Amphiphilic Polyethylene Block Copolymers and their Application as Wax Crystal Modifiers in Middle-Distillate Fuels

By

Paul Derek Goring

A thesis submitted in partial fulfilment of the requirements for the degree of Doctor of Philosophy in Chemistry

Department of Chemistry, University of Warwick

September 2017

Contents

List of Figures

List of Schemes

List of Tables

Acknowledgements

First and foremost, my sincere thanks go to my supervisor Peter Scott for choosing to give me the opportunity to work on this project and for the support, guidance and always asking the most awkward questions. Quite apart from my development as a scientist, I will also be thankful for the dramatic improvement in my knowledge of Latin, the reminders of the benefits of the library and the understanding of when full stops are correctly used in abbreviations.

I would also like to thank both past and present members of the Infineum fuels team: Colin Morton, Ben Hornby, Giles Theaker (now at Celotex), Ken Lewtas, Sally Hopkins, Mike Capaldi and Richard Hart. Your ideas, hard work and financial support are greatly appreciated. Hopefully the work proves useful and the materials do well in the tests.

My thanks go to the Scott group members over the 4 years that I've been here, who were forced to put up with me on a daily basis but did so graciously: Connah, Dan, Hualong, Shaun, Tom, Anish, Guy, Ellis, Chris, Becky and Alan, as well as many, many MChems. Thanks are also due to current and former colleagues in Chemistry for their help with some chemical, but mainly instrument-based difficulties: David Fox for humouring a polymer chemist during some very useful mechanism discussions; Dan Lester (ably assisted by Sam Lawton and Rachel Hand) for maintaining the GPC, thermal analysis and particle size facilities and in particular for his determination to keep the PL220 running high temperature GPC samples despite the ever-present temptation to throw it out of the window; Ivan Prokes and Rob Perry for their patience and persistence in persuading Ozric to run VT NMRs and for their knowledge and advice with the DOSY experiments; Kayleigh McEwan (now at MAHLE) for GPC training and David

Hammond for DSC training. Thanks to Rob Jenkins for the safety input and for arranging the emergency first aid course for me, and also to Jason Noone for solving various computer problems over the years. The final Warwick thanks goes to those from the department who played football on Monday evenings for providing a way to keep me sane while I was writing up.

I have leant on a small army of people from outside Warwick during my PhD and they all deserve recognition. Firstly, thanks to my friends from Loughborough for providing constant support and very welcome regular breaks from work: Danny, Wilson, Sam, Forster, Lynch, Gracey, Charley, Greg, Cram, Jon, Tom, Carl and Emma. A special mention ought to go to Danny, Charley and Wilson again for being there in the immediate aftermath of the most difficult period during my time here and making it so much easier. Equal appreciation goes to my friends from home in and around Eastbourne for your patience while I ranted about PhD life and the ease with which you provided much-needed distraction with anything other than chemistry: Gill, Matt, Amy, Paul, Emily, Ellie, Dan, Claire, Ros and Toms Nolan and Gosling. You all managed to be a source of empathy, advice and support regardless of which town or even which time zone you were living in and I will be forever grateful for that. Congratulations are also due to Gill and Matt, Amy and Paul, and Ellie and Dan who even managed to get married while supporting me all the way through this.

Last but not least I would like to thank all of my family, many of whom I don't get to see very often. In particular, I would like to thank my mum Andrea, my dad Derek, my stepmum Anwen and my sister Sarah. Without you I wouldn't have got anywhere near this far.

Funding

The work reported in this thesis was conducted with funding from the EPSRC and Infineum UK Ltd, a company based in Oxfordshire who produce additives for fuels and oils. Many of the materials discussed in this work were sent to Infineum for testing, as well as being tested in-house at University of Warwick using equipment provided by Infineum.

Declaration

The work performed in this thesis was carried out in the Department of Chemistry, University of Warwick between September 2013 and September 2017. Unless otherwise stated, it is the work of the author and has not been submitted in whole or in part for any degree at this or any other university.

Publications

The following paper has arisen from this thesis:

Chapters 2 and 4

C. J. Kay, C. A. Burnett, P. D. Goring, *et al*, Interface active polyolefins from versatile new macromonomers – in preparation.

Summary

Chapter 1 reviews the synthesis of polyolefin block copolymers, focussing on strategies involving catalytic coordination polymerisation to produce end-functionalised polyolefins followed by the growth of a second block from the reactive end group using living/controlled techniques. The advantages and disadvantages of the various literature methods are discussed.

Chapter 2 discusses the utilisation of the Catalytic Hydride Insertion Polymerisation (CHIP) mechanism for the synthesis of low molecular weight polyethylene macromonomers by manipulating the relative concentrations of dihydrogen and ethylene in the reactions. The application of the mechanism is investigated further with the introduction of two non-styrenic comonomers 5-vinyl-2-norbornene and 5-ethylidene-2-norbornene. Observations made when we studied the effects of comonomer concentration and dihydrogen partial pressure on the products are discussed and some mechanistic insights for the copolymerisation between ethylene and norbornene derivatives in the presence of dihydrogen are proposed.

Chapter 3 focusses on the investigation of the mechanism for the copolymerisation between the PE-*i*-DIB macromonomer and *n*-butyl acrylate using a small-scale batch process and a larger scale starved feed semi-batch process. Observations are found to be consistent with a reversible cross-propagation mechanism between PE-*i*-DIB and the propagating P(*n*-BA) chain in which the continued availability of monomer is key to the lifetime of the process, as demonstrated by the difference in the evolution of molecular weight in the batch and semi-batch processes. The semi-batch process also provides superior control over the copolymerisation compared to the batch process.

Chapter 4 investigates the versatility of the PE-*i*-DIB macromonomer in copolymerisations with several other types of polar monomer. Copolymer products with vinyl esters, methacrylates and styrenes are synthesised and the challenges provided by the new monomer types are discussed. The products discussed here and in Chapter 3 are characterised by NMR, GPC, DLS and DSC and the evidence is found to be consistent with the presence of block copolymers.

Chapter 5 describes the testing of some of the block copolymers synthesised in Chapters 3 and 4 for their wax crystal modification properties in one type of diesel fuel. The block copolymers were tested as neat additives and in formulation with commercial nucleators and growth arrestors in the Cold Filter Plugging Point (CFPP) test to assess performance and to indicate mode of action. The mode of action was then investigated further by observing the effect of the additives on the crystallisation events using DSC. The performance in CFPP and the observations in DSC are consistent with the block copolymers generally acting as nucleating agents, though some also display single-shot activity. There is an observable trend in performance with the varying size of the polar block as well as varying the polar block itself.

Chapter 6 details the experimental procedures used to carry out the work in this thesis.

Abbreviations

2-VP = 2-vinylpyridine

9-BBN = 9-borabicyclononane

AIBN = 2,2'-azobis(2-methylpropionitrile)

AMS = α-methylstyrene

ATRP = Atom Transfer Radical Polymerisation

BHT = 2,6-di-*tert*-butyl-4-methylphenol

BP = benzoyl peroxide

CCT = Catalytic Chain Transfer

CCTA = Catalytic Chain Transfer Agent

CCTP = Catalytic Chain Transfer Polymerisation

$CDCl_3$ = Chloroform-*d*

CFPP = Cold Filter Plugging Point

CHIP = Catalytic Hydride Insertion Polymerisation

COBF = Bis(boron difluorodimethylglyoximate)cobaltate(II)

COSY = Correlation Spectroscopy

Cp = Cyclopentadienyl

Cp^* = Pentamethylcyclopentadienyl

CRP = Controlled Radical Polymerisation

CTA = Chain Transfer Agent

d^2-TCE = 1,1,2,2-tetrachloroethane-d^2

$Đ$ = Dispersity

DIBAL-H = Diisobutylaluminium hydride

DIB = 1,3-diisopropenylbenzene

DLS = Dynamic Light Scattering

DOSY = Diffusion-Ordered Spectroscopy

DP = Degree of Polymerisation

DSC = Differential Scanning Calorimetry

ENB = 5-Ethylidene-2-norbornene

EO = Ethylene oxide

EVA = Ethylene/vinyl acetate copolymer

FI = Phenoxyimine

Flu = Fluorenyl

FTIR = Fourier Transform Infa-Red Spectroscopy

GPC = Gel Permeation Chromatography

HMBC = Heteronuclear Multiple-Bond Correlation

HMQC = Heteronuclear Multiple-Quantum Correlation

IF = Indenyl-fluorenyl

Ind = Indenyl

k = Boltzmann constant (1.38×10^{-23} m^2 kg s^{-2} K^{-1})

LIM = Limonene

MAO = Methylaluminoxane

MCPBA = 3-Chloroperbenzoic acid

MCR = Mid-chain radical

MMA = Methyl methacrylate

M_n = Number average molecular weight

M_p = Peak average molecular weight

M_W = Weight average molecular weight

n-BA = *n*-butyl acrylate

NIPAM = *N*-isopropylacrylamide

NMP = Nitroxide Mediated Polymerisation

NMR = Nuclear Magnetic Resonance Spectroscopy

PBd = Polybutadiene

PE-Al = Aluminium-terminated polyethylene

PE = Polyethylene

PEB = Poly(ethylene-butylene)

PEG = Polyethylene glycol

PE-*i*-AMS = Polyethylene initiated with AMS

PE-*i*-DIB = Polyethylene initiated with DIB

PE-*i*-LIM = Polyethylene initiated with LIM

PEO = Poly(ethylene oxide)

PE-OH = Hydroxy-terminated polyethylene

PEP = Poly(ethylene-propylene)

PE-SH = Thiol-terminated polyethylene

PE-*t*-PMS Polyethylene terminated with PMS

PIB = Polyisobutylene

PMDETA = *N''*-pentamethyldiethylenetriamine

PMS = *para*-methylstyrene

P(*n*-BA) = Poly(*n*-butyl acrylate)

P(MMA) = Poly(methyl methacrylate)

P(C14MA) = Poly(myristyl methacrylate)

PO = Polyoctene

PP = Polypropylene

PS = Polystyrene

P(V2EH) = Poly(vinyl-2-ethylhexanoate)

P(VAc) = Poly(vinyl acetate)

P(VOH) = Poly(vinyl alcohol)

RAFT = Reversible Addition-Fragmentation Chain Transfer

RCM = Reactive comonomer

ROMP = Ring Opening Metathesis Polymerisation

ROP = Ring Opening Polymerisation

SG1 = *N*-(2-methyl-2-propyl)-*N*-(1-diethylphosphono-2,2-dimethylpropyl)-*N*-oxyl

STY = Styrene

TBA = *tert*-butyl acrylate

T_c = Crystallisation temperature

TEMPO = 2,2,6,6-tetramethyl-1-piperidinyloxy

TFA = Trifluoroacetic acid

T_g = Glass transition temperature

THF = Tetrahydrofuran

T_m = Melting temperature

TMEDA = *N*,*N*,*N'*,*N''*-tetramethylethylidenediamine

TP = *tert*-butyl peroxide

VNB = 5-Vinyl-2-norbornene

VT = Variable temperature

WAT = Wax appearance temperature

Chapter 1: Modification of Polyolefins *via* Synthesis of Polyolefin-Polar Monomer Block Copolymers.

1.1 Introduction

Polyolefins are by far the largest volume polymers, making up 50% of plastic production worldwide.[1] Properties such as chemical stability, flexibility, mechanical strength, recyclability, processability and low production cost already mean that they are used in a wide range of commercial applications.[2, 3, 4] However lack of reactivity, poor adhesion and incompatibility with other polymers have thus far limited their use in many commercially important areas in favour of materials that are far less environmentally friendly and more expensive to produce. The functionalisation of polyolefins, *i.e.* the addition of polar groups, is a synthetic challenge that has been relentlessly pursued in recent decades because of the substantial improvement gained in terms of compatibility, adhesion and rheological properties that would allow polyolefins to be utilised in many more commercial fields, such as blends or composites.[4, 5]

In the last two decades the functionalisation of polyolefins has progressed substantially. This is because the range of applicable monomers has dramatically widened due to the development and utilisation of an increasing range of polymerisation methods. This in turn has allowed the synthesis of an almost endless variety of materials and architectures whose properties are just as varied. By introducing varying amounts of a range of polar functionalities, it has become possible to utilise the original properties of unfunctionalised polyolefins in combination with new properties introduced by the polar groups, thus broadening the potential applications.

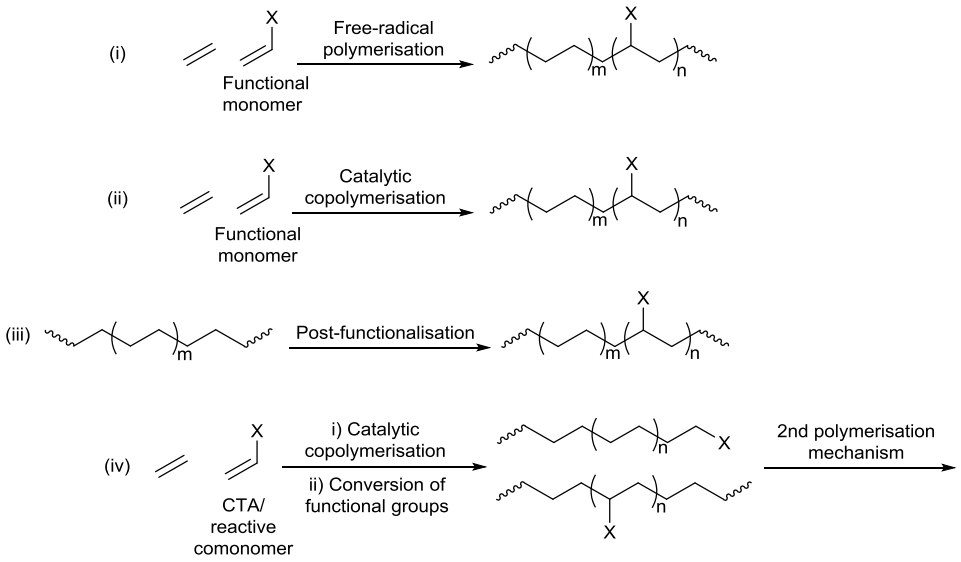

Scheme 1.1 - Main synthetic pathways for functionalised polyolefins.

Four main methods have emerged for the preparation of functional polyolefins (Scheme 1.1): (i) free radical copolymerisation of olefins (usually ethylene) with polar monomers; (ii) direct catalytic copolymerisation of olefins and polar monomers; (iii) modifying pre-formed polyolefins or; (iv) catalytic olefin polymerisation followed by other polymerisation strategies like living ionic polymerisation, ring-opening polymerisation (ROP) or controlled radical polymerisation (CRP).[2, 4, 6] Direct free radical copolymerisation of olefins with polar monomers and modification of pre-formed polyolefins (methods i and ii) are currently used in industry, though both suffer from the disadvantage of requiring harsh reaction conditions with unwanted side reactions like cross-linking or bond cleavage often occurring as a consequence.[7] Direct catalytic copolymerisation of olefins with polar monomers (iii) has found little use due to the uncontrollable reactivity between the transition metal catalysts and the functional groups of the monomers.[2] The final method (iv) involves the introduction of a reactive comonomer, a chain transfer agent or vinyl groups to the metal-catalysed olefin polymerisation to yield a reactive polyolefin, whose functional groups can be utilised in

the initiation of a second polymerisation mechanism, such as anionic or radical.[2, 4] Although this method often involves extra reaction steps, the benefits of a wider compatible monomer range and superior control of the characteristics of the final product outweigh the drawbacks and make successive catalytic olefin polymerisation and living/controlled polymerisation techniques the most promising current method for modified polyolefin synthesis.

Several reviews reporting functional polyolefin synthesis based on final structure,[4] end group nature[8] or synthetic strategy[2, 6] have been published in the last two decades while a more recent article provided a wide, updated overview of progress the field.[9] In that work functionalised polyolefins were divided into four structure-based categories: linear randomly functionalised copolymers, branched randomly functionalised copolymers, end-functionalised copolymers, block copolymers and graft copolymers. This chapter will provide an updated review specifically on the synthesis of polyolefin block copolymers and will focus on strategies involving catalytic coordination polymerisation to produce end-functionalised reactive polyolefins followed by the growth of a second block from the reactive end group *via* living/controlled techniques. Strategies involving living olefin polymerisation and combined ring opening metathesis and controlled radical polymerisations are also covered.

1.2 Approaches for the end-functionalisation of polyolefins

The synthesis of end-functionalised polyolefins is often the first step in the process for preparing copolymers with more complex architectures *e.g.* block and graft and as such is very important in polyolefin synthesis. Polyolefins can be prepared with a terminal functional group on one end or on both ends (telechelic polymers), thus allowing the synthesis of diblock and triblock copolymers. There are four major synthetic methods

for incorporating functional end groups into polyolefins (Scheme 1.2): 1) end-capping of catalytic living olefin polymerisation, 2) reaction of pre-formed unsaturated end groups, 3) *in situ* chain transfer reactions through addition of a metallic or non-metallic chain transfer agent, or 4) copolymerisation of an olefin with a reactive comonomer (reactive polyolefin approach).[2, 4, 9, 10, 11]

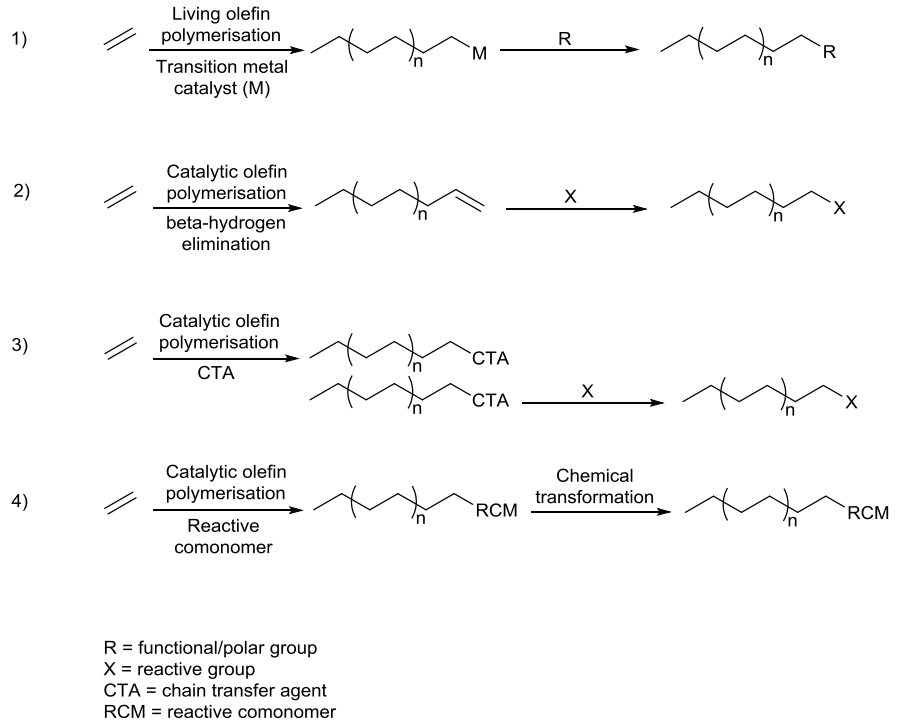

Scheme 1.2 - General synthetic pathways for end-functionalised polyolefins.

1.2.1. End-functionalisation *via* catalytic living olefin polymerisation

Rather like direct catalytic copolymerisation of olefins with polar monomers, end-capping of living polymerisations suffers from two major disadvantages. Reactions involving end groups containing polar functionalities are generally problematic[10] and there is little practical use as only one chain is produced by each metal centre so the process is metal-consuming. On top of this, there is a requirement for specific catalyst

systems and reaction conditions.[12] These practical complications have limited the number of reported examples in academic literature.

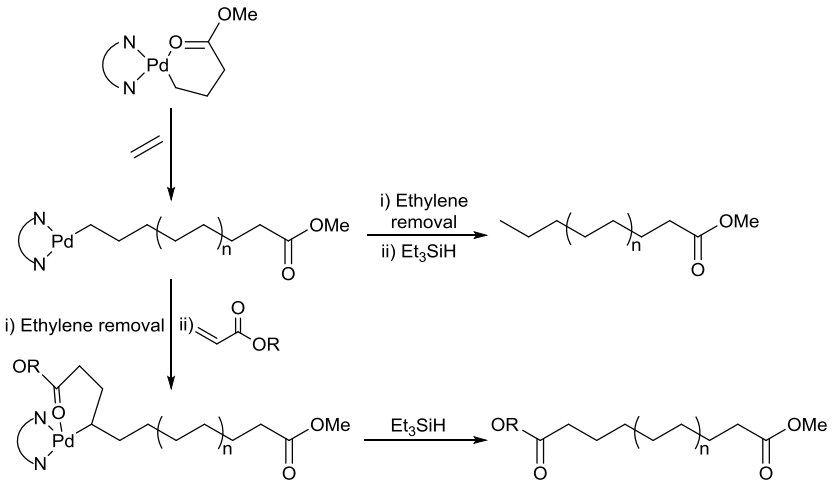

Scheme 1.3 - Synthesis of PE functionalised with an acrylate unit *via* end-capping of living olefin polymerisation catalysed by palladium. Functionalisation can be achieved at one or at both chain ends.[15]

The introduction of polar end groups to living olefin polymerisation relies on the use of either early or, mostly, late transition metal catalysts. Brookhart and co-workers[13] reported the synthesis of end-functionalised polyethylene (PE) through the use of a cobalt catalyst containing *para*-substituted phenyl groups, which were able to introduce terminal functional groups in the initiation step having initiated the living olefin polymerisation. Palladium-diimine catalysts have more recently been used to prepare PE with an acrylate end group using the same strategy *i.e.* the ethylene polymerisation is initiated by the chelated acrylate which enables the incorporation of the end group in the initiation stage of the reaction (Scheme 1.3).[14, 15] In the same publication,[15] the synthesis of telechelic PE was also reported by addition of another acrylate unit following the ethylene polymerisation. However ligand, catalyst and macromonomers required multiple reaction steps in their preparation and macromonomer yields were modest. The

need for rigorous air- and moisture-sensitive conditions for the living polymerisation step is also a drawback.

The end-capping of living olefin polymerisations is not restricted to ethylene. Syndiotactic polypropylene (PP) end-capped with iodine was achieved by Doi *et al* using a vanadium catalyst at low temperature where the iodine was added at the end of the polymerisation.[16, 17, 18, 19] Fujita and co-workers[20] developed a method for synthesis of aluminium- and silyl-end-capped PE and PP using titanium catalysts bearing phenoxyimine ligands (Scheme 1.4). Telechelic polymers could also be synthesised using this method by insertion of functionalised monomers after the olefin polymerisation. These end-groups could then be converted to hydroxyl end-groups post-polymerisation by treatment with acid.

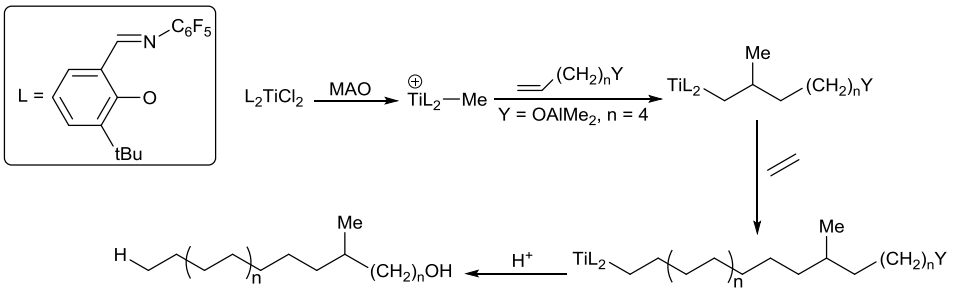

Scheme 1.4 - Use of titanium catalyst bearing phenoxyimine (FI) ligands to introduce functional groups during initiation of polyethylene growth.[20]

1.2.2. End-functionalisation *via* chain transfer

The use of chain transfer reactions in the end-functionalisation of polyolefins has the advantage of being catalyst-efficient *i.e.* each active species is able to produce multiple polymer chains, unlike catalytic living olefin polymerisation (*vide supra*).[12, 21] This keeps the end group fidelity high and means that simple manipulation of the chain transfer agent/monomer ratio can be used to tune the polymer molecular weight. Chain

transfer reactions used in this context can be divided into the use of metallic chain transfer agents, non-metallic chain transfer agents and β-hydrogen elimination. The first two are discussed in more detail below, but β-hydrogen elimination is a chain transfer process common in olefin polymerisations which normally yields low molecular weight products containing a terminal vinyl group.[9] These vinyl groups can then be chemically altered post-polymerisation (*vide infra*).

1.2.2.1 Metallic chain transfer agents

Both catalytic and irreversible chain transfer reactions to metals have been utilised in polyolefin synthesis. These strategies are appealing because the behaviour of transition metal and metal alkyl catalysts is well-studied and the reactivity of the metal-carbon bonds allows the quantitative introduction of a variety of functional groups (*vide infra*).[22, 23]

Through optimisation of the conditions that bring about the long-known chain transfer reaction that occurs between a growing polymer chain and main group metal-alkyl species,[24] coordinative chain transfer polymerisation (CCTP) was developed.[25, 26] The process normally involves a transition metal catalyst and a main group metal alkyl compound that acts as the chain transfer agent and allows the highly controlled synthesis of entirely metal-end-capped polyolefins whilst adding the aforementioned catalytic quality to the system. Zinck and co-workers[27] reviewed the use of a variety of transition metal/main group metal combinations in the CCTP of a range of olefins; however the functionalisation of these polymers were not included and the authors point out that the nature of the active species is still uncertain, although this has recently been examined kinetically and computationally by Ribeiro and co-workers.[28]

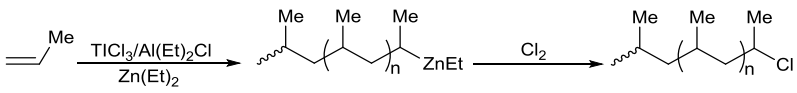

Scheme 1.5 - End-functionalisation of polypropylene with halogens *via* intermediate chain transfer to zinc.[31]

Chain transfer from early transition metals to zinc resulting in Zn-alkyl terminated polyolefins is commonly found in literature. The high reactivity of the Zn-C bonds has been used to impart vinyl,[29, 30] halogen[31] (Scheme 1.5), hydroxyl[32], carbonyl[31] and amine[33] end groups onto polypropylene. More recently alkyne- and azide-terminated polypropylene has also been reported using chain transfer to zinc.[34] The synthesis of PE terminated with zinc was pioneered by Gibson and co-workers,[35, 36, 37] uncovering a range of highly active catalytic systems across the transition metal series. Arriola[38] then took the technology further to develop a dual-catalyst system for the preparation of olefin block copolymers using a high-throughput catalyst screening approach. The reader is also referred to Sita,[39] who provides a more general review of the achievements and potential of coordinative chain transfer to zinc in olefin polymerisation.

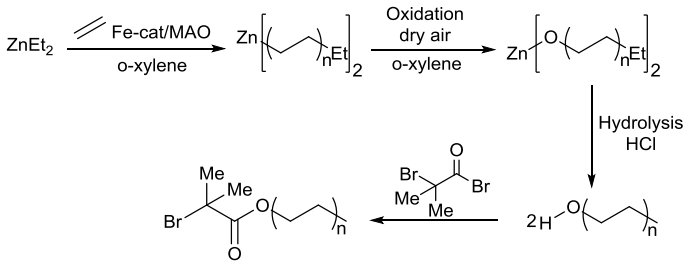

Scheme 1.6 - Synthesis of PE-OH by oxidation of a mid-chain zinc atom, followed by conversion to an ATRP macroinitiator.[40]

Matyjaszewski and co-workers[40] reported that the mid-chain Zn-carbon bonds formed in the iron-catalysed ethylene polymerisation in the presence of diethyl zinc could be converted *in situ* to hydroxyl end groups by hydrolysis (Scheme 1.6). These hydroxyl

end groups could then be treated with 2-bromo-2-methylpropionyl bromide to produce a PE-based ATRP macroinitiator (*vide infra*). A similar approach was used by Zhu and co-workers to produce an ATRP macroinitiator.[41] Macroinitiators synthesised in this way are not restricted to ATRP; ring-opening polymerisation of lactide was reported from a hydroxyl-terminated PE by Dubois *et al*[42] and Zhu and co-workers[43] were able to produce a PE terminated with a trithiocarbonate, which was useable in a subsequent RAFT polymerisation of NIPAM and 2-vinylpyridine.

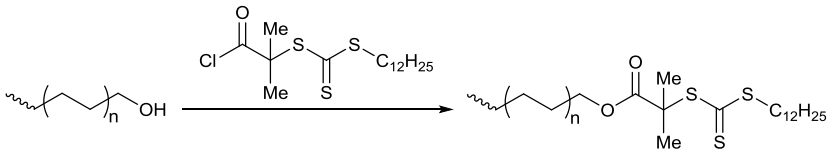

Scheme 1.7 - Synthesis of trithiocarbonate-terminated PE from PE-OH.[43]

Transition metal-catalysed polymerisations conducted in the presence of aluminium alkyls produce similar products to those conducted with zinc alkyls, namely the synthesis of polyolefins containing terminal hydroxyl groups. Kim and co-workers[44, 45] reported that during metallocene-catalysed copolymerisations between ethylene and allylbenzene in the presence of methylaluminoxane (MAO), a chain transfer to aluminium was strongly favoured following allylbenzene insertion. They found that the mode of chain transfer depended on the ligand structure of the catalysts but that chain transfer to aluminium was preferred when using highly substituted species. PE-OH could then be formed by oxidative work-up (Scheme 1.8). The same group also reported the use of PE-OH synthesised using the above method as an ROP macroinitiator.[46]

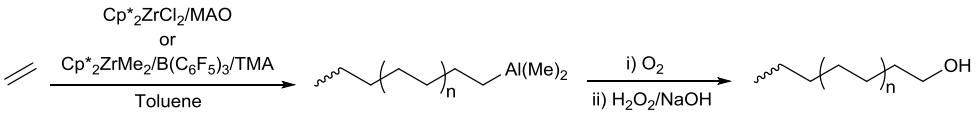

Scheme 1.8 - Synthesis of OH-terminated PE *via* chain transfer to aluminium and oxidative workup.[46]

The use of Zr-FI catalysts and an aluminium chain transfer agent allowed Fujita and co-workers to produce a wide range of molecular weight PE-Al species simply by varying the reaction time and the concentration of chain transfer agent.[47] Kashiwa and co-workers described the development of a one-pot synthesis of hydroxyl-capped PE using allyl alcohol as a comonomer and a novel metallocene indenyl-fluorenyl (IF) catalyst in the presence of MAO.[48] Selective end-incorporation of the allyl alcohol and chain transfer to aluminium allowed the synthesis of PE-OH by oxidative work-up (Scheme 1.9).

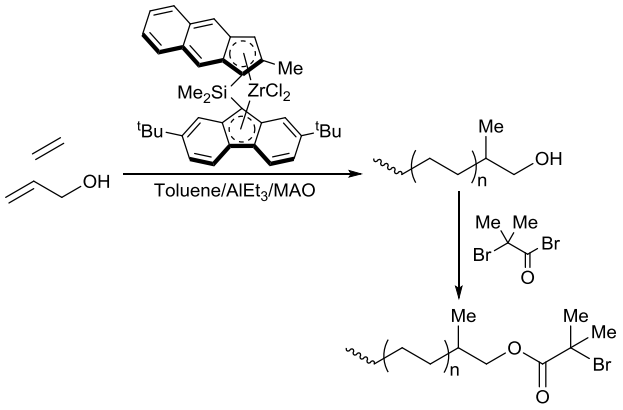

Scheme 1.9 - Copolymerisation of ethylene with allyl alcohol in presence of metallocene IF catalyst yielding PE-OH, and conversion to an ATRP macroinitiator.[48]

The same authors converted the PE-OH into an ATRP macroinitiator for block copolymer synthesis, preceding similar work published by Matyjaszewski (*vide supra*). More recently the synthesis of PE-OH using cationic yttrium complexes with aluminium chain transfer agents was reported by Kempe and co-workers.[49] Other functionalities

including bromo, chloro, α-bromoacetate and α-bromoisobutyrate were successfully synthesised by conversion of the hydroxyl groups in very high yields.

Hydroxyl-terminated polypropylene has been prepared using Ziegler-Natta catalytic systems in the presence of aluminium alkyl co-catalysts. Ikeda and co-workers utilised the classic $MgCl_2$-supported $TiCl_3$ catalyst in the presence of $AlEt_3$[50] and $Al(i\text{Bu})_3$[51] to produce both isotactic and atactic Al-terminated PP, which was then quenched with oxygen to convert the Al end groups to hydroxyl groups. The synthesis of both hydroxyl- and iodine-terminated isotactic PP was described by Soga et al[52] using a [2,6-$^{i}Pr_2C_6H_3N(CH_2)_3N2,6$-$^{i}Pr_2C_6H_3$]$TiCl_2$/MAO catalyst system followed by reaction with oxygen and iodine respectively.

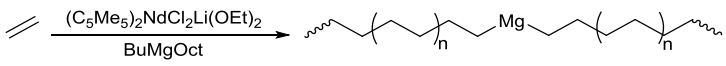

Scheme 1.10 - Synthesis of PE-Mg-PE.[26]

Mortreux and co-workers first described the use of alkyl magnesium compounds as metallic chain transfer agents in lanthanocene-catalysed PE synthesis (Scheme 1.10).[26] The product of the reaction was a PE-Mg-PE species where the PE chains were of low dispersity and could contain between four and two hundred carbons depending on the conditions. This was later utilised by Boisson and co-workers in the production of a range of end-functionalised PE's by various post-polymerisation reactions of the $Mg(PE)_2$ species.[22] Alkoxyamine-functionalised PE (Scheme 1.11) was reported by the same authors by reaction of the in-chain Mg-C bonds with 2,2,6,6-tetramethy-1-piperidinyloxy (TEMPO) with around 63% of the chains bearing a terminal TEMPO unit.[53] Prior to this Hawker and co-workers described the preparation of not only PE-TEMPO, but also PE bearing another stable radical *N*-(2-methyl-2-propyl)-*N*-(1-

diethylphosphono-2,2-dimethylpropyl)-*N*-oxyl (SG1), though the end group fidelities differed substantially for the two macroalkoxyamines (70% and 45%).[54] In a later publication Boisson *et al* described the synthesis of two new nitroxides (DD1 and DD2) and the subsequent addition to PE chains.[55] The nitroxide DD2 required a substantially lower temperature (60°C) than either TEMPO or SG1 to cleave the C-ON bond and thus initiate nitroxide mediated polymerisation, though the end group fidelity was low again (40%).

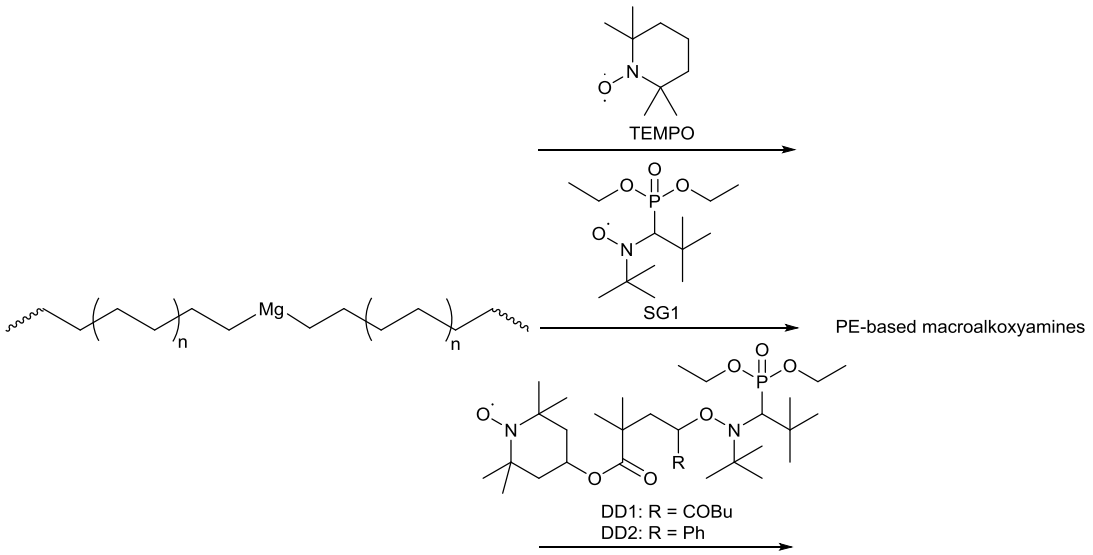

Scheme 1.11 - Synthesis of PE-based macroalkoxyamines for NMP.[53, 54, 55]

The conversion of $MgPE_2$ species into macro-RAFT agents was investigated by the same group using dithiocarbonylates (Scheme 1.12).[56, 57] Despite the low conversion and the presence of side reactions, examples of thiocarbonylate-terminated PE were synthesised for subsequent reversible addition-fragmentation chain transfer (RAFT) polymerisations. The same authors have also reported the efficient conversion of $Mg(PE)_2$ to iodine-terminated PE, from which PE terminated with an azide group was synthesised.[23] Reduction of the azide to an amine was conducted, from which another macro-RAFT agent was prepared (Scheme 1.13).

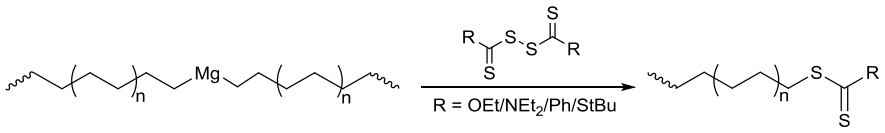

Scheme 1.12 - Synthesis of PE-based macroRAFT agents.[56, 57]

A variety of methods for the conversion of $Mg(PE)_2$ to thiol-terminated PE were conducted by Boisson and co-workers, the most successful of which involved the reduction of dithiocarbonylate-terminated PE using $LiAlH_4$ (Scheme 1.14).[58] The resulting PE-SH materials were used in later publications to initiate the ROP of lactide[59] and as nucleophiles in thia-Michael addition reactions with acrylic and methacrylic monomers.[60]

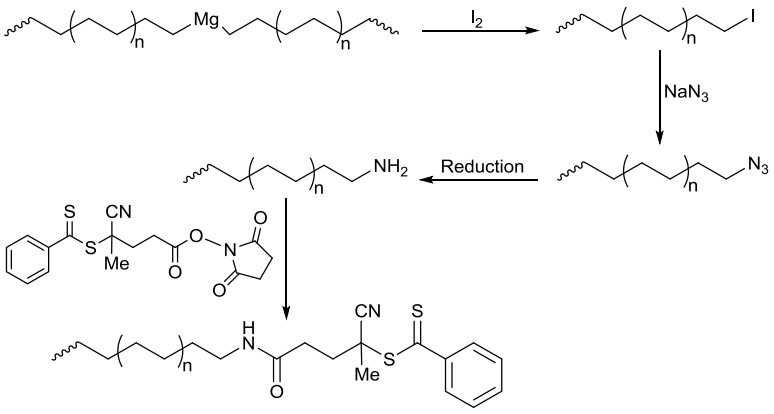

Scheme 1.13 - Strategies to functionalised PE from the PE-Mg-PE species, including synthesis of a macroRAFT agent.[23]

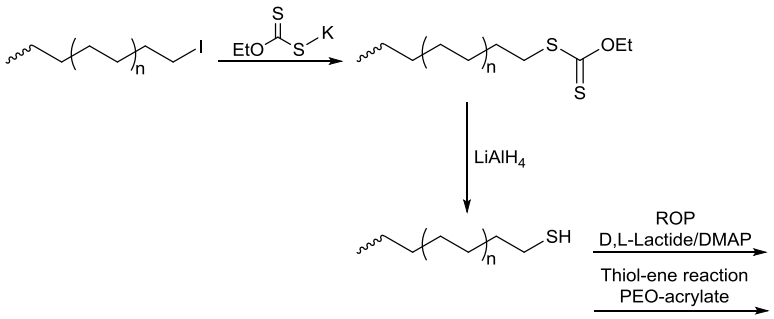

Scheme 1.14 - Synthesis of PE-SH from PE-I and further reactions.[58, 59, 60]

1.2.2.2 Non-metallic chain transfer agents

Marks and co-workers reviewed the use of chain transfer agents for the end functionalisation of polyolefins with a number of heteroatoms.[61] A variety of chain transfer agents have been shown to be highly active in catalytic olefin polymerisation and a diverse range of end groups have been reported. These chain transfer agents are compatible with both d- and f-block metal catalysts without the need for protection chemistry. The Marks group themselves have described the synthesis of silane-terminated polyolefins using Ziegler-Natta,[62, 63] metallocene[64] and organolanthanide catalysts.[65] They later reported that amine and phospine groups could also be incorporated as end groups using organolanthanide catalysts.[66, 67]

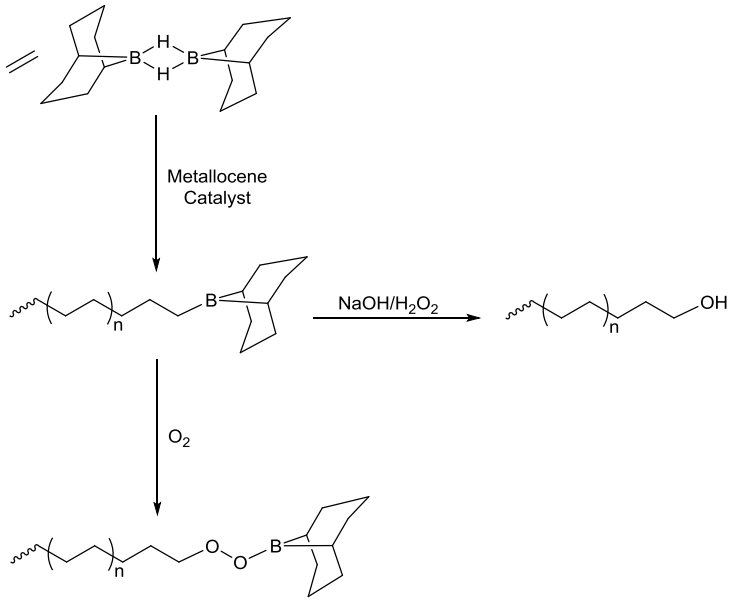

Scheme 1.15 - Synthesis of borane-terminated PE and further reactions.[68, 69]

Polyolefins with a terminal borane group can be synthesised by chain transfer to organoboranes during metallocene-catalysed olefin polymerisation. Chung and co-workers reported the formation of 9-borabicyclo[3.3.1]nonane (9-BBN)-terminated PE through chain transfer to the commercially available 9-BBN dimer (Scheme 1.15).[68, 69] In the same publication the group also reported the possibility of quantitatively converting the borane end group to a hydroxyl end group by an oxidative work-up or to a terminal peroxide unit (-BOOC-) by exposure to oxygen. Interestingly this peroxide moiety is suitable for use as a free-radical initiator for the synthesis of block copolymers (*vide infra*). A range of polyolefin anionic macroinitiators were also described by Chung,[70] prepared by oxidation of terminal borane units to produce hydroxyl end groups and followed by metalation with potassium naphthalide (*vide infra*). More recently, Dong and co-workers[71] found trialkylboranes to be efficient chain transfer agents in metallocene-catalysed olefin polymerisation which, after an oxidative work-up, also resulted in hydroxyl-terminated PE.

Chain transfer to vinyl chloride *via* β-Cl elimination was found to produce polyolefins with a single vinyl end group by Gaynor.[72] By comparison to the aforementioned silanes and boranes, vinyl chloride is inexpensive and was reportedly able to produce vinyl-terminated PE and PP in the presence of a variety of metallocene catalysts. Despite this vinyl chloride has not found widespread use in olefin polymerisation.

1.2.3 End Functionalisation using vinyl end groups

Polyethylene with high vinyl end-group fidelity (70-90%) can be synthesised under mild conditions using group IV metal catalysts, of which a range have been reported with high activities bearing phenoxy/imine ligands (FI catalysts, *vide supra*) by Fujita and co-workers to prepare low molecular weight PE.[73, 74, 75, 76, 77] In separate publications the same authors described post-polymerisation reactions to further functionalise the PE. An Alder-ene reaction followed by hydrolysis yielded disodium succinate end groups;[78] whereas oxidation of the vinyl end groups led to diol- and triol-terminated PE which could be used to initiate ROP of ethylene oxide.[79]

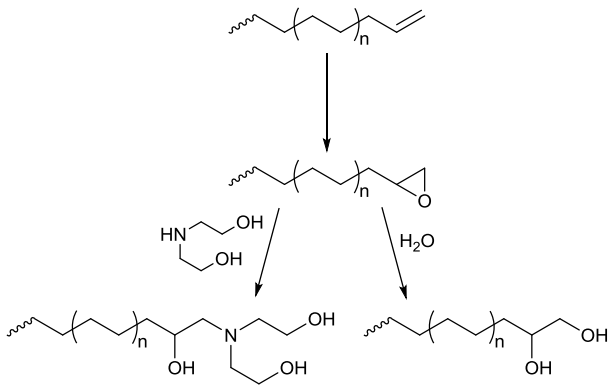

Scheme 1.16 - Synthesis of diol- and triol-terminated PE.[79]

Low molecular weight PE with 100% vinyl end group fidelity was produced using a nickel phosphanylenolate catalyst,[80] which Mazzolini and co-workers utilised in an investigation into reactions of vinyl-terminated PE with a series of thiols, yielding high degrees of functionalisation.[58] The addition of a thiol to vinyl-terminated PE was first published by Sengupta and co-workers[81] and was subsequently used to produce PE with a silane functionality. The application of a silyl functionality has also been described by Matyjaszewski for the conversion of pre-formed vinyl-terminated PP into an ATRP macroinitiator for block copolymer synthesis (Scheme 1.17).[82]

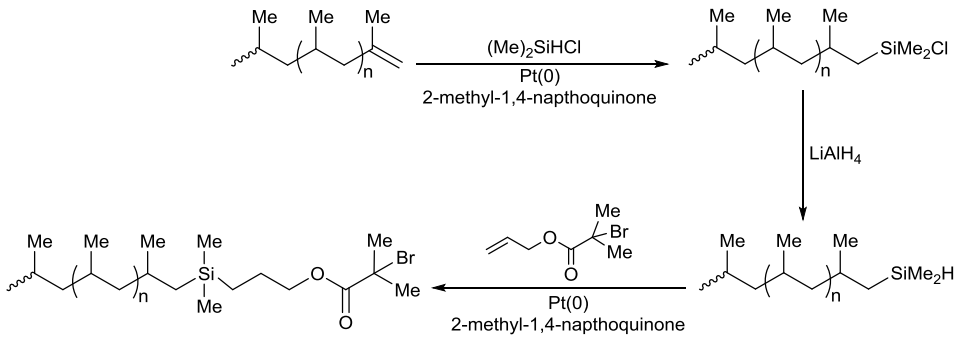

Scheme 1.17 - Synthesis of PP macroinitiator for ATRP by hydrosilylation of vinyl-terminated PE.[82]

Functionalisation of pre-formed unsaturated end groups has also been achieved by hydroalumination and hydroboration reactions.[10, 11] As with the chain transfer processes to aluminium alkyls (*vide supra*), the hydroalumination reactions of unsaturated polyolefin chain ends are often followed by oxidation to add hydroxyl functionality,[51, 83] though this method has also been shown to introduce halogen functionalities to the polyolefin chain end.[31] Matyjaszewski and co-workers have utilised a hydroalumination process in the four-step synthesis of an α-bromoester-terminated PE which could be used as an ATRP macroinitiator.[84] Also noteworthy is the work of Kashiwa and co-workers who utilised a similar process to synthesise a hydroxyl-terminated ethylene/propylene

macromonomer which could then be converted into a methacrylate macromonomer by reaction with methacryloyl chloride.[83, 85]

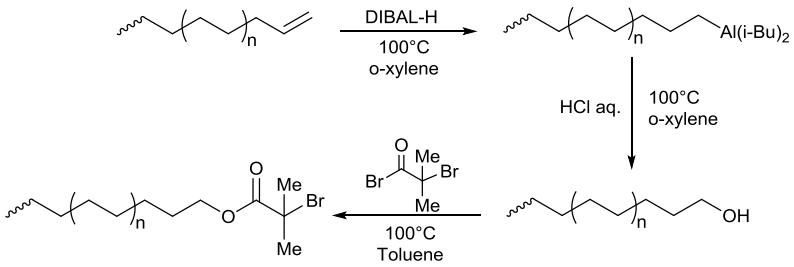

Scheme 1.18 - Synthesis of a PE-based ATRP macroinitiator from vinyl-terminated PE.[84]

Hydroboration reactions have proved to be more successful than either hydrosilation or hydroalumination in the functionalisation of vinyl-terminated polyolefins. This is attributed to the superior reactivity and solubility of the alkyl borane reagents, which go some way to overcoming the typical disadvantages of this general approach *i.e.* low functional group concentration and poor polymer solubility in the reaction medium.[2, 4] Borane-functionalised PP has been prepared from vinyl-terminated PP[86] and polyethylene-*co*-hexadiene[87] using alkylboranes and subsequently transformed into hydroxyl,[86, 87] amine,[87] silyl[87] and maleic anhydride end functionalities (Scheme 1.19).[88, 89]

The Matyjaszewski group have also described the preparation of ATRP macroinitiators directly from vinyl-terminated PE by triflic acid catalysed treatment with 2-bromoisobutyric acid. This in turn led to the controlled radical polymerisation of *n*-BA, MMA and styrene for the synthesis of block copolymers in 3 steps.[90]

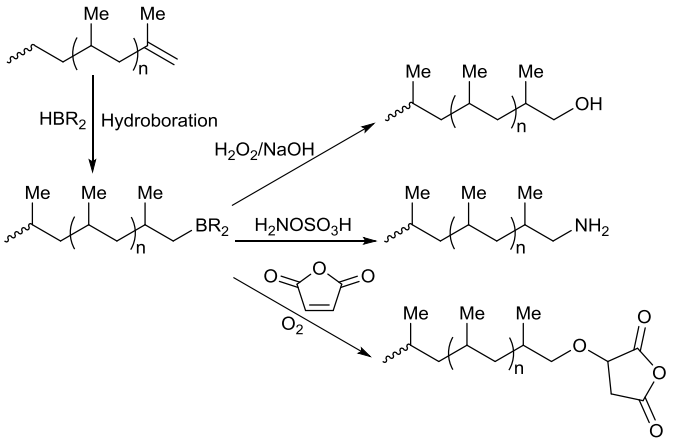

Scheme 1.19 - End-functionalisation of PP via hydroboration reactions of vinyl end groups.

1.2.4 End Functionalisation using reactive comonomers

In his book from 2002,[91] Chung described the concept of reactive comonomers for end-functionalisation of polyolefins. The comonomers in question are carefully chosen to fulfil certain criteria: compatibility with early transition metal catalysts; effective incorporation; a range of possible transformation reactions and the ability to perform "living" graft-from polymerisations. Organoborane monomers (*vide supra*) were investigated and their end-functionalisation reactions with polyolefins have been discussed earlier.[68, 69, 70, 71] The other comonomer investigated by Chung was *para*-methylstyrene (PMS).

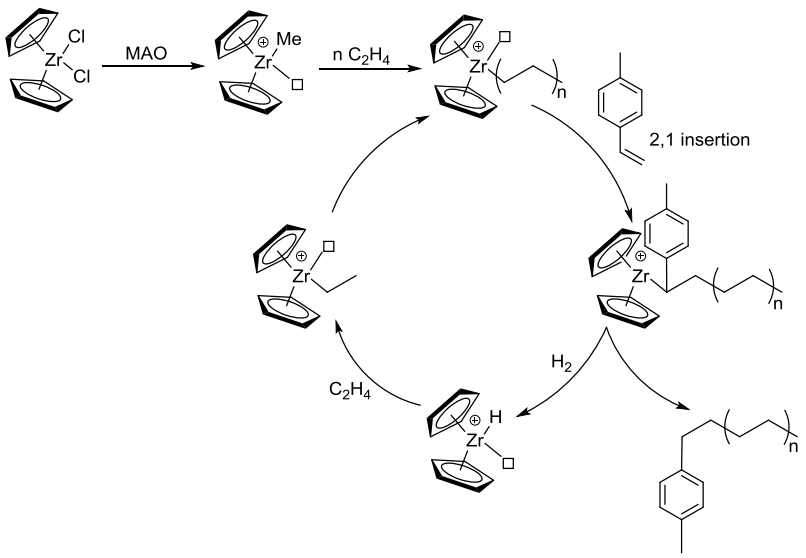

Scheme 1.20 - Chain transfer to PMS followed by hydrogenolysis to yield PE-*t*-PMS.[92]

Chung has described the synthesis of PMS-terminated PE and PP in the presence of hydrogen using several group IV metal catalysts.[92, 93] The authors also described the mechanism resulting in the polyolefin-*t*-PMS species as relying on the formation of a dormant state following selective 2,1-insertion of the PMS into a zirconium-carbon bond (Scheme 1.20). This mechanism has recently been probed by Scott and co-workers who, along with an amendment to the original Chung mechanism, reported a range of suitable reactive comonomers for end-functionalisation of polyethylene.[94]

1.3. Living olefin polymerisation for the synthesis of block copolymers

Living olefin polymerisation has been utilised to prepare block copolymers, typically achieved *via* sequential monomer addition. There are numerous examples of block copolymers made from non-polar monomers[12] but the large reactivity differences between polar and non-polar vinyl monomers mean that block copolymer synthesis *via* sequential monomer addition using any single polymerisation mechanism is problematic.[4] The use of living olefin polymerisation to this end has been hampered

either by oxophilic early transition catalysts, or inactive late transition metal catalysts towards polar monomers. Despite these setbacks, some examples of polyolefin-polar block copolymers prepared by living olefin polymerisation have been reported.

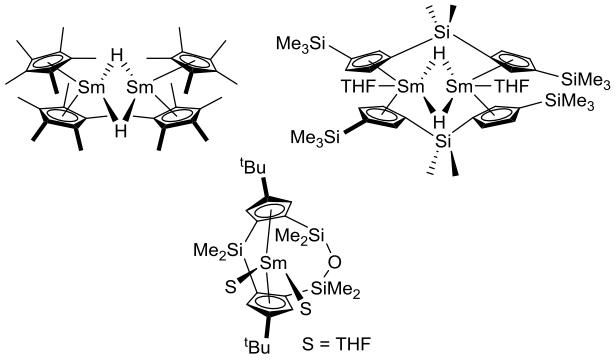

Scheme 1.21 - Rare earth metal catalysts for block copolymerisation.[12]

Yasuda and co-workers described the synthesis of PE block copolymers of narrow dispersity with acrylates, methacrylates and lactones *via* sequential monomer addition using Cp_2^*Sm derived catalysts (Scheme 1.21) and, interestingly, it was found that block copolymers could not be formed by reversing the monomer addition order.[95, 96] Similar catalysts have been utilised by the same group to produce triblock copolymers with a PE mid-block.[97] Block copolymers of higher α-olefins with polar monomers have also been reported, this time using bridged Cp-bearing scandium and yttrium catalysts.[98] Again the order of monomer addition is key, but with sequential addition of 1-pentene or 1-hexene followed by the polar monomer, block copolymers with MMA and ε-caprolactone could be formed.

Höcker and co-workers reported the synthesis of a PE-*b*-PMMA diblock at low temperatures by sequential monomer addition in the presence of a zirconium catalyst capable of mechanistic cross-over from coordination to addition polymerisation.[99] While it cannot be described as a living process, the proposed mechanism is similar to the living

processes involving the samarocene-based catalysts described above in that a cationic ester enolate zirconocene complex is thought to be the active species for the MMA polymerisation.[100, 101] This may provide encouragement that this type of process can be achieved using more commercially suitable catalysts, given the similarity of the zirconocene species to those already used in industry.

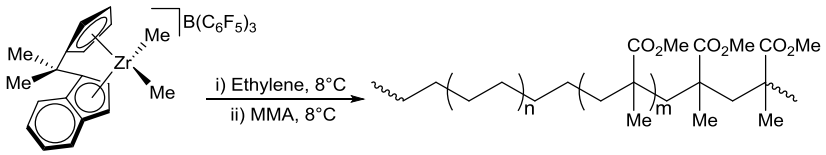

Scheme 1.22 - Synthesis of PE-*b*-PMMA by mechanistic cross-over from coordination to addition polymerisation using a zirconocene catalyst.[99]

Although the ability to synthesise block copolymers in a controlled fashion in one pot is undoubtedly convenient, the requirement for specific, expensively-made late transition metal or lanthanide catalysts and the still-limited polar monomer range somewhat restricts the current scope of this technology.

1.4. Coordination polymerisation and living ionic polymerisation for synthesis of block copolymers

The synthesis of polyolefin-polar monomer block copolymers is often accomplished by the use of multiple distinct polymerisation mechanisms in order to circumvent the practical complications associated with the incompatibility of most single mechanisms with different types of monomers. One such strategy involves the combination of catalytic coordination polymerisation of an olefin *e.g.* ethylene or propylene followed by conversion of the polyolefin into a macroinitiator for the living ionic polymerisation of another monomer to produce a block copolymer.

Although the second polymerisation mechanism in this area is almost always anionic; in 1983 a number of PP-*b*-P(THF) diblock copolymers were synthesised by Doi using coordination polymerisation followed by living cationic polymerisation.[102] Synthesis of iodine-terminated polypropylene using a vanadium (acac) catalyst was followed by conversion to a macroinitiator for cationic polymerisation of THF by reaction with $AgClO_4$.

Chung and co-workers found that the use of various metallocene catalysts activated by MAO could be used to incorporate terminal *p*-MS units during ethylene or propylene polymerisation in the presence of hydrogen (*vide supra*). These *p*-MS end groups could then be metallated in the presence of *s*-BuLi and *N, N, N', N'*-tetramethylethylenediamine (TMEDA) to convert the polyolefin into a macroinitiator for the living anionic polymerisation of styrene yielding PE-*b*-PS and PP-*b*-PS diblock copolymers (Scheme 1.23).[92, 93] It was found by Chung that polyolefins containing vinylbenzene functionalities could be used to prepare graft copolymers with styrene in a similar fashion,[103] though the synthesis of block copolymers was not reported.

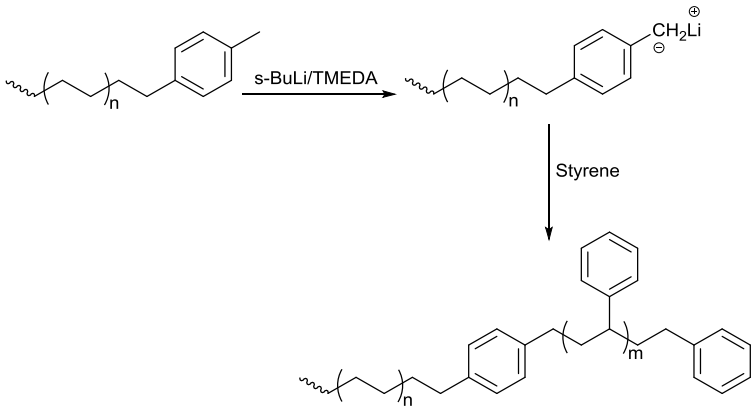

Scheme 1.23 - Synthesis of PE-*b*-PS from PE-*t*-PMS.[92]

The Chung group have also studied the synthesis and reactions of polyolefins containing 9-BBN end groups.[70] As well as being able to initiate free-radical polymerisation (*vide infra*), oxidation of the 9-BBN end groups followed by metalation converts the boranes into efficient initiators for the anionic polymerisation of ethylene oxide to yield block copolymers (Scheme 1.24). A similar process was also used for the synthesis of PE-*b*-P(ε-caprolactone) and PS-*b*-P(*ε*-caprolactone) block copolymers *via* anionic ring-opening polymerisation.[104]

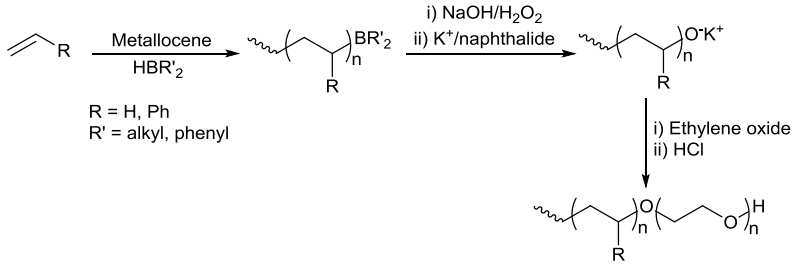

Scheme 1.24 - Synthesis of amphiphilic block copolymers from borane-terminated polyolefins.[70]

1.5. Coordination polymerisation and controlled radical polymerisation for synthesis of block copolymers

1.5.1. 9-Borobicyclononane oxidation

As well as being able to initiate anionic polymerisation from oxidised alkyl borane end groups, Chung and co-workers have demonstrated that exposure of a 9-BBN-terminated polyolefin to oxygen produces a borane peroxide that can either be reduced by another alkyl borane or cleaved homolytically to generate a stable 9-BBN-O• radical, along with alkyl and alkoxy radicals capable of initiating radical polymerisation of various polar monomers at ambient temperature.[105] The B-O• radical does not initiate polymerisation itself, but can react reversibly with the growing radical, resulting in an equilibrium

between active and dormant species. The group utilised the oxophilicity of alkyl boranes to develop two methods for the preparation of polyolefins bearing terminal 9-BBN functionalities, namely hydroboration of preformed unsaturated PE and PP and chain transfer to H-9-BBN compounds during catalytic olefin polymerisation (*vide supra*).[68, 69, 106] Following oxidation of the 9-BBN end group, the polyolefins could be used as initiators for the free radical polymerisation of methyl methacrylate to produce PE-*b*-PMMA and PP-*b*-PMMA block copolymers (Scheme 1.25).

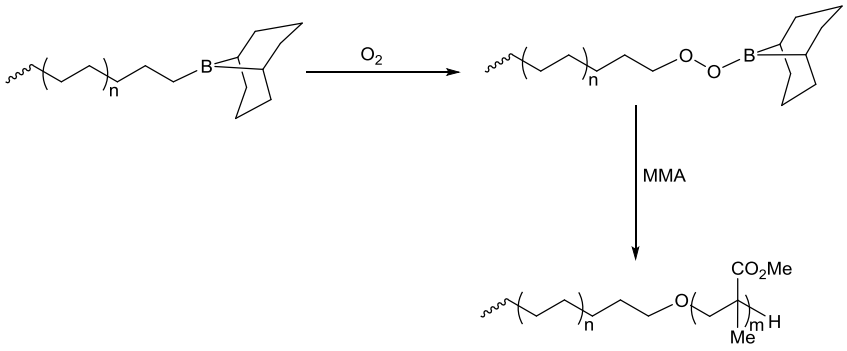

Scheme 1.25 - Oxidation of borane end group and subsequent radical polymerisation of MMA.[68, 69]

1.5.2. Nitroxide-mediated radical polymerisation (NMP)

The transformation of polyolefins into macroalkoxyamines for nitroxide-mediated graft polymerisation of various polar monomers has been fairly well-studied by various groups, but successful block copolymer synthesis by catalytic coordination polymerisation and NMP is much rarer in the literature. Hawker and Boisson have both reported the synthesis of TEMPO- and SG1-terminated PE from $Mg(PE)_2$ species (*vide supra*), though with fairly modest end group fidelities, and the high cleavage temperatures (180°C and 160°C) prevented conducting free radical polymerisation under mild conditions.[53, 54] The Boisson group subsequently went on to design nitroxides (DD1 and DD2) based on SG1 that were cleavable at lower temperatures and, though

the end group fidelities were low again, macroalkoxyamines based PE were produced and NMP of *n*-butyl acrylate was performed to yield a block copolymer in 3 steps (Scheme 1.26).[55]

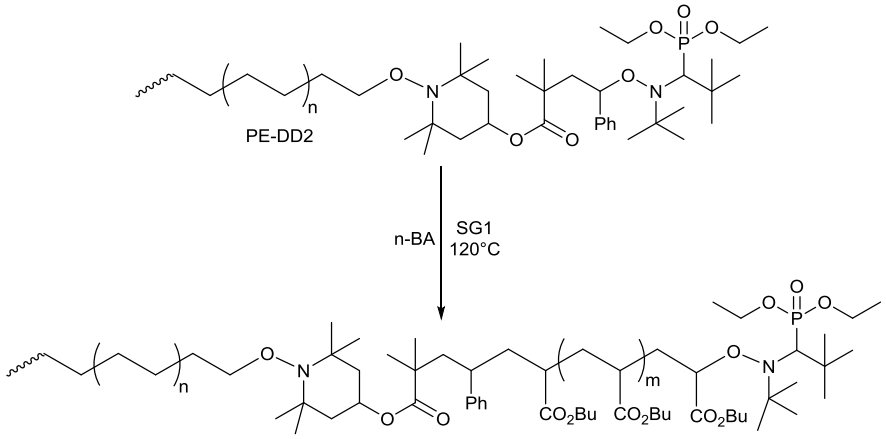

Scheme 1.26 - Synthesis of a block copolymer by NMP from a PE-macroalkoxyamine.

1.5.3. Atom transfer radical polymerisation (ATRP)

The conversion of functionalised polyolefins to macroinitiators for the subsequent ATRP of polar monomers is by far the most studied strategy to produce both polyolefin-polar block and graft copolymers. The main differences in the literature reports are to be found in the method for obtaining the polyolefin macroinitiator; while some authors modified terminal vinyl functionality to obtain macroinitiators, others utilised coordination chemistry to impart specific functionalities on polyolefins that could be converted to macroinitiators.

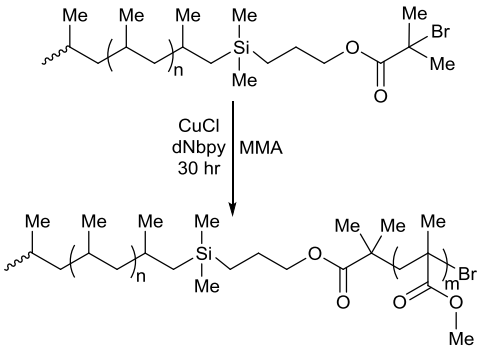

Scheme 1.27 - Synthesis of a block copolymer by ATRP of MMA in the presence of PP macroinitiator.[82]

Matyjaszewski and co-workers[82] described two methods for the synthesis of halogenated macroinitiators based on PP, involving the chemical transformation of terminal vinylidene groups synthesised using a dichloride [1,2-*bis*-(η5-9-fluorenyl)-1-(*R*)-phenylethane]zirconocene/MAO catalyst system. In the first strategy hydrosilylation followed by reduction with $LiAlH_4$ produces a terminal Si-H function which is then converted to a macroinitiator with >95% end group fidelity by reaction with 2-bromoisobutyrate. The second strategy also involved a hydrosilylation reaction but this time using the specially synthesised 1-(2-bromoisobutyryloxy)propyltetramethyldisiloxane in the presence of Karstedt's catalyst and 2-methyl-1,4-napthoquinone to yield a PP bearing a 2-bromoisobutyrate end group. PP ATRP macroinitiators made using the first strategy were then used in the synthesis of PP-*b*-PMMA and PP-*b*-P(*n*-BA) block copolymers of low dispersity and good conversion, though with long reaction times (Scheme 1.27).

A more straightforward synthesis was proposed for PE block copolymers by the same group (Scheme 1.28).[90] Vinyl-terminated PE produced using a phenoxyimine zirconium catalyst was reacted directly with 2-bromopropanoic acid in the presence of triflic acid

to yield a 75% functionalised PE ATRP macroinitiator. PE-*b*-PMMA, PE-*b*-P(*n*-BA) and PE-*b*-PS copolymers of low dispersity were then prepared.

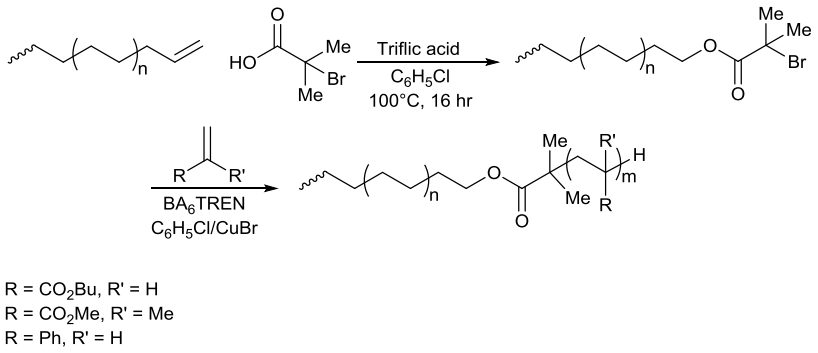

Scheme 1.28 - Direct synthesis of a PE-based macroinitiator and ATRP of MMA, n-BA and S.[90]

Matsugi and co-workers[107] described their preparation of vinyl-terminated PP from commercial PP by *via* pyrolysis and its subsequent conversion to an allylic bromide group by reaction with *N*-bromosuccinimide. They then used this Br-terminated PP to initiate the ATRP of styrene, MMA and *n*-BA respectively to yield block copolymers. The authors recently extended this technology substantially, reporting a range of different Br-terminated polyolefins and their subsequent use in ATRP of polar monomers including MMA, *t*-butyl acrylate, ethyl acrylate and styrene to yield a great variety of pololefin block copolymers.[108]

The use of catalytic coordination polymerisation to synthesise polyolefins with specific functions is an interesting alternative to modification of terminal vinyl groups, which often requires several reaction steps for the conversion and long polymerisation times for the second block synthesis. Hydroxy-terminated PE, produced from the metallocene-catalysed copolymerisation of ethylene and allyl alcohol in the presence of trialkyl aluminium CTA,[48] has been used to synthesise macroinitiators by reaction with α-bromoisobutyryl bromide in the presence of Et_3N for block copolymer synthesis by

ATRP of MMA (Scheme 1.29).[109] The effective compatibilisation of PE and PMMA homopolymers by the block copolymer was also reported.

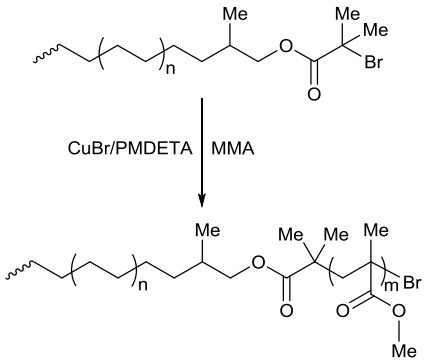

Scheme 1.29 - ATRP of MMA in the presence of a PE-Br macroinitiator to form a block copolymer.[48, 105]

Matyjaszewski and co-workers[40] reported ATRP of *n*- or *t*-butyl acrylate from a PE ATRP macroinitiator prepared by chain transfer to Zn (*vide supra*) to afford PE block copolymers with substantially faster polar monomer conversion than that achieved by modification of vinyl-terminated polyolefins.

Also noteworthy are macromonomers based on PE that have been copolymerised with acrylate monomers to yield PE chains bearing methacrylic end groups, achieved by Matyjaszewski and co-workers utilising Pd(II) α-diimine catalysts.[14] The functional PE was then able to copolymerise with *n*-BA under ATRP conditions. A novel functionalised palladium diimine catalyst containing a 2-bromoisobutyryl substituting group allowed Ye and co-workers[110] to directly synthesise 2-bromoisobutyryl-terminated PE (Scheme 1.30). The terminal groups could then be used to initiate ATRP of styrene or *n*-butyl acrylate to produce block copolymers in two steps, a significant achievement given the number of strategies described here that require more steps to achieve the same.

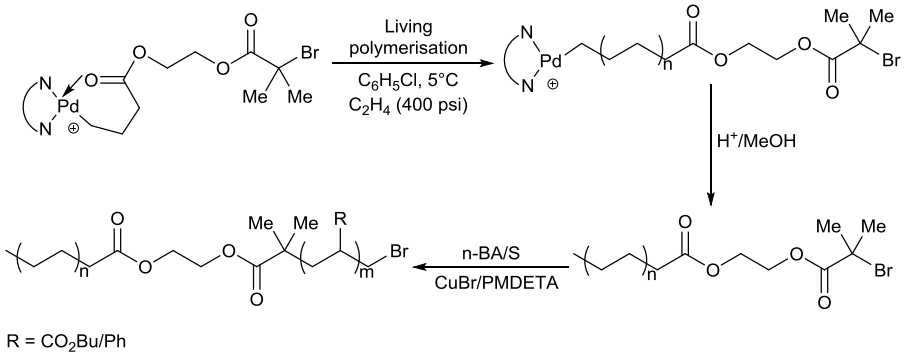

Scheme 1.30 - Tandem strategy for functionalised PE block copolymers.[106]

Other organometallic mediated methods include a very recent contribution from Yagci and co-workers[111] who demonstrated the use of $Mn_2(CO)_{10}$ for the thermally-induced controlled radical polymerisation of styrene and MMA to produce PE block copolymers of relatively low dispersity from iodo-terminated PE (Scheme 1.31). The PE macroinitiator was formed from catalysed chain growth on magnesium followed by reaction with iodine. The authors also report the synthesis of a triblock copolymer under the same conditions by polymerisation of styrene in the presence of the PE-*b*-PMMA-I species.

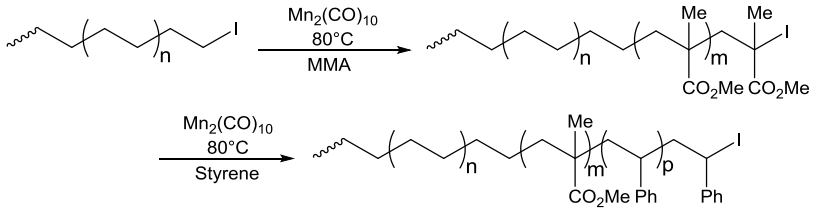

Scheme 1.31 - Synthesis of a diblock and a triblock copolymer by sequential thermally induced polymerisation with MMA and styrene.[107]

Detrembleur and co-workers[112] recently described the one-pot organometallic-mediated radical copolymerisation of ethylene with a variety of polar monomers where the transition metal complex reversibly traps the growing polymer chains. The authors

report the controlled synthesis of block-like copolymers where modification of the composition is possible by altering the ethylene feed pressure.

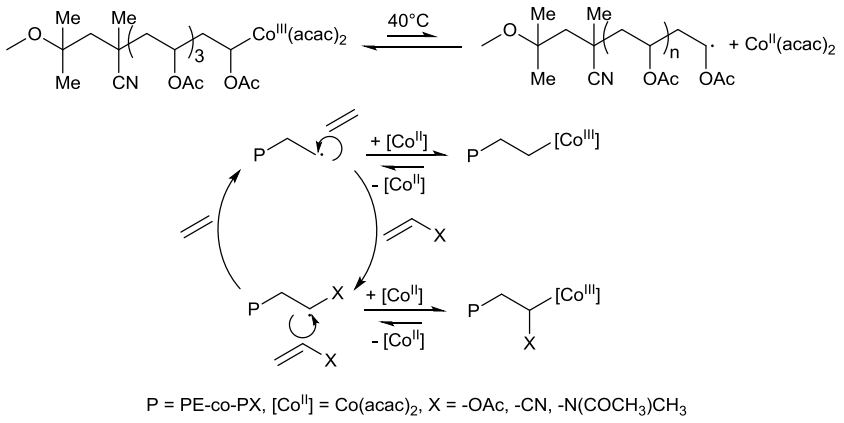

P = PE-co-PX, [Co^{II}] = Co(acac)$_2$, X = -OAc, -CN, -N(COCH$_3$)CH$_3$

Scheme 1.32 - Organometallic-mediated polymerisation of ethylene with polar monomers.[108]

1.5.4. Reversible addition-fragmentation chain transfer polymerisation (RAFT)

Polyolefin macro-RAFT agents are, like polyolefin macroalkoxyamines, scarce in literature. Kawahara and co-workers reported that a PE-PMMA polymer hybrid could be made by RAFT polymerisation. The PE macro-RAFT agent was prepared by sequential functionalisation of an ethylene copolymerisation with allyl alcohol, yielding a RAFT agent bearing a dithiobenzoate group.[113]

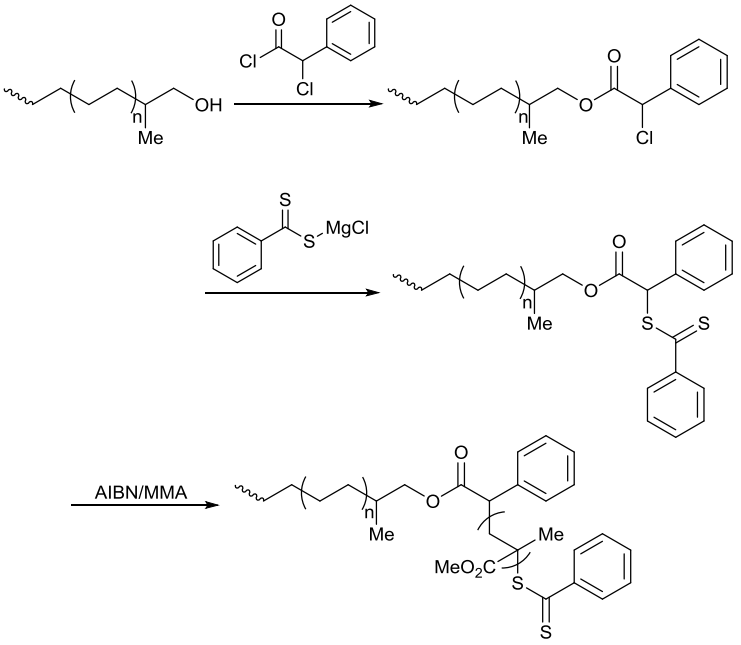

Scheme 1.33 - Synthesis of a PE macroRAFT agent from OH-terminated PE, followed by RAFT polymerisation of MMA.[109]

Boisson and co-workers reacted $Mg(PE)_2$ species with a number of thiocarbonylated compounds to yield dithiocarbonylate-terminated PE, which were suitable for use as mediators in RAFT polymerisation of *n*-butyl acrylate to provide a path to PE-based block copolymers (*vide supra*).[56] The same authors also described the conversion of $Mg(PE)_2$ to a macro-RAFT agent *via* conversion to PE-I, then to PE-N_3 and reduction to an amine. PE block copolymers were then prepared using the PE macro-RAFT agent to mediate the polymerisation of *n*-butyl acrylate.[23]

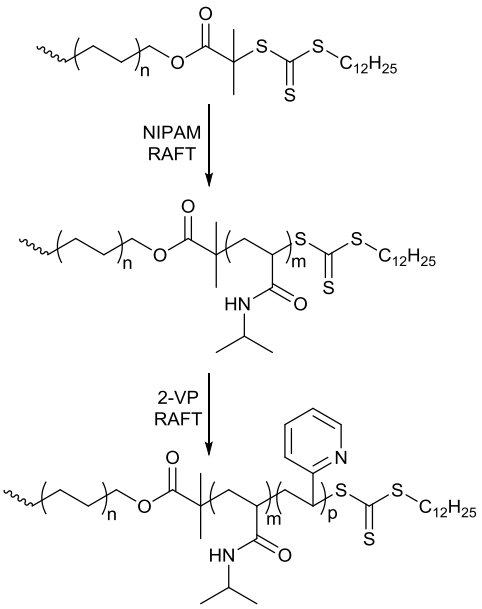

Scheme 1.34 - Use of a PE-based macroRAFT agent in the synthesis of PE-*b*-P(NIPAM) and PE-*b*-P(NIPAM)-*b*-P(2-VP) copolymers.[43]

Koning and co-workers[114] have studied the preparation of multiblock copolymers from multifunctional RAFT agents, a feat that would require many polymerisation steps using a conventional monofunctional RAFT agent. They reported the preparation of a poly(ethylene-*co*-butylene)-*b*-PBA-*b*-poly(ethylene-*co*-butylene) triblock copolymer in one step using a difunctional RAFT agent based on 'Kraton', a monohydroxyl end-capped poly(ethylene-*co*-butylene). More recently Zhu and co-workers described the production of thermo- and pH-responsive PE-based di- and triblock copolymers with NIPAM and 2-vinylpyridine by RAFT polymerisation mediated by a RAFT agent made from hydroxyl-terminated PE (Scheme 1.34).[43]

While it does not involve catalytic coordination polymerisation, it is nonetheless noteworthy that Monteil and co-workers have recently reported the first RAFT polymerisation of ethylene using xanthates as mediators.[115] They also report the copolymerisation of ethylene with small amounts of vinyl acetate mediated by xanthates

under far milder conditions (70°C, 200 bar) than those required for free-radical ethylene polymerisation.

1.6. Coordination polymerisation and ring opening polymerisation (ROP) for synthesis of block copolymers

Combining catalytic coordination polymerisation with ring-opening polymerisation provides a useful route to copolymers with novel and controlled structures that are generally considered inaccessible by more conventional techniques.[116] ROP can be accomplished thermally, ionically or by a transition metal catalyst and in order to achieve block and graft copolymers; synthesis of hydroxyl group-bearing polyolefins is overwhelmingly the preferred method.[6, 116]

The addition of hydroxyl functionalisation to polyolefin chains has been discussed in previous sections (*vide supra*) and generally involves *in situ* chain transfer to one of a number of species including organoboranes, alkyl aluminiums and alkyl zincs during catalytic olefin polymerisation, followed by oxidation. Chung and co-workers reported the synthesis of PE-*b*-PEO by anionic ROP of ethylene oxide following oxidation and metalation of a borane-functionalised PE synthesised in the presence of a 9-BBN CTA.[70] The resulting block copolymers contained between 40 and 80 mol% ethylene oxide. Using a similar approach, the same authors also synthesised a series of PO-*b*-P(ε-caprolactone) copolymers which found use as a polymeric compatibilisers.[104] Fujita and co-workers[79] reported the use of diol- and triol-terminated PE, prepared from vinyl-terminated PE (*vide supra*), as initiators for ROP of ethylene oxide to yield PE/polyethylene glycol hybrid materials.

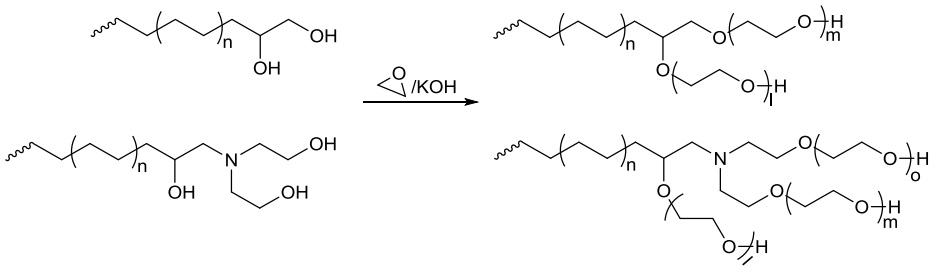

Scheme 1.35 - Synthesis of PE-PEG AB_2- and AB_3-type hybrid materials by ROP.[79]

Kim and co-workers described their synthesis of PE-*b*-P(*ε*-caprolactone) *via* catalytic ring-opening polymerisation in the presence of preformed OH-terminated PE using stannous octoate as the catalyst.[46] The OH-terminated PE in this case was prepared by sequential oxidation and hydrolysis of Al-terminated PE (*vide supra*). A similar approach was taken by Dubois and co-workers to prepare PE-*b*-P(lactide).[42] Zn-terminated PE, produced by chain transfer to diethyl zinc during metallocene-catalysed ethylene oligomerisation, was converted to OH-terminated PE by exposure to air and was then used as a macroinitiator for the ROP of lactide in the presence of stannous octoate (Scheme 1.36).

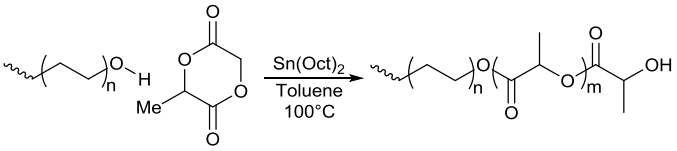

Scheme 1.36 - ROP of lactide initiated by PE-OH/$Sn(Oct)_2$.[42]

1.7. Sequential ring opening methathesis polymerisation (ROMP) and controlled radical polymerisation for synthesis of block copolymers

To this point, the strategies covered for the synthesis of polyolefin-polar monomer block copolymers have involved the use of catalytic coordination polymerisation followed by controlled radical or ionic polymerisation. Ring-opening metathesis polymerisation has

been utilised in certain examples to generate the olefinic first block before being used for the initiation of controlled radical polymerisations to produce the second block. ROMP has also been used to develop telechelic polymers which can be used for the synthesis of triblocks.[117, 118]

1.7.1. ROMP and ATRP

ATRP macroinitiators have been prepared from ROMP synthesised polyolefins. Coca and co-workers[119] described the production of ROMP synthesised poly(norbornene) using a tetrahedral imido/alkylidene metathesis catalyst Mo(CHCPhMe$_2$)(NAr)(O-*t*-Bu)$_2$, and its subsequent conversion to an ATRP macroinitiator by reaction with *p*-(bromomethyl)-benzaldehyde. The ATRP of styrene and methyl acrylate were then described to yield diblock copolymers. The same method has also been used to make block copolymers using poly(dicyclopentadiene) as the olefin block.

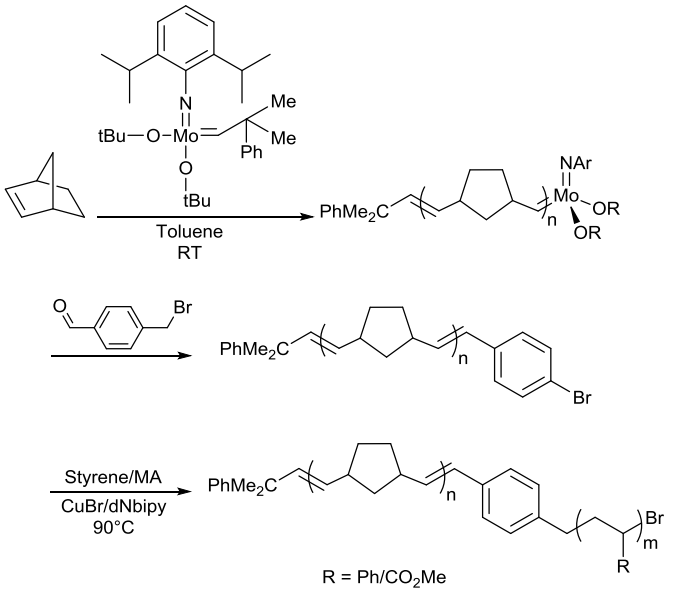

Scheme 1.37 - Successive living ROMP and ATRP to produce block copolymers.[115]

The use of a functional CTA during the ROMP of 1,5-dicyclooctadiene in the presence of a ruthenium catalyst allowed Bielawski and co-workers to obtain telechelic polybutadiene bearing chlorine or 2-bromopropionyl ester end groups; from which ATRP of styrene and MMA could be efficiently conducted to yield poly(styrene-*b*-butadiene-*b*-styrene) and poly(MMA-*b*-butadiene-*b*-MMA) triblock copolymers with good control over the radical polymerisation.

1.7.2. ROMP and RAFT

A ROMP produced polyolefin has also been converted into a macroRAFT agent through the synthesis of polybutadiene with dithiocarbonylate functions at both ends. Similar to the ATRP example mentioned above, Bates and co-workers[120] conducted the ROMP of 1,5-cyclooctadiene in the presence of another ruthenium catalyst and functional CTA. The double-end functionalised polymer could then be used to mediate the RAFT polymerisation of styrene and *t*-butyl acrylate respectively to produce triblock copolymers. The cross-metathesis of the triblock copolymers successfully cleaved the PS and P(*t*-BA) blocks so that they could be analysed and thus the control of the RAFT polymerisation could be demonstrated.

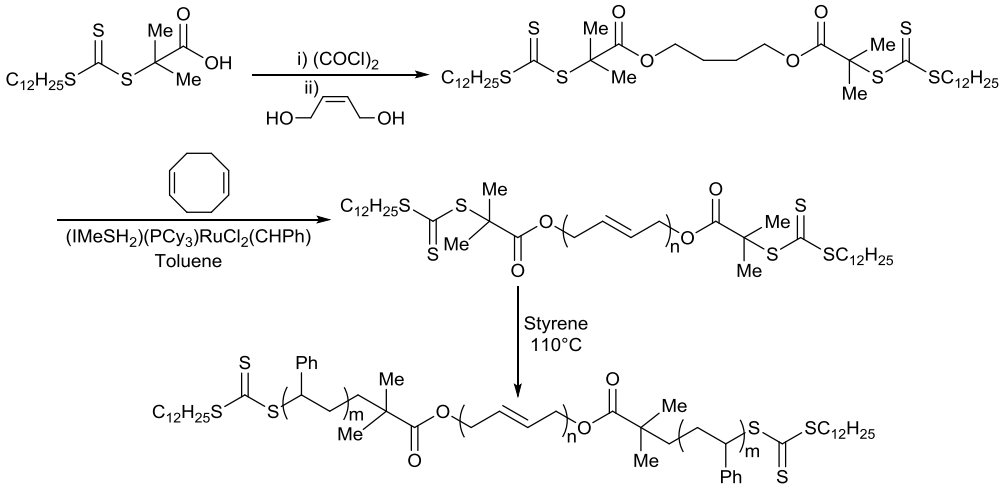

Scheme 1.38 - Tandem ROMP and RAFT strategy for triblock copolymer synthesis.[116]

1.8. Use of C1 polymerisation and alternative polar monomers in synthesis of block copolymers

Attempts thus far to obtain polar-functionalised polyolefins *via* direct catalytic coordination polymerisation with metal catalysts have met with limited success, mainly due to compatibility problems between the metal catalysts and the polar monomers (*vide supra*). The development of C1 polymerisation, or polyhomologation strategies,[121, 122] circumvents the incompatibility of polar monomers with most metal catalysts (though specific metal catalysts are required) by building up perfectly linear PE chains one carbon unit at a time with very narrow molecular weight distribution. These one-carbon monomers are able to directly impart polar functionality on the polymer chains and, especially in the case of carbene polymerisation, a wide range of polar groups can be incorporated by varying the substituents of the carbene precursors. In the vast majority of cases in literature this technique is used in the synthesis of random copolymers. However there are reports of block or block-like copolymers being prepared directly, or by using C1 polymerisation in combination with either controlled radical or living ionic polymerisation.

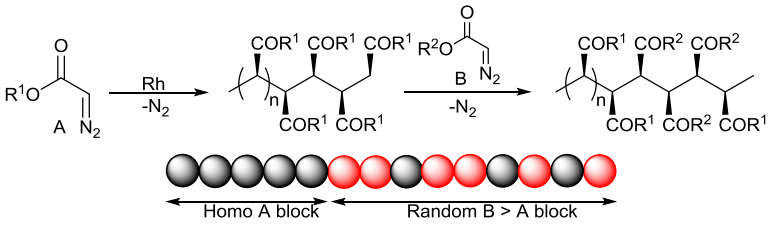

Scheme 1.39 - Rh-mediated carbene polymerisation for synthesis of [homo-A]-[random-B>A] block copolymers.[120]

De Bruin and co-workers have reported the stereoselective polymerisation of a variety of functionalised diazoester-based carbene precursors using rhodium(diene) catalysts,[123] which allowed the production of syndiotactic homo-, random and [homo-A]-[random-B>A]-type block copolymers (Scheme 1.39).[124] More recently, the same group also showed that functionalised and non-functionalised carbenes formed from either diazomethane or sulfoxonium ylides could be copolymerised using these rhodium catalysts, with the resulting copolymers exhibiting a blocky microstructure.[125, 126] The composition and, thus, also the functional group content could be tuned by varying the monomer feed ratio over a large range.

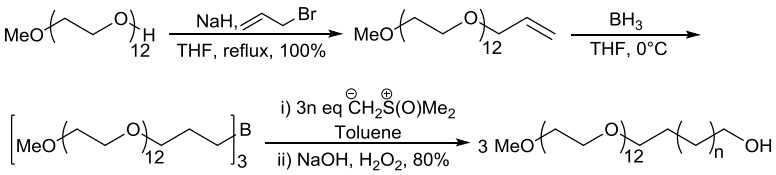

Scheme 1.40 - Synthesis of a poly(methylene-*b*-ethylene glycol) copolymer *via* hydroboration and polyhomologation.[123]

Shea and co-workers[127] reported the synthesis of poly(methylene-*b*-ethylene glycol) diblocks by conversion of commercially available methoxy-terminated poly(ethylene-glycol) to a trialkylborane initiator for the subsequent polyhomolgation of dimethylsulfoxonium methylide, leading to well-defined, low dispersity diblock

copolymers (Scheme 39). In the same publication, the group also report the first example of a poly(methylene-*b*-dimethylsiloxane-*b*-methylene) triblock from *α,ω*-divinylpoly(dimethylsiloxane) using a similar strategy. The authors then looked into the possibility of combining polyhomologation with NMP in a sequential living polymerisation (Scheme 1.40).[128] Starting from a specially prepared TEMPO PS initiator, which was hydrolysed to convert the benzoyloxy group to a hydroxyl group, TEMPO-mediated polymerisation of styrene was conducted to produce the hydroxyl-terminated PS. From there a similar hydroboration reaction to that described above followed by polyhomologation using dimethylsulfoxonium methylide yielded the block copolymer in a six step process.

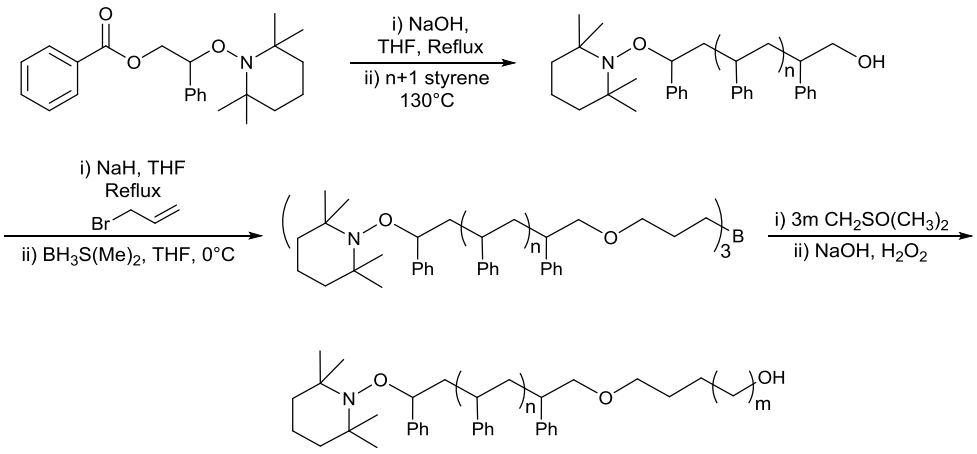

Scheme 1.41 - Synthesis of poly(methylene-*b*-styrene) *via* NMP and polyhomologation.[124]

Ma and co-workers[129] described the preparation of a hydroxyl-terminated poly(methylene) *via* polyhomologation of dimethylsufoxonium ylides and quantitative oxidation. An ATRP macroinitiator was then synthesised by transformation of the hydroxyl end group to an α-haloester. ATRP of *t*-butyl acrylate followed to afford poly(methylene-*b*-*t*-butyl acrylate) diblocks of controllable molecular weight and very narrow dispersities (Scheme 1.41). Hydrolysis of the ester groups yielded finally yielded

poly(methylene-*b*-acrylic acid) copolymers, whose self-assembly behaviour in water was studied. The same strategy was used by the same authors to produce a series of poly(methylene-*b*-styrene) diblocks from a poly(methylene)-based ATRP macroinitiators.[130] ATRP has also been used in this strategy to grow a styrene-*co*-2,3,4,5,6-pentafluorostyrene copolymer as a second block from a poly(methylene) macroinitiator.[131]

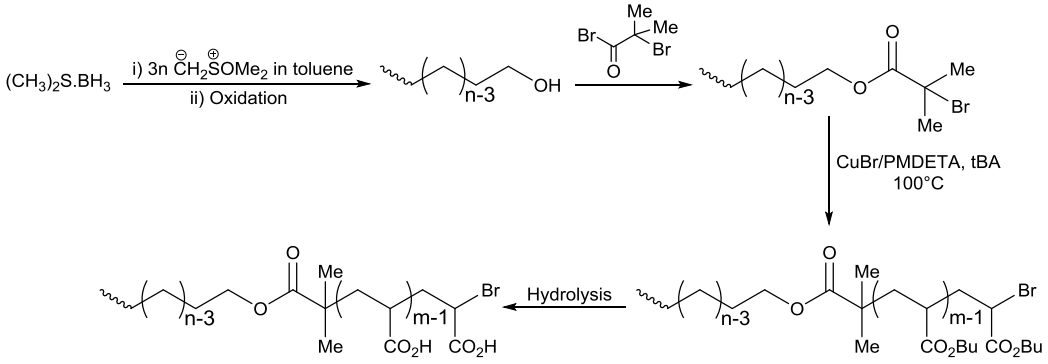

Scheme 1.42 - Synthesis of amphiphilic poly(methylene-*b*-acrylic acid) copolymers.[125]

The authors then progressed to combine polyhomologation first with ROP and then with ATRP to produce a poly(methylene-*b*-*ε*-caprolactone-*b*-*t*-butyl acrylate) triblock copolymer (Scheme 1.42).[132] OH-terminated poly(methylene) prepared as discussed above was used as a macroinitiator for catalytic ROP in the presence of stannous octoate and the resulting diblock copolymer was converted into an ATRP macroinitiator for the polymerisation of *t*-butyl acrylate. Finally hydrolysis of the acrylate ester groups converted the third block into poly(acrylic acid).

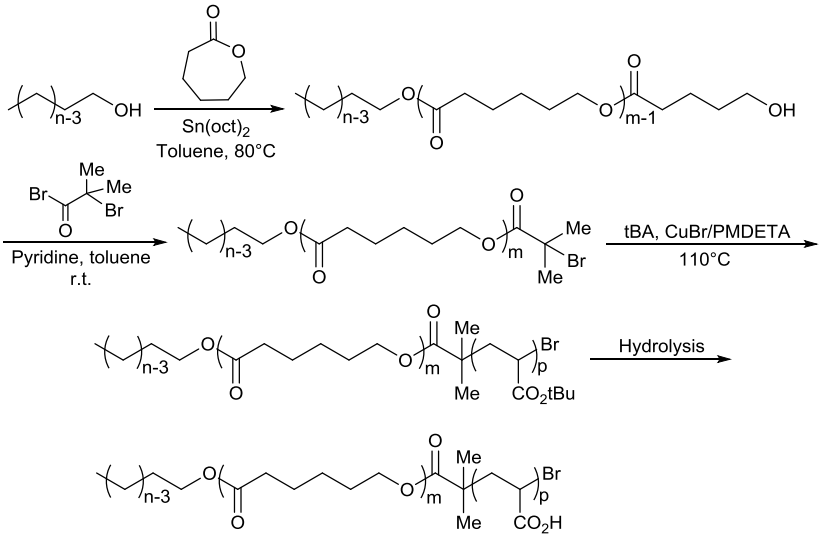

Scheme 1.43 - Synthesis of a poly(methylene-*b*-*ε*-caprolactone-*b*-acrylic acid) triblock.[128]

The tandem strategy of polyhomologation and controlled radical polymerisation has allowed a great deal of control over the synthesis of all components of both diblock and triblock copolymers; indeed often far better control than that achieved by tandem catalytic coordination and controlled radical polymerisation strategies (*vide supra*). These strategies often require cumbersome multi-step processes however and that is a significant disadvantage also shared by the combined coordination/radical polymerisation processes.

In the last three years Hadjichristidis and co-workers[133] described the one-pot combination of polyhomologation and living anionic polymerisation to produce PE block copolymers. The process involves the synthesis of living macroanions of poly(butadiene) or poly(styrene), from which the triakylborane macroinitiator is synthesised by reaction with BF_3OEt_2. The polyhomologation of dimethylsulfonium methylide was then carried out *in situ* to produce PBd-*b*-PE and PS-*b*-PE block copolymers. This method accounts for the incompatibility of ethylene with anionic

polymerisation as well as having the advantage of only requiring one pot to achieve the desired product.

The same group also reported a more familiar tandem strategy involving living cationic polymerisation followed by polyhomologation to yield hydroxyl-terminated poly(ethylene-*b*-isobutylene) diblock copolymers.[134] Allyl-terminated poly(isobutylene) (PIB-allyl) was prepared by living cationic polymerisation followed by *in situ* functionalisation with allyltrimethylsilane. Hydroboration of the PIB-allyl to form a trifunctional alkylborane initiator preceded the polyhomologation of dimethylsulfonium methylide to generate a 3-arm star polymer. The linear hydroxyl-terminated diblock copolymer was finally afforded by oxidation. The restricted compatible monomer range in ionic polymerisations is a limitation of these strategies but the terminal hydroxyl group imparted in this method creates the potential for further reaction.

1.9. Conclusions

The importance of the field of polyolefins and the incentive for the development of efficient, commercially-viable functionalisation strategies is very much reflected in the level of interest it has received in recent decades. The modification of polyolefins through the synthesis of block copolymers, just one of many strategies in a vast area of research, has seen the development of a large variety of continuously improving methods for the production of some truly remarkable materials. The various strategies described in this review have their own advantages and drawbacks and, while substantial progress has been made, it is clear that polyolefin-polar block copolymer synthesis remains a significant challenge.

The biggest obstacle remains the large intrinsic reactivity differences between unfunctionalised olefins and polar vinyl monomers, with no single polymerisation mechanism currently capable of handling substantial quantities of both types of monomer. Sequential monomer addition during a living olefin polymerisation process allows block copolymer synthesis of olefins and polar monomers, but only under strict conditions and in the presence of specific late transition metal or lanthanide catalysts that are more tolerant of polar functional groups. This strategy may prove more applicable in the future as catalyst technologies develop and this may also improve the currently limited range of compatible polar monomers.

The majority of reports of block copolymers containing olefins and polar monomers involve the synthesis of chain-end functionalised polyolefins, either by catalytic coordination polymerisation or ROMP, then conversion of the chain ends to specific functional groups to initiate a second polymerisation mechanism to generate the second block. The production of end-functionalised polyolefins of high end group fidelity has benefitted hugely from advances in chain transfer processes and reactive comonomers and they make excellent building blocks for block copolymers. The combination of distinct polymerisation mechanisms substantially increases the polymerisable monomer range and also means that more readily available catalysts can be used to generate the first block. The main drawback is the requirement for multi-step procedures, particularly in order to convert the terminal functional groups for controlled radical or anionic polymerisation. The use of anionic polymerisation for the growth of the second block also requires challenging reaction conditions and has a limited compatible monomer range. Similarly to living olefin polymerisation methods, future advances in the development of late transition metal catalysts may yet allow block copolymer synthesis using a coordination polymerisation mechanism. The recent reports of organometallic-

mediated radical polymerisation of ethylene and polar vinyl monomers is also encouraging.

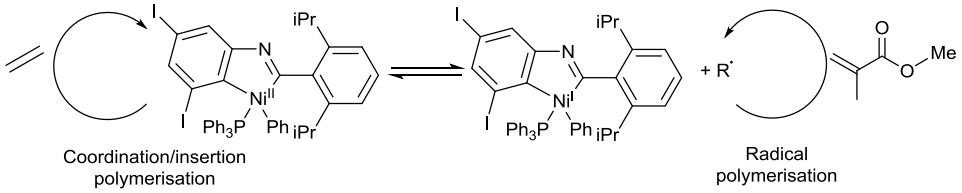

Scheme 1.44 - Reversible shuttling process between Ni^{II} and Ni^{I} species responsible for coordination/insertion ethylene polymerisation and controlled radical acrylate polymerisation respectively.[131, 132]

A recent alternative is ethylene-polar monomer block copolymer synthesis *via* a reversible shuttling process between catalytic insertion and radical polymerisation mechanisms at one metal centre, as proposed by Monteil and co-workers (Scheme 1.44),[135, 136] though the need for a specific Ni catalyst to mediate this shuttling process is a familiar limitation. Another alternative is the use of coupling reactions to link two preformed polymer segments together to produce block copolymers. The current scarcity of polyolefins containing terminal functional end groups suitable for coupling reactions means that this method is not often used for linking polyolefin and polar polymer segments; however the availability of coupling reactions that can be applied to polymers suggests that this method will grow in importance in the future.[137] Indeed the first example of such an approach for coupling PE and poly(acrylate) segments using hetero Diels-Alder chemistry has been described by D'Agosto and co-workers (Scheme 1.45).[138]

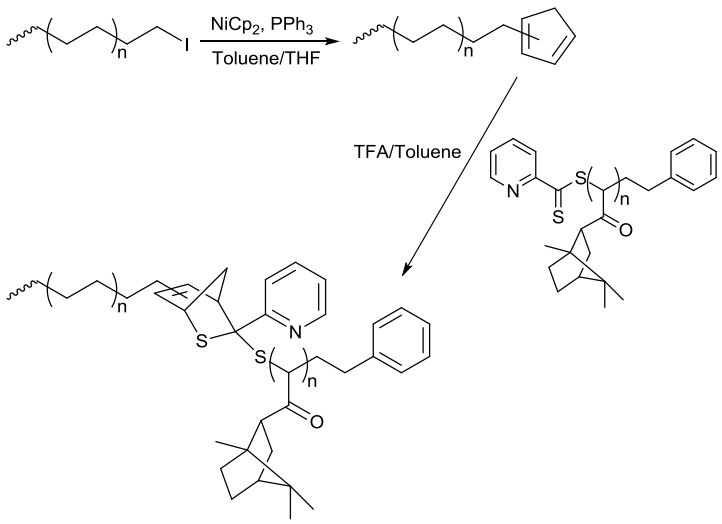

Scheme 1.45 - Formation of a block copolymer by coupling preformed non-polar and polar segments by a hetero Diels-Alder reaction.[138]

The polyhomologation of functionalised carbenes (C1 polymerisation) is also a promising emerging method with which to produce functionalised polyolefins and block copolymers. Copolymers can be formed either in a single transition metal-catalysed step to overcome some of the previously mentioned challenges, or in combination with another polymerisation mechanism. Though reports of block copolymer synthesis are currently scarce, the ability to produce tuneable molecular weight, highly stereoregular polymers with very low dispersities and access to a large range of functionalities will push development in this area.

1.10. References

1. Tabba, H. D.; Hijji, Y. M.; Abu-Surrah, A. S., Olefin Polymerization. In *Polyolefin Compounds and Materials: Fundamentals and Industrial Applications*, Al-Ali AlMa'adeed, M.; Krupa, I., Eds. Springer International Publishing: Cham, 2016; pp 51-77.
2. Godoy Lopez, R.; D'Agosto, F.; Boisson, C., Synthesis of well-defined polymer architectures by successive catalytic olefin polymerization and living/controlled polymerization reactions. *Prog. Polym. Sci.* **2007,** *32* (4), 419-454.
3. Kashiwa, N.; Matsugi, T.; Kojoh, S.-I.; Kaneko, H.; Kawahara, N.; Matsuo, S.; Nobori, T.; Imuta, J.-I., Functionalization of polyethylene based on metallocene catalysis and its application to syntheses of new graft copolymers possessing

polar polymer segments. *J. Polym. Sci. A: Polym. Chem.* **2003,** *41* (22), 3657-3666.
4. Chung, T. C., Synthesis of functional polyolefin copolymers with graft and block structures. *Prog. Polym. Sci.* **2002,** *27* (1), 39-85.
5. Boffa, L. S.; Novak, B. M., Copolymerization of Polar Monomers with Olefins Using Transition-Metal Complexes. *Chem. Rev.* **2000,** *100* (4), 1479-1494.
6. Zhao, Y.; Wang, L.; Xiao, A.; Yu, H., The synthesis of modified polyethylene via coordination polymerization followed by ATRP, RAFT, NMRP or ROP. *Prog. Polym. Sci.* **2010,** *35* (10), 1195-1216.
7. Boaen, N. K.; Hillmyer, M. A., Post-polymerization functionalization of polyolefins. *Chem. Soc. Rev.* **2005,** *34* (3), 267-275.
8. Chung, T. C.; Lu, H. L., Functionalization and block reactions of polyolefins using metallocene catalysts and borane reagents. *J. Mol. Catal. A: Chem.* **1997,** *115* (1), 115-127.
9. Franssen, N. M. G.; Reek, J. N. H.; de Bruin, B., Synthesis of functional 'polyolefins': state of the art and remaining challenges. *Chem. Soc. Rev.* **2013,** *42* (13), 5809-5832.
10. Dong, J.-Y.; Hu, Y., Design and synthesis of structurally well-defined functional polyolefins via transition metal-mediated olefin polymerization chemistry. *Coord. Chem. Rev.* **2006,** *250* (1–2), 47-65.
11. Yanjarappa, M. J.; Sivaram, S., Recent developments in the synthesis of functional poly(olefin)s. *Prog. Polym. Sci.* **2002,** *27* (7), 1347-1398.
12. Domski, G. J.; Rose, J. M.; Coates, G. W.; Bolig, A. D.; Brookhart, M., Living alkene polymerization: New methods for the precision synthesis of polyolefins. *Prog. Polym. Sci.* **2007,** *32* (1), 30-92.
13. Brookhart, M.; DeSimone, J. M.; Grant, B. E.; Tanner, M. J., Cobalt(III)-Catalyzed Living Polymerization of Ethylene: Routes to End-Capped Polyethylene with a Narrow Molar Mass Distribution. *Macromolecules* **1995,** *28* (15), 5378-5380.
14. Hong, S. C.; Jia, S.; Teodorescu, M.; Kowalewski, T.; Matyjaszewski, K.; Gottfried, A. C.; Brookhart, M., Polyolefin graft copolymers via living polymerization techniques: Preparation of poly(n-butyl acrylate)-graft-polyethylene through the combination of Pd-mediated living olefin polymerization and atom transfer radical polymerization. *J. Polym. Sci. A: Polym. Chem.* **2002,** *40* (16), 2736-2749.
15. Gottfried, A. C.; Brookhart, M., Living and block Copolymerization of Ethylene and α-Olefins using palladium(II)−α-diimine Catalysts. *Macromolecules* **2003,** *36* (9), 3085-3100.
16. Doi, Y.; Ueki, S.; Keii, T., "Living" Coordination Polymerization of Propene Initiated by the Soluble V(acac)3-Al(C2H5)2Cl System. *Macromolecules* **1979,** *12* (5), 814-819.
17. Doi, Y.; Ueki, S.; Keii, T., Preparation of “living” polypropylenes by a soluble vanadium-based Ziegler catalyst. *Makromol. Chem.* **1979,** *180* (5), 1359-1361.
18. Doi, Y.; Suzuki, S.; Soga, K., Living coordination polymerization of propene with a highly active vanadium-based catalyst. *Macromolecules* **1986,** *19* (12), 2896-2900.
19. Doi, Y.; Keii, T., Synthesis of “living” polyolefins with soluble Ziegler-Natta catalysts and application to block copolymerization. In *Chromatography/Foams/Copolymers*, Springer Berlin Heidelberg: Berlin, Heidelberg, 1986; pp 201-248.

20. Makio, H.; Fujita, T., Synthesis of Chain-End Functionalized Polyolefins with a Bis(phenoxy imine) Titanium Catalyst. *Macromol. Rapid Commun.* **2007,** *28* (6), 698-703.
21. Coates, G. W.; Hustad, P. D.; Reinartz, S., Catalysts for the Living Insertion Polymerization of Alkenes: Access to New Polyolefin Architectures Using Ziegler–Natta Chemistry. *Angew. Chem. Int. Ed.* **2002,** *41* (13), 2236-2257.
22. Mazzolini, J.; Espinosa, E.; D'Agosto, F.; Boisson, C., Catalyzed chain growth (CCG) on a main group metal: an efficient tool to functionalize polyethylene. *Polym. Chem.* **2010,** *1* (6), 793-800.
23. Briquel, R.; Mazzolini, J.; Le Bris, T.; Boyron, O.; Boisson, F.; Delolme, F.; D'Agosto, F.; Boisson, C.; Spitz, R., Polyethylene Building Blocks by Catalyzed Chain Growth and Efficient End Functionalization Strategies, Including Click Chemistry. *Angew. Chem. Int. Ed.* **2008,** *47* (48), 9311-9313.
24. Ziegler, K.; Holzkamp, E.; Breil, H.; Martin, H., Das Mülheimer Normaldruck-Polyäthylen-Verfahren. *Angew. Chem.* **1955,** *67* (19-20), 541-547.
25. Kempe, R., How to Polymerize Ethylene in a Highly Controlled Fashion? *Chem. Eur. J.* **2007,** *13* (10), 2764-2773.
26. Pelletier, J.-F.; Mortreux, A.; Olonde, X.; Bujadoux, K., Synthesis of New Dialkylmagnesium Compounds by Living Transfer Ethylene Oligo- and Polymerization with Lanthanocene Catalysts. *Angew. Chem. Int. Ed.* **1996,** *35* (16), 1854-1856.
27. Valente, A.; Mortreux, A.; Visseaux, M.; Zinck, P., Coordinative Chain Transfer Polymerization. *Chem. Rev.* **2013,** *113* (5), 3836-3857.
28. Ribeiro, R.; Ruivo, R.; Nsiri, H.; Norsic, S.; D'Agosto, F.; Perrin, L.; Boisson, C., Deciphering the mechanism of coordinative chain transfer polymerization of rthylene using neodymocene catalysts and dialkylmagnesium. *ACS Catal.* **2016,** *6* (2), 851-860.
29. Shiono, T.; Kurosawa, H.; Soga, K., Isospecific Polymerization of Propene over TiCl3 Combined with Bis(omega-alkenyl)zinc Compounds. *Macromolecules* **1995,** *28* (2), 437-443.
30. Kurosawa, H.; Shiono, T.; Soga, K., Synthesis of vinyl-terminated isotactic poly(propylene) using the coupling reaction between Zn-terminated polymer and allyl halides. *Macromol. Chem. Phys.* **1994,** *195* (4), 1381-1388.
31. Shiono, T.; Kurosawa, H.; Soga, K., Synthesis of carboxy- and chloro-terminated poly(propylene)s using Zn(C2H5)2 as chain transfer reagent. *Makromol. Chem.* **1992,** *193* (11), 2751-2761.
32. Burfield, D. R., The synthesis of low molecular weight hydroxy-tipped polyethylene and polypropylene by the intermediacy of Ziegler—Natta catalysts. *Polymer* **1984,** *25* (12), 1817-1822.
33. Shiono, T.; Kurosawa, H.; Soga, K., Synthesis of Isotactic Polypropylene Functionalized with a Primary Amino Group at the Initiation Chain End. *Macromolecules* **1994,** *27* (9), 2635-2637.
34. Zhang, C.; Niu, H.; Dong, J.-Y., Facile functionalization of isotactic polypropylene by azide and alkyne groups for click chemistry application. *Appl. Organomet. Chem.* **2011,** *25* (8), 632-637.
35. Britovsek, G. J. P.; Cohen, S. A.; Gibson, V. C.; van Meurs, M., Iron Catalyzed Polyethylene Chain Growth on Zinc: A Study of the Factors Delineating Chain Transfer versus Catalyzed Chain Growth in Zinc and Related Metal Alkyl Systems. *J. Am. Chem. Soc.* **2004,** *126* (34), 10701-10712.

36. Britovsek, G. J. P.; Cohen, S. A.; Gibson, V. C.; Maddox, P. J.; van Meurs, M., Iron-Catalyzed Polyethylene Chain Growth on Zinc: Linear α-Olefins with a Poisson Distribution. *Angew. Chem.* **2002,** *114* (3), 507-509.
37. van Meurs, M.; Britovsek, G. J. P.; Gibson, V. C.; Cohen, S. A., Polyethylene Chain Growth on Zinc Catalyzed by Olefin Polymerization Catalysts: A Comparative Investigation of Highly Active Catalyst Systems across the Transition Series. *J. Am. Chem. Soc.* **2005,** *127* (27), 9913-9923.
38. Arriola, D. J.; Carnahan, E. M.; Hustad, P. D.; Kuhlman, R. L.; Wenzel, T. T., Catalytic Production of Olefin Block Copolymers via Chain Shuttling Polymerization. *Science* **2006,** *312* (5774), 714-719.
39. Sita, L. R., Ex Uno Plures ("Out of One, Many"): New Paradigms for Expanding the Range of Polyolefins through Reversible Group Transfers. *Angew. Chem. Int. Ed.* **2009,** *48* (14), 2464-2472.
40. Kaneyoshi, H.; Inoue, Y.; Matyjaszewski, K., Synthesis of Block and Graft Copolymers with Linear Polyethylene Segments by Combination of Degenerative Transfer Coordination Polymerization and Atom Transfer Radical Polymerization. *Macromolecules* **2005,** *38* (13), 5425-5435.
41. Wang, W.; Liu, R.; Li, Z.; Meng, C.; Wu, Q.; Zhu, F., Synthesis and Self-Assembly of New Double-Crystalline Amphiphilic Polyethylene-block-Poly[oligo(ethylene glycol) Methyl Ether Methacrylate] Coil-Brush Diblock Copolymer. *Macromol. Chem. Phys.* **2010,** *211* (13), 1452-1459.
42. Ring, J. O.; Thomann, R.; Mülhaupt, R.; Raquez, J.-M.; Degée, P.; Dubois, P., Controlled Synthesis and Characterization of Poly[ethylene-block-(L,L-lactide)]s by Combining Catalytic Ethylene Oligomerization with "Coordination-Insertion" Ring-Opening Polymerization. *Macromol. Chem. Phys.* **2007,** *208* (8), 896-902.
43. Zhao, Y.; Shi, X.; Gao, H.; Zhang, L.; Zhu, F.; Wu, Q., Thermo- and pH-sensitive polyethylene-based diblock and triblock copolymers: synthesis and self-assembly in aqueous solution. *J. Mater. Chem.* **2012,** *22* (12), 5737-5745.
44. Byun, D.-J.; Shin, D.-K.; Kim, S. Y., Copolymerization of ethylene with allylbenzene using rac-ethylenebis(indenyl)zirconium dichloride/methylaluminoxane as a catalyst. *Macromol. Rapid Commun.* **1999,** *20* (8), 419-422.
45. Byun, D.-J.; Kim, S. Y., Selective Chain Transfer Reactions in Metallocene Catalyzed Copolymerization of Ethylene with Allylbenzene. *Macromolecules* **2000,** *33* (6), 1921-1923.
46. Han, C. J.; Lee, M. S.; Byun, D.-J.; Kim, S. Y., Synthesis of Hydroxy-Terminated Polyethylene via Controlled Chain Transfer Reaction and Poly(ethylene-*b*-caprolactone) Block Copolymer. *Macromolecules* **2002,** *35* (24), 8923-8925.
47. Saito, J.; Tohi, Y.; Matsukawa, N.; Mitani, M.; Fujita, T., Selective Synthesis of Al-Terminated Polyethylenes Using a Bis(Phenoxy-Imine)Zr Complex with Methylalumoxane. *Macromolecules* **2005,** *38* (12), 4955-4957.
48. Imuta, J.-i.; Kashiwa, N.; Toda, Y., Catalytic Regioselective Introduction of Allyl Alcohol into the Nonpolar Polyolefins: Development of One-Pot Synthesis of Hydroxyl-Capped Polyolefins Mediated by a New Metallocene IF Catalyst. *J. Am. Chem. Soc.* **2002,** *124* (7), 1176-1177.
49. Kretschmer, W. P.; Bauer, T.; Hessen, B.; Kempe, R., An efficient yttrium catalysed version of the "Aufbaureaktion" for the synthesis of terminal functionalised polyethylene. *Dalton Trans.* **2010,** *39* (29), 6847-6852.

50. Shiono, T.; Kang, K. K.; Hagihara, H.; Ikeda, T., Novelty of Vinylidene-Terminated Polypropylene Prepared by a MgCl2-Supported TiCl4 Catalyst Combined with AlEt3 as Cocatalyst. *Macromolecules* **1997,** *30* (20), 5997-6000.
51. Kang, K. K.; Shiono, T.; Ikeda, T., Synthesis of Aluminum-Terminated Polypropylene by a MgCl2-Supported TiCl4 Catalyst Combined with Al(i-Bu)3 as Cocatalyst. *Macromolecules* **1997,** *30* (4), 1231-1233.
52. Tsubaki, S.; Jin, J.; Sano, T.; Uozumi, T.; Soga, K., Synthesis of Terminally Functionalized Isotactic Poly(propylene) with a [ArN(CH2)3NAr]TiCl2 (Ar = 2,6-iPr2C6H3) – MAO Catalyst System. *Macromol. Chem. Phys.* **2001,** *202* (9), 1757-1760.
53. Lopez, R. G.; Boisson, C.; D'Agosto, F.; Spitz, R.; Boisson, F.; Bertin, D.; Tordo, P., Synthesis and Characterization of Macroalkoxyamines Based on Polyethylene. *Macromolecules* **2004,** *37* (10), 3540-3542.
54. Benoit, D.; Chaplinski, V.; Braslau, R.; Hawker, C. J., Development of a Universal Alkoxyamine for "Living" Free Radical Polymerizations. *J. Am. Chem. Soc.* **1999,** *121* (16), 3904-3920.
55. Godoy Lopez, R.; Boisson, C.; D'Agosto, F.; Spitz, R.; Boisson, F.; Gigmes, D.; Bertin, D., Catalyzed chain growth of polyethylene on magnesium for the synthesis of macroalkoxyamines: Application to the production of block copolymers using controlled radical polymerization. *J. Polym. Sci. A: Polym. Chem.* **2007,** *45* (13), 2705-2718.
56. Godoy Lopez, R.; Boisson, C.; D'Agosto, F.; Spitz, R.; Boisson, F.; Gigmes, D.; Bertin, D., New Functional Polyolefins: Towards a Bridge Between Catalytic and RAFT Polymerizations *Macromol. Rapid Commun.* **2006,** *27* (3), 173-181.
57. D'Agosto, F.; Boisson, C., A RAFT Analogue Olefin Polymerization Technique Using Coordination Chemistry. *Aust. J. Chem.* **2010,** *63* (8), 1155-1158.
58. Mazzolini, J.; Mokthari, I.; Briquel, R.; Boyron, O.; Delolme, F.; Monteil, V.; Bertin, D.; Gigmes, D.; D'Agosto, F.; Boisson, C., Thiol-End-Functionalized Polyethylenes. *Macromolecules* **2010,** *43* (18), 7495-7503.
59. Lefay, C.; Glé, D.; Rollet, M.; Mazzolini, J.; Bertin, D.; Viel, S.; Schmid, C.; Boisson, C.; D'Agosto, F.; Gigmes, D.; Barner-Kowollik, C., Block copolymers via macromercaptan initiated ring opening polymerization. *J. Polym. Sci. A: Polym. Chem.* **2011,** *49* (3), 803-813.
60. Mazzolini, J.; Boyron, O.; Monteil, V.; D'Agosto, F.; Boisson, C.; Sanders, G. C.; Heuts, J. P. A.; Duchateau, R.; Gigmes, D.; Bertin, D., Polyethylene end functionalization using thia-Michael addition chemistry. *Polym. Chem.* **2012,** *3* (9), 2383-2392.
61. Amin, S. B.; Marks, T. J., Versatile Pathways for In Situ Polyolefin Functionalization with Heteroatoms: Catalytic Chain Transfer. *Angew. Chem. Int. Ed.* **2008,** *47* (11), 2006-2025.
62. Koo, K.; Marks, T. J., Silanolytic Chain Transfer in Ziegler−Natta Catalysis. Organotitanium-Mediated Formation of New Silapolyolefins and Polyolefin Architectures. *J. Am. Chem. Soc.* **1998,** *120* (16), 4019-4020.
63. Koo, K.; Marks, T. J., Silicon-Modified Ziegler−Natta Polymerization. Catalytic Approaches to Silyl-Capped and Silyl-Linked Polyolefins Using "Single-Site" Cationic Ziegler−Natta Catalysts. *J. Am. Chem. Soc.* **1999,** *121* (38), 8791-8802.
64. Fu, P.-F.; Marks, T. J., Silanes as Chain Transfer Agents in Metallocene-Mediated Olefin Polymerization. Facile in Situ Catalytic Synthesis of Silyl-Terminated Polyolefins. *J. Am. Chem. Soc.* **1995,** *117* (43), 10747-10748.

65. Koo, K.; Fu, P.-F.; Marks, T. J., Organolanthanide-Mediated Silanolytic Chain Transfer Processes. Scope and Mechanism of Single Reactor Catalytic Routes to Silapolyolefins. *Macromolecules* **1999,** *32* (4), 981-988.
66. Amin, S. B.; Seo, S.; Marks, T. J., Organo-fn,d0-Mediated Synthesis of Amine-Capped Polyethylenes. Scope and Mechanism. *Organometallics* **2008,** *27* (11), 2411-2420.
67. Kawaoka, A. M.; Marks, T. J., Organolanthanide-Catalyzed Synthesis of Phosphine-Terminated Polyethylenes. Scope and Mechanism. *J. Am. Chem. Soc.* **2005,** *127* (17), 6311-6324.
68. Xu, G.; Chung, T. C., Borane Chain Transfer Agent in Metallocene-Mediated Olefin Polymerization. Synthesis of Borane-Terminated Polyethylene and Diblock Copolymers Containing Polyethylene and Polar Polymer. *J. Am. Chem. Soc.* **1999,** *121* (28), 6763-6764.
69. Chung, T. C.; Xu, G.; Lu, Y.; Hu, Y., Metallocene-Mediated Olefin Polymerization with B−H Chain Transfer Agents: Synthesis of Chain-End Functionalized Polyolefins and Diblock Copolymers. *Macromolecules* **2001,** *34* (23), 8040-8050.
70. Lu, Y.; Hu, Y.; Wang, Z. M.; Manias, E.; Chung, T. C., Synthesis of new amphiphilic diblock copolymers containing poly(ethylene oxide) and poly(α-olefin). *J. Polym. Sci. A: Polym. Chem.* **2002,** *40* (20), 3416-3425.
71. Lin, W.; Niu, H.; Chung, T. C. M.; Dong, J.-Y., Borane chain transfer reaction in olefin polymerization using trialkylboranes as chain transfer agents. *J. Polym. Sci. A: Polym. Chem.* **2010,** *48* (16), 3534-3541.
72. Gaynor, S. G., Vinyl Chloride as a Chain Transfer Agent in Olefin Polymerizations: Preparation of Highly Branched and End Functional Polyolefins. *Macromolecules* **2003,** *36* (13), 4692-4698.
73. Ishii, S.-i.; Mitani, M.; Saito, J.; Matsuura, S.; Kojoh, S.-i.; Kashiwa, N.; Fujita, T., Zirconium Complexes Having Phenoxy/Cycloalkylimine Chelate Ligands for the Polymerization of Ethylene for Vinyl-Terminated Low Molecular Weight Polyethylenes. *Chem. Lett.* **2002,** *31* (7), 740-741.
74. Ishii, S.-i.; Mitani, M.; Saito, J.; Matsuura, S.; Furuyama, R.; Fujita, T., 6 Ethylene polymerization behavior of polymethylene-bridged bis (phenoxy-imine) Zr complexes. In *Studies in Surface Science and Catalysis*, Masakazu Anpo, M. O.; Hiromi, Y., Eds. Elsevier: 2003; Vol. Volume 145, pp 49-54.
75. Terao, H.; Ishii, S.-i.; Saito, J.; Matsuura, S.; Mitani, M.; Nagai, N.; Tanaka, H.; Fujita, T., Phenoxycycloalkylimine Ligated Zirconium Complexes for Ethylene Polymerization: Formation of Vinyl-Terminated Low Molecular Weight Polyethylenes with High Efficiency. *Macromolecules* **2006,** *39* (25), 8584-8593.
76. Makio, H.; Terao, H.; Iwashita, A.; Fujita, T., FI Catalysts for Olefin Polymerization—A Comprehensive Treatment. *Chem. Rev.* **2011,** *111* (3), 2363-2449.
77. Matoishi, K.; Nakai, K.; Nagai, N.; Terao, H.; Fujita, T., Value-added olefin-based materials originating from FI catalysis: Production of vinyl- and Al-terminated PEs, end-functionalized PEs, and PE/polyethylene glycol hybrid materials. *Catal. Today* **2011,** *164* (1), 2-8.
78. Sesha Sainath, A. V.; Isokawa, M.; Suzuki, M.; Ishii, S.; Matsuura, S.; Nagai, N.; Fujita, T., Synthesis and Characteristics of Succinic Anhydride- and Disodium Succinate-Terminated Low Molecular Weight Polyethylenes. *Macromolecules* **2009,** *42* (13), 4356-4358.

79. Matoishi, K.; Nakatsuka, S.; Nakai, K.; Isokawa, M.; Nagai, N.; Fujita, T., Preparation and Characteristics of Well-defined Polyethylene/Poly(ethylene glycol) Hybrid Materials of Different Molecular Architectures. *Chem. Lett.* **2010,** *39* (10), 1028-1029.
80. Kuhn, P.; Sémeril, D.; Jeunesse, C.; Matt, D.; Neuburger, M.; Mota, A., Ethylene Oligomerisation and Polymerisation with Nickel Phosphanylenolates Bearing Electron-Withdrawing Substituents: Structure–Reactivity Relationships. *Chem. Eur. J.* **2006,** *12* (20), 5210-5219.
81. Sengupta, S. S.; Parent, J. S., Comparative analysis of radical-mediated polyethylene modifications: Vinyltriethoxysilane versus mercaptopropyltriethoxysilane addition. *Polym. Eng. Sci.* **2006,** *46* (4), 480-485.
82. Matyjaszewski, K.; Saget, J.; Pyun, J.; Schlögl, M.; Rieger, B., Synthesis of polypropylene-poly(methacrylate) block copolymers using metallocene catalysed processes and subsequent atom transfer radical polymerisation. *J. Macromol. Sci. A* **2002,** *39* (9), 901-913.
83. Kaneko, H.; Kojoh, S.-i.; Kawahara, N.; Matsuo, S.; Matsugi, T.; Kashiwa, N., Syntheses of graft and star copolymers possessing polyolefin branches by using polyolefin macromonomer. *J. Polym. Sci. A: Polym. Chem.* **2005,** *43* (21), 5103-5118.
84. Kaneyoshi, H.; Matyjaszewski, K., Synthesis of a linear polyethylene macromonomer and preparation of polystyrene-graft-polyethylene copolymers via grafting-through atom transfer radical polymerization. *J. Appl. Polym. Sci.* **2007,** *105* (1), 3-13.
85. Kaneko, H.; Kojoh, S.-i.; Kawahara, N.; Matsuo, S.; Matsugi, T.; Kashiwa, N., Polymacromonomers with polyolefin branches synthesized by free-radical homopolymerization of polyolefin macromonomer with a methacryloyl end group. *Macromol. Symp.* **2004,** *213* (1), 335-346.
86. Chung, T. C.; Rhubright, D., Functionalization of polypropylene by hydroboration. *J. Polym. Sci. A: Polym. Chem.* **1993,** *31* (11), 2759-2763.
87. Chung, T. C.; Lu, H. L.; Li, C. L., Synthesis and Functionalization of Unsaturated Polyethylene: Poly(ethylene-co-1,4-hexadiene). *Macromolecules* **1994,** *27* (26), 7533-7537.
88. Lu, B.; Chung, T. C., Maleic Anhydride Modified Polypropylene with Controllable Molecular Structure: New Synthetic Route via Borane-Terminated Polypropylene. *Macromolecules* **1998,** *31* (17), 5943-5946.
89. Lu, B.; Chung, T. C., New Maleic Anhydride Modified PP Copolymers with Block Structure: Synthesis and Application in PP/Polyamide Reactive Blends. *Macromolecules* **1999,** *32* (8), 2525-2533.
90. Inoue, Y.; Matyjaszewski, K., Preparation of polyethylene block copolymers by a combination of postmetallocene catalysis of ethylene polymerization and atom transfer radical polymerization. *J. Polym. Sci. A: Polym. Chem.* **2004,** *42* (3), 496-504.
91. Chung, T. C. M., *Functionalization of Polyolefins*. Elsevier Science: 2002.
92. Chung, T. C.; Dong, J. Y., A Novel Consecutive Chain Transfer Reaction to p-Methylstyrene and Hydrogen during Metallocene-Mediated Olefin Polymerization. *J. Am. Chem. Soc.* **2001,** *123* (21), 4871-4876.
93. Dong, J. Y.; Chung, T. C., Synthesis of Polyethylene Containing a Terminal p-Methylstyrene Group: Metallocene-Mediated Ethylene Polymerization with a Consecutive Chain Transfer Reaction to p-Methylstyrene and Hydrogen. *Macromolecules* **2002,** *35* (5), 1622-1631.

94. Kay, C. J. Polyethylene Block Copolymers. University of Warwick, PhD, 2014.
95. Yasuda, H.; Furo, M.; Yamamoto, H.; Nakamura, A.; Miyake, S.; Kibino, N., New approach to block copolymerizations of ethylene with alkyl methacrylates and lactones by unique catalysis with organolanthanide complexes. *Macromolecules* **1992,** *25* (19), 5115-5116.
96. Desurmont, G.; Li, Y.; Yasuda, H.; Maruo, T.; Kanehisa, N.; Kai, Y., Reaction Pathway for the Formation of Binuclear Samarocene Hydride from Monomeric Alkyl Samarocene Derivative and the Effective Catalysis of Samarocene Hydride for the Block Copolymerization of Ethylene with Polar Monomers. *Organometallics* **2000,** *19* (10), 1811-1813.
97. Desurmont, G.; Tanaka, M.; Li, Y.; Yasuda, H.; Tokimitsu, T.; Tone, S.; Yanagase, A., New approach to block copolymerization of ethylene with polar monomers by the unique catalytic function of organolanthanide complexes. *J. Polym. Sci. A: Polym. Chem.* **2000,** *38* (22), 4095-4109.
98. Desurmont, G.; Tokimitsu, T.; Yasuda, H., First Controlled Block Copolymerizations of Higher 1-Olefins with Polar Monomers Using Metallocene Type Single Component Lanthanide Initiators. *Macromolecules* **2000,** *33* (21), 7679-7681.
99. Frauenrath, H.; Balk, S.; Keul, H.; Höcker, H., First Synthesis of an AB Block Copolymer with Polyethylene and Poly(methyl methacrylate) Blocks Using a Zirconocene Catalyst. *Macromol. Rapid Commun.* **2001,** *22* (14), 1147-1151.
100. Ihara, E.; Morimoto, M.; Yasuda, H., Living Polymerizations and Copolymerizations of Alkyl Acrylates by the Unique Catalysis of Rare Earth Metal Complexes. *Macromolecules* **1995,** *28* (23), 7886-7892.
101. Yasuda, H.; Ihara, E., Rare earth metal initiated polymerizations of polar and nonpolar monomers to give high molecular weight polymers with extremely narrow molecular weight distribution. *Macromol. Chem. Phys.* **1995,** *196* (8), 2417-2441.
102. Doi, Y.; Watanabe, Y.; Ueki, S.; Soga, K., Synthesis of a propylene-tetrahydrofuran block copolymer via "living" coordination polymerization. *Makromol. Chem., Rapid Commun.* **1983,** *4* (8), 533-537.
103. Dong, J. Y.; Hong, H.; Chung, T. C.; Wang, H. C.; Datta, S., Synthesis of Linear Polyolefin Elastomers Containing Divinylbenzene Units and Applications in Cross-Linking, Functionalization, and Graft Reactions. *Macromolecules* **2003,** *36* (16), 6000-6009.
104. Lu, Y.; Hu, Y.; Chung, T. C. M., Syntheses of diblock copolymers polyolefin-b-poly(ε-caprolactone) and their applications as the polymeric compatilizer. *Polymer* **2005,** *46* (23), 10585-10591.
105. Chung, T. C.; Janvikul, W.; Lu, H. L., A Novel "Stable" Radical Initiator Based on the Oxidation Adducts of Alkyl-9-BBN. *J. Am. Chem. Soc.* **1996,** *118* (3), 705-706.
106. Chung, T. C.; Lu, H. L.; Janvikul, W., A novel synthesis of PP-b-PMMA copolymers via metallocene catalysis and borane chemistry. *Polymer* **1997,** *38* (6), 1495-1502.
107. Kaneko, H.; Saito, J.; Kawahara, N.; Matsuo, S.; Matsugi, T.; Kashiwa, N., Synthesis and characterization of polypropylene-based block copolymers possessing polar segments via controlled radical polymerization. *J. Polym. Sci. A: Polym. Chem.* **2009,** *47* (3), 812-823.
108. Sugimoto, R.; Kaneko, H.; Saito, J.; Kawahara, N.; Matsuo, S.; Matsugi, T., Controlled radical polymerization with polyolefin macroinitiator: a convenient

and versatile approach to polyolefin-based block and graft copolymers. *Polym. Bull.* **2014,** *71* (6), 1421-1431.
109. Matsugi, T.; Kojoh, S.-I.; Kawahara, N.; Matsuo, S.; Kaneko, H.; Kashiwa, N., Synthesis and morphology of polyethylene-block-poly(methyl methacrylate) through the combination of metallocene catalysis with living radical polymerization. *J. Polym. Sci. A: Polym. Chem.* **2003,** *41* (24), 3965-3973.
110. Zhang, K.; Ye, Z.; Subramanian, R., Synthesis of Block Copolymers of Ethylene with Styrene and n-Butyl Acrylate via a Tandem Strategy Combining Ethylene "Living" Polymerization Catalyzed by a Functionalized Pd−Diimine Catalyst with Atom Transfer Radical Polymerization. *Macromolecules* **2008,** *41* (3), 640-649.
111. Ciftci, M.; Norsic, S.; Boisson, C.; D'Agosto, F.; Yagci, Y., Synthesis of Block Copolymers Based on Polyethylene by Thermally Induced Controlled Radical Polymerization Using Mn2(CO)10. *Macromol. Chem. Phys.* **2015,** *216* (9), 958-963.
112. Kermagoret, A.; Debuigne, A.; Jérôme, C.; Detrembleur, C., Precision design of ethylene- and polar-monomer-based copolymers by organometallic-mediated radical polymerization. *Nat. Chem.* **2014,** *6* (3), 179-187.
113. Kawahara, N.; Kojoh, S.-i.; Matsuo, S.; Kaneko, H.; Matsugi, T.; Saito, J.; Kashiwa, N., Synthetic method of polyethylene-poly(methylmethacrylate) (PE-PMMA) polymer hybrid via reversible addition-fragmentation chain transfer (RAFT) polymerization with functionalized polyethylene. *Polym. Bull.* **2006,** *57* (6), 805-812.
114. Bussels, R.; Bergman-Göttgens, C.; Meuldijk, J.; Koning, C., Multiblock copolymers synthesized in aqueous dispersions using multifunctional RAFT agents. *Polymer* **2005,** *46* (19), 8546-8554.
115. Dommanget, C.; D'Agosto, F.; Monteil, V., Polymerization of Ethylene through Reversible Addition–Fragmentation Chain Transfer (RAFT). *Angew. Chem. Int. Ed.* **2014,** *53* (26), 6683-6686.
116. Cho, I., New ring-opening polymerizations for copolymers having controlled microstructures. *Prog. Polym. Sci.* **2000,** *25* (8), 1043-1087.
117. Chung, T. C.; Chasmawala, M., A new synthetic route to telechelic polymers. *Macromolecules* **1991,** *24* (12), 3718-3720.
118. Chung, T. C.; Chasmawala, M., Synthesis of telechelic 1,4-polybutadiene by metathesis reactions and borane monomers. *Macromolecules* **1992,** *25* (20), 5137-5144.
119. Coca, S.; Paik, H.-J.; Matyjaszewski, K., Block Copolymers by Transformation of Living Ring-Opening Metathesis Polymerization into Controlled/"Living" Atom Transfer Radical Polymerization. *Macromolecules* **1997,** *30* (21), 6513-6516.
120. Mahanthappa, M. K.; Bates, F. S.; Hillmyer, M. A., Synthesis of ABA Triblock Copolymers by a Tandem ROMP−RAFT Strategy. *Macromolecules* **2005,** *38* (19), 7890-7894.
121. Shea, K. J.; Walker, J. W.; Zhu, H.; Paz, M.; Greaves, J., Polyhomologation. A Living Polymethylene Synthesis. *J. Am. Chem. Soc.* **1997,** *119* (38), 9049-9050.
122. Shea, K. J.; Busch, B. B.; Paz, M. M., Polyhomologation: Synthesis of Novel Polymethylene Architectures by a Living Polymerization of Dimethylsulfoxonium Methylide. *Angew. Chem. Int. Ed.* **1998,** *37* (10), 1391-1393.

123. Hetterscheid, D. G. H.; Hendriksen, C.; Dzik, W. I.; Smits, J. M. M.; van Eck, E. R. H.; Rowan, A. E.; Busico, V.; Vacatello, M.; Van Axel Castelli, V.; Segre, A.; Jellema, E.; Bloemberg, T. G.; de Bruin, B., Rhodium-Mediated Stereoselective Polymerization of "Carbenes". *J. Am. Chem. Soc.* **2006,** *128* (30), 9746-9752.
124. Jellema, E.; Jongerius, A. L.; van Ekenstein, G. A.; Mookhoek, S. D.; Dingemans, T. J.; Reingruber, E. M.; Chojnacka, A.; Schoenmakers, P. J.; Sprenkels, R.; van Eck, E. R. H.; Reek, J. N. H.; de Bruin, B., Rhodium-Mediated Stereospecific Carbene Polymerization: From Homopolymers to Random and Block Copolymers. *Macromolecules* **2010,** *43* (21), 8892-8903.
125. Franssen, N. M. G.; Remerie, K.; Macko, T.; Reek, J. N. H.; de Bruin, B., Controlled Synthesis of Functional Copolymers with Blocky Architectures via Carbene Polymerization. *Macromolecules* **2012,** *45* (9), 3711-3721.
126. Suarez, A. I. O.; del Río, M. P.; Remerie, K.; Reek, J. N. H.; de Bruin, B., Rh-Mediated C1-Polymerization: Copolymers from Diazoesters and Sulfoxonium Ylides. *ACS Catal.* **2012,** *2* (9), 2046-2059.
127. Shea, K. J.; Staiger, C. L.; Lee, S. Y., Synthesis of Polymethylene Block Copolymers by the Polyhomologation of Organoboranes. *Macromolecules* **1999,** *32* (9), 3157-3158.
128. Zhou, X.-Z.; Shea, K. J., Synthesis of Poly(methylene-b-styrene) by Sequential Living Polymerization. *Macromolecules* **2001,** *34* (9), 3111-3114.
129. Lu, H.-C.; Xue, Y.; Zhao, Q.-L.; Huang, J.; Xu, S.-G.; Cao, S.-K.; Ma, Z., Well-defined amphiphilic polymethylene-b-poly(acrylic acid) diblock copolymers: New synthetic strategy and their self-assembly. *J. Polym. Sci. A: Polym. Chem.* **2012,** *50* (17), 3641-3647.
130. Chen, J.-Z.; Cui, K.; Zhang, S.-Y.; Xie, P.; Zhao, Q.-L.; Huang, J.; Shi, L.-P.; Li, G.-Y.; Ma, Z., New Strategy Targeting Well-Defined Polymethylene-block-Polystyrene Copolymers: The Combination of Living Polymerization of Ylides and Atom Transfer Radical Polymerization. *Macromol. Rapid Commun.* **2009,** *30* (7), 532-538.
131. Xue, Y.; Lu, H.-C.; Zhao, Q.-L.; Huang, J.; Xu, S.-G.; Cao, S.-K.; Ma, Z., Polymethylene-b-poly(styrene-co-2,3,4,5,6-pentafluoro styrene) copolymers: synthesis and fabrication of their porous films. *Polym. Chem.* **2013,** *4* (2), 307-312.
132. Yuan, C.; Lu, H.-C.; Li, Q.-Z.; Yang, S.; Zhao, Q.-L.; Huang, J.; Wei, L.-H.; Ma, Z., Synthesis of well-defined amphiphilic polymethylene-b-poly(ε-caprolactone)-b-poly(acrylic acid) triblock copolymer via a combination of polyhomologation, ring-opening polymerization, and atom transfer radical polymerization. *J. Polym. Sci. A: Polym. Chem.* **2012,** *50* (12), 2398-2405.
133. Zhang, H.; Alkayal, N.; Gnanou, Y.; Hadjichristidis, N., Anionic polymerization and polyhomologation: an ideal combination to synthesize polyethylene-based block copolymers. *Chem. Comm.* **2013,** *49* (79), 8952-8954.
134. Zhang, H.; Banerjee, S.; Faust, R.; Hadjichristidis, N., Living cationic polymerization and polyhomologation: an ideal combination to synthesize functionalized polyethylene-polyisobutylene block copolymers. *Polym. Chem.* **2016,** *7* (6), 1217-1220.
135. Leblanc, A.; Grau, E.; Broyer, J.-P.; Boisson, C.; Spitz, R.; Monteil, V., Homo- and Copolymerizations of (Meth)Acrylates with Olefins (Styrene, Ethylene) Using Neutral Nickel Complexes: A Dual Radical/Catalytic Pathway. *Macromolecules* **2011,** *44* (9), 3293-3301.

136. Leblanc, A.; Broyer, J.-P.; Boisson, C.; Spitz, R.; Monteil, V., Synthesis of copolymers of ethylene and (meth)acrylates or styrene by an original dual radical/catalytic mechanism. In *Pure Appl. Chem.*, 2012; Vol. 84, p 2113.
137. Kempe, K.; Krieg, A.; Becer, C. R.; Schubert, U. S., "Clicking" on/with polymers: a rapidly expanding field for the straightforward preparation of novel macromolecular architectures. *Chem. Soc. Rev.* **2012,** *41* (1), 176-191.
138. Espinosa, E.; Glassner, M.; Boisson, C.; Barner-Kowollik, C.; D'Agosto, F., Synthesis of Cyclopentadienyl Capped Polyethylene and Subsequent Block Copolymer Formation Via Hetero Diels-Alder (HDA) Chemistry. *Macromol. Rapid Commun.* **2011,** *32* (18), 1447-1453.

Chapter 2: Investigation of the Catalytic Hydride Insertion Polymerisation (CHIP) mechanism for the **S**ynthesis and characterisation of polyethylene macromonomers

2.1 Introduction

As discussed in section 1.2.4 (Chapter 1), Chung and co-workers showed that ethylene polymerisations in the presence of dihydrogen and styrenes yielded polyolefins containing terminal styrene units.[1, 2] This was proposed to proceed *via* the mechanism of Scheme 1.20. Scott and co-workers[3] reproduced this work successfully in these laboratories and, for example, using styrene as the comonomer under suitable conditions, very high levels of styrene end groups were reported with no detectable mid-chain insertions. When the comonomer concentration was increased beyond that used by Chung[2] however, the styrene end group fidelity was found to be >100%. This could only occur if some of the chains contained such units at both ends, an observation which required a new mechanism (Scheme 2.1).

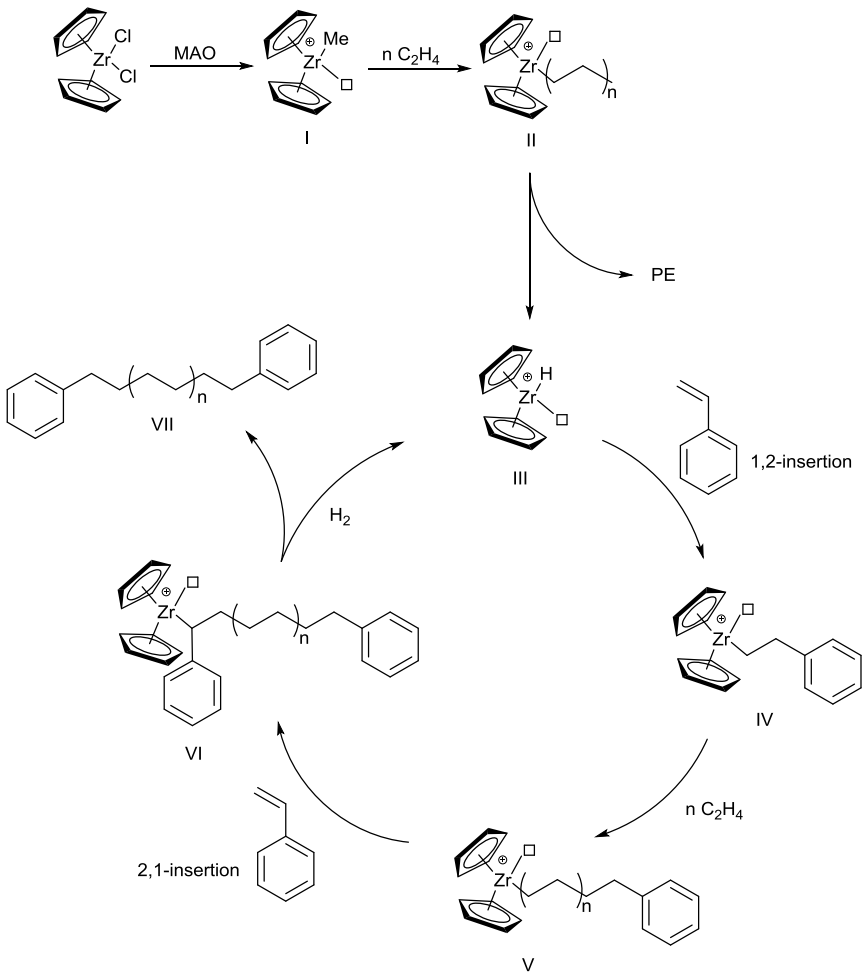

Scheme 2.1 - Proposed Catalytic Hydride Insertion Polymerisation (CHIP) mechanism forming PE double end-capped with styrene.[3]

The proposed catalytic hydride insertion polymerisation (CHIP)[3] mechanism required the rate of 1,2-insertion of styrene to compete favourably with ethylene insertion into a cationic zirconium hydride **III** at high concentrations, an observation that was also reported by Oliva and co-workers,[4] resulting in the formation of a zirconium alkyl species **IV**. Ethylene would then as expected outcompete styrene for insertion into the zirconium alkyl intermediate to form a polymeric intermediate **V**. From this point a 2,1-insertion of styrene into a zirconium-carbon bond would lead to species **VI**, analogous to that described by Chung, before hydrogenation generates the double end-capped polymer chain **VII** and reforms the zirconium hydride.

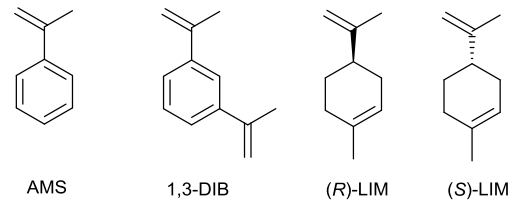

Figure 2.1 - AMS and related olefins.

It was recognised that, in contrast to styrene, α-methylstyrene (AMS, Figure 2.1) is not copolymerised with ethylene under metallocene catalysis. This is a result of the reluctance of this bulkier monomer to insert into metal-carbon bonds.[5, 6] Nevertheless, AMS would be expected to undergo insertion into zirconium hydrides (*vide infra*). Subsequently, the group went on to show that PE *initiated* with an AMS unit *i.e.* PE-*i*-AMS (Figure 2.2) could be prepared by polymerisation of ethylene in the presence of AMS and dihydrogen. The mechanism proposed is shown in Scheme 2.2.[3]

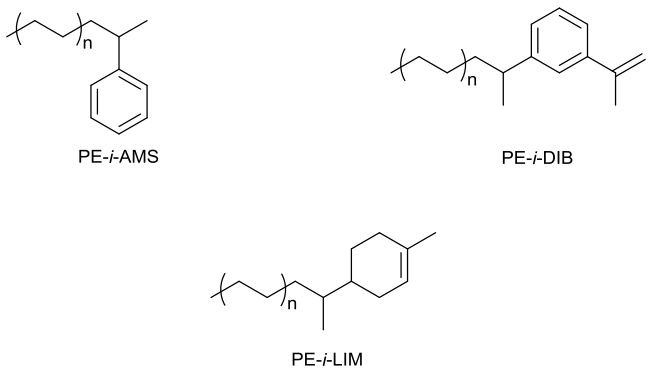

Figure 2.2 - End-functionalised PE copolymers made using CHIP.

The cation **I** is expected to undergo ethylene insertion to give **II**, and indeed some PE was detected in most reactions. Nevertheless, hydride **III** formed by hydrogenation of any alkyl species such as **I** or **II** may insert either ethylene or AMS. The conditions of the reaction *i.e.* a fairly high concentration of comonomer favours the latter. Further, a selective 1,2-insertion of AMS into the zirconium hydride **III** is expected on the basis of work by Chirik and Bercaw;[7] in addition to steric effects, the cationic nature of **III**

leads to build-up of positive charge at the benzylic centre in **IV**, and the transition state is thus stabilised by the presence of the arene.

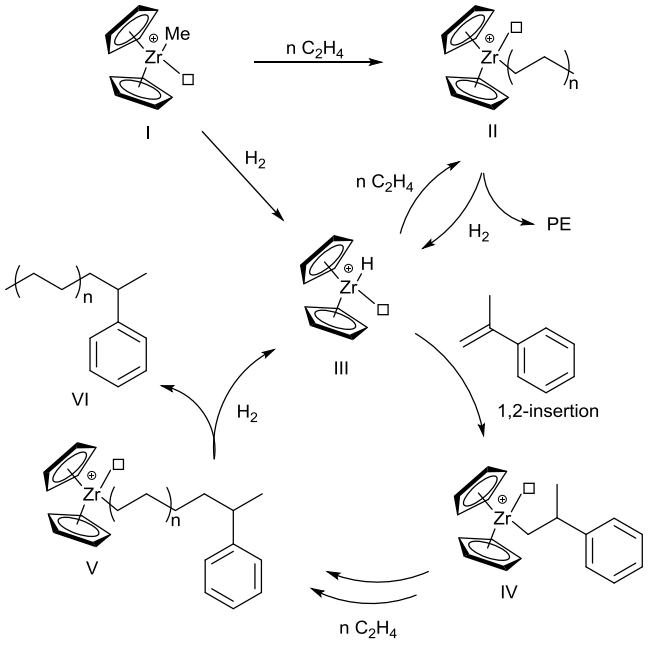

Scheme 2.2 - Proposed CHIP mechanism for the formation of PE-*i*-AMS.[3]

Ethylene insertion into the primary alkyl **IV** evidently outcompetes hydrogenation under these conditions to yield **V**. AMS insertion into the zirconium carbon bond is not expected (*vide supra*). Eventually termination by hydrogenation of **V** would result in the regeneration of **III** and form the final product PE *initiated* by AMS.

In extension of this work, 1,3-diisopropenylbenzene (DIB) was successfully used to form PE-*i*-DIB (Figure 2.2) and in further preliminary work, limonene (LIM) was also incorporated to yield PE-*i*-LIM (Figure 2.2) although the end group fidelity in this case peaked at *ca* 50%.

This chapter is divided into two main parts. The first aims to demonstrate the utilisation of the CHIP mechanism to produce PE-*i*-DIB of varying molecular weights – in particular low molecular weights – which it was hoped would give more soluble products, and also to improve the end-group fidelity of the PE-*i*-LIM materials. The second part aims to further develop the range of end-functionalised PE materials by introducing further non-styrenic comonomers, 5-vinyl-2-norbornene and 5-ethylidene-2-norbornene (Figure 2.3).

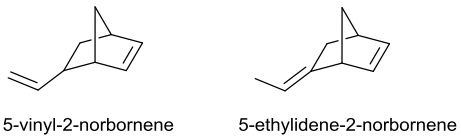

Figure 2.3 - Non-aromatic bicylic comonomers used in this chapter.

2.2 Use of CHIP mechanism to vary molecular weight of PE-*i*-DIB

A series of polymerisations of ethylene were conducted in the presence of various concentrations of dihydrogen and DIB comonomer (Table 2.1). Runs 1 and 2 show the effect of an increase in dihydrogen partial pressure on ethylene homopolymerisation, which resulted in higher productivity, lower molecular weight (with accompanying fall in melting temperature T_m) and lower dispersity.[8] The addition of DIB to an ethylene homopolymerisation in the absence of dihydrogen (Run 3) had little impact on the molecular weight of the product and no styrenic end groups were detected. When hydrogen was present however, a high proportion of chains were end-functionalised with DIB (Run 5) as previously reported.[3] Increasing the DIB concentration in the presence of dihydrogen (Runs 4 and 5) resulted in similar molecular weights but higher end group fidelities, consistent with a greater proportion of DIB insertions into the zirconium hydride species **III** (Scheme 2.2). The higher DIB concentration was also

found to have a detrimental effect on productivity. Runs 5 and 6 show that increasing the dihydrogen partial pressure whilst keeping the ethylene partial pressure constant in a copolymerisation with DIB caused a reduction in molecular weight while retaining end group fidelity. This is consistent with the proposed mechanism as we expect a higher rate of hydrogenolysis *versus* propagation, but for the initiation step to be unaffected. The observed increase in productivity is also expected.[8]

Table 2.1 - Ethylene copolymerisations with 1,3-DIB in the presence of dihydrogen.

Run[a]	**H_2 (psi)**	**[DIB] mol/L**	**M_p (g/mol)**[c]	**M_n (g/mol)**[c]	**M_w (g/mol)**[c]	**Đ**[c]	**Yield (g)**	**Productivity**[d]	**Incorporation (mol%)**	**End Groups (%)**[e]	**T_m (°C)**
1	0	0	80400	31500	172000	5.5	2.2	2700	n/a	n/a	135
2	20	0	4100	2300	5000	2.3	7.2	8600	n/a	n/a	122
3	0	2	76400	16200	82900	5.1	2.2	2700	0	0	135
4	20	0.5	4300	2700	5900	2.2	12.5	14900	1.7	76	122
5	20	2	6200	3800	8000	2.1	6.0	7100	2.0	88	125
6	60	2	3200	2400	4600	1.9	9.2	11000	2.3	90	121
7[b]	30	2	5600	3200	6200	2.0	13.5	16200	1.5	78	124
8[b]	60	2	3500	2500	5100	2.0	13.7	16400	2.1	87	121
9[b]	90	2	3000	2100	4000	2.0	11.9	14200	2.3	94	120

[a] Reaction conditions: Cp_2ZrCl_2 = 2.5x10^{-6} mol; MAO 1800 equivalents; solvent = toluene; reaction volume = 90 ml; ethylene partial pressure = 30 psi; reaction time = 20 min; reaction temperature = 60°C.
[b] Ethylene delivery pressure = 100 psig.
[c] GPC data obtained at 160°C in 1,2,4-trichlorobenzene using universal calibration. PS standards were used to calibrate the system (see Chapter 6, Section 6.1 for further details).
[d] (kg polymer/(mol[Zr].h))
[e] percentage of chains bearing single comonomer unit at one end.

The results thus far complement the work conducted previously in the group and are consistent with the proposed CHIP mechanism.[3, 7, 9] Runs 7-9 show that increasing the dihydrogen partial pressure (and, since the system pressure is also fixed at 100 psig, decreasing the ethylene partial pressure) also caused a reduction in molecular weight, culminating in Run 9 which produced the lowest molecular weight material to date. The increase in the hydrogen:ethylene ratio also led to higher end group fidelity as a result

of reduced competition from ethylene for insertion into the zirconium hydride. Most pleasingly, the productivity was maintained even at such low partial pressure of ethylene – probably < 1 atm.

The ^{1}H NMR spectrum shown in Figure 2.4 of the PE-*i*-DIB product from Run 9 is typical of the products recovered. As before,[3] the styrenic end group fidelity of the product was determined using the ratio of integrals for the peaks in the spectrum corresponding to the benzylic methine proton and the methyl end group environments (X and Y, Figure 2.5). The peak assigned to the PE methyl end group (Y) appears at 0.92 ppm (Figure 2.4) and the peak assigned to the benzylic methine proton (X) is found at 2.70 ppm. The integrals of these signals are used in equation (1).

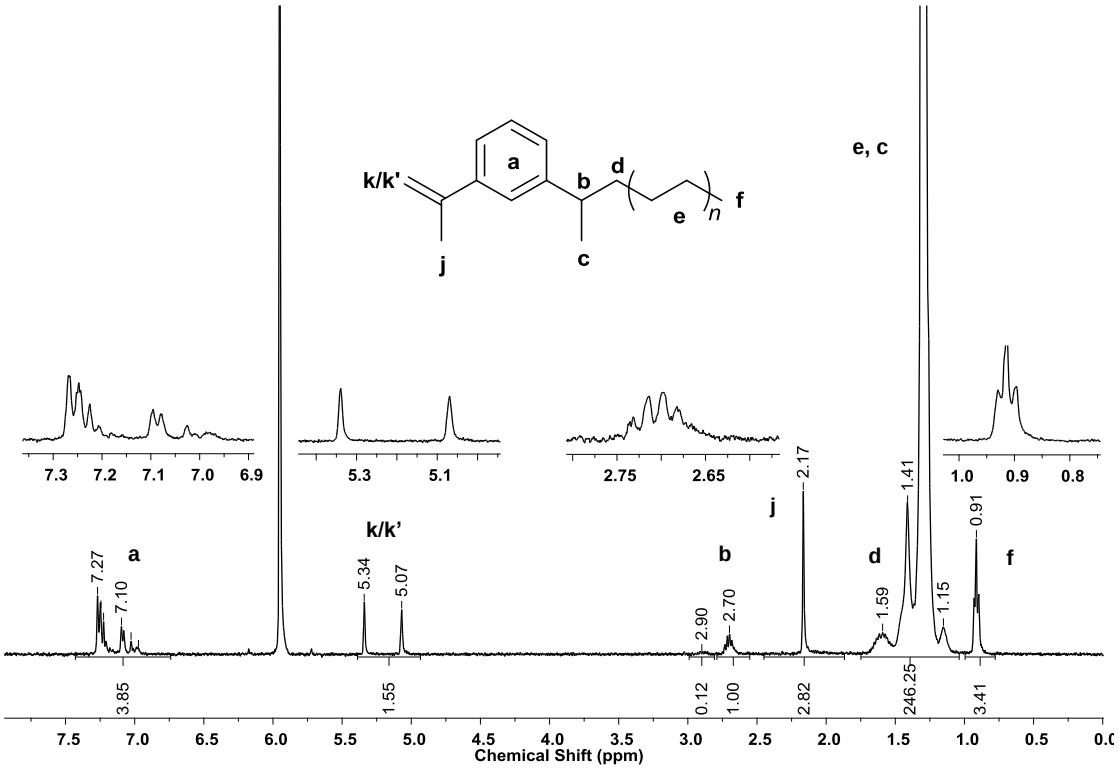

Figure 2.4 - ^{1}H NMR spectrum of the product from Run 9 in d^{2}-TCE at 100°C (400 MHz) Relaxation delay = 1 s. The top of the peak at 1.30 ppm corresponding to the PE main chain methylene protons has been omitted for clarity.

$$(1)\ \frac{X}{X+(Y/3)} \times 200$$

As an example, when the relevant integral values taken from Figure 2.6 are used in equation (1), a value of 94% is yielded for the number of PE chains containing a DIB unit at one end. One apparent advantage of reducing the molecular weight of the PE chains is that end group fidelity may be more accurately estimated. In these samples there is less overlap of the methyl end group signal at 0.92 ppm with the broad PE backbone methylene signal at 1.30 ppm. The more significant overlap between the two signals in the higher molecular weight samples tends to increase the integral of the methyl signal leading to an underestimation of end group fidelity.

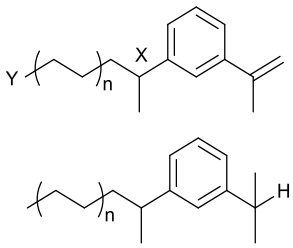

Figure 2.5 – (Above) PE-*i*-DIB. (Below) PE bearing the 3-isopropylphenyl end group.

We also note that signals corresponding to another aryl end group are detectable in the ^{1}H NMR spectra of the recovered products. This was observed previously and was assigned as a 3-isopropylphenyl end group appearing at one end of the polymer chain, presumably a result of hydrogenation of the 2-propenyl groups. NMR analysis of the DIB monomer recovered from the polymerisations showed no isopropyl groups, and previous attempts to hydrogenate DIB monomer under the polymerisation conditions yielded no reaction.[3] The proportion of these end groups present in the products was determined by integration of the peak at 2.90 ppm relative to the DIB methine signal as discussed above.

This highly end-functionalised, low molecular weight PE formed with high productivity is used as a macromonomer in Chapters 3 and 4. In Chapter 5, it is shown to be advantageous in the production of relatively soluble materials for the intended applications.

2.3 Attempts to improve end group fidelity of PE-*i*-LIM

Since the CHIP mechanism does not require the formation of a dormant state to selectively incorporate a comonomer (*vide supra*); it follows that potential comonomers do not necessarily need to contain an aromatic ring so as to be selectively incorporated at the beginning of a polymer chain. The commercial availability of large quantities of limonene from sustainable sources, and the potential for post-polymerisation reactions from the chain end prompted our group to investigate its incorporation as an example of a non-styrenic comonomer.[3] To the best of our knowledge, the work of Shiono *et al*[10] remains the only other report to date on metal-catalysed copolymerisation of ethylene with limonene; low productivities and low incorporations were reported.

Both isomers of limonene were previously investigated by our group and both were successfully incorporated at the beginning of the PE chain, but the end group fidelity was found to reach a maximum of *ca* 50%. At the time it was speculated that the lower incorporations may be because the arene generates greater electrophilicity to accelerate insertion into the metal hydride (**III**, Scheme 2.2) and stabilises the positive charge that develops during insertion (*vide supra*). However we hypothesised that in the presence of higher dihydrogen partial pressure, *i.e.* under the same conditions as run 9 for the PE-*i*-DIB synthesis, there would be less competition from ethylene for insertion into the metal hydride. This would be expected to lead to a higher rate of limonene insertion and therefore higher end group fidelities.

Table 2.2 - Ethylene copolymerisations with (*R*)- and (*S*)-limonene in the presence of dihydrogen.

Run[a]	H_2 (psi)	[Comon.] mol/L	M_p (g/mol)[d]	M_n (g/mol)[d]	M_w (g/mol)[d]	Đ [d]	Yield (g)	Productivity[e]	Incorporation (mol%)	End Groups (%)[f]	T_m (°C)
10	0	2.0	76100	25100	118500	4.7	2.9	3500	0	0	133
11	70	0.5	4100	2700	5900	2.3	7.1	8450	0.47	17	121
12	20	2.0	3100	2600	4600	1.8	8.2	9800	1.0	54	120
13	40	2.0	2600	1900	3700	2.0	8.9	10700	1.2	56	119
14	70	2.0	3000	1800	3500	1.9	8.5	10200	1.3	50	117
15[c]	70	2.0	1700	1500	2600	1.7	7.9	9700	1.4	50	116
16[b]	30	2.0	7600	4600	10100	2.2	7.7	9300	0.5	36	125
17[b]	60	2.0	3200	2000	4200	2.1	4.7	5600	1.1	45	118
18[b]	90	2.0	2200	1600	2400	1.5	0.85	1000	1.7	52	84
19[b, c]	90	2.0	2300	1700	2700	1.6	0.78	950	1.8	54	85

[a] Reaction conditions: Cp_2ZrCl_2 = 2.5x10^{-6} mol; MAO 1800 equivalents; solvent = toluene; comonomer = (*R*)-LIM; reaction volume = 90 ml; ethylene partial pressure = 30 psi; reaction time = 20 min; reaction temperature = 60°C.
[b] Ethylene delivery pressure = 100 psig.
[c] Comonomer = (*S*)-LIM.
[d] GPC data obtained at 160°C in 1,2,4-trichlorobenzene using universal calibration. PS standards were used to calibrate the system (see Chapter 6, Section 6.1 for further details).
[e] (kg polymer/(mol[Zr].h))
[f] percentage of chains bearing single comonomer unit at one end.

Runs 11 and 14 (Table 2.2) were conducted to see the effect of increasing (*R*)-LIM concentration. A slight drop in molecular weight and T_m were observed, as well as a significant increase in end group fidelity from 17% to 54%. This is consistent with an increased rate of comonomer insertion into the zirconium hydride species **III** (Scheme 2.2) relative to ethylene. Runs 12-14 show that as the partial pressure of dihydrogen was increased whilst keeping the partial pressure of ethylene constant at 30 psi, the molecular weights decreased and productivity increased slightly. This is consistent with the formation of more zirconium hydride species for the comonomer to insert into as a result of an increased rate of hydrogenolysis of alkyl species **I** or **II** (Scheme 2.2). However,

LIM end group fidelity remains essentially the same. The use of the (*S*) isomer also led to the same end group fidelity under these conditions (run 15).

Runs 16-18 were conducted to test our hypothesis that increasing the dihydrogen partial pressure still further could improve the end group fidelity by reducing the competition from ethylene for insertion into the zirconium hydride. When the total pressure of the system was maintained at 100 psig, as with the PE-*i*-DIB runs, raising the dihydrogen partial pressure again led to lower molecular weights and a gradual increase in end group fidelity. However, *ca* 50% was the limit again while we also observe a substantial reduction in productivity. Similar results were also obtained with (*S*)-LIM (Run 19). It should be noted that under the conditions of Runs 18 and 19, low molecular weight, highly end-functional PE-*i*-DIB had been produced with good productivity (*vide supra*).

The lack of improvement in the end group fidelity of PE-*i*-LIM when compared to the highly end-functional PE-*i*-DIB made under the same conditions is indicative of a substantial difference in the rate of insertion of the two comonomers in to the metal hydride. It also adds support to the suggestion made previously that LIM cannot provide the stabilisation to the cationic metal centre, while the aromaticity of DIB could not only provide the stabilisation, but also enable fast coordination.

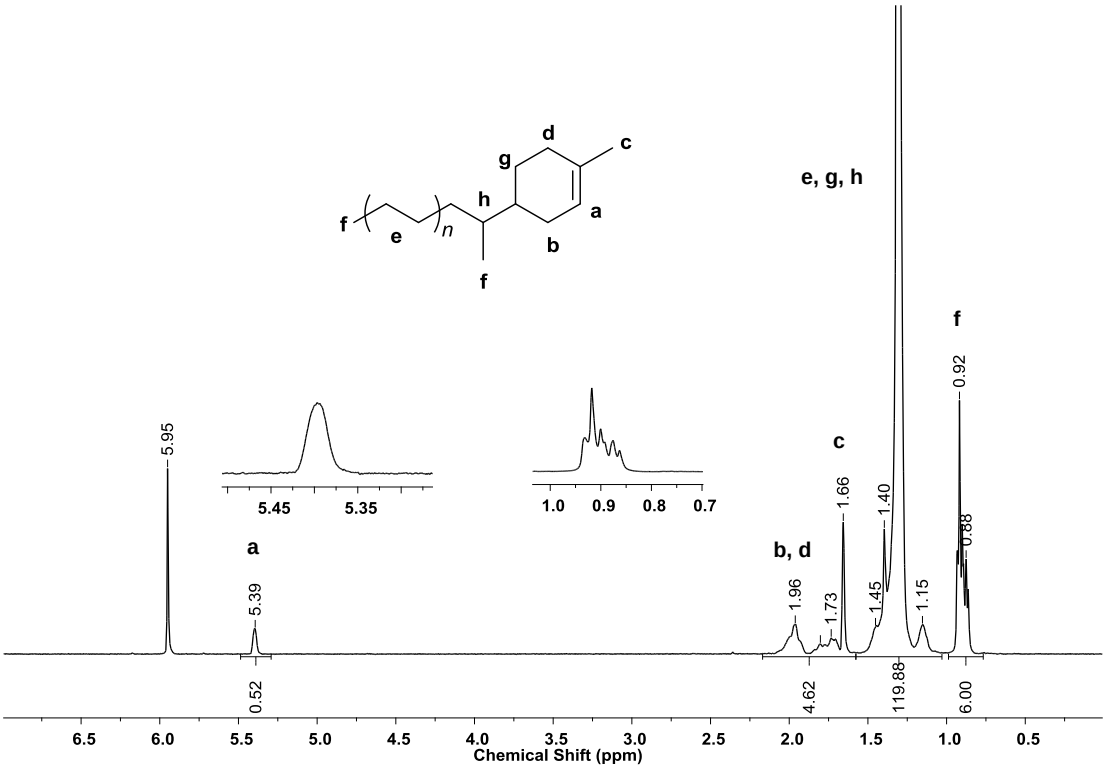

Figure 2.6 - ^{1}H NMR spectrum of the product from Run 18 in d^2-TCE at 100°C (400 MHz) Relaxation delay = 1 s. The top of the peak at 1.30 ppm corresponding to the PE main chain methylene protons has been omitted for clarity.

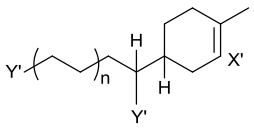

Figure 2.7 - PE-*i*-LIM.

A typical ^{1}H NMR spectrum of the products obtained from the copolymerisation of ethylene and LIM is shown in Figure 2.6. The expansion of the methyl region at 0.8-1.0 ppm shows the PE methyl triplet and the two doublets caused by the two diastereomeric proton environments (Figure 2.7). End group fidelity of the product was determined using the ratio of integrals for the peaks in the spectrum corresponding to the cycloalkene proton X' at 5.39 ppm and the methyl group environments Y' at 0.8-1.0 ppm (Figure 2.7). In a sample where 100% of chains were capped at one end with a LIM unit, we

would expect a 1:6 ratio for the integrals of the signals corresponding to the alkene proton at 5.39 ppm (X') and the methyl protons at 0.8-1.0 ppm (Y'). We therefore determine end group fidelity by the integral of X' when the integral of Y' is set to 6, corresponding to the number of protons per chain it would represent if this were the case. For example, when the integral for the methyl signals Y' in the spectrum given in Figure 2.6 is set to 6, the integral of the alkene proton X' suggests an end group fidelity of *ca* 52%.

Terminal epoxides have been used previously to initiate ring opening polymerisations from polyolefins to yield block copolymers (Chapter 1). Although this would require an extra reaction step to obtain the required functional group, being able to produce a PE macromonomer for ring opening polymerisation in just two steps would be very noteworthy. Epoxidation (Scheme 2.3) of the limonene end groups (Run 14) was conducted in refluxing toluene with excess 3-chloroperbenzoic acid (MCPBA) as the oxidant and the quantitative conversion of the end groups was confirmed by ^{1}H NMR spectroscopy through the absence of the unsaturated CH signal at 5.39 ppm and the presence of a signal 2.96 ppm, corresponding to the CH environment adjacent to the epoxide.

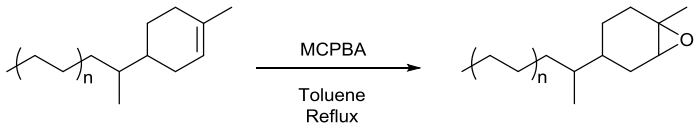

Scheme 2.3 - Epoxidation of PE initiated with limonene (PE-*i*-LIM).

2.4 Further investigation of the CHIP mechanism with the introduction of new non-styrenic comonomers

Copolymers of olefins and cycloolefins have received a great deal of interest in recent years because of properties such as their high glass transition temperatures, heat resistance and transparency;[11, 12, 13] the best-known examples are copolymerisations of ethylene and propylene with norbornene.[14, 15, 16, 17]

Related examples of copolymerisations of olefins with bifunctional comonomers that provide a route to functional polyolefins include polymerisations of ethylene or propylene with linear,[18, 19, 20] cyclic[21, 22, 23] or bicyclic dienes[24, 25, 26] where the retained double bonds can be converted to provide polar functionality. The main technical challenge appears to be achieving significant incorporation whilst preventing cross-linking.[26]

2.4.1 5-Vinyl-2-norbornene (VNB)

Sivaram[27] and Pakkanen[28] reported the copolymerisation of ethylene with the commercially available 5-vinyl-2-norbornene and, more recently, the synthesis of the analogous propylene copolymer was published by Bochmann.[29] All three teams observed selective incorporation of the comonomer *via* the endocyclic double bond in the presence of metallocene/MAO catalyst systems, leaving the pendant double bond available for further functionalisation *e.g.* epoxidation, hydroboration and hydroxylation (see Chapter 1). The concentration of comonomer, olefin partial pressure and the choice of catalyst can be used to control the incorporation of VNB.[28, 29] To the best of our knowledge there is no report of such a copolymerisation conducted in the presence of

dihydrogen and given the results above we were interested to investigate the selective incorporation of comonomer at the beginning of the polymer chain.

We note that Pakkanen[28] and Bochmann[29] utilised metallocene catalysts with larger active sites in order to obtain higher comonomer incorporations, whereas Sivaram[27] reported modest VNB incorporation using the classic $ZrCp_2Cl_2$/MAO system. Since we were trying to incorporate VNB selectively as an end group, the use of a catalyst system that is known to incorporate low levels of comonomer seemed prudent.

Table 2.3 - Ethylene copolymerisations with VNB in the presence of hydrogen.

Run[a]	**H_2 (psi)**	**[VNB] mol/L**	**M_p (g/mol)**[d]	**M_n (g/mol)**[d]	**M_w (g/mol)**[d]	**Đ**[d]	**Yield (g)**	**Productivity**[e]	**Incorporation (mol%)**[f]	**VNB:methyl Ratio**[f]	**T_m (°C)**
20	0	0.75	43600	18000	137000	7.6	3.0	3600	6.0	n/d[g]	85
21	20	0.75	4900	3200	7500	2.4	7.4	8800	8.6	3.7:1	82
22	20	1.5	5500	2900	8700	3.0	9.2	11000	12.2	4.8:1	58
23	20	0.5	6200	3700	8500	2.3	10.2	12300	5.3	2.4:1	98
24	20	0.25	6300	3400	7500	2.2	10.5	12600	3.9	1.05:1	104
25	40	0.25	5800	2600	5300	2.1	6.5	7800	2.9	1:1.3	108
26	60	0.25	2700	1900	3400	1.8	6.6	7900	2.7	1:1.7	107
27[b]	20	0.25	2700	2000	3400	1.7	5.2	6200	5.6	1.5:1	95
28[c]	20	0.25	5400	3000	6500	2.2	11.1	13300	2.6	1.1:1	111

[a] Reaction conditions: $Cp_2ZrCl_2 = 2.5x10^{-6}$ mol; MAO 1800 equivalents; solvent = toluene; reaction volume = 90 ml; ethylene partial pressure = 40 psi unless otherwise stated; reaction time = 20 min; temperature = 60°C.
[b] Ethylene partial pressure = 20 psi.
[c] Ethylene partial pressure = 60 psi.
[d] GPC data obtained at 160°C in 1,2,4-trichlorobenzene using universal calibration. PS standards were used to calibrate the system (see Chapter 6, Section 6.1 for further details).
[e] (kg polymer/(mol[Zr].h))
[f] Determined from ^{1}H NMR.
[g] Not determined.

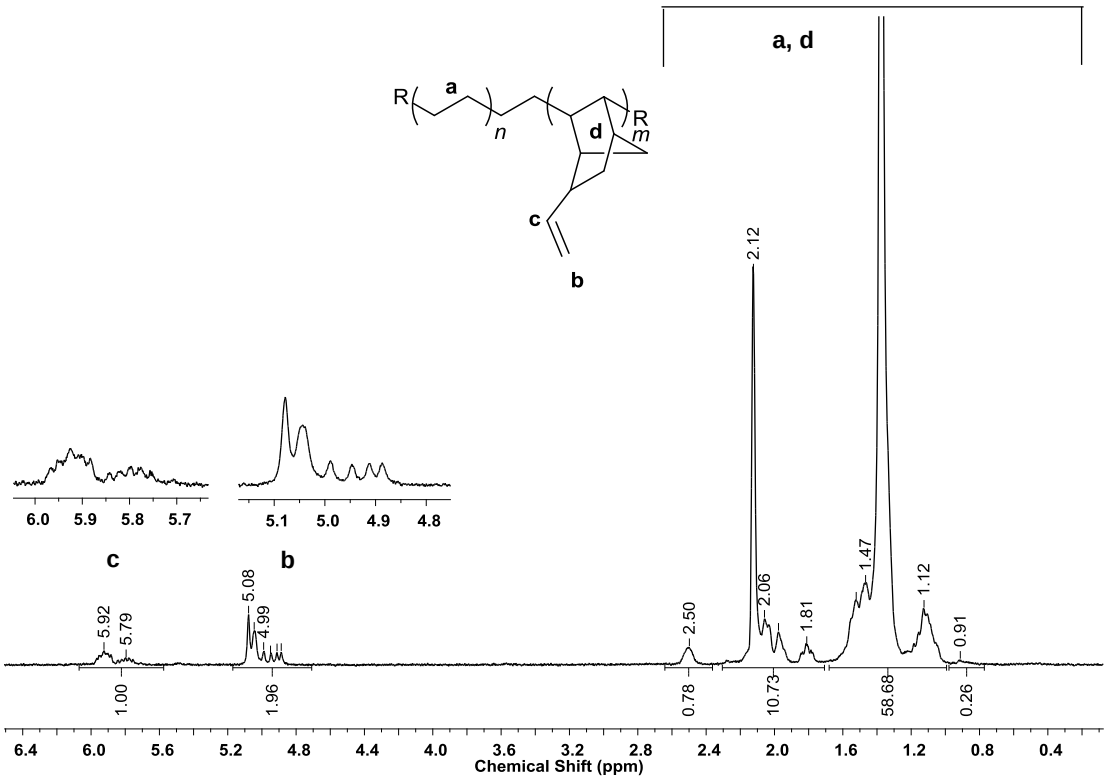

Figure 2.8 - ^{1}H NMR spectrum of the product from Run 20 in d^{8}-toluene at 100°C (400 MHz) Relaxation delay = 1 s. The top of the peak at 1.30 ppm has been omitted for clarity.

As expected a copolymerisation of ethylene and VNB using $ZrCp_2Cl_2$/MAO as a catalyst in the absence of dihydrogen (Run 20, Table 2.3) led to modest incorporation of VNB according to ^{1}H NMR spectroscopy. The ^{1}H NMR spectrum of the product recovered from Run 20 is shown in Figure 2.8. Assignments were found to be consistent with NMR studies of a similar P(E-*co*-VNB) material published by Pakkanen and co-workers.[30] Thought to be a consequence of the alleviation of ring strain,[27, 28] the selective incorporation of VNB *via* the endocyclic double bond was confirmed by the absence of a cyclic olefin signal at *ca* 6.1 ppm.[27] The VNB content of the copolymers in Table 2.3 was determined from ^{1}H NMR spectra *e.g.* in Figure 2.8 according to equations (2) and (3), as outlined by Pakkanen.[28]

$$(2)\ VNB = \frac{(\frac{b}{2}+c)}{2}$$

$$(3)\ VNB\ (mol\ \%) = \frac{VNB}{(A-9VNB)/4\ +VNB} \times 100$$

a corresponds to the set of integrals over the ^{1}H signals at 0.75-2.7 ppm, **b** is the integral of the vinyl CH_2 signals at 4.8-5.2 ppm and **c** is the integral of the vinyl CH signals at 5.7-6.0 ppm. For example when the calculation is performed using the integrals from Figure 2.8, the VNB content is determined to be 6 mol%.

Interestingly the integral for PE methyl end groups in the ^{1}H NMR spectrum of this P(E-*co*-VNB) product prepared in the absence of dihydrogen was very low. Published spectra by others are similar but we have been unable to find reference to this phenomenon in the literature.

The use of dihydrogen (Run 21) resulted in lowering of molecular weight, dispersity and T_m and led to higher productivity. In contrast with *e.g.* Run 20, we observe PE methyl end group signals at *ca* 0.9 ppm in the ^{1}H NMR spectrum *e.g.* in Figure 2.9. These observations are consistent with the introduction of a new hydrogen-based termination mechanism and, since we only observe methyl end groups in the presence of dihydrogen, it is reasonable to assume that they appear at the end of the chain rather than the start *via* termination of some chains by hydrogenation following an ethylene insertion. Increasing the VNB concentration further (Run 22) yielded a similar molecular weight and, as expected, led to a higher VNB incorporation and a lower ratio of PE methyl end groups to VNB. This is consistent with a greater proportion of chains terminating by hydrogenation following a VNB insertion.

Decreasing the concentration of VNB (Runs 23 and 24) did not substantially affect the molecular weight but decreased the overall comonomer incorporation, while also increasing the productivity and the proportion of PE methyl end groups in the product. The near 1:1 ratio of methyl groups to VNB vinyl groups in Run 24 is consistent with more polymer chains containing a single VNB unit at the beginning on average and suggests that a greater proportion of chains are terminating by hydrogenolysis following ethylene insertion. The higher T_m suggests an increase in the crystallinity as a result of lower levels of mid-chain comonomer.

Increasing the dihydrogen partial pressure (Run 25) led to lower molecular weight along with a reduction in VNB incorporation. The VNB:methyl end group ratio fell further, this time below 1:1 indicating again that, at least on average, there is 1 VNB unit per polymer chain. A further increase in dihydrogen pressure (Run 26) resulted in a further reduction in molecular weight, as well as VNB incorporation and VNB:methyl group ratio. This is very similar to observations in this laboratory[3] and by Chung[2] during copolymerisations with styrene and suggests that hydrogenation of ethylene chain ends is competitive with that of VNB chain ends, particularly at higher partial pressures of dihydrogen. Decreasing the ethylene partial pressure (Run 27) resulted in a similar molecular weight, but the productivity and T_m decreased and the VNB incorporation increased significantly. This is consistent with a higher rate of comonomer insertion. Correspondingly, increasing the ethylene partial pressure (Run 28) in the presence of dihydrogen led to increases in molecular weight, productivity and T_m along with lower levels of comonomer.

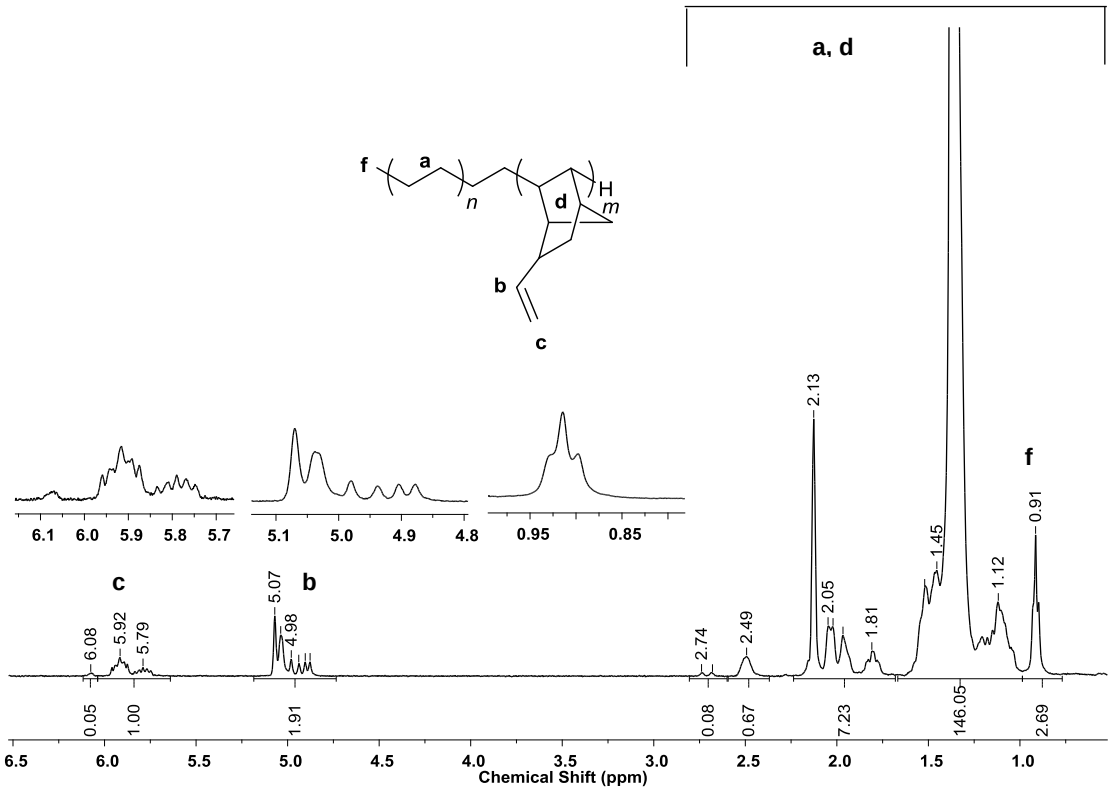

Figure 2.9 - ^{1}H NMR spectrum of the product from Run 28 in d^{8}-toluene at 100°C (400 MHz) Relaxation delay = 1 s. The top of the peak at 1.30 ppm has been omitted for clarity.

Figure 2.9 shows a ^{1}H NMR spectrum of the product obtained from a copolymerisation of ethylene and VNB in the presence of dihydrogen (Run 28). Here we observe the presence of a PE methyl end group signal at 0.91 ppm and VNB vinyl signals in almost a 1:1 ratio. We note the less intense VNB signals with smaller integrals, consistent with a reduced VNB incorporation, and a larger integral for the signal at 1.30 ppm, consistent with a larger ethylene segment.

We also note for such samples the presence of a small signal at 6.07 ppm which corresponds to an endocyclic vinylic CH environment (**c**', Figure 2.10), with the other vinylic CH signal expected to fall under the side chain vinylic CH signals at 5.7-6.0 ppm. Other small signals at 2.73 and 2.68 ppm caused by the saturated CH environments adjacent to the endocyclic vinyl group (**a**' and **b**', Figure 2.10) are also observed. These signals were not removed after washing the product with THF which indicates that they

are part of the polymer and not free VNB monomer; much sharper signals would be expected in any event. The signals are therefore consistent with a small amount of side chain incorporation of the comonomer leaving the cyclic vinyl group detectable in the product, as depicted in Figure 2.10. The insertion of comonomer *via* the side chain, which had been reported previously in VNB homopolymerisation and in copolymerisation with butenes but in the presence of $TiCl_3$-alkylaluminium catalysts,[31] is particularly interesting when we consider that this is not observed in the absence of dihydrogen (*vide supra*).

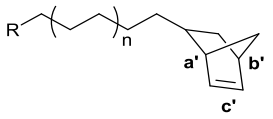

Figure 2.10 – P(E-*co*-VNB) with side chain comonomer insertion.

The above observations led us to some mechanistic proposals for the copolymerisation of VNB with ethylene in the presence of dihydrogen (*vide infra*).

The low methyl integral observed in the absence of dihydrogen raises questions with regard to the mechanism for the copolymerisation: what is the origin of the apparent ability of VNB to be the first inserted monomer; how does the polymerisation terminate so as to produce so few methyl end groups in the product; what is the nature of the active catalyst species that is generated after termination?

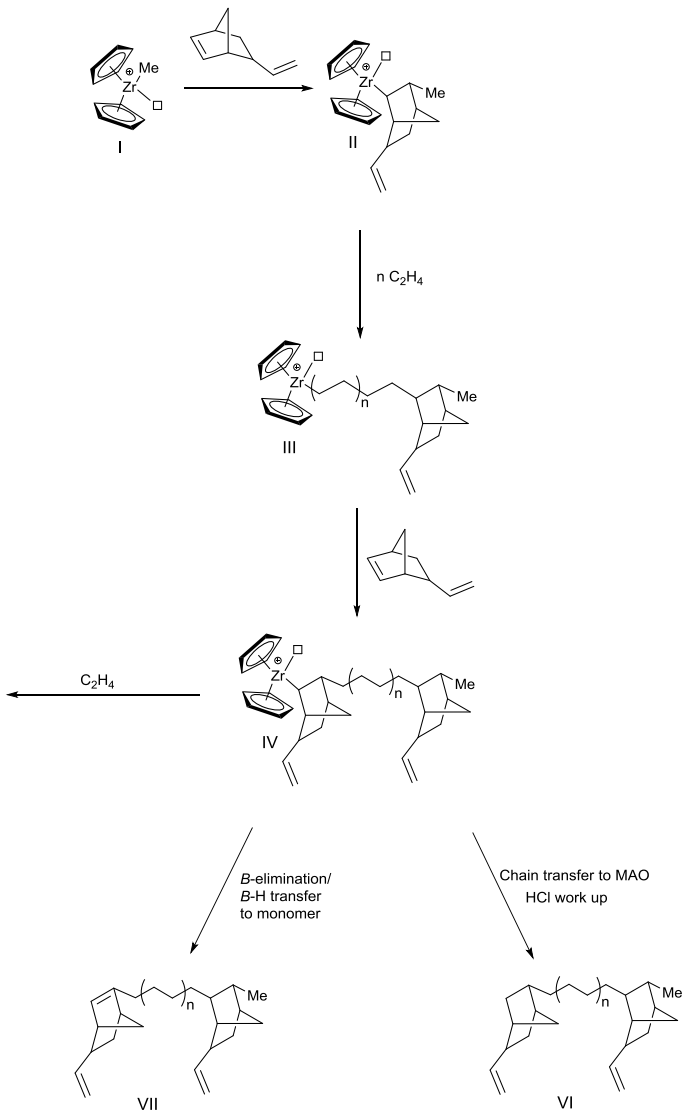

Scheme 2.4 – Proposed mechanism for the copolymerisation of ethylene with VNB in the absence of dihydrogen, including termination following VNB insertion.

As mentioned above, on the basis of the lack of methyl end groups in the NMR spectra of the polymer product, VNB appears to outcompete ethylene for the initial insertion into **I** to form metal alkyl species **II** (Scheme 2.4). Consecutive VNB insertions are unlikely because of steric demands[28] so ethylene would be expected to insert into the zirconium alkyl **II** more easily to give polymeric alkyl **III**. The two monomers would then compete for further insertion and, as the steric demands reduce, VNB may insert again to form *e.g.* species **IV**. Termination directly following a VNB insertion is unlikely

for several reasons: β-elimination and β-hydride transfer to monomer would both result in the formation of a highly strained alkene product (species **VII**); while chain transfer to the MAO cocatalyst would lead to a more favourable saturated product (**VI**) following an acid work up, the resulting metal alkyl would initiate a chain containing a methyl end group; such polymers are formed infrequently if at all (Figure 2.8). It should also be noted that transfer to the aluminium cocatalyst is predominantly found when the olefin monomer concentration is low,[32, 33] which is not the case here.

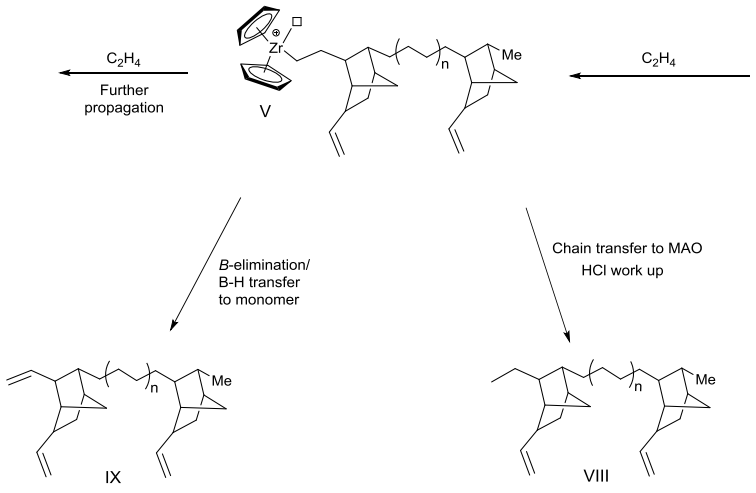

Scheme 2.5 - Proposed mechanism for the copolymerisation of ethylene with VNB in the absence of dihydrogen. Termination following ethylene insertion.

Therefore, termination is more likely to occur following an ethylene insertion into species **IV** *e.g.* in species **V** (Scheme 2.5). As was mentioned earlier, chain transfer to MAO cocatalyst (forming species **VIII**) is unlikely under these conditions and we would also expect to see more methyl end groups in the product if this termination step were prevalent. Various theoretical studies suggest that β-elimination to form **IX** is also not prevalent under the usual experimental conditions,[34, 35] which leaves us with β-hydride transfer to monomer as the most plausible mechanism of the three in this scenario. Although transfer to either ethylene or VNB is possible, we propose that the alleviation of ring strain during transfer to VNB monomer to form species **IX** would make this the

more favoured option. This would lead to a vinyl-termination that is indistinguishable from the VNB side chain vinyl group by NMR and a metal-VNB species which could reinitiate the polymerisation with a chain containing a VNB unit at the start.

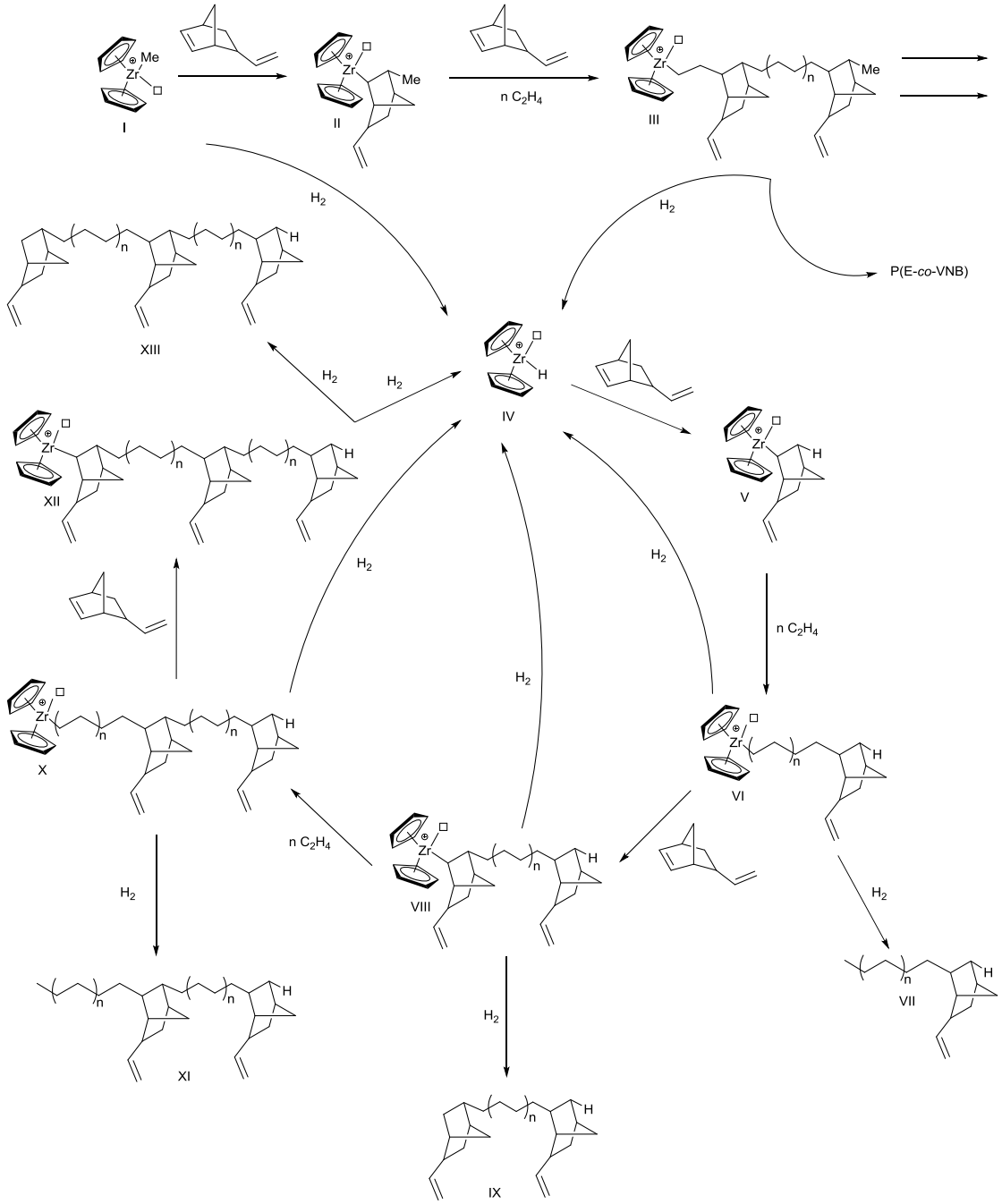

Scheme 2.6 – Proposed mechanism for the copolymerisation of ethylene with VNB in the presence of dihydrogen.

We now turn to the reaction in the presence of dihydrogen. While observations are consistent with the CHIP mechanism, the introduction of the hydrogen-based termination step and the ability of VNB to insert into zirconium carbon bonds introduces a greater number of possibilities at each point in the process than with DIB and LIM (Scheme 2.6). As before, VNB apparently outcompetes ethylene for insertion into active catalyst **I** to form zirconium alkyl **II**. The steric demands of **II** dictate that ethylene would be more likely to insert next, but as the steric demands reduce another VNB unit may insert to yield a polymeric species *e.g.* **III**, (*c.f.* Scheme 2.4). In this case however, hydrogenation of species **I** or **III** to form zirconium hydride **IV** is expected to be highly competitive with monomer insertion. VNB is again expected to outcompete ethylene for insertion at **IV** to yield **V**, into which ethylene can insert to form polymeric species **VI**. At this point termination by hydrogenation may occur to form **VII** and reform the hydride, though further ethylene propagation is also possible, as is insertion of another VNB unit as the steric constraints of the zirconium-polymeryl species are reduced, which would form **VIII**. As well as termination by hydrogenation of **VIII** to form double end-capped species **IX**, propagation by ethylene insertion may occur forming polymeric species **X**. Here, as well as hydrogenation to yield **XI** and further ethylene propagation, insertion of VNB is possible to form species **XII** where again hydrogenation to yield the polymer product **XIII** will compete with further ethylene insertion.

Even when VNB (0.25 mol/L) and ethylene (<0.3 mol/L)[2, 36] were present in similar concentrations in *e.g.* Runs 24-26, the chains still appear to be initiated by VNB. For comparison, a large molar excess of DIB was required to obtain high end group fidelity (*vide supra*) and we have observed already that AMS-like comonomers will not insert readily into zirconium carbon bonds.[5, 6] The ability of VNB to insert multiple times per chain is reminiscent of similar work on ethylene copolymerisations with styrene, where

a high comonomer concentration (2 mol/L) resulted in a double end-capped polymer in the presence of dihydrogen (Scheme 2.1).[3] In the case of VNB this apparently occurs at far lower concentrations, suggesting the rate of VNB insertion into zirconium hydrides and zirconium carbon species is faster than that of styrene.

We know from literature reports and our own runs that VNB will insert selectively into zirconium carbon bonds *via* the endocyclic double bond whether hydrogen is present or not, which means that VNB insertion must be competitive with ethylene insertion provided the steric demands are not substantial. Given this competitiveness and noting that the expected chemical shift differences between end-chain and mid-chain VNB are not as significant as with aromatic comonomers, it would be difficult to justify completely ruling out the presence of multiple VNB units per chain in the products formed in these copolymerisations. What we can say with confidence is that in an optimised reaction with low VNB concentration and high dihydrogen partial pressure, a much lower VNB incorporation is observed and a higher proportion of methyl end groups is obtained, leading to an average ratio of methyl end groups to VNB groups of 1:1 (*e.g.* Runs 24-26). Although this is *consistent* with a single end-functionalised polymer, we cannot safely conclude that this is the exclusive product even under those conditions. The best we can say is that there is a 1:1 ratio of the two sets of signals on average across a distribution of chains.

The observation that VNB inserts very selectively at the endocyclic double bond has been attributed to the accompanying relief of ring strain.[27, 28] We were concerned however that this argument may address the stability of the product rather than of the relevant transition state. In section 2.2, we considered the idea that the rate of AMS insertion at a cationic zirconium hydride is promoted by stabilisation of the charge at the

tertiary benzylic centre. Here we investigate a similar notion that insertion of the endocyclic double bond of VNB is promoted *via* the presence of a non-classical carbocation at the norbornyl system.

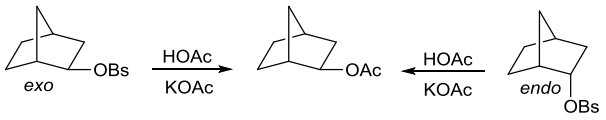

Scheme 2.7 - Acetolysis of 2-norbornyl brosylate.

The structure of the 2-norbornyl carbocation has been the source of debate over many years since the first reports of the unusual behaviour of norbornyl systems in solvolytic displacement reactions.[37] Winstein observed that 2-*exo*-norbornyl brosylate and 2-*endo*-norbornyl brosylate both underwent acetolysis (Scheme 2.7) to form a racemic mixture of the same product, 2-*exo*-norbornyl acetate. The same observations were also made with the equivalent tosylates. In order to explain the abnormal stereochemistry of the product and the enhanced reactivity of the *exo* isomer, Winstein and co-workers concluded that both reactions were proceeding *via* a common cationic intermediate. They proposed that the C1-C6 σ-bond can assist the ionisation of the starting material by acting as a neighbouring group, leading to an achiral non-classical carbocation intermediate which is stabilised by σ-bond delocalisation (Scheme 2.8). The symmetric intermediate would allow access to both enantiomers.[38] This was disputed by Brown[39] who argued that all the available data could be explained by a rapid equilibrium between classical carbocations, such as that shown in Scheme 2.8.

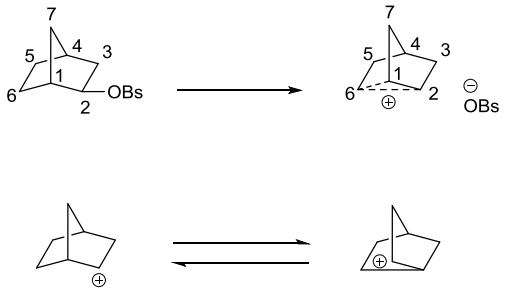

Scheme 2.8 – (Above) Formation of a non-classical 2-norbornyl carbocation intermediate. (Below) Rapid equilibration between classical carbocations.

Despite mounting spectroscopic[40, 41, 42] and theoretical[43, 44] evidence for the non-classical structure, this debate continued until the long-sought crystallographic data was recently published by Scholz and co-workers.[45]

We propose that the formation of a non-classical carbocation species on insertion of VNB into either a metal hydride or metal alkyl (Scheme 2.9) provides the stability for the build-up of positive charge and thus explains why norbornene derivatives insert so readily in the mechanisms discussed above.

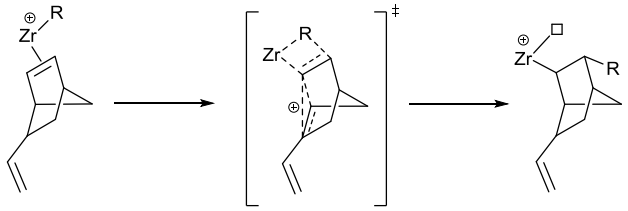

Scheme 2.9 - Formation of non-classical carbocation after insertion of VNB into zirconium centre.

Epoxidation (Scheme 2.10) of the VNB groups (Run 21) was conducted in hot toluene in the presence of excess 3-chloroperbenzoic acid (MCPBA) as previously reported by Bochmann and co-workers.[29] Again, quantitative conversion of the end groups was confirmed by ^{1}H NMR spectroscopy. As mentioned earlier, the epoxide group facilitates

the possibility of initiating ring-opening polymerisation to offer further functionalisation potential.

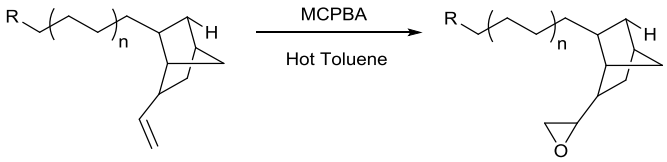

Scheme 2.10 - Epoxidation of VNB groups.

2.4.2 5-Ethylidene-2-norbornene (ENB)

5-Ethylidene-2-norbornene is another commercially available bifunctional norbornene derivative that has been successfully copolymerised with ethylene in the presence of metallocene catalyst systems to afford functionalised olefin copolymers.[46, 47] According to the literature the comonomer is selectively incorporated *via* the endocyclic double bond and the proportion of comonomer in the product varies with the concentration of comonomer and the particular catalyst system used.[48, 49, 50] As with VNB, the side chain double bond is retained in the product thus allowing quantitative functionalisation with a similar range of standard organic reactions as mentioned previously. Again there are no previous reports of copolymerisations of ethylene and ENB in the presence of hydrogen as far as we are aware, leading us to investigate the selective incorporation of ENB at the beginning of the polymer chain to yield an end-functionalised polyethylene.

Table 2.4 - Ethylene copolymerisations with ENB in the presence of dihydrogen.

Run[a]	H_2 (psi)	[ENB] mol/L	M_p (g/mol)[d]	M_n (g/mol)[d]	M_w (g/mol)[d]	$Đ$[d]	Yield (g)	Productivity[e]	Incorporation (mol%)[f]	ENB:methyl Ratio[f]	T_m (°C)
29	0	0.75	76800	12800	80000	6.2	0.61	730	22.1	n/d[g]	n/a[h]
30	20	0.75	3600	2200	4200	1.9	6.1	7300	18.4	5.3:1	n/a[h]
31	20	1.5	4800	2100	6600	3.1	7.3	8800	31.9	n/d[g]	n/a[h]
32	20	0.5	3900	2600	4600	1.7	8.8	10600	12.1	4.0:1	81
33	20	0.25	3800	2300	4300	1.9	6.8	8100	6.8	2.1:1	100
34	40	0.25	2400	2200	3700	1.7	5.9	7100	6.0	1.7:1	102
35	60	0.25	1800	1400	2100	1.6	5.3	6400	5.7	1.6:1	95
36[b]	20	0.25	1500	1200	2100	1.8	2.0	2400	12.7	2.6:1	76
37[c]	20	0.25	5300	3000	6000	2.0	10.5	12600	5.6	2.4:1	105

[a] Reaction conditions: Cp_2ZrCl_2 = 2.5x10^{-6} mol; MAO 1800 equivalents; solvent = toluene; reaction volume = 90 ml; ethylene partial pressure = 40 psi unless otherwise stated; reaction time = 20 min; reaction temperature = 60°C.
[b] Ethylene partial pressure = 20 psi.
[c] Ethylene partial pressure = 60 psi.
[d] GPC data obtained at 160°C in 1,2,4-trichlorobenzene using universal calibration. PS standards were used to calibrate the system (see Chapter 6, Section 6.1 for further details).
[e] (kg polymer/(mol[Zr].h))
[f] Determined from ^{1}H NMR.
[g] Not determined.
[h] Not applicable.

A copolymerisation of ethylene with ENB catalysed by $ZrCp_2Cl_2$/MAO in the absence of dihydrogen (Run 29, Table 2.4) yielded the expected P(E-*co*-ENB). Again PE methyl end groups were not detected in significant proportion, suggesting a similar mechanism as discussed with VNB (*vide supra*). Also noteworthy is that the incorporation of comonomer was far higher (22%) than with VNB under the same conditions which indicates a far larger number of mid-chain insertions.

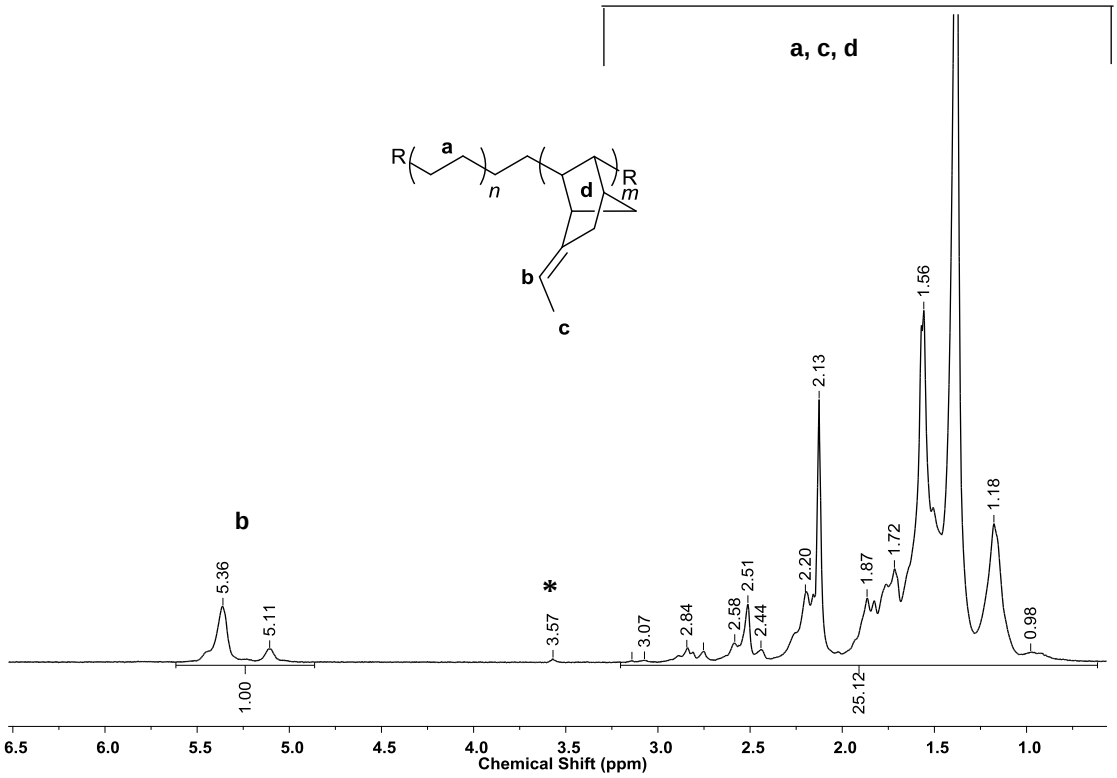

Figure 2.11 - ^{1}H NMR spectrum of the product from Run 29 in d^{8}-toluene at 100°C (400 MHz) Relaxation delay = 1 s. The top of the peak at 1.30 ppm has been omitted for clarity.

The ^{1}H NMR spectrum of the product recovered from Run 29 is shown in Figure 2.11 and peak assignments were found to be consistent with those of analogous materials found in the literature.[46, 48, 50] As with the analogous VNB copolymerisation, the absence of the endocyclic double bond signal at 5.8-6.0 ppm confirms the regioselective incorporation of the comonomer. The ENB content of the copolymers in Table 2.4 was determined from ^{1}H NMR spectra *e.g.* in Figure 2.11 according to equation (4), as outlined by Mu and co-workers.[46]

$$(4)\ ENB\ (mol\ \%) = \frac{b}{(A-11B)/4 + b} \times 100$$

A is the set of integrals over the ^{1}H signals at 0.5-3.2 ppm and **B** is the integral of the ethylidene ^{1}H signals at 4.8-5.5 ppm. As an example, when the calculation is performed using the integrals from Figure 2.11, the ENB content is determined to be 22 mol%.

As shown in Table 2.4, the use of dihydrogen (Run 30) yielded substantially higher productivity along with lower molecular weight, dispersity and a reduction in comonomer incorporation. Consistent with the analogous copolymerisation with VNB, PE methyl end group signals at *ca* 0.9 ppm were detectable in the ^{1}H NMR spectrum of the product (Figure 2.12), which is an indication of the same hydrogen-based termination mechanism shown in Scheme 2.6. Increasing the ENB concentration (run 31) led to higher comonomer incorporation and fewer PE methyl end groups, while reduction of ENB concentration (Runs 32 and 33) led to an increasing proportion of methyl end groups and lower incorporations of comonomer. This effect was again enhanced when the dihydrogen partial pressure was increased (Runs 34 and 35) and the ENB:methyl group ratio fell further. Lower molecular weights were also obtained as the dihydrogen partial pressure was increased. As with VNB, lowering the ethylene partial pressure (Run 36) had little effect on molecular weights, but productivity and T_m decreased which is consistent with reduced rate of ethylene insertion and a greater rate of comonomer insertion. Correspondingly, increasing the ethylene partial pressure (Run 37) resulted in greater productivity and higher molecular weight materials with a corresponding increase in T_m, consistent with a higher rate of ethylene insertion.

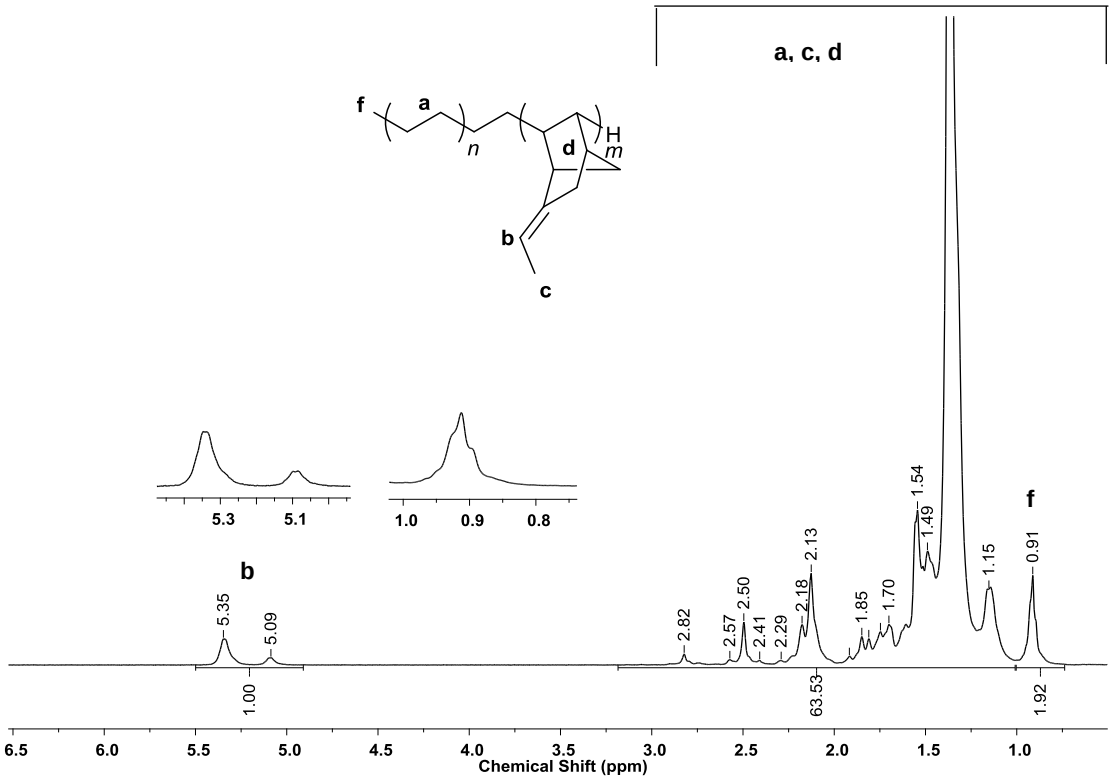

Figure 2.12 - ^{1}H NMR spectrum of the product from Run 35 in d^{8}-toluene at 100°C (400 MHz) Relaxation delay = 1 s. The top of the peak at 1.30 ppm has been omitted for clarity.

Figure 2.12 shows a ^{1}H NMR spectrum of the product obtained from a copolymerisation of ethylene and ENB in the presence of dihydrogen (Run 35). In contrast to the analogous run with VNB, here we still observe no endocyclic vinyl group signals suggesting that the regioselectivity of insertion is fully retained with ENB in the presence of dihydrogen.

Across the range of conditions used here, even in Runs 30 and 31, there were still multiple insertions of ENB per chain that did not reduce significantly below *ca* 2 ENB units per methyl group on average by NMR. Under the same conditions with VNB materials with an average ratio of 1:1 methyl:comonomer were obtained. This indicates a significant difference between VNB and ENB in terms of rate of insertion which is interesting given the structural similarity of the two comonomers.

2.5 Conclusions

Dihydrogen partial pressure rather than comonomer concentration, as for Chung,[1, 2] may be used to control the molecular weight of the products formed in the synthesis of PE-*i*-DIB. Raising the partial pressure also leads to improved productivity of the reaction. By these means rather low molecular weight, and more soluble polyethylenes could be produced with high end group fidelity of DIB.

These observations prompted us to investigate the use of dihydrogen concentration to attempt to improve the end group fidelity of the PE-*i*-LIM materials. While end group fidelity of the PE-*i*-LIM increased slightly as the hydrogen:ethylene ratio increased, this still peaked at between 50-60%. We conclude that the rate of insertion of LIM must be insufficient to produce high end group fidelities; unlike for DIB, the transition state for insertion of LIM is not stabilised by delocalisation of cationic charge arising from the zirconium alkyl centre.

The scope of the CHIP mechanism was then investigated further using the non-styrenic bifunctional monomer VNB. Runs conducted in the absence of dihydrogen led to a copolymer product that contained very few methyl end groups by NMR; an observation not previously made in the literature on this copolymerisation. Similar reactions conducted in the presence of dihydrogen yielded lower molecular weight products that contained methyl end groups, consistent with the CHIP mechanism. Productivity was also improved.

This raised questions about the termination mechanism in the absence of dihydrogen and about the nature of the metal alkyl species that initiated subsequent chains. We subsequently proposed a mechanism involving β-hydride transfer to monomer following

an ethylene insertion that would result in a vinyl end group indistinguishable from the comonomer side chain vinyl group. We also suggested that transfer to VNB comonomer would be more favourable on the basis that ring strain would be alleviated and because the resulting metal-comonomer species would produce a polymer chain with a VNB unit at the beginning.

In the presence of dihydrogen the CHIP mechanism was more complex because, unlike AMS or DIB, VNB can insert into a zirconium alkyl as well as a zirconium hydride. In the presence of low comonomer concentrations and high dihydrogen partial pressures, a material with almost 1:1 VNB:methyl groups was formed. While this ratio is consistent with a single end-capped polymer chain, we could not confirm this by NMR due to the similarity of expected chemical shifts between mid-chain and end-chain VNB, thus leading to the conclusion that the ratio was probably an average over a distribution of chains. A similar investigation conducted on copolymerisations of ethylene and ENB yielded similar observations but in the presence of dihydrogen, the ratio of comonomer to methyl end group did not reduce as much as with VNB under the same range of conditions.

We propose that VNB and ENB are similar to AMS and DIB in that they are able to insert so readily into a metal hydride because of the stability they provide to the resulting cationic metal alkyl intermediate. In the case of VNB and ENB a non-classical carbocation stabilises the transition state. The major difference between the two sets of monomers is that, while AMS and DIB will not insert into metal carbon bonds, VNB and ENB do so readily making it more difficult to control the number of comonomer insertions per chain.

2.6 References

1. Chung, T. C.; Dong, J. Y., A Novel Consecutive Chain Transfer Reaction to p-Methylstyrene and Hydrogen during Metallocene-Mediated Olefin Polymerization. *J. Am. Chem. Soc.* **2001,** *123* (21), 4871-4876.
2. Dong, J. Y.; Chung, T. C., Synthesis of Polyethylene Containing a Terminal p-Methylstyrene Group: Metallocene-Mediated Ethylene Polymerization with a Consecutive Chain Transfer Reaction to p-Methylstyrene and Hydrogen. *Macromolecules* **2002,** *35* (5), 1622-1631.
3. Kay, C. J. Polyethylene Block Copolymers. University of Warwick, 2014.
4. Galdi, N.; Izzo, L.; Oliva, L., Comparison of the Regiochemical Behavior of Zirconium and Hafnium in the Polyinsertion of Styrenes. *Organometallics* **2010,** *29* (20), 4434-4439.
5. Schwecke, C.; Kaminsky, W., Homo- and Copolymerization of Styrene and Alkylstyrenes with the Highly Active Catalyst System CpTiF3/MAO. *Macromol. Rapid Commun.* **2001,** *22* (7), 508-512.
6. Rabagliati, F. M.; Pérez, M. A.; Rodríguez, F. J.; Caro, C. J.; Crispel, N., Further studies on styrene/styrene derivative copolymerizations using combined diphenylzinc-additive initiator systems. *Polym. Int.* **2005,** *54* (2), 437-441.
7. Chirik, P. J.; Bercaw, J. E., Cyclopentadienyl and Olefin Substituent Effects on Insertion and β-Hydrogen Elimination with Group 4 Metallocenes. Kinetics, Mechanism, and Thermodynamics for Zirconocene and Hafnocene Alkyl Hydride Derivatives. *Organometallics* **2005,** *24* (22), 5407-5423.
8. Blom, R.; Swang, O.; Heyn, R. H., Semi-Batch Polymerisations of Ethylene with Metallocene Catalysts in the Presence of Hydrogen, 3. Correlation Between Hydrogen Sensitivity and Molecular Parameters. *Macromol. Chem. Phys.* **2002,** *203* (2), 381-387.
9. McCormick, H. W., Ceiling temperature of α-methylstyrene. *J. Polym. Sci.* **1957,** *25* (111), 488-490.
10. Nakayama, Y.; Sogo, Y.; Cai, Z.; Shiono, T., Copolymerization of ethylene with 1,1-disubstituted olefins catalyzed by ansa-(fluorenyl)(cyclododecylamido)dimethyltitanium complexes. *J. Polym. Sci. A: Polym. Chem.* **2013,** *51* (5), 1223-1229.
11. Kaminsky, W.; Bark, A.; Arndt, M., New polymers by homogenous zirconocene/aluminoxane catalysts. *Makromol. Chem. Macromol. Symp.* **1991,** *47* (1), 83-93.
12. Arndt, M.; Kaminsky, W., Microstructure of poly(cycloolefins) produced by metallocene/methylaluminoxane (mao) catalysts. *Macromol. Symp.* **1995,** *97* (1), 225-246.
13. Cherdron, H.; Brekner, M. J.; Osan, F., Cycloolefin-copolymere: Eine neue klasse transparenter thermoplaste. *Angew. Makromol. Chem.* **1994,** *223* (1), 121-133.
14. McKnight, A. L.; Waymouth, R. M., Ethylene/Norbornene Copolymerizations with Titanium CpA Catalysts. *Macromolecules* **1999,** *32* (9), 2816-2825.
15. Arndt-Rosenau, M.; Beulich, I., Microstructure of Ethene/Norbornene Copolymers. *Macromolecules* **1999,** *32* (22), 7335-7343.
16. Tritto, I.; Marestin, C.; Boggioni, L.; Zetta, L.; Provasoli, A.; Ferro, D. R., Ethylene−Norbornene Copolymer Microstructure. Assessment and Advances

Based on Assignments of 13C NMR Spectra. *Macromolecules* **2000,** *33* (24), 8931-8944.
17. Tritto, I.; Marestin, C.; Boggioni, L.; Sacchi, M. C.; Brintzinger, H.-H.; Ferro, D. R., Stereoregular and Stereoirregular Alternating Ethylene−Norbornene Copolymers. *Macromolecules* **2001,** *34* (17), 5770-5777.
18. Nam, Y.-G.; Murayama, S.; Shiono, T.; Ikeda, T., Copolymerization of Propene and 1,2,4-Trivinylcyclohexane by a MgCl2-Supported TiCl4 Catalyst. *Macromolecules* **2001,** *34* (19), 6533-6535.
19. Hustad, P. D.; Coates, G. W., Insertion/Isomerization Polymerization of 1,5-Hexadiene: Synthesis of Functional Propylene Copolymers and Block Copolymers. *J. Am. Chem. Soc.* **2002,** *124* (39), 11578-11579.
20. Song, F.; Pappalardo, D.; Johnson, A. F.; Rieger, B.; Bochmann, M., Derivatization of propene/methyloctadiene copolymers: A flexible approach to side-chain-functionalized polypropenes. *J. Polym. Sci. A: Polym. Chem.* **2002,** *40* (10), 1484-1497.
21. Li, X.; Baldamus, J.; Nishiura, M.; Tardif, O.; Hou, Z., Cationic Rare-Earth Polyhydrido Complexes: Synthesis, Structure, and Catalytic Activity for the cis-1,4-Selective Polymerization of 1,3-Cyclohexadiene. *Angew. Chem. Int. Ed.* **2006,** *45* (48), 8184-8188.
22. Kobayashi, S.; Lu, C.; Hoye, T. R.; Hillmyer, M. A., Controlled Polymerization of a Cyclic Diene Prepared from the Ring-Closing Metathesis of a Naturally Occurring Monoterpene. *J. Am. Chem. Soc.* **2009,** *131* (23), 7960-7961.
23. Pan, L.; Ye, W.-P.; Liu, J.-Y.; Hong, M.; Li, Y.-S., Efficient, Regioselective Copolymerization of Ethylene with Cyclopentadiene by the Titanium Complexes Bearing Two β-Enaminoketonato Ligands. *Macromolecules* **2008,** *41* (9), 2981-2983.
24. Pan, L.; Hong, M.; Liu, J.-Y.; Ye, W.-P.; Li, Y.-S., Living Copolymerization of Ethylene with Dicyclopentadiene Using Titanium Catalyst: Formation of Well-Defined Polyethylene-block-poly(ethylene-co-dicyclopentadiene)s and Their Transformation into Novel Polyolefin-block-(functional polyolefin)s. *Macromolecules* **2009,** *42* (13), 4391-4393.
25. Mönkkönen, K.; Pakkanen, T. T., Synthesis and characterization of poly(ethylene-co-norbornadiene). *Macromol. Chem. Phys.* **1999,** *200* (12), 2623-2628.
26. Hong, M.; Pan, L.; Ye, W.-P.; Song, D.-P.; Li, Y.-S., Facile, efficient functionalization of polyethylene via regioselective copolymerization of ethylene with cyclic dienes. *J. Polym. Sci. A: Polym. Chem.* **2010,** *48* (8), 1764-1772.
27. Marathe, S.; Sivaram, S., Regioselective Copolymerization of 5-Vinyl-2-norbornene with Ethylene Using Zirconocene-Methylaluminoxane Catalysts: A Facile Route to Functional Polyolefins. *Macromolecules* **1994,** *27* (5), 1083-1086.
28. Lasarov, H.; Pakkanen, T. T., Copolymerization of ethylene with 5-vinyl-2-norbornene in the presence of the Ph2C(Flu)(Cp)ZrCl2 /MAO catalyst. *Macromol. Chem. Phys.* **2000,** *201* (14), 1780-1786.
29. Sarazin, Y.; Fink, G.; Hauschild, K.; Bochmann, M., Copolymerization of Propene and 5-Vinyl-2-Norbornene: A Simple Route to Polar Poly(propylene)s. *Macromol. Rapid Commun.* **2005,** *26* (15), 1208-1213.
30. Lasarov, H.; Pakkanen, T. T., 2D NMR characterization of poly(ethylene-co-5-vinyl-2-norbornene). *Macromol. Rapid Commun.* **1999,** *20* (6), 356-360.

31. Endo, K.; Fujii, K.; Otsu, T., Polymerization of 5-vinyl-2-norbornene with TiCl3 and alkylaluminium catalysts. *Macromol. Chem. Phys.* **1996,** *197* (1), 97-104.
32. Resconi, L.; Bossi, S.; Abis, L., Study on the role of methylalumoxane in homogeneous olefin polymerization. *Macromolecules* **1990,** *23* (20), 4489-4491.
33. Naga, N.; Mizunuma, K., Chain transfer reaction by trialkylaluminum (AIR3) in the stereospecific polymerization of propylene with metallocene — AIR3/Ph3CB(C6F5)4. *Polymer* **1998,** *39* (21), 5059-5067.
34. Deng, L.; Margl, P.; Ziegler, T., Mechanistic Aspects of Ethylene Polymerization by Iron(II)−Bisimine Pyridine Catalysts: A Combined Density Functional Theory and Molecular Mechanics Study. *J. Am. Chem. Soc.* **1999,** *121* (27), 6479-6487.
35. Margl, P.; Deng, L.; Ziegler, T., A Unified View of Ethylene Polymerization by d0 and d0fn Transition Metals. 3. Termination of the Growing Polymer Chain. *J. Am. Chem. Soc.* **1999,** *121* (1), 154-162.
36. Wu, J.; Pan, Q.; Rempel, G. L., Solubility of ethylene in toluene and toluene/styrene–butadiene rubber solutions. *J. Appl. Polym. Sci.* **2005,** *96* (3), 645-649.
37. March, J., *Advanced organic chemistry: reactions, mechanisms, and structure*. Wiley: 1992.
38. Winstein, S.; Trifan, D. S., The structure of the bicyclo[2.2.1]2-heptyl (norbornyl) carbonium ion. *J. Am. Chem. Soc.* **1949,** *71* (8), 2953-2953.
39. Brown, H. C., *The Nonclassical Ion Problem*. Springer: New York, 1977.
40. Perera, S. A.; Bartlett, R. J., Structure and NMR Spectra of the 2-Norbornyl Carbocation: Prediction of 1J(13C13C) for the Bridged, Pentacoordinate Carbon Atom. *J. Am. Chem. Soc.* **1996,** *118* (33), 7849-7850.
41. Koch, W.; Liu, B.; DeFrees, D. J.; Sunko, D. E.; Vanččik, H., Experimental and Theoretical IR Spectra of the 2-Norbornyl Cation. *Angew. Chem. Int. Ed.* **1990,** *29* (2), 183-185.
42. Olah, G. A., Carbocations and Electrophilic Reactions. *Angew. Chem. Int. Ed.* **1973,** *12* (3), 173-212.
43. Hong, Y. J.; Tantillo, D. J., Perturbing the Structure of the 2-Norbornyl Cation through C−H···N and C−H···π Interactions. *J. Org. Chem.* **2007,** *72* (23), 8877-8881.
44. Koch, W.; Liu, B.; DeFrees, D. J., Structure of the 2-norbornyl cation. *J. Am. Chem. Soc.* **1989,** *111* (4), 1527-1528.
45. Scholz, F.; Himmel, D.; Heinemann, F. W.; Schleyer, P. v. R.; Meyer, K.; Krossing, I., Crystal Structure Determination of the Nonclassical 2-Norbornyl Cation. *Science* **2013,** *341* (6141), 62-64.
46. Li, H.; Li, J.; Zhang, Y.; Mu, Y., Homo- and copolymerization of 5-ethylidene-2-norbornene with ethylene by [2-C5Me4-4,6-tBu2C6H2O]TiCl2/AliBu3/Ph3CB(C6F5)4 catalyst system and epoxidation of the resulting copolymer. *Polymer* **2008,** *49* (12), 2839-2844.
47. Hasan, T.; Ikeda, T.; Shiono, T., Homo- and copolymerization of norbornene derivatives with ethene by ansa-fluorenylamidodimethyltitanium activated with methylaluminoxane. *J. Polym. Sci. A: Polym. Chem.* **2007,** *45* (20), 4581-4587.
48. Arabi, H.; Mobarakeh, H. S.; Balzadeh, Z.; Nejabat, G.-R., Copolymerization of ethylene/5-ethylidene-2-norbornene with bis (2-phenylindenyl) zirconium dichloride catalyst: I. Optimization of the operating conditions by response surface methodology. *J. Appl. Polym. Sci.* **2013,** *129* (5), 3047-3053.

49. Meshkova, I. N.; Grinev, V. G.; Kiseleva, E. V.; Paspopov, L. N.; Kuznetsov, S. P.; Udovenko, A. I.; Shchegolikhin, A. N.; Ladygina, T. A.; Novokshonova, L. A., Polymer materials based on ethylene copolymers with substituted norbornene. *Polym. Sci. Series A* **2007,** *49* (11), 1165-1172.
50. Meshkova, I. N.; Shchegolikhin, A. N.; Kiseleva, E. V.; Novokshonova, L. A., Homopolymerization of ethylene and copolymerization of ethylene and 5-ethylidene-2-norbornene with the use of C2-symmetric ansa-zirconozenes catalysts of different composition. *Polym. Sci. Series B* **2015,** *57* (2), 77-84.

Chapter 3: Synthesis of polyethylene-*b*-Poly(*n*-butyl acrylate) copolymers

3.1 Introduction

AMS is added to some radical polymerisations to control the molecular weight and end group fidelity.[1, 2] The high chain transfer to monomer constant ($C_M = k_{tr}/k_p$), low propagation rate and low ceiling temperature[1, 2, 3, 4] mean that AMS adds rapidly to the end of a growing polymer radical but further propagation is slow. Even at low concentrations this is effective in styrene polymerisations[5] and the monomer has been used extensively in the synthesis of vinyl-terminated polymers *via* catalytic chain transfer polymerisation (CCTP) in the presence of a chain transfer agent such as bis(boron difluorodimethylglyoximate)cobaltate(II) (COBF).[2, 5, 6, 7, 8, 9]

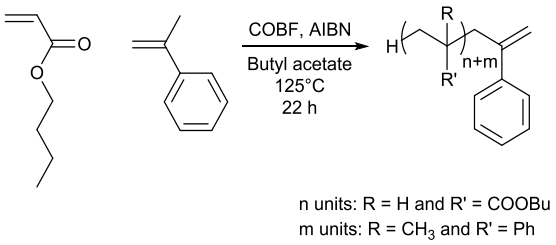

Scheme 3.1 - Copolymerisation of *n*-BA and AMS in the presence of COBF.[2]

Barner-Kowollik and co-workers[2] utilised this method to synthesise macromonomers of P(*n*-BA) containing a terminal AMS group, noting that the addition of AMS not only improved the efficiency of the CCT process, but also produced macromonomers whose vinyl end functionalities were far more reactive than those of a pure P(*n*-BA) macromonomer prepared by CCTP. Copolymerisations between styrene and maleic anhydride have also been demonstrated to terminate to AMS in a CCTP reaction with

COBF, forming a macromonomer capable of graft polymerisation with styrene and *n*-butyl acrylate.[9]

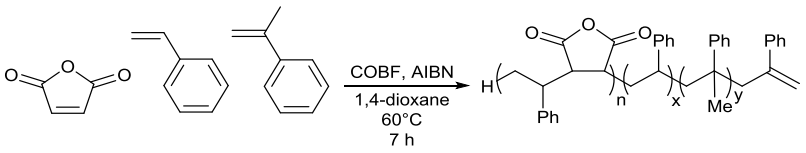

Scheme 3.2 - Copolymerisation of maleic anhydride, styrene and AMS in the presence of COBF.[9]

These reports led Scott and co-workers[10] to propose that the AMS-like end group of PE-*i*-DIB could be utilised as an end-capping agent in free radical polymerisation with a suitable polar monomer in a similar way to form a polyethylene copolymer. Noting the reported similarity in reactivity of double bonds in macromonomers to their corresponding small monomer,[11] initial attempts at the copolymerisation simply aimed to replace the AMS comonomer in the aforementioned CCTP reactions with PE-*i*-DIB to produce block copolymers. It was found however, that the presence of the CCTP catalyst did not lead to generation of vinylic groups, presumably for steric reasons, but that heating the macromonomer and *n*-butyl acrylate (*n*-BA) with a peroxide initiator formed copolymer products.

In this chapter the mechanism of the copolymerisation of PE-*i*-DIB with *n*-BA was investigated further utilising both a small scale batch process and a starved feed semi-batch method, the likes of which are commonly found in industry. This starved feed approach was found to enable the production of a range of molecular weight copolymers on a larger scale and with greater control, as well as straightforward optimisation through tuning of experimental conditions.

3.2 Free radical polymerisation of *n*-BA

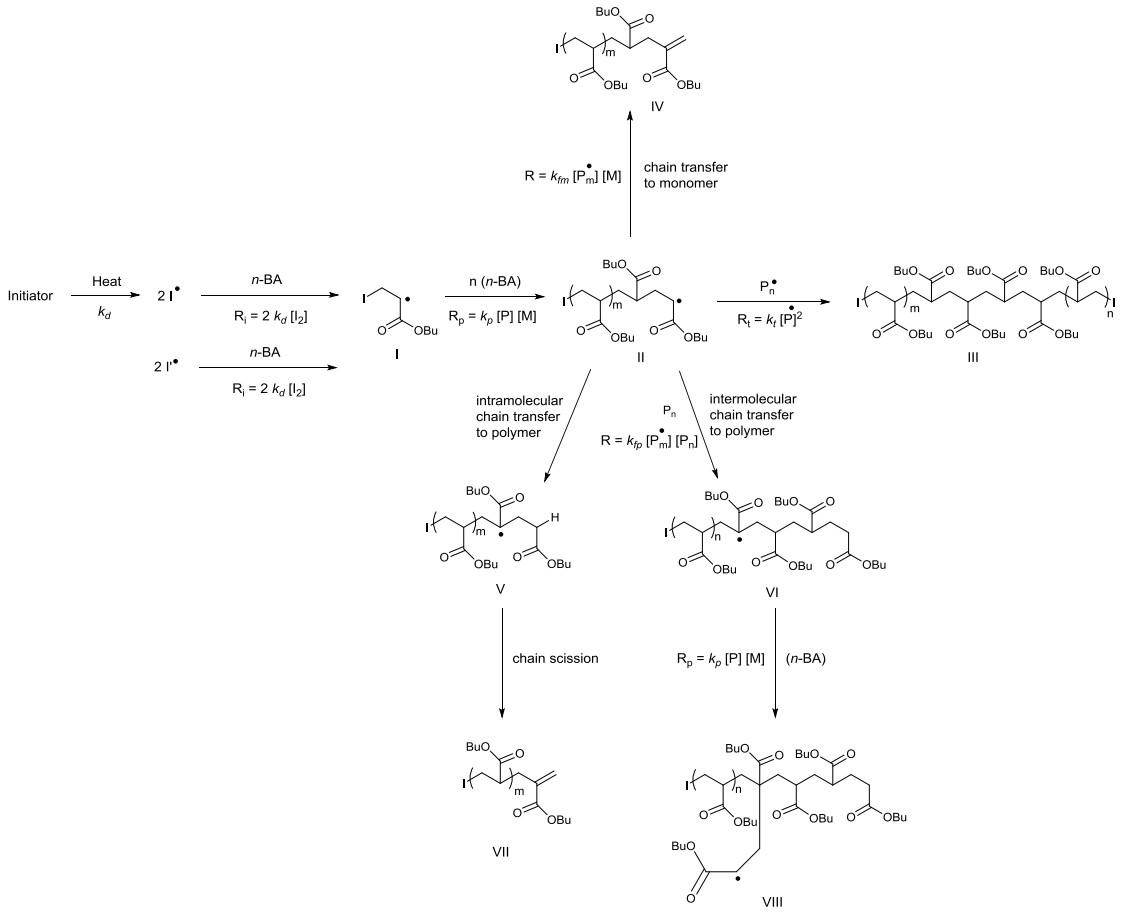

Scheme 3.3 - Free radical polymerisation of *n*-butyl acrylate.

A typical mechanism for the free radical polymerisation of *n*-BA is shown in Scheme 3.3. The initiator decomposes to form two primary radicals I$^•$, which can fragment further to form secondary radicals I'$^•$. Both primary and secondary radicals can initiate the polymerisation by addition of monomer (rate = 2 k_d [I_2]) to start the growth of polymer chains *e.g.* species **I**; further monomer units are then added to the secondary radical **I** to form polymer radical **II** (rate = k_p [P$^•$] [M]). Traditional termination of acrylate polymerisation occurs by radical-radical combination with rate = k_t [P$^•$]^2 to form a dead chain **III**, but several chain transfer reactions may also occur. Chain transfer to monomer (rate = k_m [P$^•$] [M]) would form vinylic species **IV** and a new radical capable

of re-initiating polymerisation. Chain transfer to polymer can occur *via* and intra- (backbiting) or an intermolecular (abstraction from a dead polymer chain) mechanism depending on the conditions of the polymerisation (*vide infra*) and both result in the formation of a mid-chain tertiary radical (**V** or **VI**). The addition of monomer to either of these tertiary radicals would result in branch formation as in species **VIII**, while under certain conditions *β*-scission of the mid-chain radical species may also occur to yield a vinyl-terminated polymer chain **VII** and a new secondary radical.

Given that the end group of PE-*i*-DIB is essentially an AMS unit, we wouldn't expect the macromonomer to homopropagate readily due to the low ceiling temperature of AMS;[3] but, depending on the reactivity ratios of AMS and *n*-BA, the addition of a significant concentration of PE-*i*-DIB macromonomer to a free radical polymerisation of *n*-BA provides another species for the P(*n*-BA) chains to react with which would result in the formation of copolymers. It would therefore be expected to have a significant effect on the molecular weight of the P(*n*-BA) chains formed in its presence given that cross-propagation with the macromonomer would be expected to effectively act as a chain stopping mechanism. The presence of PE-*i*-DIB also increases the number of possible reactions involving the initiator radicals that escape the solvent cage (*vide infra*).

3.3 Free radical polymerisation of *n*-BA in the presence of PE-*i*-DIB

Copolymerisations of PE-*i*-DIB (M_n = 2300, $Đ$ = 2.0) with varying *n*-BA concentrations were conducted in toluene at 125°C using benzoyl peroxide (BP) as the initiator. Several ampoules were set up in parallel for each kinetic run and the progress of the reactions were followed by NMR and GPC, including plotting the GPC traces. Given its substantially shorter half-life at the reaction temperature,[12] BP ($t_{1/2}$ *ca* 1 min at 130°C)

was chosen over *tert*-butyl peroxide (TP) ($t_{1/2}$ *ca* 10 hr at 125°C) for these runs so that a large number of propagating chains would be formed at the beginning of the reaction. This had previously been discovered to convert the PE-*i*-DIB more quickly[10] and its rapid consumption would also allow us to see if the molecular weight would change with time after macromonomer and initiator consumption. At the appropriate time, the ampoules were opened and the mixture poured into stirring methanol. Macromonomer conversions in Table 3.1 were determined by comparison of the integrals of the sharp vinylidene proton signals of the DIB end group at 5.07 and 5.34 ppm in the ^{1}H NMR spectrum of each of the precipitated products, to those in the ^{1}H NMR spectrum of the PE-*i*-DIB macromonomer sample used for the run. †

Run 1 is a control run conducted to show how the *n*-BA polymerisation progresses in the absence of PE-*i*-DIB which yielded a high dispersity polymer in a yield corresponding to 90% of the monomer feed. The P(*n*-BA) produced in Run 1 was worked up by precipitation in methanol. Having worked up the product of Run 1 using methanol, using the same again to separate the PE-containing species from the P(*n*-BA) by-products seems counter-intuitive. However, it was found that much lower molecular weight P(*n*-BA) was produced in the presence of PE-*i*-DIB in most cases and was therefore soluble in methanol. The success of this process in the various runs will be discussed throughout the chapter.

† Integrated against the benzylic proton environment at 2.70 ppm corresponding to PE chains initiated by DIB (Chapter 2).[10]

Table 3.1 - Free radical polymerisations of *n*-BA in presence of PE-*i*-DIB.

Run	Time (min)	Yield (g/%)	M_p [e] (g/mol)	M_n [e] (g/mol)	M_w [e] (g/mol)	Đ [e]	PE-*i*-DIB Conversion (%)[f]
1[a]	180	4.43/90	91100	22100	202300	9.2	-
2[b]	5	0.252/9	7500	4000	12700	3.2	37
	10	0.339/23	12100	6000	16300	2.7	89
	20	0.388/31	11800	6900	14400	2.1	100
	40	0.394/32	13400	7800	17300	2.3	100
	60	0.395/33	11000	7400	15600	2.1	100
	120	0.400/34	11500	7700	17500	2.3	100
	180	0.368/28	11500	7000	15700	2.2	100
3[c]	5	1.38/49	76600	26800	125800	4.7	100
	10	1.48/53	51400	23500	85700	3.7	100
	20	1.55/56	56600	23700	97200	4.1	100
	40	1.63/60	47200	24000	81800	3.4	100
	60	1.68/62	56500	23800	104200	4.4	100
	120	1.70/63	51000	23700	85400	3.6	100
	180	1.46/53	39000	19200	69200	3.6	100
4[d]	5	3.36/64	88000	39800	161700	4.1	100
	10	3.36/64	183400	39700	251300	6.3	100
	20	3.56/69	172700	46500	297800	6.4	100
	40	3.35/64	133800	44800	271300	6.1	100
	60	3.47/67	159000	42100	256800	6.1	100
	120	3.42/66	180300	42500	278300	6.5	100
	180	3.43/66	135100	40200	298500	7.4	100

[a] Polymerisation conditions: comonomer = *n*-BA; total mass *n*-BA added = 4.9 g (5.5 ml); initiator = BP; [initiator] solution = 0.011 mol/L; solvent = toluene; total volume = 8.2 ml; temperature = 125°C.
[b] Polymerisation conditions: PE-*i*-DIB = 0.2 g, M_n = 2300 g/mol, Đ = 2.0; initial [PE-*i*-DIB] = 0.011 mol/L; comonomer = *n*-BA; total mass *n*-BA added = 0.61 g (0.68 ml); *n*-BA:PE = 50:1; initiator = BP; [initiator] solution = 0.011 mol/L; solvent = toluene; total volume = 8.2 ml; temperature = 125°C.
[c] mass *n*-BA added = 2.4 g (2.7 ml); *n*-BA:PE = 200:1.
[d] mass *n*-BA added = 4.9 g (5.5 ml); *n*-BA:PE = 400:1.
[e] GPC data obtained at 160°C in 1,2,4-trichlorobenzene using universal calibration. PS standards were used to calibrate the system (see Chapter 6, Section 6.1 for further details).
[f] Calculated from ^{1}H NMR.

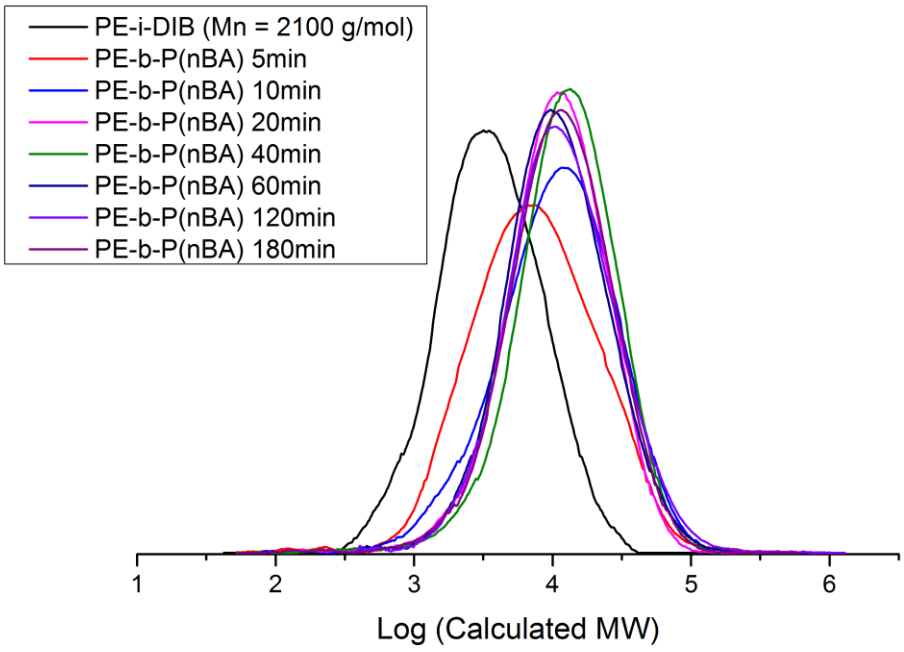

Figure 3.1 - GPC traces following the progress of the free radical polymerisation of *n*-BA in the presence of PE-*i*-DIB (Run 2, Table 3.1).

Runs 2-4 in Table 3.1 follow the progress of the copolymerisations with PE-*i*-DIB over time at increasing *n*-BA:PE-*i*-DIB molar ratios (50:1, 200:1 and 400:1). In Run 2 complete macromonomer conversion was observed by t = 20 min by ^{1}H NMR and this coincides with an increase in recorded yield, molecular weight and dispersity with time up to t = 10 min, which is consistent with copolymerisation. After t = 10 min the dispersities and the molecular weights differ very little, which is no surprise given the consumption of macromonomer and initiator by this point. The GPC traces shown in Figure 3.1 support the molecular weight increase with time up to t = 10 min, but the overlap of the subsequent traces indicates that little further molecular weight change has occurred after this time. As shown in Table 3.2, the molecular weight and dispersity of the P(*n*-BA) homopolymer by-product for Run 2 was very low (M_n 2000 g/mol, $Đ \sim 1.7$) by comparison to Run 1 (M_n 22,000 g/mol, $Đ \sim 9.2$). As a consequence, when the

reaction mixture was poured into methanol the homopolymer remained in solution while the PE-containing copolymer was precipitated. ^{1}H NMR spectra for both species (Figures 3.4 and 3.5) and mass balance are consistent with this.

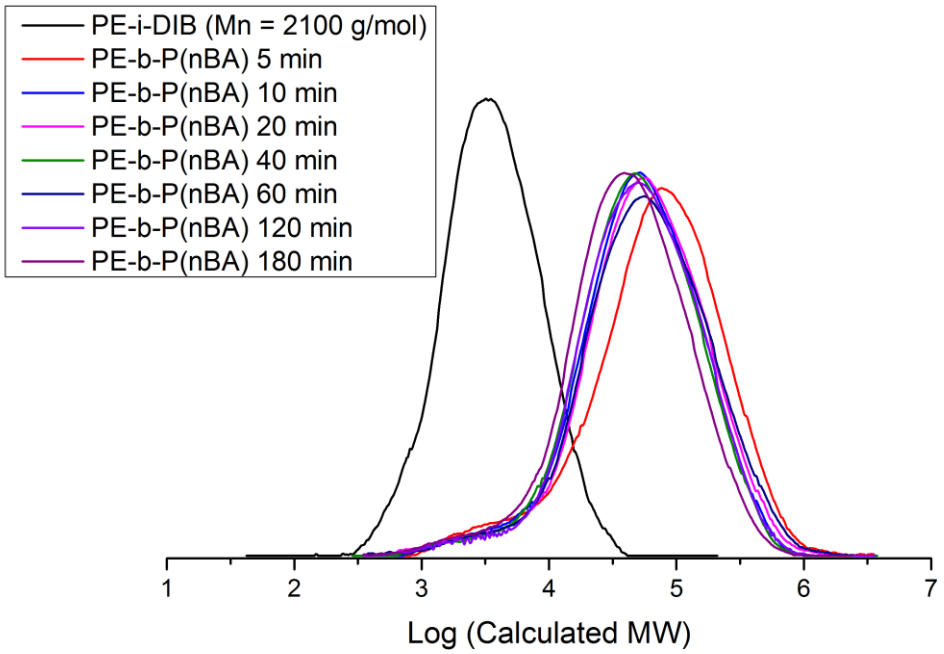

Figure 3.2 - GPC traces following the progress of the free radical polymerisation of *n*-BA in the presence of PE-*i*-DIB (Run 3, Table 3.1).

Macromonomer conversion was achieved more quickly in Run 3 in the presence of a higher concentration of *n*-BA monomer. The molecular weight data is more akin to that of the data after *t* = 10 min from Run 2 which, given the far more rapid consumption of PE-*i*-DIB, is perhaps not surprising. We would expect little difference in yield or molecular weight of the precipitated products for most of the reaction on this basis. This was indeed the case with Run 3 and the GPC traces shown in Figure 3.2 are consistent with these observations, indicating little change in molecular weight once the macromonomer was converted. Again the molecular weight of the homopolymer by-product was apparently sufficiently low to remain in solution in methanol while the PE-

containing materials were precipitated, as suggested by the mass balance and ^{1}H NMR data (Figure C.1. and C.3.).

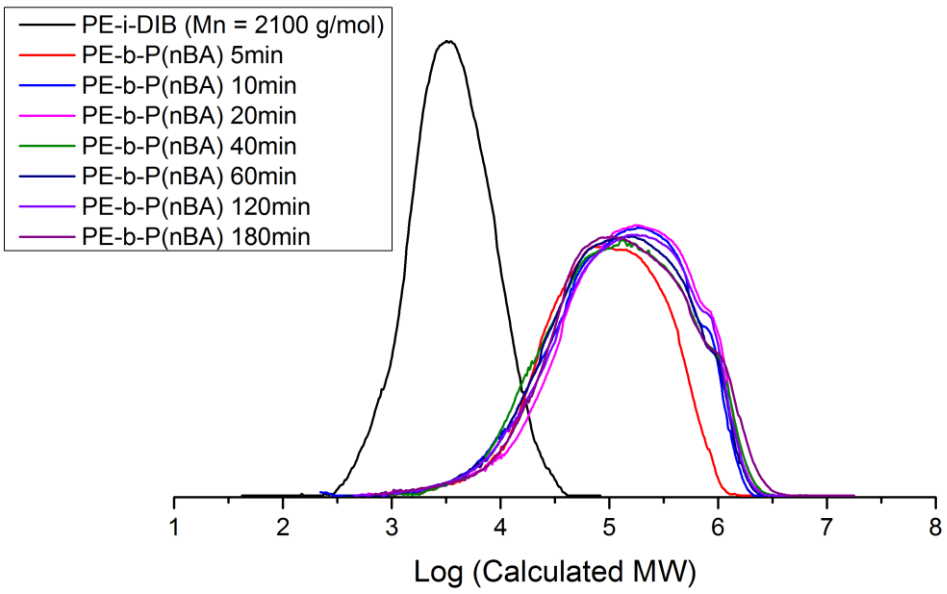

Figure 3.3 - GPC traces following the progress of the free radical polymerisation of *n*-BA in the presence of PE-*i*-DIB (Run 4, Table 3.1).

In Run 4 the macromonomer was again converted in the first 5 min of the reaction. The consistency of the recorded yields and the molecular weights would suggest that again, very little is happening following macromonomer conversion. The high monomer concentration has also resulted in very broad GPC traces for the copolymer products (Figure 3.3). Although they still seem to show that very little change in molecular weight had occurred, the dispersities are all broad and they increased substantially after t = 5 min. The broadness is likely to be partially a result of the co-precipitation of P(*n*-BA) homopolymer given that its molecular weight (Table 3.2) in this run was far higher than in Runs 2 and 3 and more similar to that of Run 1 where the homopolymer product was precipitated in methanol.

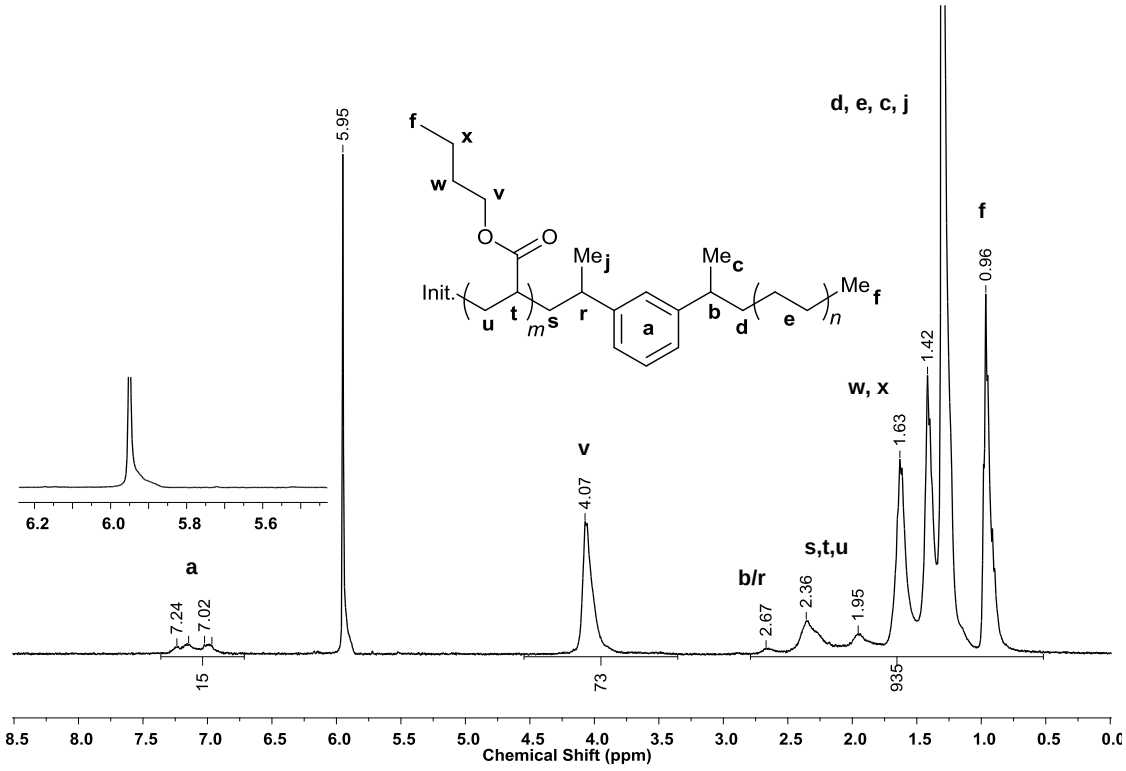

Figure 3.4 - ^{1}H NMR spectrum of P(*n*-BA)-*b*-PE-*i*-DIB from Run 2 in d^2-TCE at 100°C (400MHz).

^{1}H NMR spectra of the PE-containing material from Runs 2 and 3 (Figures 3.4 and C.1.) showed signals corresponding to PE and P(*n*-BA) (more detailed analysis in Chapter 4) and contained no signals at 5.5 and 6.2 ppm corresponding to P(*n*-BA) macromonomer end groups (*vide infra*);[13] the ^{1}H NMR spectrum for Run 4 (Figure C.2.) however, did show such vinyl end group signals. This would suggest that this sample does contain some P(*n*-BA) macromonomer and thus, in all likelihood, also contains some higher molecular weight, non-macromonomer P(*n*-BA) given the molecular weight of the homopolymer formed in this run (Table 3.2). This would suggest that the separation by precipitation was successful for Runs 2 (above) and 3 but not for Run 4, which is not necessarily surprising.

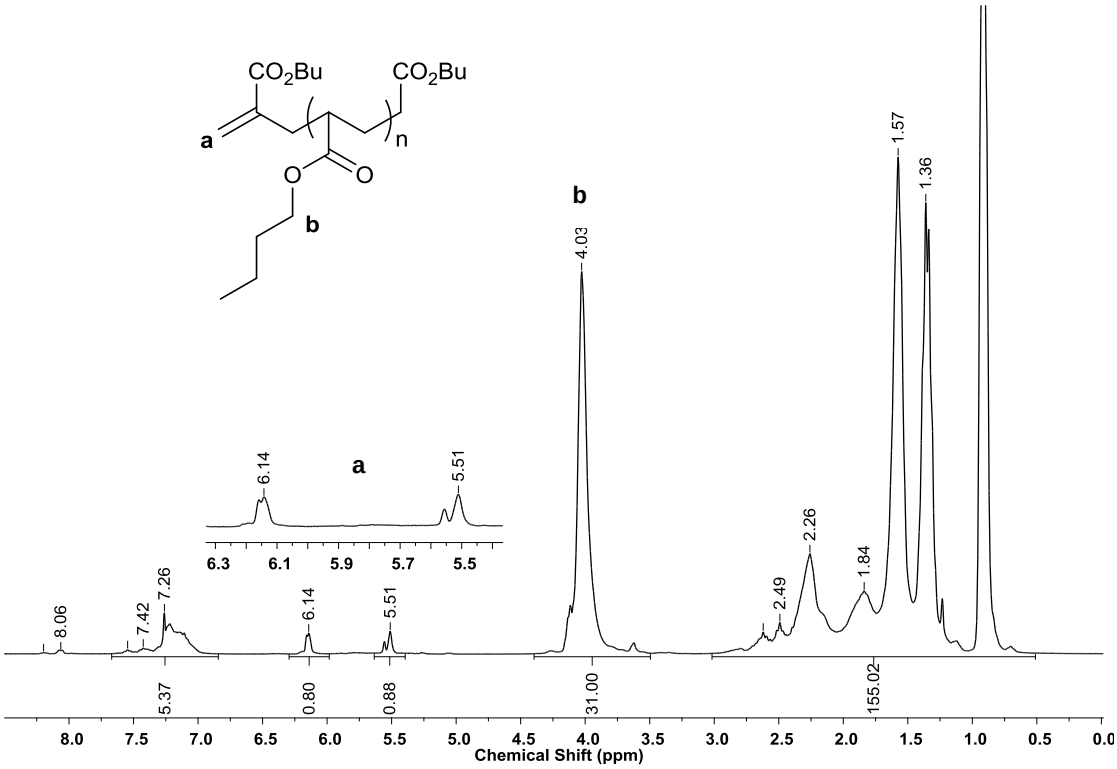

Figure 3.5 - ^{1}H NMR spectrum of P(*n*-BA) by-product (M_n = 2000 g/mol, $Đ$ = 1.7) from Run 2 in $CDCl_3$ at 25°C (400MHz).

^{1}H NMR spectra of the soluble homopolymer formed in Runs 2-4 (*e.g.* Figure 3.4) showed no signals corresponding to PE, which indicated that all PE-containing materials were recovered by precipitation. Signals corresponding to P(*n*-BA) were detected however, as well as vinyl signals at 6.2 and 5.5 ppm. These were assignable to end-group protons for P(*n*-BA) macromonomer, consistent with those observed by Moad and co-workers that were proposed to be formed by chain scission following chain transfer to the P(*n*-BA) backbone.[13]

Both fragmentation by chain scission[14, 15] and chain transfer to polymer backbone are known processes; indeed the latter has been studied previously in poly(acrylate) synthesis in which branch formation was reported.[16] Chain transfer to the polymer backbone can occur either by an intermolecular (another radical) or intramolecular (backbiting) H abstraction and the results provided by Moad[13] and Lovell[16] respectively

suggest that the predominant mechanism is monomer concentration-dependent, *i.e.* at lower monomer concentration the intramolecular mechanism is more prevalent, while at higher concentrations the intermolecular mechanism becomes more important. Once chain transfer to polymer has occurred, monomer can either add to the resulting radical to form branches, or fragmentation (β-scission) can occur to yield a vinyl-terminated macromonomer and a new propagating radical. In the same publication as discussed above, Moad reports that the molecular weight of the synthesised P(*n*-BA) macromonomers can be controlled by varying both reaction temperature and monomer concentration; it was found that increasing the temperature and decreasing the monomer concentration both resulted in lower molecular weight polymers. Based on these reports, and noting that the incidence of backbone H abstraction in ethylene polymerisation is known to increase with temperature,[17, 18] an acrylate polymerisation conducted at low monomer concentration and high temperature could be expected to undergo a significant number of incidences of both backbone methine H abstraction and of fragmentation, the result of which would be a lower molecular weight polymer containing a terminal vinyl group.

The reported temperature range of 80-240°C[13] for this chemistry to occur suggests that P(*n*-BA) macromonomer formation ought to be significant under our conditions and, sure enough, both the homopolymer formed in the reactions involving PE-*i*-DIB and that formed in the runs without both show vinyl signals in the ^{1}H NMR spectrum at 5.5 and 6.2 ppm that are consistent with those reported to be formed from such a process. The relative integrals[†] of the vinyl end-group signals at 5.5 and 6.2 ppm and the first

[†] Expected integral of P(*n*-BA) butyl ester CH_2 at 4.1 ppm was calculated based on the homopolymer M_n of 2000 g/mol and, with the ester integral set to that expected value, the integral of the vinyl proton signals at 5.5 and 6.2 ppm gave an estimate of the relative macromonomer amount (vinyl integral = 2 indicates that 100% of the polymer in the sample contains these end groups).

methylene signals of the butyl ester at 4.1 ppm can be used to estimate the relative amount of P(*n*-BA) macromonomer compared to non-macromonomer products;[13] as an example, in Run 2 (Figure 3.4) the integrals would suggest that at this high temperature and lower monomer concentration the proportion of the P(*n*-BA) isolated that contains vinyl end groups is *ca* 84%. As discussed above, the lower the monomer concentration, more P(*n*-BA) macromonomer would be expected to form and this, combined with the yields and % yields of the block copolymer and homopolymer reported in Tables 3.1 and 3.2, accounts for much of the P(*n*-BA) species formed in runs 2 and 3 (Figure C.3.); although this gets less reliable for Run 4 (Figure C.4.) where the monomer concentration is much higher, so consequently the P(*n*-BA) molecular weight is higher, and vinyl signals from unreacted *n*-BA monomer overlap with the P(*n*-BA) end group signals. It is worth noting at this point that P(*n*-BA) chains that have terminated by radical-radical combination would be much higher in molecular weight, so would look the same as the polar component of the copolymer by NMR, and that as the concentration of monomer increases the number of these terminations will increase, as will the addition of monomer to mid-chain radicals to form branches. Hence, in the reactions with higher monomer concentration and therefore also higher molecular weight, possibly branched P(*n*-BA) chains (*e.g.* Run 4), we cannot rule out co-precipitation of some higher molecular weight homopolymer chains. The moleculear weight limit for solubility of the P(*n*-BA) macromonomer would appear to be *ca* 8000 – 9000 g/mol based on the data obtained for runs 1-4; we therefore speculate that any chains of higher molecular weight than this could well co-precipitate with the PE-containing materials.

Table 3.2 – GPC data of P(*n*-BA) homopolymer by-product from free radical polymerisations of *n*-BA in the presence of PE-*i*-DIB.

Run[a]	Time (min)	Yield (g/%)	M_p [d] (g/mol)	M_n [d] (g/mol)	M_w [d] (g/mol)	Đ [d]
2	5	0.012/2	2000	1600	2600	1.6
	10	0.074/12	1900	1500	2400	1.6
	20	0.179/29	2200	1700	2900	1.7
	40	0.241/40	2300	1900	3200	1.7
	60	0.257/42	2300	1800	3000	1.7
	120	0.278/45	2500	1800	3300	1.9
	180	0.293/48	2600	2000	3500	1.8
3[b]	5	0.147/6	11000	7200	14400	2.0
	10	0.638/27	9400	3400	9300	2.7
	20	0.774/32	9400	3500	9400	2.7
	40	0.830/35	9500	4200	11000	2.6
	60	0.813/34	9100	3700	8900	2.4
	120	0.754/31	8300	3200	7700	2.4
	180	1.01/42	7400	2800	6900	2.5
4[c]	5	0.916/19	15900	7000	17000	2.4
	10	0.907/19	19100	8800	28700	3.3
	20	1.03/21	23800	11600	33700	2.9
	40	0.961/20	21200	10500	27700	2.6
	60	0.876/18	18500	8400	20600	2.4
	120	0.737/15	21200	12400	24900	2.0
	180	0.730/15	14300	7700	18300	2.4

[a] Polymerisation conditions: Polymerisation conditions: PE-*i*-DIB = 0.2 g, M_n = 2300 g/mol, Đ = 2.0; initial [PE-*i*-DIB] = 0.011 mol/L; comonomer = *n*-BA; total mass *n*-BA added = 0.61 g (0.68 ml); *n*-BA:PE = 50:1; initiator = BP; [initiator] solution = 0.011 mol/L; solvent = toluene; total volume = 8.2 ml; temperature = 125°C.

[b] *n*-BA added = 2.4 g (2.7 ml); *n*-BA:PE = 200:1.

[c] mass *n*-BA added = 4.9 g (5.5 ml); *n*-BA:PE = 400:1.

[d] GPC data obtained at 30°C in $CHCl_3$ using conventional calibration vs PMMA standards.

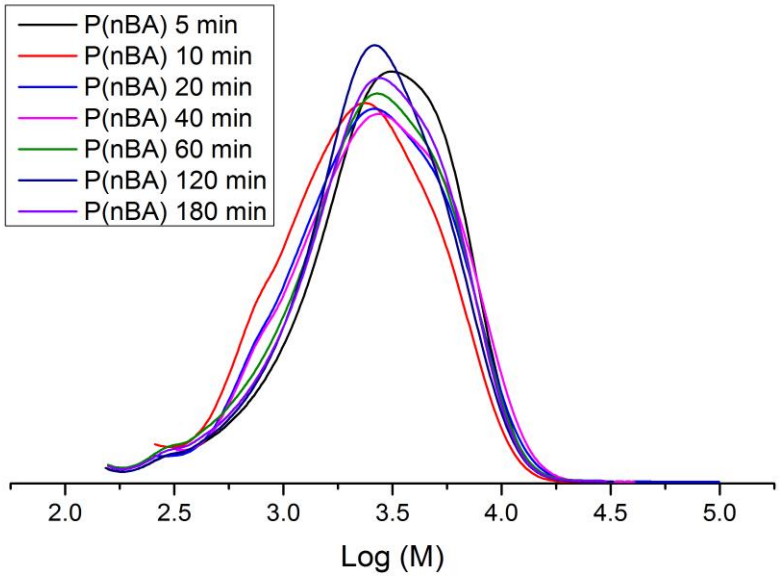

Figure 3.6 - GPC traces following the production of P(*n*-BA) homopolymer in the copolymerisation of *n*-BA with PE-*i*-DIB (Run 2, Table 3.1).

The P(*n*-BA) samples from Runs 2-4 were analysed by GPC (Table 3.2) and their traces plotted for comparison. The recorded yields increased with time in both runs up to a certain point, before dropping slightly with more extended reaction times. In Run 2 the homopolymer molecular weights and dispersities remained consistent and consistently low throughout (M_n ~ 1800 g/mol, $Đ$ ~ 1.7) and this is supported by the GPC traces in Figure 3.6. In Run 3, after t = 5 min the P(*n*-BA) homopolymer samples were formed with similar molecular weights (M_n ~ 3500 g/mol) and dispersities (~2.5). However in Run 4, where the monomer concentration was much higher, the molecular weight was correspondingly much higher which is consistent with the difference in solubility of this homopolymer in methanol compared to Runs 2 and 3. The general trend in this case is an initial increase in molecular weight and dispersity with time followed by a drop with more extended reaction times.

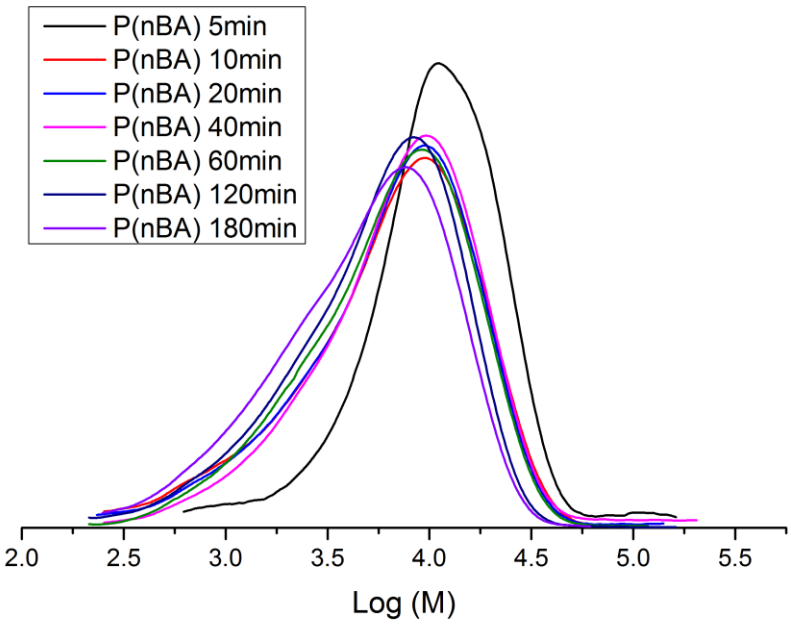

Figure 3.7 - GPC traces following the production of P(*n*-BA) homopolymer in the copolymerisation of *n*-BA with PE-*i*-DIB (Run 3, Table 3.1).

The GPC traces for Run 3 (Figure 3.7) do indeed show that the molecular weights and dispersities of the homopolymer samples remained fairly consistent for the remainder of the reaction, following the substantial drop in molecular weight and rise in dispersity between $t = 5$ and $t = 10$ min. Given the consistent yields and molecular weights obtained for the copolymer samples, this indicates that the majority of the monomer feed was consumed in the first 5 min of the reaction. After this point backbiting and subsequent β-scission of the homopolymer chains is likely to have taken effect at the high temperature and in the presence of a now far lower monomer concentration,[8, 7, 13, 19, 20] thus accounting for the substantial fall in molecular weight of the subsequent sample and the similarity of the molecular weights of the samples thereafter.

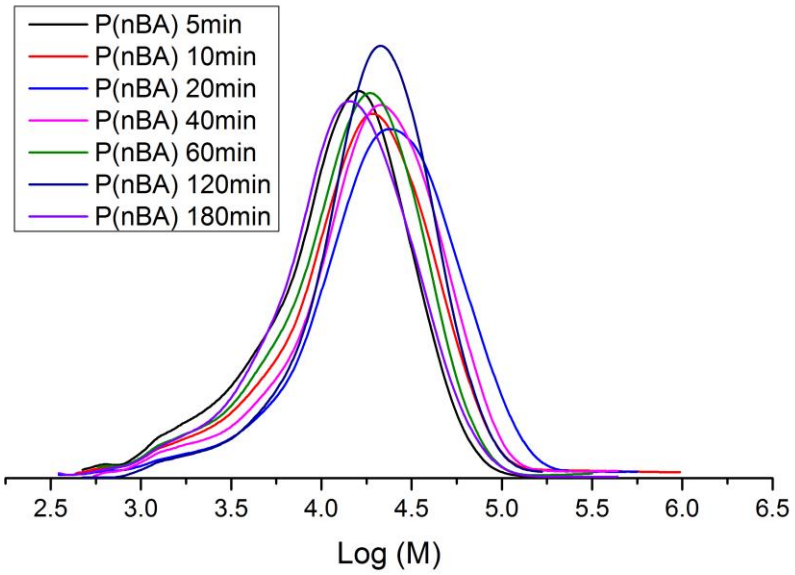

Figure 3.8 - GPC traces following the production of P(*n*-BA) homopolymer in the copolymerisation of *n*-BA with PE-*i*-DIB (Run 4, Table 3.1).

Figure 3.8 shows the traces for the homopolymer samples from Run 4, which again are consistent with the corresponding molecular weight data, showing an initial increase in homopolymer molecular weight before a slight drop as time went on. Like Run 3, the macromonomer was converted in the first 5 min of the reaction; however in this case, presumably due to the larger initial monomer feed, the monomer concentration apparently remained sufficiently high after PE-*i*-DIB conversion to facilitate the continued molecular weight growth of the homopolymer for a significant period of time while there was still initiator present before the conditions eventually favoured the backbiting and chain scission process which is likely to have been responsible again for lowering the P(*n*-BA) molecular weight with longer reaction times.

These observations provide a potential explanation for that fact that the molecular weight of the homopolymer samples is substantially lower than the P(*n*-BA) component of the

polar block. The larger chains are likely to have been produced at the beginning of the reaction when the monomer and initiator concentrations were at their highest. Many of these larger chains will have been rapidly consumed by the PE-*i*-DIB, which was also at its highest concentration. After the PE was converted, a much smaller monomer concentration would be present in a much more viscous reaction medium at a high reaction temperature. Under these conditions further propagation and termination processes would be much slower as a result of slower diffusion of molecules,[21] but intramolecular chain transfer to polymer would still be expected to occur. We propose that an increase in backbiting and *β*-scission of P(*n*-BA) chains under these conditions leads to the drop in homopolymer molecular weight observed after macromonomer conversion. In run 4, the higher monomer concentration would have led to longer P(*n*-BA) chains which were consumed even more quickly by the macromonomer. It is possible that the faster consumption of the macromonomer and the higher initial monomer concentration would, despite the visibly more viscous reaction medium, have led to a situation where sufficient monomer remained to favour propagation over backbiting and cause an increase in homopolymer molecular weight up to a certain point. After this the rate of diffusion and monomer concentration would have decreased such that backbiting predominates and the molecular weight decreases with time accordingly.

3.4 Free radical polymerisation of *n*-BA in the presence of PE-*i*-DIB under starved-feed semi-batch conditions

The copolymerisations discussed in the previous section, as well as in previous work,[10] showed that a range of molecular weight PE-*b*-P(*n*-BA) copolymers could be synthesised and purified under very practical conditions with efficient conversion of the PE-*i*-DIB macromonomer. Analysis of both the precipitated copolymer products and the

soluble homopolymer by-products also yielded valuable information as to the mechanism for the copolymerisation (*vide infra*). However, the molecular weight distributions of many of the materials presented and the amount of P(*n*-BA) homopolymer produced in the runs imply a distinct limitation in the degree of control we currently have over the process under batch conditions. This is undoubtedly compounded by the high reaction temperature, high monomer and initiator concentrations, the efficiency with which the macromonomer is converted under these conditions and the apparently limited ability of the macromonomer to mediate the *n*-BA polymerisation during its lifetime in the reaction.

Starved-feed polymerisations are semi-batch reactions where the monomer and initiator are fed continuously into the reaction vessel containing a fixed volume of solvent, thus enabling effective control over the molecular weight of the products by the ratio of addition rates of monomer and initiator.[22] The high reaction temperatures remain but the monomer and initiator concentrations are kept low due to their almost instantaneous consumption as they are fed in, resulting in the production of low molecular weight polymers and copolymers.[23] Due to the low molecular weight materials being produced, the gel effect is also far weaker under these conditions and the viscosity of the mixture is substantially reduced.[22, 24] These factors considered, a starved-feed process seemed likely to provide the improvement in control over the polymerisation we were looking for, giving us access to low molecular weight materials as well as a far more practical process for potential scale up.

3.4.1 Control reactions in the absence of macromonomer

Free radical polymerisations of *n*-butyl acrylate (7.3 g, 8 ml) in the absence of PE-*i*-DIB were conducted in toluene at 110°C under dinitrogen using BP as the initiator. 2.5 ml

samples of the reaction mixture were taken by syringe periodically for analysis. Runs 5 and 6 (Table 3.3) were conducted under different monomer and initiator delivery conditions. Run 5 was conducted with all monomer and initiator added at t = 0 min, similar to the ampoule runs (*vide supra*), while Run 6 was conducted under starved feed conditions with controlled addition of both monomer and initiator over the course of the reaction.

^{1}H NMR and GPC data show low molecular weight P(*n*-BA) was produced in both runs but the method of delivery of the monomer and initiator feeds affects the evolution of molecular weight and dispersity with time, as well as monomer conversion. In Run 5 90% monomer conversion was achieved in 60 min but very little change in molecular weight or dispersity with time was observed throughout this run. This is not surprising given the rapid consumption of initiator and monomer feed under these conditions. In contrast, steady molecular weight increase with time and a reduced monomer conversion (63%) were observed in Run 6 where the monomer and initiator were fed in over the course of the polymerisation. As expected, the starved feed setup seemed to allow greater control over the polymerisation, as evidenced by the lower and more consistent dispersities in Run 6.

Table 3.3 - Free radical polymerisations of *n*-butyl acrylate in absence of PE-*i*-DIB. How polymerisation is affected by changes in monomer and initiator feed delivery.

Run[a]	Time (min)	Yield (g/%)	M_p [c] (g/mol)	M_n [c] (g/mol)	M_w [c] (g/mol)	$Đ$ [c]
5	10	0.165	9600	4400	12100	2.8
	20	0.178	8200	3500	11100	3.1
	30	0.206	7900	3200	9700	3.0
	40	0.207	7700	3100	9400	3.0
	50	0.201	7700	2900	9100	3.2
	60	0.222	7400	2800	9300	3.3
	Remainder	5.37/90	7700	2900	9500	3.3
6[b]	10	0.003	-	-	-	-
	20	0.018	2400	1400	2700	1.9
	30	0.045	3400	2000	4200	2.1
	40	0.080	5300	2300	4900	2.1
	50	0.121	5800	2600	5400	2.0
	60	0.281	5200	2800	5600	2.0
	Remainder	4.16/63	7000	3100	7600	2.5

[a] Polymerisation conditions: Monomer = *n*-BA; total mass *n*-BA added = 7.3 g; initiator solution = 0.11 mol/L in 10 ml solvent; solvent = toluene; initial reaction volume = 78 ml; temperature = 110°C; total polymerisation time = 1 hour.
[b] Initial reaction volume = 60 ml; initiator addition rate = 10 ml/hr (1.14×10^{-3} mol/hr); monomer addition rate = 8 ml/hr (0.057 mol/hr).
[c] GPC data obtained at 30°C in $CHCl_3$ using conventional calibration vs PMMA standards.

3.4.2 Copolymerisation of macromonomer with *n*-BA

Having observed the behaviour of the *n*-BA homopolymerisation under the two monomer and initiator delivery strategies, the effect of introducing PE-*i*-DIB macromonomer was investigated by conducting analogous free radical polymerisations of *n*-butyl acrylate in the presence of PE-*i*-DIB (2.4 g, M_n = 2100 g/mol, $Đ$ = 2.0) at a *n*-BA:PE molar ratio of 50:1. Copolymerisations were conducted in toluene at 110°C to ensure complete dissolution of the PE-*i*-DIB and samples were taken periodically from the main mixture by syringe for analysis as before. The copolymer samples were isolated by pouring the mixture into excess methanol after exposure to air, where the PE

component would force the copolymer out of solution while the soluble homopolymer and unreacted monomer remained dissolved. The precipitates were then filtered and dried in a vacuum oven overnight.

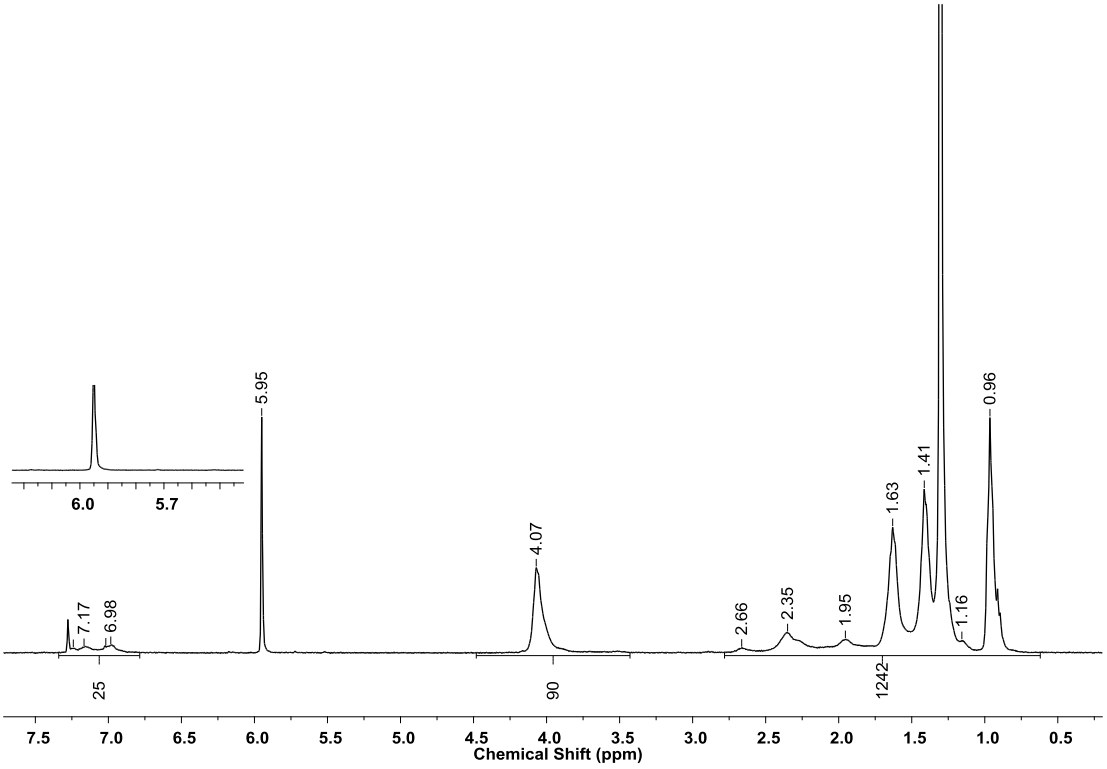

Figure 3.9 - ^{1}H NMR spectrum of P(*n*-BA)-*b*-PE-*i*-DIB from Run 8, Chapter 3 in d^{2}-TCE at 100°C (400MHz).

The ^{1}H NMR spectrum of the final precipitated product (Figure 3.9) contained signals corresponding to both PE and P(*n*-BA) after multiple reprecipitations; the absence of DIB vinylidene proton signals at 5.07 and 5.34 ppm indicate complete conversion of the PE-*i*-DIB starting material. The absence of P(*n*-BA) vinylidene signals at 5.5 and 6.2 ppm indicates the successful separation of copolymer from low molecular weight homopolymer by precipitation. The absence of PE-containing material in the soluble fraction by ^{1}H NMR (Figure 3.10) indicates complete recovery of PE-containing species. Signals at 5.5 and 6.2 ppm corresponding to vinyl-terminated P(*n*-BA) formed by backbiting and subsequent chain scission at high temperatures were detected as in the

batch runs (*vide supra*). The use of relative integrals, based on a polymer M_n of 1900 g/mol, $Đ$ = 1.8 by GPC, was used again to estimate the relative amount of macromonomer present; in the case of Figure 3.10, the analysis suggests that *ca* 50% of the homopolymer contained a vinyl end group. The molecular weight of the homopolymer is very similar to that isolated by working up the soluble fractions from runs 2 and 3, where the P(*n*-BA) was apparently soluble in methanol and no evidence of homopolymer contaminant was detected in NMR. It is also far below that obtained in Run 1 where pouring into methanol was found to precipitate the P(*n*-BA), and Run 4 where the copolymer NMR spectrum showed evidence of P(*n*-BA) macromonomer in the precipitated sample.

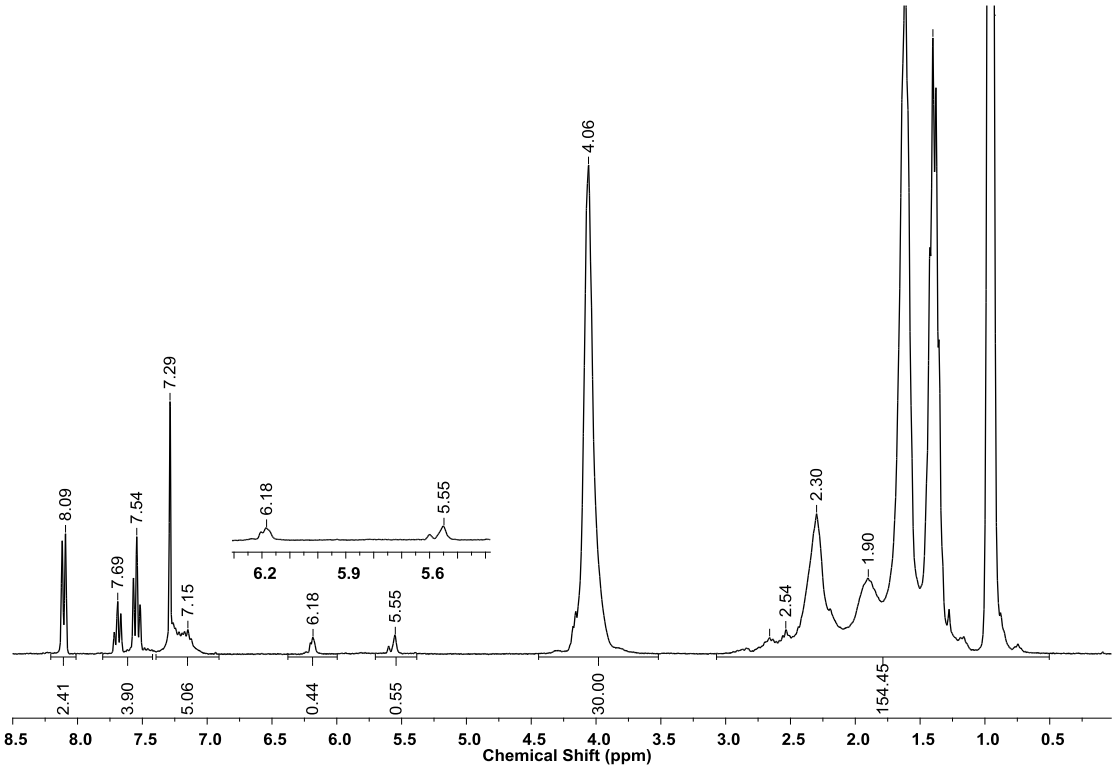

Figure 3.10 - ^{1}H NMR spectrum of P(*n*-BA) by-product (M_n = 1900 g/mol, $Đ$ = 1.8) from Run 8 in $CDCl_3$ at 25°C (400MHz).

In Run 7 (Table 3.4) complete DIB end group conversion was observed by ^{1}H NMR from the early stages (t = 10 min) and molecular weight did not change substantially

while an increase in dispersity towards the end of the polymerisation was noted. The recovered yields remain consistent throughout the polymerisation. While overall monomer conversion was high (88%) only 40% of that was incorporated in the copolymer by mass.

Table 3.4 - Free radical polymerisations of *n*-butyl acrylate in presence of PE-*i*-DIB. How copolymerisation is affected by changes in monomer and initiator feed delivery.

Run[a]	**Time (min)**	**Yield (g/%)**	M_p [c] **(g/mol)**	M_n [c] **(g/mol)**	M_w [c] **(g/mol)**	$Đ$ [c]	**PE-*i*-DIB Conversion (%)**[d]
7	20	0.166	15800	7700	18500	2.4	100
	30	0.172	20500	11000	21800	2.0	100
	40	0.17	17600	8400	19400	2.3	100
	50	0.173	17800	7700	20200	2.6	100
	60	0.173	16700	6700	19200	2.8	100
	Remainder	4.3/38	15600	6800	22200	3.2	100
8[b]	20	0.091	2600	2500	5000	2.0	16
	30	0.104	3200	2900	6800	2.3	53
	40	0.123	13000	4500	12400	2.7	87
	50	0.139	14600	6800	14200	2.0	97
	60	0.180	16000	7900	17300	2.2	100
	Remainder	3.5/24	17600	7900	16200	2.0	100

[a] Polymerisation conditions: PE-*i*-DIB = 2.4 g, M_n = 2100 g/mol, Đ = 2.0; initial [PE-*i*-DIB] = 0.019 mol/L; comonomer = *n*-BA; total mass *n*-BA added = 7.3 g (8 ml); *n*-BA:PE = 50:1; [initiator] solution = 0.11 mol/L in 10 ml solvent; solvent = toluene; initial volume = 78 ml; temperature = 110°C; polymerisation time = 1 hour.
[b] Initial reaction volume = 60 ml; initiator addition rate = 10 ml/hr (1.14×10^{-3} mol/hr), monomer addition rate 8 ml/hr (0.057 mol/hr); *n*-BA:PE = 50:1.
[c] GPC data obtained at 160°C in 1,2,4-trichlorobenzene using universal calibration. PS standards were used to calibrate the system (see Chapter 6, Section 6.1 for further details).
[d] Calculated from ^{1}H NMR.

^{1}H NMR and GPC of the methanol soluble fractions of the aliquots for Run 7 showed that low molecular weight, low dispersity P(*n*-BA) was also produced, fairly similar to that produced in the corresponding homopolymerisation (Run 5, Table 3.3). Consistent with the hompolymerisation described earlier, the P(*n*-BA) molecular weight and

dispersity did not change significantly with time and the recovered yield did not significantly change from t = 20 min when the macromonomer was present. The molecular weight data suggests that both the copolymerisation and the homopolymerisation were completed rapidly in the presence of high initial monomer and initiator concentrations.

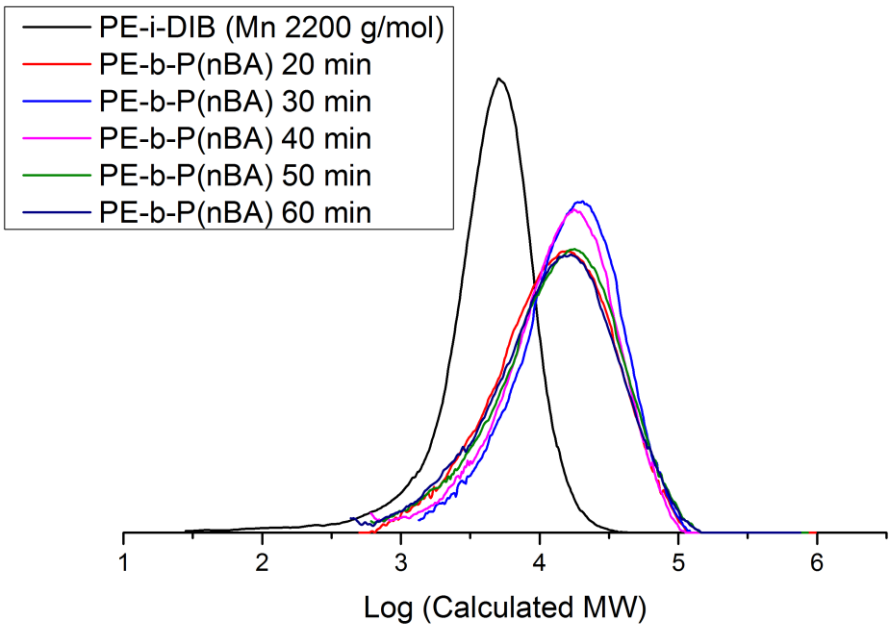

Figure 3.11 - GPC traces following progress of free radical polymerisation of n-BA in presence of PE-*i*-DIB (Run 7, Table 3.4).

This is supported by the GPC traces in Figure 3.11 that show the shift to higher molecular weight with time from t = 0 to t = 20 min, but then the traces for the samples taken from this point onwards overlap with each other. Given that the monomer and initiator were all added at the start of the reaction, we would expect both to be consumed quickly at this high reaction temperature. This means the reaction is likely to have been completed in the first 20 min and unlikely to continue further due to the small monomer and initiator concentrations remaining by this point. This run was very similar to Run 2

in section 3.2 and this is reflected in the similar trends observed in the data obtained for both the copolymer and the soluble homopolymer.

In Run 8 slower conversion of the DIB end groups (97% at t = 50 min) was observed due to the lower monomer and initiator concentrations under starved feed conditions, as well as a steady increase in copolymer yield with time. Monomer conversion by mass was also substantially lower, 64% of which only 26% was converted to copolymer. Analysis of the copolymer samples showed that P(*n*-BA) NMR signal integrals and copolymer molecular weight increased with time throughout the polymerisation, similar to the corresponding homopolymerisation control reaction discussed earlier. Analysis of the methanol soluble fractions (Figures C.5. – C.7.) showed that, interestingly, no P(*n*-BA) homopolymer was detectable by NMR or by GPC until t = 40 min by which point 87% of the PE-*i*-DIB macromonomer had been converted. Given that only low molecular weight homopolymer was isolated at the end of the reaction and that up to this point only P(*n*-BA) homopolymer of M_n ~10,000+ g/mol had been precipitated (Runs 1 and 4), it is reasonable to suggest that in the time up to t = 40 min any P(*n*-BA) that was being produced was cross-propagating with the macromonomer while it was present in higher concentration than the propagating P(*n*-BA) radicals as opposed to terminating by radical-radical combination or *via* backbiting and chain scission. However, at lower macromonomer concentration the P(*n*-BA) may terminate by other mechanisms resulting in the formation of significant amounts of homopolymer.

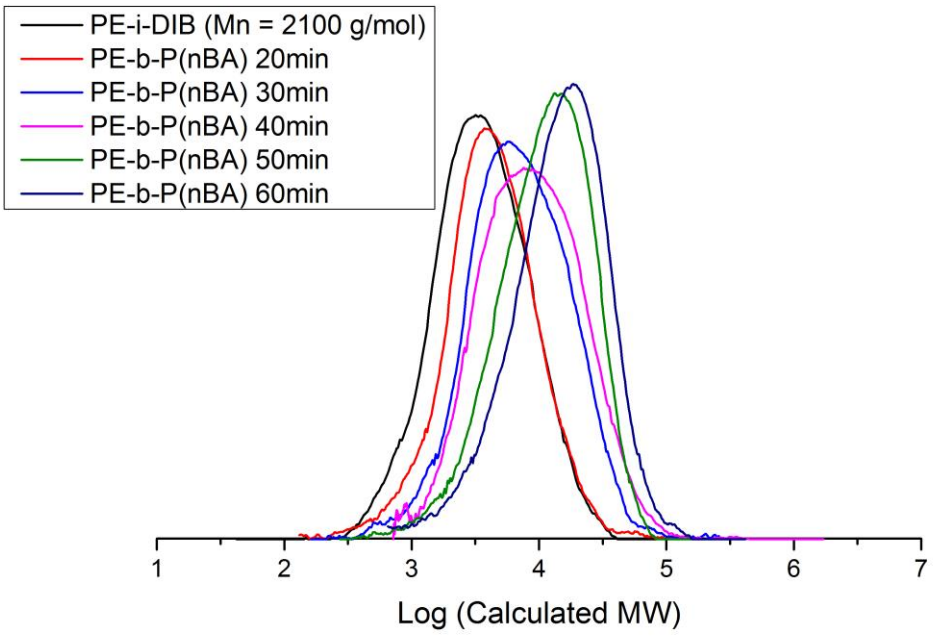

Figure 3.12 - GPC traces following progress of free radical polymerisation of n-BA in presence of PE-*i*-DIB (Run 8, Table 3.4).

The progress of the copolymerisation can be followed by plotting the GPC traces of the samples taken over the course of the reaction (Figure 3.12). The broadening of the GPC traces and the increase in dispersity up to t = 40 min is indicative of the presence of both the copolymer product and significant amounts of PE-*i*-DIB starting material, with consumption of the latter responsible for the narrowing of the traces and dispersities of subsequent samples. Under starved feed conditions the molecular weight of the copolymer continued to increase throughout the reaction, as evidenced both by the data in Table 3.4 and the GPC traces in Figure 3.12.

3.4.3 Effect of monomer addition rate

The controlled addition of both monomer and initiator allowed greater control over the process and enabled the continuous increase in molecular weight of the P(*n*-BA)

component with time throughout while macromonomer remained available to terminate to. Under starved feed conditions the molecular weight of the product is known to be controllable by the ratio of monomer and initiator feed rates[22] and thus, Runs 9-11, conducted at *n*-BA:PE molar ratios of 100:1, 25:1 and 12.5:1 respectively, were conducted to establish the effect of monomer addition rate on the characteristics of the copolymer products, as well as to assess the reproducibility of the observations from the original run.

The runs in Table 3.5 follow the same trend as Run 8 in Table 3.4, showing the reproducibility of the results under a range of conditions. A steady increase in mass yield with time was recorded, along with a continued increase in molecular weight. Dispersities initially broaden due to the presence of both copolymer and macromonomer and the eventual consumption of the macromonomer causes the dispersities to fall towards the end of the polymerisation. Macromonomer conversion is complete, or essentially complete, by ^{1}H NMR within 60 min and conversion is slower with reducing monomer addition rate. Final molecular weights and yields are found to decrease with decreasing monomer addition rate as expected, while monomer conversions remained consistent across the range of addition rates.

Table 3.5 - Free radical polymerisations of *n*-butyl acrylate in presence of PE-*i*-DIB. How copolymerisation is affected by changes in monomer addition rate.

Run[a]	Time (min)	Yield (g/%)	M_p[d] (g/mol)	M_n[d] (g/mol)	M_w[d] (g/mol)	Đ[d]	PE-*i*-DIB Conversion (%)[e]
9	20	0.112	4300	3300	10900	3.2	66
	30	0.137	14900	5800	14800	2.5	93
	40	0.168	17900	8200	20900	2.5	100
	50	0.178	20800	10100	23600	2.3	100
	60	0.200	22200	11200	28700	2.6	100
	Remainder	6.1/31	22400	11100	28000	2.6	100
10[b]	20	0.095	2500	2500	4200	2.0	17
	30	0.110	3800	2800	5800	2.1	35
	40	0.109	6100	4300	10200	2.4	62
	50	0.119	9100	5600	11500	2.1	88
	60	0.211	9200	6600	13400	2.0	100
	Remainder	2.8/29	10500	6700	13200	2.0	100
11[d]	20	0.098	3200	2500	4900	2.0	15
	30	0.094	4000	2900	5500	1.9	35
	40	0.097	4400	3200	6000	2.0	62
	50	0.100	5800	3800	6800	1.9	77
	60	0.106	9100	4700	10100	2.1	92
	Remainder	2.2/16	9100	4900	10500	2.1	92

[a] Polymerisation conditions: PE-*i*-DIB = 2.4 g, M_n = 2100 g/mol, Đ = 2.0; initial [PE-*i*-DIB] = 0.019 mol/L; comonomer = *n*-BA; total mass *n*-BA added = 14.6 g (16 ml); *n*-BA:PE = 100:1; [initiator] solution = 0.11 mol/L in 10 ml solvent; solvent = toluene; initial volume = 60 ml; temperature = 110°C; polymerisation time = 1 hour; initiator addition rate = 10 ml/hr (1.14×10^{-3} mol/hr); monomer addition rate = 16 ml/hr (0.114 mol/hr).
[b] Monomer addition rate = 4 ml/hr (0.0279 mol/hr); *n*-BA:PE = 25:1.
[c] Monomer addition rate = 2 ml/hr (0.0140 mol/hr); *n*-BA:PE = 12.5:1.
[d] GPC data obtained at 160°C in 1,2,4-trichlorobenzene using universal calibration. PS standards were used to calibrate the system (see Chapter 6, Section 6.1 for further details).
[e] Calculated from ^{1}H NMR.

Analysis of the methanol soluble P(*n*-BA) homopolymer in Runs 9-11 revealed a similar trend to that of Run 8 *i.e.* that homopolymer was not detectable by NMR or GPC until a large proportion (*ca.* 90%) of the macromonomer had been converted to copolymer. As would be expected, the time taken for this scenario to occur increased with decreasing

monomer addition rate from t = 30 min in Run 9 to Run 11 where after t = 60 min the reaction finished with 92% of the macromonomer converted.

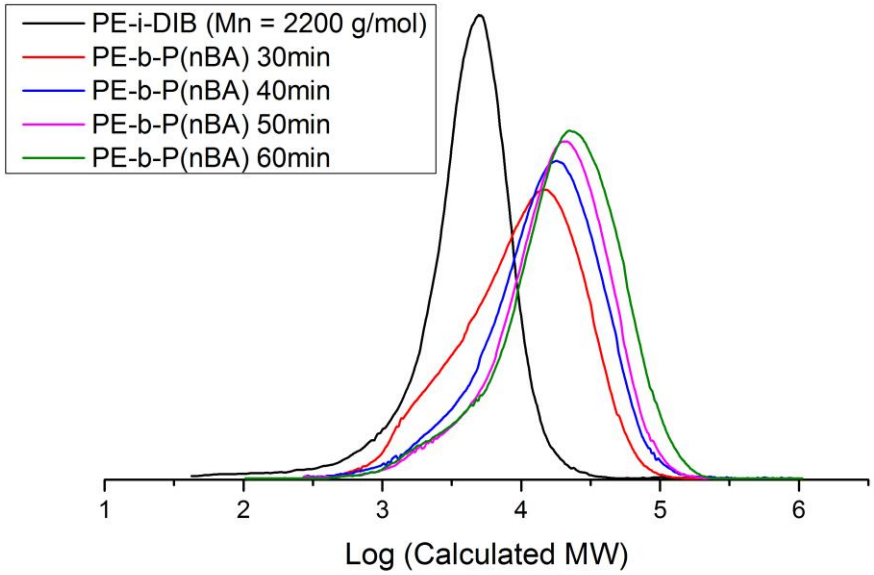

Figure 3.13 - GPC traces following progress of free radical polymerisation of *n*-BA in presence of PE-*i*-DIB (Run 9, Table 3.5).

The evolution of molecular weight and dispersity in Run 9 is well-demonstrated by the GPC traces (Figure 3.13) for the aliquots taken during the kinetic run.[†] The traces show a gradual shift from one material of low molecular weight (PE-*i*-DIB), through two materials (t = 30 min), to one material of higher molecular weight. The GPC traces for Runs 10 and 11 (Figures 3.14 and 3.15) were also plotted and a similar trend was observed in both cases, though the broadening and narrowing effect is less pronounced due to the smaller monomer addition rates.

[†] 20 min sample is not shown due to run failure.

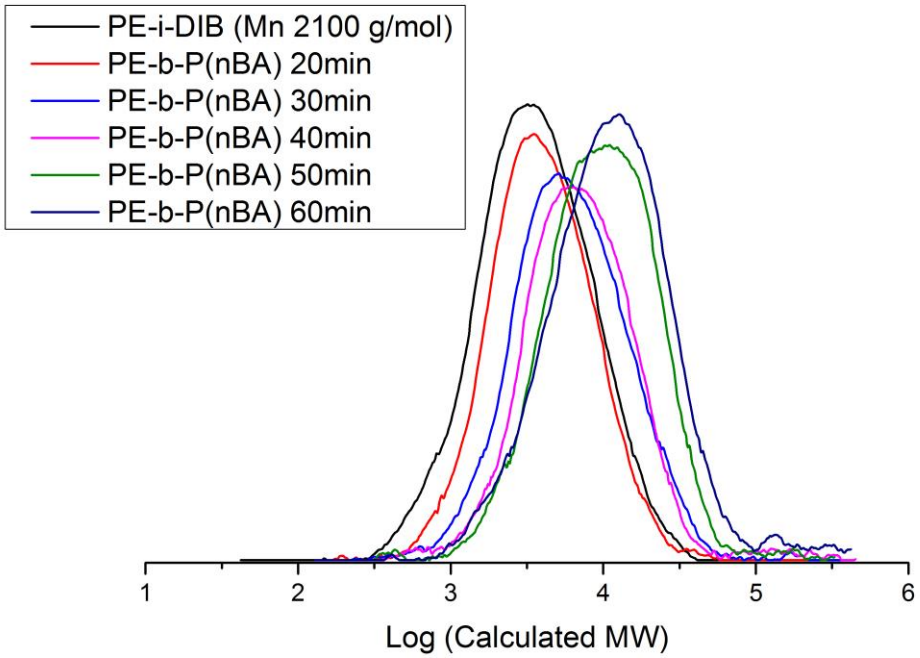

Figure 3.14 - GPC traces following progress of free radical polymerisation of *n*-BA in presence of PE-*i*-DIB (Run 10, Table 3.5).

Run 9 (Figure 3.13), where the macromonomer is converted before the end of the reaction as a result of a higher monomer addition rate, revealed another interesting observation. The molecular weight appeared to increase with time after the macromonomer was fully converted in the continued presence of initiator and free monomer. This was the first starved feed run conducted where the macromonomer was fully converted so early on in the reaction and the GPC traces apparently support this molecular weight increase.

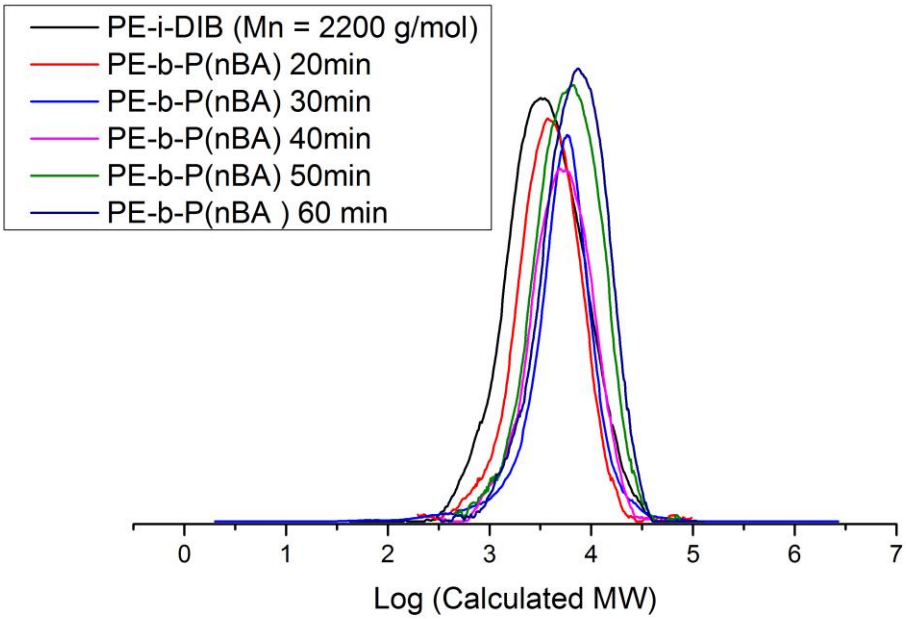

Figure 3.15 - GPC traces following progress of free radical polymerisation of n-BA in presence of PE-*i*-DIB (run 11, table 3.5).

An extended copolymerisation was conducted to investigate this further. The monomer addition was continued for 180 min with the other conditions remaining the same *i.e.* the monomer addition was continued long after the initiator addition was finished at t = 60 min and even longer after the consumption of the macromonomer. BP has a $t_{1/2}$ of *ca* 6 min at 110°C[12] so we would expect the initiator to have been essentially consumed *ca* 25 min after the last of the solution was added, bearing in mind the initiator concentration is not going to be high under these conditions regardless due to its rapid consumption.

Table 3.6 - Free radical polymerisation of *n*-butyl acrylate in presence of PE-*i*-DIB with extended monomer addition.

Run[a]	Time (min)	Yield (g/%)	M_p[b] (g/mol)	M_n[b] (g/mol)	M_w[b] (g/mol)	Đ[b]	PE-*i*-DIB Conversion (%)[c]
12	20	0.117	2500	2400	6700	2.7	21
	30	0.143	3800	3500	16200	4.6	53
	60	0.179	19600	6700	19600	2.8	100
	120	0.188	16300	8600	20900	2.4	100
	180	0.198	24700	10000	23000	2.3	100
	Remainder	5.7/29	24500	10200	26300	2.6	100

[a] Polymerisation conditions: PE-*i*-DIB = 2.4 g, M_n = 2200 g/mol, Đ = 2.0; initial [PE-*i*-DIB] = 0.019 mol/L; comonomer = *n*-BA; total mass *n*-BA added = 14.3 g (16 ml); *n*-BA:PE = 100:1; [initiator] solution = 0.11 mol/L in 10 ml solvent; solvent = toluene; initial volume = 60 ml; temperature = 110°C; polymerisation time = 3 hour; initiator addition rate = 10 ml/hr (1.14×10^{-3} mol/hr); monomer addition rate = 5.3 ml/hr (0.038 mol/hr).
[b] GPC data obtained at 160°C in 1,2,4-trichlorobenzene using universal calibration. PS standards were used to calibrate the system (see Chapter 6, Section 6.1 for further details).
[c] Calculated from ^{1}H NMR.

The GPC data in Table 3.6 appears to show that although the DIB end groups were converted by t = 60 min by ^{1}H NMR, the recovered yield increased throughout and molecular weight of the copolymer samples continued to increase steadily until t = 180 min. This continued molecular weight increase after macromonomer conversion is supported by the GPC traces (Figure 3.16) which further indicate that even after the macromonomer is converted, further molecular weight increase occurs. These observations are consistent with those of run 9 and suggest that in the presence of sufficient monomer feed throughout the polymerisation, the molecular weight can continue to grow even after consumption of initiator and macromonomer. The formation of branching points could also provide some explanation for this molecular weight increase, though the production of branching points in the P(*n*-BA) chains would be detectable in the form of quarternary carbon signals at *ca* 48 ppm.[16, 25] The ^{13}C NMR of the copolymer products show no signals corresponding to quarternary branch point carbons (*e.g.* Figure C.17.) and as such we suggest that branch formation is not prevalent

here. Quaternary branching points are normally found in reactions with very low polymer concentration and high monomer concentration which,[16, 25, 26] given the significant concentration of macromonomer present from the beginning, of copolymer present as these runs progress and the controlled, slow monomer feed, clearly is not the case here.

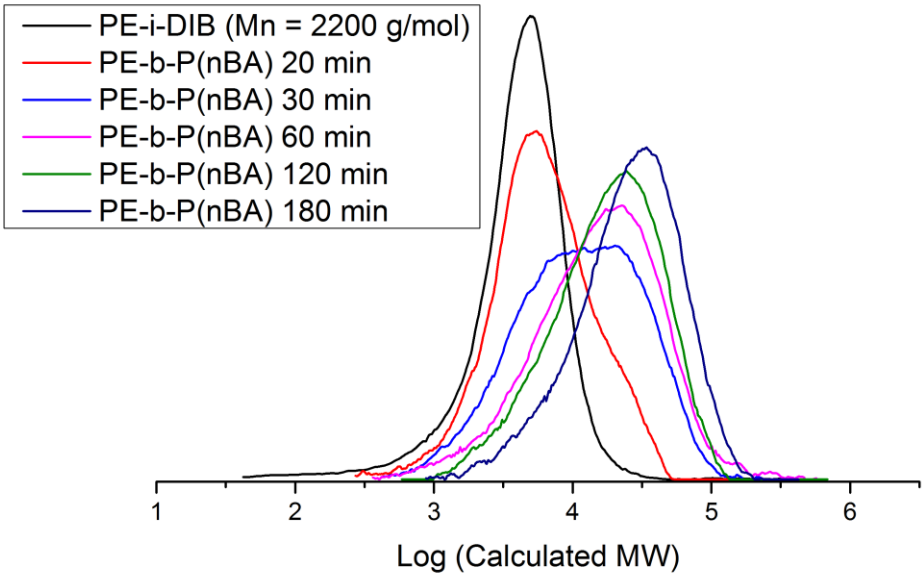

Figure 3.16 - GPC traces following progress of free radical polymerisation of *n*-BA in presence of PE-*i*-DIB with extended monomer addition (Table 3.6).

To test this further still, a similar copolymerisation (Run 13) was conducted where the initiator was added at the start of the reaction to see if the molecular weight would still continue to grow as monomer was added if the initiator and macromonomer were consumed even earlier in the reaction. Table 3.7 shows the higher concentration of initiator at the start of the reaction resulted in faster DIB end group conversion (t = 30 min), with the continuous monomer addition appearing to facilitate continued increase in molecular weight with time up to t = 120 min.

Table 3.7 - Free radical polymerisation of *n*-butyl acrylate in presence of PE-*i*-DIB with extended monomer addition. Initiator added at t = 0 min.

Run[a]	Time (min)	Yield (g/%)	M_p[b] (g/mol)	M_n[b] (g/mol)	M_w[b] (g/mol)	Đ[b]	PE-*i*-DIB Conversion (%)[c]
13	20	0.107	3200	3100	6100	2.0	79
	30	0.139	9800	4500	9100	2.0	100
	60	0.148	12400	5600	12400	2.2	100
	120	0.177	14800	6900	18400	2.7	100
	180	0.183	15000	7100	20700	2.9	100
	Remainder	7.39/40	27000	7100	18900	2.7	100

[a] Polymerisation conditions: PE-*i*-DIB = 2.4 g, M_n = 2100 g/mol, Đ = 2.0; initial [PE-*i*-DIB] = 0.019 mol/L; comonomer = *n*-BA; total mass *n*-BA added = 14.3 g (16 ml); *n*-BA:PE = 100:1; [initiator] solution = 0.11 mol/L in 10 ml solvent; solvent = toluene; initial volume = 60 ml; temperature = 110°C; polymerisation time = 3 hour; monomer addition rate = 5.3 ml/hr (0.038 mol/hr).
[b] GPC data obtained at 160°C in 1,2,4-trichlorobenzene using universal calibration. PS standards were used to calibrate the system (see Chapter 6, Section 6.1 for further details).
[c] Calculated from ^{1}H NMR.

The GPC traces shown in Figure 3.17 appear to support this, though since they appear multimodal it would not be safe to say this for certain. The traces are far broader for this run which is likely to be a result of the reduced control over the reaction due to the high initiator concentration at the start, as well as the possibility of co-precipitation of P(*n*-BA) homopolymer, the molecular weight of which was higher in these samples (M_n ~ 5000 g/mol, $Đ$ ~ 2.7) than for Runs 8-12. The main observation however is that there is still evidence of molecular weight increase with time between the samples taken from t = 30 min onwards. This is consistent with the results from the previous run and indicates that, despite the obvious loss of control in this case, even when the macromonomer and initiator are consumed far more quickly, evolution of molecular weight with time is still achievable in the presence of a continuous monomer feed.

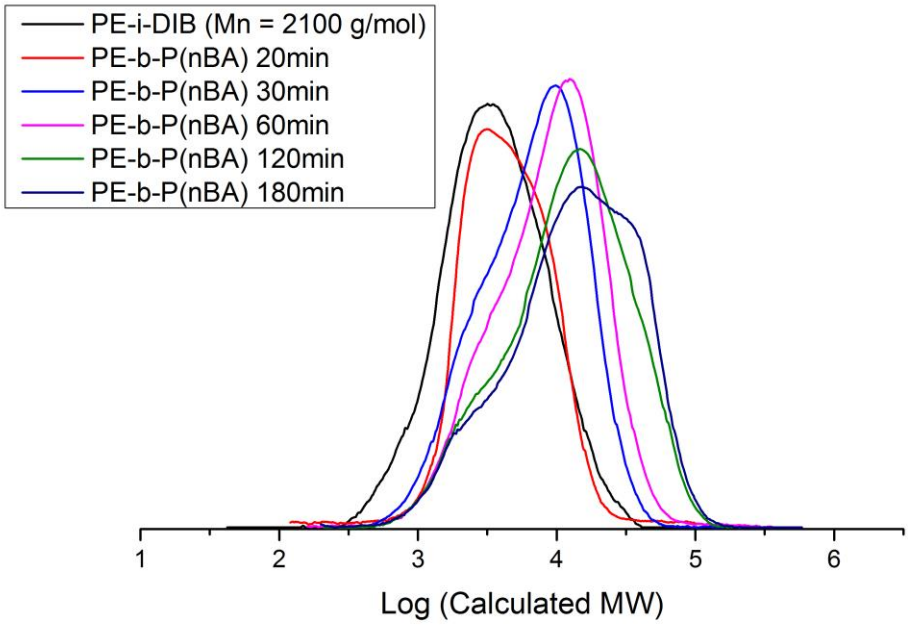

Figure 3.17 - GPC traces following progress of free radical polymerisation of *n*-BA in presence of PE-*i*-DIB with extended monomer addition (Table 3.7).

3.4.4 Effect of temperature

The requirement for high temperatures is often seen as a disadvantage of a radical process because the reaction is more difficult to control.[27] It must be pointed out however that starved feed polymerisations are regularly carried out at high temperature to keep the concentration of monomer and initiator in the reactor at any given time low, which allows control over the process.[22, 23, 24] Another noteworthy consideration is that in this case the insolubility of the PE-*i*-DIB macromonomer at ambient temperature meant that polymerisation temperatures >100°C were typically necessary for the free radical step. This being said, the molecular weight of the macromonomer used in these runs (M_n = 2100 g/mol) was found to be sufficiently low that dissolution was achievable below 100°C, leading us to investigate running the copolymerisation at both higher and lower temperatures to see what effect it would have on the reaction and the properties of the

products. Runs 14 and 15 (Table 3.8) were conducted under the same conditions as Run 8 (Table 3.4), but at 90°C (BP $t_{1/2}$ *ca* 60 min) and 130°C (BP $t_{1/2}$ *ca* 1 min) respectively rather than the 110°C used in all the starved feed runs up to this point.

Table 3.8 - Free radical polymerisation of *n*-butyl acrylate in presence of PE-*i*-DIB with variation in reaction temperature.

Run[a]	Time (min)	Yield (g/%)	M_p[c] (g/mol)	M_n[c] (g/mol)	M_w[c] (g/mol)	Đ[c]	PE-*i*-DIB Conversion (%)[d]
14	20	0.098	3100	2200	4400	2.1	0
	30	0.101	6100	4600	10400	2.3	39
	40	0.109	9500	5500	14500	2.6	63
	50	0.128	19800	8100	18700	2.3	99
	60	0.165	21200	10100	23000	2.3	100
	Remainder	4.04/32	20700	9800	22700	2.3	100
15[b]	20	0.100	5900	2800	7600	2.7	35
	30	0.111	7100	4000	7800	2.0	86
	40	0.125	8500	4700	10100	2.1	100
	50	0.126	8200	5200	10100	2.0	100
	60	0.131	10700	6000	12100	2.0	100
	Remainder	3.48/23	10900	6100	12300	2.0	100

[a] Polymerisation conditions: PE-*i*-DIB = 2.4 g, M_n = 2100 g/mol, Đ = 2.0; initial [PE-*i*-DIB] = 0.019 mol/L; comonomer = *n*-BA; total mass *n*-BA added = 7.3 g (8 ml); [initiator] solution = 0.11 mol/L; solvent = toluene; initial volume = 60 ml; temperature = 110°C; polymerisation time = 1 hour; initiator addition rate = 10 ml/hr (1.14×10^{-3} mol/hr); monomer addition rate = 8 ml/hr (0.057 mol/hr).
[b] Temperature = 130°C.
[c] GPC data obtained at 160°C in 1,2,4-trichlorobenzene using universal calibration. PS standards were used to calibrate the system (see Chapter 6, Section 6.1 for further details).
[d] Calculated from ^{1}H NMR.

Steady increases in yield and molecular weight with time were observed for precipitated samples from Runs 14 and 15 (Table 3.8), though it is less pronounced in Run 15. This is consistent with results obtained for the runs described earlier and likewise DIB end group conversion is achieved by t = 60 min in both cases. Macromonomer conversion

was slower at the lower temperature as expected and this coincides with an improvement in the conversion of monomer to copolymer, 32% compared to 26% at 110°C (*vide supra*) and 24% at 130°C. A higher degree of polymerisation by ^{1}H NMR and final molecular weight by GPC were also observed at the lower temperature, which is consistent with expectations because the reduced rate of cross-propagation and termination at the lower temperature would allow the P(*n*-BA) chains to grow for longer before they eventually cross-propagate with the PE-*i*-DIB or terminate *via* other mechanisms depending on the stage of the polymerisation.

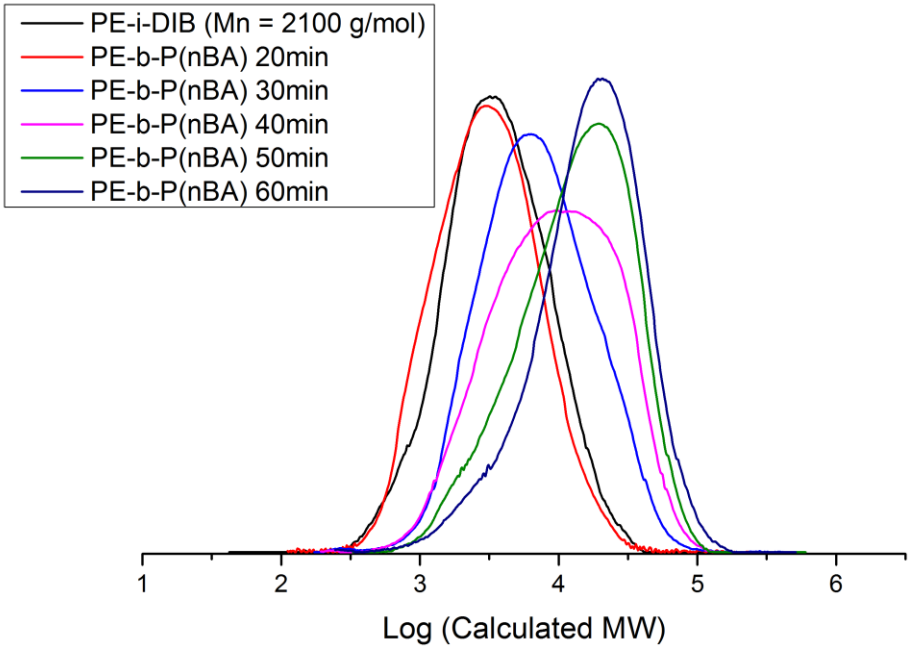

Figure 3.18 - GPC traces following progress of free radical polymerisation of n-BA in presence of PE-i-DIB at 90°C (Run 14, Table 3.8).

Analysis of the soluble P(*n*-BA) homopolymer for both runs was conducted. Interestingly in Run 14 no homopolymer is detectable by NMR or GPC until t = 50 min, by which point 99% of the macromonomer had been converted to copolymer by NMR. This again suggests that any P(*n*-BA) being produced is reacting with the

macromonomer for the majority of the polymerisation and that homopolymer is only being produced in significant amounts once the macromonomer is essentially consumed and other sources of termination have to be found. This is consistent with observations from starved feed runs discussed earlier (Runs 8-11), the first of which was conducted under identical conditions to Run 14 but at a higher temperature (110°C). In fact the first detection of homopolymer took significantly longer at the lower temperature (t = 50 min) than at the higher temperature (t = 30 min).

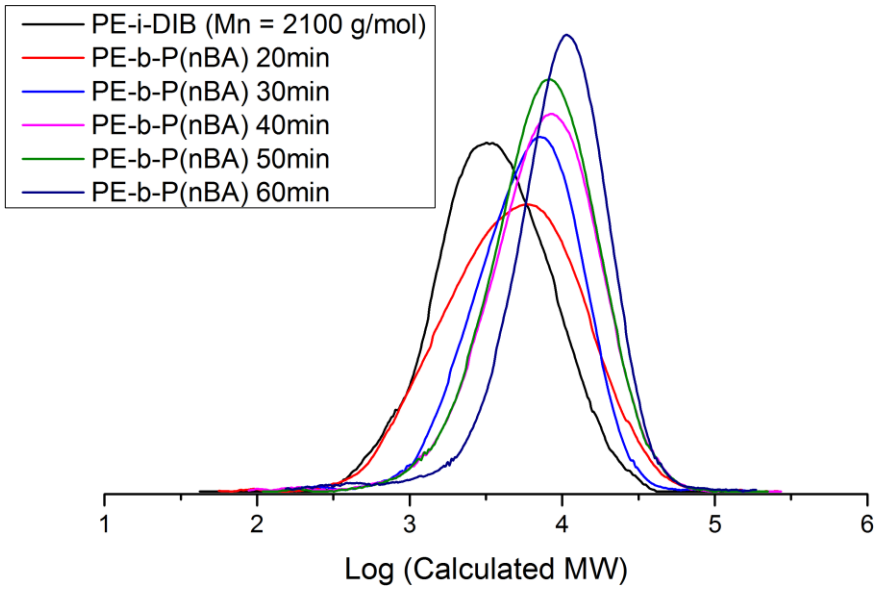

Figure 3.19 - GPC traces following progress of free radical polymerisation of *n*-BA in presence of PE-*i*-DIB at 130°C (Run 15, Table 3.8).

3.5 Mechanism for the copolymerisation of *n*-BA with PE-*i*-DIB

Considering the observations discussed in sections 3.3 and 3.4, and bearing in mind the expected rates of the various reactions, we propose a reversible cross-propagation mechanism between the propagating P(*n*-BA) radical and the PE-*i*-DIB macromonomer

which competes with other possible reactions of the cross-propagation product, as depicted in Scheme 3.4. The BP initiator decomposes with rate coefficient k_d into two benzoyloxy primary radicals I$^{\bullet}$, which can either initiate polymerisation themselves or fragment further to form secondary phenyl initiating radicals I''$^{\bullet}$. In order to initiate polymerisation of *n*-BA, a proportion of the initiator-derived radicals must escape the solvent cage (avoiding recombination or reaction with solvent), avoid primary radical termination with a propagating radical and, in this case, they must also avoid reaction with the PE-*i*-DIB macromonomer which is also present in significant concentration. The radicals derived from BP are reported to have a relatively high cage efficiency *i.e.* cage reactions are limited, but are highly susceptible to radical-induced decomposition *i.e.* the initiator is decomposed by initiating radicals or propagating radicals (transfer to initiator).[28] All of these factors will impact on the initiator efficiency, in particular primary radical termination and induced decomposition given the susceptibility of BP to such a process and the high radical concentrations in the batch reactions.[28] Under the starved-feed conditions the rates of induced decomposition and primary radical termination ought to be reduced in the early stages given the lower radical concentration in the polymerisation medium (though they might well increase with time as the macromonomer is consumed) but reaction with the PE-*i*-DIB macromonomer becomes more likely which would affect both the initiator efficiency and potentially reduce the concentration of available macromonomer.

Given its high propagation rate coefficient[29] and high ceiling temperature (T_c),[30] fast and irreversible propagation of *n*-BA would be expected to follow to give species **I**.[2, 31] Many of these chains would then be involved in a cross-propagation process with PE-*i*-DIB, which could have an even higher rate coefficient as a consequence of the reactivity ratios for AMS and *n*-BA at these temperatures, as shown in Equation (1).[31] The value for r_1

suggests that the rate constants for homopropagation and cross-propagation are similar but the T_c of AMS means that at this temperature depropagation is at least as fast as homopropagation. The value for r_2 suggests that the rate constant for cross-propagation of the P(*n*-BA) radical with AMS is much higher than homopropagation. This would seem to imply that the rate coefficient of the cross-propagation of the P(*n*-BA) radical with the AMS-like PE-*i*-DIB will be fast. We also note that the macromonomer is present at substantially higher molar concentrations than that of a control agent in a typical nitroxide-mediated polymerisation.[32] This would result in rapid consumption of the macromononer to form species **III**.

$$(1)\ r_1 = \frac{k_{AA}}{k_{AB}} = 0.524 \quad r_2 = \frac{k_{BB}}{k_{BA}} = 0.181$$

Where AMS = A and *n*-BA = B at T = 120°C.

The species **III** is a tertiary benzylic radical[1, 19, 33] afforded still greater stability by steric protection from the bulky PE chain. As a consequence, transfer reactions, including propogation, would be expected to be slow. There is however some evidence in the starved feed runs *e.g.* Figures 3.7-3.11 that molecular weight of the copolymer product continues to increase after essentially complete macromonomer conversion. We propose that this is a result of unimolecular *β*-scission of **III**, which is expected to be appreciable at this high temperature,[7] to give **I** ($\underline{k_{12}}$) and thus the process is competitive with irreversible termination *via* hydrogen transfer from solvent (k_S) to give **V**. This would allow further *n*-BA propagation at **I**, particularly under conditions where polar monomer concentration is maintained (*e.g.* Runs 8-12). In contrast, under the batch conditions of *e.g.* Runs 2-4 the molecular weight of the product does not evolve significantly after the early stages of the polymerisation. Further, we note that the presence of radical initiator

is not required to furnish this apparent increase in molecular weight with time (Figure 3.11). The sterically protected nature of **III** suggests that intermolecular chain transfer reactions would be slow; however given that toluene has the highest concentration of any reagent in the reaction, the most likely source of termination is chain transfer from **III** to solvent (k_S) to form final product **V**.

We also took into account the possibility of mid-chain radical migration as another consequence of the backbiting reaction given its significance in *n*-BA homopolymerisation.[34] In this case the process would lead to the conversion of **III** to **VI** with rate coefficient k_{Intra}. Fairly rapid β-scission would then be expected to follow in two directions,[35, 20] one of which would yield copolymer **IX** with a vinylic end group. Given that complete prevention of the formation of such species is unlikely when significant quantities of P(*n*-BA) macromonomer were detected, the failure to detect these species in NMR experiments led us to the conclusion that intramolecular chain transfer of **III** to another tertiary carbon must be very slow. Addition of monomer or macromonomer to the tertiary carbon would lead to the formation of branches (species **VII**) but fragmentation could be significant at these high temperatures[8] and quarternary branch points in the P(*n*-BA) chain are not detected in the copolymer ^{13}C NMR spectra (*e.g.* Figure C.17.).[16, 25]

Under these conditions we expect the cross-propagation of **III** with *n*-BA to form **X** to be slow.[2] This is also supported by the work of Moad and co-workers, wherein they note that even in low concentrations AMS becomes incorporated as an end-group in copolymerisation with *n*-BA at high temperatures because of the lack of propagation from the tertiary benzylic radical formed by cross-propagation between the two monomers.[36] Nonetheless, we acknowledged that this is a possibility, which would then

lead to further fast propagation with *n*-BA to produce a graft copolymer **XI**. However the graft copolymer based on **XI** that would be formed after propagation through **III** would be expected to contain vinylic termination products, which are not observed. NMR studies conducted on these materials, as well as thermal analyses and investigations into their behaviour in solution, are also consistent with the formation of the block copolymer product **V** (see Chapter 4).

Another interesting observation came from attempted chain extension reactions, which produced no detectable change in copolymer molecular weight by NMR or GPC, suggesting that once species **III** is removed from the system by termination it cannot be made active again under the same reaction conditions. The results of this reaction also appear to rule out the post-polymerisation introduction of branches for the same reasons as discussed above. The far lower molecular weight distributions of the P(*n*-BA) homopolymer by-product suggest that the PE-*i*-DIB plays a key role in controlling the *n*-BA polymerisation. An observation that is confirmed by the lack of control observed in reactions that contain no macromonomer (*e.g.* Run 1).

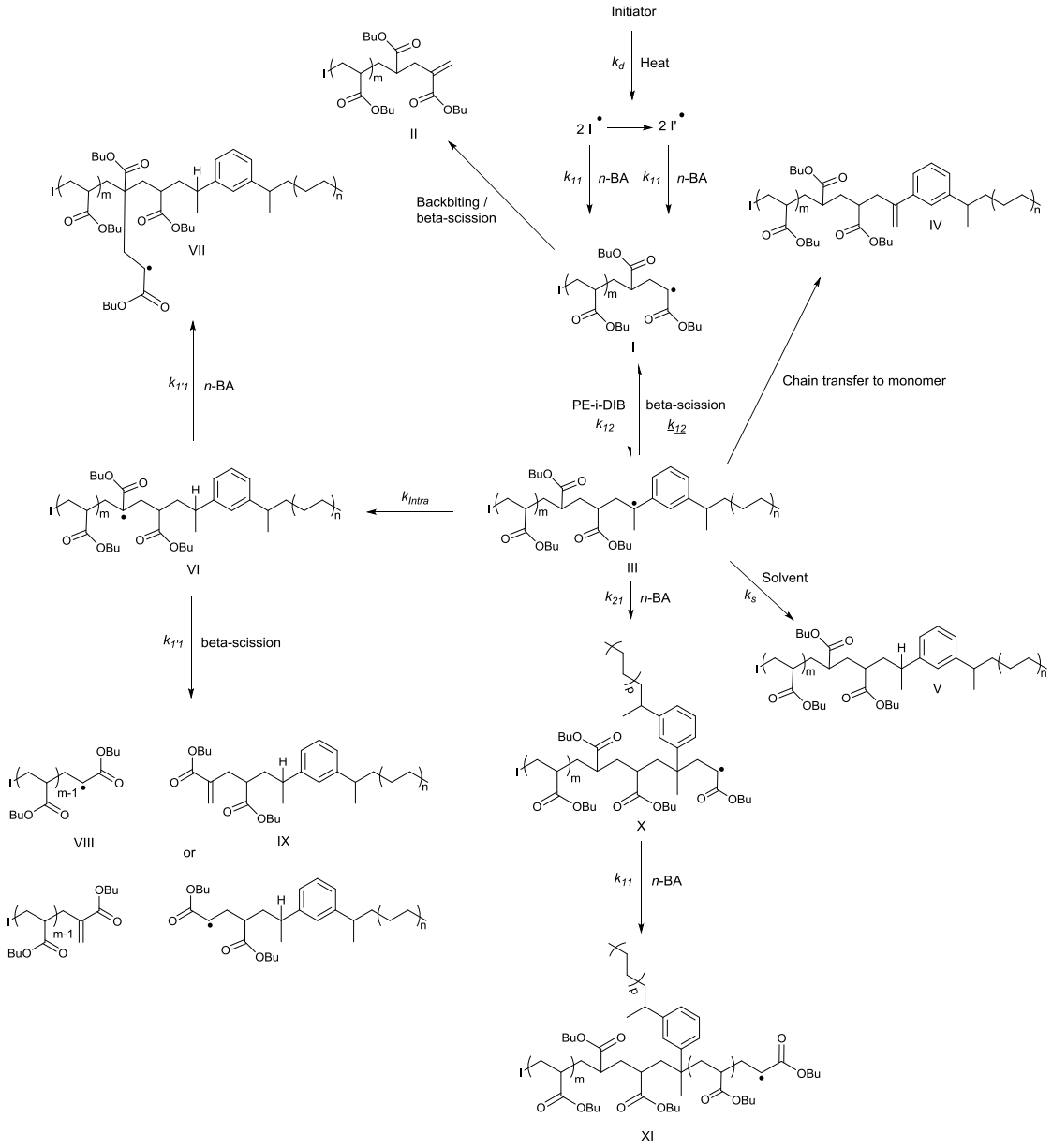

Scheme 3.4 - Proposed mechanism for the free radical copolymerisation of *n*-BA with PE-*i*-DIB.

Under batch conditions, the viscosity of the reaction mixture became visibly much higher rather quickly (especially at higher monomer concentrations), so the P(*n*-BA) chains that did not cross-propagate with PE-*i*-DIB would be expected to remain an active part of the system for longer given the substantially decreased rates of propagation and bimolecular termination.[21] As a result of the high reaction temperature and the low monomer concentration at this point,[7] backbiting and subsequent β-scission could predominate[7, 8, 13, 19, 20] leading to the formation of a significant amount of P(*n*-BA)

macromonomer as the fastest path to termination. P(*n*-BA) macromonomer could also be produced by backbiting and *β*-scission of species **I** after its reformation following *β*-scission of **III**. We propose that a combination of the two leads to the drop in molecular weight observed for the some of the recovered homopolymer after the macromonomer was fully converted, as well as the reduction in molecular weight in some copolymer samples at extended reaction times, and that this is why the molecular weight of the recovered homopolymer was substantially smaller than that of the polar block in the copolymer. At the highest monomer concentration (Run 4) the homopolymer molecular weight continued to increase for a time after macromonomer consumption. We propose that the higher initial monomer concentration and faster macromonomer consumption led to a higher concentration of available monomer after PE-*i*-DIB conversion, which was sufficient to allow continued growth of the P(*n*-BA) chains for a period of time despite the increased viscosity. Once the monomer concentration decreased further and the viscosity increased further however, the backbiting and *β*-scission process became dominant leading to the reduction in homopolymer molecular weight observed as time went on.

Under starved feed conditions, the monomer and initiator concentrations at any given point are normally very low due to their rapid consumption,[22] though the reaction temperatures used in our runs were significantly lower than those normally used in starved feed (*n*-BA) polymerisations. For the vast majority of the polymerisation low molecular weight P(*n*-BA) chains were being formed and cross-propagating to PE-*i*-DIB due to the higher macromonomer concentration compared to propagating P(*n*-BA) chains. It was only once the macromonomer had been almost entirely converted that low MW homopolymer was produced as the concentration of growing P(*n*-BA) chains increased, which occurred towards the end of the reaction as a result of the fairly slow

feed rates. The far lower viscosity of the reaction under starved feed conditions[22, 23, 24] would allow the P(*n*-BA) chains to propagate and terminate more readily, which accounts for the slight growth in homopolymer molecular weight with time observed towards the end of the reaction, though the high temperature and relatively low monomer concentration limited this and meant that there were significant amounts of P(*n*-BA) macromonomer detected.

It has been argued that in starved feed *n*-BA homopolymerisation, the potential propagation of P(*n*-BA) macromonomer must be considered. Hutchinson *et al.* concluded it was the only explanation for the disparity between experimental and modelled molecular weight profiles and for the reduction in macromonomer concentration with time.[24] Indeed, Yamada and co-workers suggested that acrylate macromonomer reactivity is comparable to its monomer.[37, 38, 39] In the presence of PE-*i*-DIB however, we detected no homopolymer at all until the PE-*i*-DIB macromonomer was essentially converted towards the end of the reaction under starved-feed conditions and only low molecular weight material was detected in those final stages. Given that the vast majority of the PE-*i*-DIB was converted before any homopolymer was apparently produced, it is highly unlikely that P(*n*-BA) macromonomer propagation could have affected the copolymerisation. The small increase in P(*n*-BA) molecular weight, the consistent dispersities and the similar macromonomer concentrations in the NMR spectra of the soluble fractions are also inconsistent with macromonomer propagation.

Under batch conditions however, despite the observation that P(*n*-BA) macromonomer produced by the backbiting and *β*-scission process is not as reactive as the analogous species yielded from a CCT process with AMS,[7] macromonomer propagation could

have had an effect because it will have been present from the early stages of the polymerisation. Addition of P(*n*-BA) macromonomer **II** to the propagating P(*n*-BA) radical **I** would lead to a tertiary radical species **XII** (Scheme 3.5, left), to which further monomer or macromonomer could add to yield a branched P(*n*-BA) chain, or *β*-scission could occur yielding another macromonomer and a new propagating P(*n*-BA) radical.[24] In Run 4, clearly P(*n*-BA) homopolymer was co-precipitated because the homopolymer molecular weight was higher and therefore less soluble, but branching could be another factor in explaining the insolubility of the P(*n*-BA) which resulted in the co-precipitation of homopolymer and the large increase in dispersity from Run 3 to Run 4. The relative rates of monomer addition at **XII** compared to chain scission would be dependent on the concentration of monomer, though given the high temperature we would still expect a significant proportion of **XII** to undergo chain scission and this proportion would only increase with time due to the consumption of monomer. Addition of P(*n*-BA) macromonomer **II** to the tertiary benzylic radical **III** (Scheme 3.5, right) is also a possibility, which would yield a new tertiary radical **XIII** that could then propagate further forming another branched species, or terminate by chain transfer to solvent to form a graft copolymer similar to species **XI**. However, this reaction seems unlikely for several reasons: a) the sterically protected nature of species **III** would make addition of macromonomer rather slow, especially when we consider the relatively unreactive nature of the P(*n*-BA) vinyl group;[7] b) we have already established that the copolymer NMR spectra showed no signals corresponding to quarternary branch points so we wouldn't expect branched species to be formed; c) NMR studies are consistent with block copolymer product **V**.

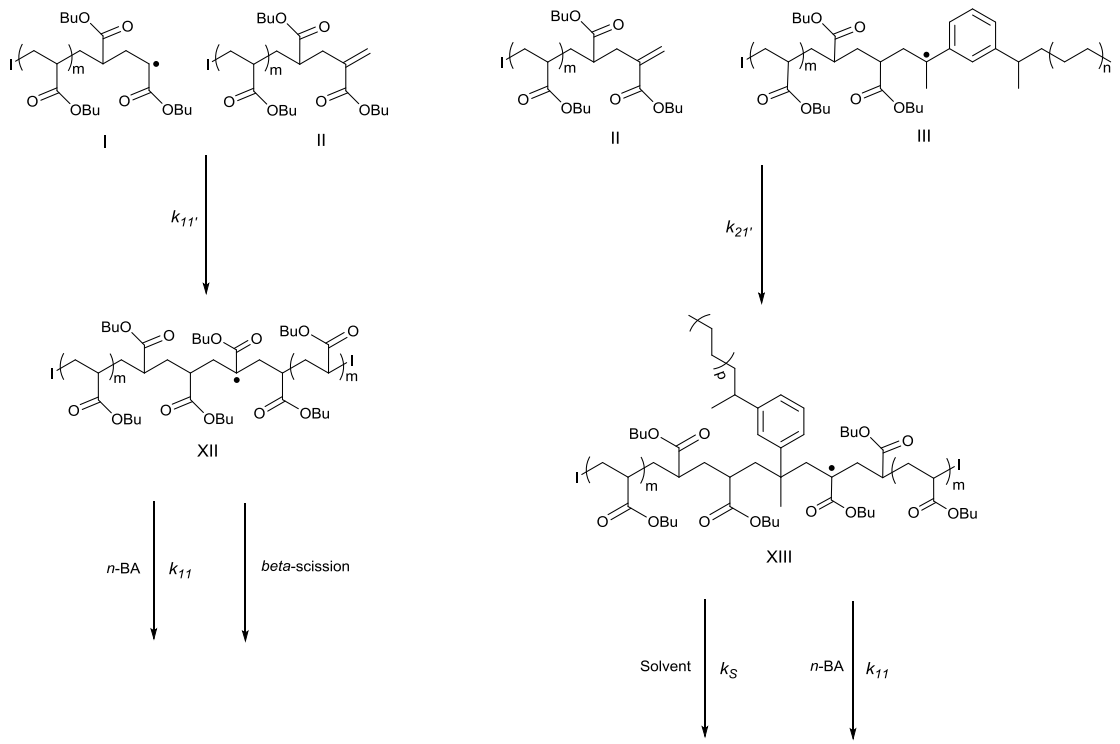

Scheme 3.5. - Possible outcomes of P(*n*-BA) macromonomer propagation in free radical copolymerisation of *n*-BA with PE-*i*-DIB.

3.6 Conclusions

The mechanism for the free-radical copolymerisation of PE-*i*-DIB and *n*-BA was investigated in detail by comparing results obtained from both batch and starved-feed copolymerisation reaction setups. Some evidence from the starved feed runs points towards a reversible cross-propagation step between PE-*i*-DIB and the propagating P(*n*-BA) chains that is at least competitive with irreversible termination once the tertiary benzylic macroradical is formed. Under batch conditions, the monomer and initiator feeds were consumed far more quickly which is likely to have caused the termination process to outcompete the reversible cross-propagation process from an earlier stage in the reaction. This could explain why the molecular weight growth was stalled after initial growth at a certain point in the reaction.

Under starved-feed conditions, the macromonomer remained part of the reaction for longer, with the initiator and, more importantly, the monomer present throughout. The continuous feed resulted in more sustained molecular weight growth with time and produced more compelling evidence for the proposed mechanism. This again was reflected in the continued shift of the GPC traces to higher molecular weight as well as the average molecular weight data; which was shown to increase even at extended reaction times in the absence of initiator as long as there was monomer available in significant concentration for the reversible cross-propagation to out-compete termination. It is also noteworthy that under these conditions, no homopolymer was produced until the macromonomer had been essentially converted to copolymer. The starved-feed setup is far more practical for scale-up purposes and was also found to provide greater control over the reaction. This in turn allowed us access to lower molecular weight polar blocks, thus increasing the range of materials that could be produced. Despite the superior control over the reaction gained while the macromonomer was present in significant concentration, the reduced monomer to copolymer conversion in the starved-feed runs suggests that this procedure needs further work. Although this was found to improve when the temperature was reduced, further optimisation is required to avoid wasting reagents and the solubility of the PE macromonomer limits the substantial further reduction of temperature.

3.7 References

1. Kukulj, D.; Davis, T. P.; Gilbert, R. G., Chain Transfer to Monomer in the Free-Radical Polymerizations of Methyl Methacrylate, Styrene, and α-Methylstyrene. *Macromolecules* **1998,** *31* (4), 994-999.
2. Chiu, T. Y. J.; Heuts, J. P. A.; Davis, T. P.; Stenzel, M. H.; Barner-Kowollik, C., Synthesis of Macromonomers via Catalytic Chain Transfer (CCT) Polymerization and their Characterization via NMR Spectroscopy and Electrospray Ionization Mass Spectrometry (ESI-MS). *Macromol. Chem. Phys.* **2004,** *205* (6), 752-761.

3. McCormick, H. W., Ceiling temperature of α-methylstyrene. *J. Polym. Sci.* **1957,** *25* (111), 488-490.
4. Barner-Kowollik, C.; Davis, T. P., Using Kinetics and Thermodynamics in the Controlled Synthesis of Low Molecular Weight Polymers in Free-Radical Polymerization. *macromol. theory simul.* **2001,** *10* (4), 255-261.
5. Kukulj, D.; Heuts, J. P. A.; Davis, T. P., Copolymerization of Styrene and α-Methylstyrene in the Presence of a Catalytic Chain Transfer Agent. *Macromolecules* **1998,** *31* (18), 6034-6041.
6. Johan, P. A. H.; David, A. M.; Thomas, P. D., End-Group Control in Catalytic Chain Transfer Polymerization. In *Controlled/Living Radical Polymerization*, American Chemical Society: 2000; Vol. 768, pp 313-331.
7. Chiefari, J.; Jeffery, J.; Krstina, J.; Moad, C. L.; Moad, G.; Postma, A.; Rizzardo, E.; Thang, S. H., Binary Copolymerization with Catalytic Chain Transfer. A Method for Synthesizing Macromonomers Based on Monosubstituted Monomers. *Macromolecules* **2005,** *38* (22), 9037-9054.
8. John, C.; Justine, J.; Roshan, T. A. M.; Graeme, M.; Ezio, R.; San, H. T., Preparation of Macromonomers via Chain Transfer with and without Added Chain Transfer Agent. In *Controlled/Living Radical Polymerization*, American Chemical Society: 2000; Vol. 768, pp 297-312.
9. Sanders, G. C.; Duchateau, R.; Lin, C. Y.; Coote, M. L.; Heuts, J. P. A., End-Functional Styrene–Maleic Anhydride Copolymers via Catalytic Chain Transfer Polymerization. *Macromolecules* **2012,** *45* (15), 5923-5933.
10. Kay, C. J. Polyethylene Block Copolymers. University of Warwick, PhD, 2014.
11. Moad, G.; Solomon, D. H., 7 - Copolymerization. In *The Chemistry of Radical Polymerization (Second Edition)*, Solomon, G. M. H., Ed. Elsevier Science Ltd: Amsterdam, 2005; pp 333-412.
12. Salamone, J. C., *Polymeric materials encyclopedia*. CRC Press: 1996.
13. Chiefari, J.; Jeffery, J.; Mayadunne, R. T. A.; Moad, G.; Rizzardo, E.; Thang, S. H., Chain Transfer to Polymer: A Convenient Route to Macromonomers. *Macromolecules* **1999,** *32* (22), 7700-7702.
14. Rizzardo, E.; Chong, Y. K.; Evans, R. A.; And, G. M.; Thang, S. H., Control of polymer structure by chain transfer processes. *Macromolecular Symposia* **1996,** *111* (1), 1-11.
15. Rizzardo, E.; Meijs, G. F.; Thang, S. H., Chain transfer by radical addition-fragmentation mechanisms: Synthesis of macromonomers and end-functional oligomers. *Macromolecular Symposia* **1995,** *98* (1), 101-123.
16. Ahmad, N. M.; Heatley, F.; Lovell, P. A., Chain Transfer to Polymer in Free-Radical Solution Polymerization of n-Butyl Acrylate Studied by NMR Spectroscopy. *Macromolecules* **1998,** *31* (9), 2822-2827.
17. McCord, E. F.; Shaw, W. H.; Hutchinson, R. A., Short-Chain Branching Structures in Ethylene Copolymers Prepared by High-Pressure Free-Radical Polymerization: An NMR Analysis. *Macromolecules* **1997,** *30* (2), 246-256.
18. Luft, G.; Kämpf, R.; Seidl, H., Synthesis conditions and structure of low density polyethylene. I. Short and long chain branching. *Die Angewandte Makromolekulare Chemie* **1982,** *108* (1), 203-217.
19. Gridnev, A. A.; Ittel, S. D., Catalytic Chain Transfer in Free-Radical Polymerizations. *Chem. Rev.* **2001,** *101* (12), 3611-3660.
20. Barner-Kowollik, C.; Junkers, T., Kinetic and mechanistic similarities between reversible addition fragmentation chain transfer intermediate and acrylate midchain radicals. *J. Polym. Sci., Part A: Polym. Chem.* **2011,** *49* (5), 1293-1297.

21. Barner-Kowollik, C.; Vana, P.; Davis, T. P., The Kinetics of Free-Radical Polymerization. In *Handbook of Radical Polymerization*, John Wiley & Sons, Inc.: 2003; pp 187-261.
22. Cao, G.-P.; Zhu, Z.-N.; Zhang, M.-H.; Yuan, W.-K., Kinetics of butylacrylate polymerization in a starved feed reactor. *J. Appl. Polym. Sci.* **2004,** *93* (4), 1519-1525.
23. Wang, W.; Hutchinson, R. A., Recent Advances in the Study of High-Temperature Free Radical Acrylic Solution Copolymerization. *Macromol. React. Eng.* **2008,** *2* (3), 199-214.
24. Wang, W.; Nikitin, A. N.; Hutchinson, R. A., Consideration of Macromonomer Reactions in n-Butyl Acrylate Free Radical Polymerization. *Macromol. Rapid Commun.* **2009,** *30* (23), 2022-2027.
25. Peck, A. N. F.; Hutchinson, R. A., Secondary Reactions in the High-Temperature Free Radical Polymerization of Butyl Acrylate. *Macromolecules* **2004,** *37* (16), 5944-5951.
26. Plessis, C.; Arzamendi, G.; Alberdi, J. M.; van Herk, A. M.; Leiza, J. R.; Asua, J. M., Evidence of Branching in Poly(butyl acrylate) Produced in Pulsed-Laser Polymerization Experiments. *Macromol. Rapid Commun.* **2003,** *24* (2), 173-177.
27. Cunningham, M. F.; Hutchinson, R., Industrial Applications and Processes. In *Handbook of Radical Polymerization*, John Wiley & Sons, Inc.: 2003; pp 333-359.
28. Moad, G.; Solomon, D. H., 3 - Initiation. In *The Chemistry of Radical Polymerization (Second Edition)*, Solomon, G. M. H., Ed. Elsevier Science Ltd: Amsterdam, 2005; pp 49-166.
29. Moad, G.; Solomon, D. H., 4 - Propagation. In *The Chemistry of Radical Polymerization (Second Edition)*, Solomon, G. M. H., Ed. Elsevier Science Ltd: Amsterdam, 2005; pp 167-232.
30. Hutchinson, R. A.; Penlidis, A., Free-Radical Polymerization: Homogeneous Systems. In *Polym. React. Eng.*, Blackwell Publishing Ltd: 2008; pp 118-178.
31. Wang, T. J.; Leamen, M. J.; McManus, N. T.; Penlidis, A., Copolymerization of Alpha-Methyl Styrene with Butyl Acrylate: Parameter Estimation Considerations. *J. Macromol. Sci., A* **2004,** *41* (11), 1205-1220.
32. Graeme, M.; Albert, G. A.; Frances, E.; Charles, H. J. J.; Julia, K.; Catherine, L. M.; Ezio, R.; Thomas, H. S.; San, H. T., Controlled-Growth Free-Radical Polymerization of Methacrylate Esters: Reversible Chain Transfer versus Reversible Termination. In *Controlled Radical Polymerization*, American Chemical Society: 1998; Vol. 685, pp 332-360.
33. Roberts, G. E.; Heuts, J. P. A.; Davis, T. P., Direct Observation of Cobalt−Carbon Bond Formation in the Catalytic Chain Transfer Polymerization of Methyl Acrylate Using Matrix-Assisted Laser Desorption Ionization Time-of-Flight Mass Spectrometry. *Macromolecules* **2000,** *33* (21), 7765-7768.
34. Vandenbergh, J.; Junkers, T., Macromonomers from AGET Activation of Poly(n-butyl acrylate) Precursors: Radical Transfer Pathways and Midchain Radical Migration. *Macromolecules* **2012,** *45* (17), 6850-6856.
35. Junkers, T.; Barner-Kowollik, C., The role of mid-chain radicals in acrylate free radical polymerization: Branching and scission. *J. Polym. Sci., Part A: Polym. Chem.* **2008,** *46* (23), 7585-7605.
36. Moad, G.; Rizzardo, E.; Moad, C. L.; Ittel, S. D.; Wilczek, L.; Gridnev, A. A., Catalytic polymerization process. Google Patents: 1997.

37. Yamada, B.; Hirano, T., Copolymerizations of macromonomer prepared by addition-fragmentation chain transfer polymerization of methyl acrylate trimer. *Polym. Bull.* **2003,** *50* (4), 243-250.
38. Yamada, B.; Oku, F.; Harada, T., Substituted propenyl end groups as reactive intermediates in radical polymerization. *J. Polym. Sci., Part A: Polym. Chem.* **2003,** *41* (5), 645-654.
39. Harada, T.; Zetterlund, P. B.; Yamada, B., Preparation of macromonomers by copolymerization of methyl acrylate dimer involving β fragmentation. *J. Polym. Sci., Part A: Polym. Chem.* **2004,** *42* (3), 597-607.

Chapter 4: Synthesis and characterisation of polyethylene-polar diblock copolymers by free-radical copolymerisation with PE-*i*-DIB

4.1 Introduction

The results from Chapter 3, following on from work conducted in the group previously,[1] showed that PE-*i*-DIB could be used as a macromonomer in a simple free radical copolymerisation with acrylates to prepare PE-containing block copolymers. Further to this, starved feed polymerisations allowed us to tune the molecular weight of the polar block. In this chapter the use of PE-*i*-DIB in simple free radical polymerisations for the synthesis of PE copolymers with a range of polar monomers will be presented. The copolymers are characterised by NMR, GPC, DLS and DSC.

4.2 Vinyl Esters

4.2.1 Vinyl acetate (VAc)

The copolymerisation of ethylene and vinyl acetate is well-established and EVA random copolymers have become very important commercial materials in a variety of fields in the last few decades.[2] EVAs are typically prepared by direct free radical copolymerisation in solution or in emulsion, requiring high temperatures and pressures. Unsurprisingly, the polymer properties depend on the vinyl acetate content, the molecular weight distribution and the degree of branching.[3, 4, 5] While the controlled homopolymerisation of vinyl acetate has been demonstrated using a range of methods,[6, 7, 8, 9] similar copolymerisations are rare. Monteil recently reported the first example of

ethylene copolymerisation with VAc *via* RAFT.[10] The use of xanthates enabled the control of molecular weight and dispersity of the copolymers under fairly mild conditions, but the pressures used were still rather high, long reaction times were needed, the VAc content reported was low and the polymerisation was hindered by a side reaction involving fragmentation of the controlling agent. Detrembleur[11] utilised an organometallic-mediated radical polymerisation strategy to synthesise copolymers of ethylene and VAc with a block-like structure under far milder conditions. Copolymers of narrow dispersity, tuneable molecular weight and variable VAc content were prepared, though pressures used were again rather high, reaction times were long, yields are not reported and there was no comment on the scalability of the process. Access to PE-*b*-P(VAc) materials prepared more easily would be of considerable academic and commercial interest given the current importance of EVA in applications such as adhesion and compatibilisation.[2, 12]

A copolymerisation of PE-*i*-DIB (M_n = 3000 g/mol, $Đ$ = 2.1) and 500 equivalents of vinyl acetate (Run 1, Table 4.1) was conducted in toluene at 125°C using *tert*-butyl peroxide (TP) as the initiator ($t_{1/2}$ *ca* 10 h at 125°C), chosen because of its availability at the time. The insolubility of the PE component meant that isolation and purification of the copolymer was simply a matter of precipitation in an appropriate anti-solvent, in this case ethanol. As with P(*n*-BA)/methanol (Chapter 3), use of ethanol to separate the copolymer from the P(VAc) homopoymer seems counter-intuitive; however, we found again that this worked because of the low molecular weight P(VAc) being produced in (most of) these runs. Complete recovery of the PE containing materials was confirmed by the absence of any signals corresponding to PE in the NMR spectra of the soluble fraction. Samples were dried overnight in a vacuum oven before being analysed for comparison to the macromonomer. The ^{1}H NMR spectrum of the precipitated product

showed complete conversion of the PE-*i*-DIB macromonomer and the presence of signals corresponding to both PE and P(VAc) after multiple reprecipitations. A copolymer molecular weight of 8000 g/mol, Đ = 2.4 by GPC was obtained.

Table 4.1 - Free radical polymerisations of VAc in presence of PE-*i*-DIB.

Run	Init.	Time (min)	Yield (g/%)	M_p [f] (g/mol)	M_n [f] (g/mol)	M_w [f] (g/mol)	Đ [f]	PE-*i*-DIB Conversion (%)[g]
1[a]	TP	360	0.860/23	16800	8000	19300	2.4	100
2[b]	BP	10	0.269/8	2900	2300	5600	2.4	86
	BP	20	0.282/10	3300	2500	5000	2.0	100
	BP	40	0.287/11	3000	2500	4400	1.7	100
	BP	60	0.286/11	3600	2500	5200	2.1	100
	BP	120	0.285/10	3200	2400	4500	1.8	100
	BP	180	0.282/10	3700	2600	5400	2.1	100
	BP	240	0.285/10	3600	2700	5200	1.9	100
3[c]	BP	10	0.432/12	6200	4000	8600	2.2	100
	BP	20	0.428/11	6400	4400	8200	1.9	100
	BP	40	0.447/12	5900	4000	7700	1.9	100
	BP	60	0.448/12	6000	4100	8400	2.0	100
	BP	120	0.447/12	6200	4000	9200	2.3	100
	BP	180	0.454/13	6300	4100	8900	2.2	100
	BP	240	0.430/12	5800	4200	8400	2.0	100
4[d]	BP	10	0.599/10	18300	5400	19900	3.7	100
	BP	20	0.612/10	17300	6000	21100	3.5	100
	BP	40	0.623/10	17300	6300	19000	3.0	100
	BP	60	0.646/11	18700	7100	20500	2.9	100
	BP	120	0.604/10	18400	6800	20500	3.0	100
	BP	180	0.644/11	19000	6700	20300	3.0	100
	BP	240	0.633/11	19400	6800	21600	3.0	100

[a] Polymerisation conditions: PE-*i*-DIB = 0.2 g, M_n = 3000 g/mol, Đ = 2.1; [PE-*i*-DIB] = 0.0083 mol/L; comonomer = VAc; mass VAc added = 2.9 g (3.1 ml); VAc:PE = 500:1; initiator = TP; [initiator] solution = 0.081 mol/L; solvent = toluene; total volume = 8.2 ml; temperature = 125°C.

[b] PE-*i*-DIB = 0.2 g, M_n = 2100 g/mol, Đ = 2.0; initial [PE-*i*-DIB] = 0.011 mol/L; mass VAc added = 0.82 g (0.88 ml); VAc:PE = 100:1; initiator = BP; [initiator] solution = 0.11 mol/L.

[c] Mass VAc added = 2.0 g (2.2 ml); VAc:PE = 250:1.

[d] Mass VAc added = 4.1 g (4.4 ml); VAc:PE = 500:1.

[e] GPC data obtained at 160°C in 1,2,4-trichlorobenzene using universal calibration. PS standards were used to calibrate the system (see Chapter 6, Section 6.1 for further details).

[f] Calculated from ^{1}H NMR.

To investigate this reaction in greater detail, kinetic runs (Table 4.1) were conducted as in Chapter 3 by setting up several ampoules in parallel and stopping the reactions at pre-defined intervals. For these runs, BP ($t_{1/2}$ *ca* 1 min at 130°C) was chosen over TP to increase the number or propagating chains at the start of the polymerisation so that the macromonomer would be converted more quickly. Runs 2-4 (Table 4.1) follow the copolymerisations of PE-*i*-DIB over time with 100:1, 250:1, and 500:1 molar ratios of VAc:PE respectively. In Run 2 the PE-*i*-DIB macromonomer was fully converted after t = 20 min according to ^{1}H NMR spectra and the recorded yields, molecular weights and dispersities did not significantly increase after this point. This indicates that little further change in the copolymer properties have occurred after macromonomer conversion, consistent with observations in Chapter 3. In Run 3 the PE-*i*-DIB was converted more quickly in the presence of a higher VAc concentration, while we also see higher molecular weight products. As expected, the molecular weight data and recorded yields alter very little with time, suggesting that the reaction was completed rapidly. In the presence of a still higher monomer concentration (Run 4), higher molecular weight materials were produced but again the yields and molecular weight data remained very similar after t = 20 min.

^{1}H NMR spectra of the homopolymer by-product from Runs 2-4 conducted in $CDCl_3$ consisted of low molecular weight P(VAc). At low monomer concentration *e.g.* Run 3 these molecular weights did not change significantly over time (M_n *ca* 2200 g/mol throughout) while in Run 4 this was seen to increase from M_n *ca* 1800 g/mol at t = 10 min to *ca* 4300 g/mol at t = 120min by ambient temperature GPC conducted on a $CHCl_3$ system. Similar observations were made for *n*-BA (Table 3.1, Chapter 3). In Runs 2 and 3, ^{1}H and ^{13}C NMR spectra (discussed in greater detail in Section 4.2.2, see also Appendix C) suggested that any homopolymer produced was apparently sufficiently low

molecular weight to be soluble in ethanol for the isolation of the copolymer (Figure C.8.); whereas in Run 4 (Figure C.10.), similar analysis contained evidence of higher molecular weight P(VAc) homopolymer that was not removed by reprecipitation. This would suggest that provided the P(VAc) by-product did not exceed M_n <5000 g/mol, the copolymer could be successfully isolated using ethanol.

4.2.2 Vinyl-2-ethylhexanoate (V2EH)

Copolymers of ethylene with vinyl esters containing long alkyl side chains are rarely described in academic literature; although such copolymers are important in a range of areas including the production of resins,[13] adhesives[14] and in wax crystal modification in oils.[15, 16] Vinyl-2-ethylhexanoate (Figure 4.1) is of particular interest because of its current use in the latter application.

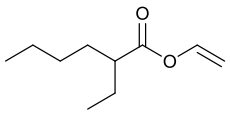

Figure 4.1 - Vinyl-2-ethylhexanoate

A copolymerisation of PE-*i*-DIB (M_n = 3000 g/mol, $Đ$ = 2.1) and 200 equivalents of V2EH (Run 5, Table 4.2) was conducted in toluene at 125°C using TP as the initiator, again because it was available at the time. The resulting polymeric mixture was found to be separable by precipitation in acetone and the ^{1}H NMR spectrum of the precipitated product showed signals corresponding to both PE and P(V2EH). The ^{1}H NMR spectrum also indicated >90% conversion of the DIB end groups, while GPC analysis gave a copolymer molecular weight of 7800 g/mol, $Đ$ = 2.0.

Table 4.2 - Free radical polymerisations of V2EH in presence of PE-*i*-DIB.

Run	Init.	Time (min)	Yield (g/%)	M_p [e] (g/mol)	M_n [e] (g/mol)	M_w [e] (g/mol)	Đ [e]	PE-*i*-DIB Conversion (%)[f]
5[a]	TP	360	0.460/11	14500	7800	16000	2.0	91
6[b]	BP	10	0.336/9	5900	3200	6600	2.1	82
	BP	20	0.366/10	6400	4100	7700	1.9	100
	BP	40	0.357/10	5900	4200	6700	1.6	100
	BP	60	0.360/10	5500	4000	6900	1.7	100
	BP	120	0.361/10	6000	4300	6900	1.6	100
	BP	180	0.361/10	6100	4000	7700	1.9	100
	BP	240	0.359/10	6600	4300	7900	1.8	100
7[c]	BP	10	0.627/13	14800	6000	17400	2.9	100
	BP	20	0.673/15	16600	7300	19100	2.6	100
	BP	40	0.600/13	16500	7100	19100	2.7	100
	BP	60	0.676/15	16500	7500	18700	2.5	100
	BP	120	0.685/15	16500	7300	18100	2.5	100
	BP	180	0.727/16	16200	7300	18600	2.5	100
	BP	240	0.649/14	17100	7500	19200	2.6	100
8[d]	BP	10	1.03/17	25600	10300	34300	3.3	100
	BP	20	0.941/15	31000	11100	42900	3.9	100
	BP	40	0.889/14	27500	10800	36400	3.4	100
	BP	60	1.07/18	28100	11200	40900	3.6	100
	BP	120	1.01/17	28600	11100	40200	3.6	100
	BP	180	1.06/18	28600	11600	42500	3.7	100
	BP	240	1.11/19	34500	12100	42400	3.5	100

[a] Polymerisation conditions: PE-*i*-DIB = 0.2 g, M_n = 3000 g/mol, Đ = 2.1; initial [PE-*i*-DIB] = 0.0083 mol/L; comonomer = V2EH; mass V2EH added = 2.3 g (2.6 ml); V2EH:PE = 200:1; initiator = TP; [initiator] solution = 0.081 mol/L; solvent = toluene; total volume = 8.2 ml; temperature = 125°C.
[b] PE-*i*-DIB = 0.2 g, M_n = 2100 g/mol, Đ = 2.0; initial [PE-i-DIB] = 0.011 mol/L; mass V2EH added = 1.6 g (1.9 ml); V2EH:PE = 100:1; initiator = BP; [initiator] solution = 0.11 mol/L.
[c] V2EH added = 3.2 g (3.7 ml); V2EH:PE = 200:1.
[d] V2EH added = 4.9 g (5.6 ml); V2EH:PE = 300:1.
[e] GPC data obtained at 160°C in 1,2,4-trichlorobenzene using universal calibration. PS standards were used to calibrate the system (see Chapter 6, Section 6.1 for further details).
[f] Calculated from ^{1}H NMR.

Kinetic runs (Runs 6-8, Table 4.2) similar to those conducted for the vinyl acetate copolymerisations (*vide supra*) were set up, with BP replacing TP in order to fully convert the macromonomer by producing more propagating chains at the start. In the presence of a molar ratio of 100:1 V2EH:PE (Run 6), PE-*i*-DIB macromonomer

conversion was shown by ^{1}H NMR to be complete after t = 20 min, while the recorded yields and molecular weight data did not significantly increase after this point. When the monomer:PE ratio was doubled (Run 7), higher molecular weight copolymers were formed and faster macromonomer conversion was observed (t = 10 min). Molecular weight data and yields were found to remain steady for the entirety of the run. Similar results were obtained in Run 8 when the monomer:PE ratio was increased further to form still higher molecular weight materials.

The ^{1}H NMR spectra of the soluble fractions from Runs 6-8 in $CDCl_3$ showed the presence of P(V2EH). Ambient temperature GPC analysis showed that the molecular weight of the The P(V2EH) homopolymer by-products from Run 7 remained constant at M_n *ca* 3200 g/mol, $Đ$ = 2.0 throughout, while those from Run 8 remained constant at M_n *ca* 5600 g/mol, $Đ$ = 2.2 after an initial increase up to t = 20 min.

4.3 Methacrylates

4.3.1 Methyl methacrylate (MMA)

Several contributors have reported the potential use of PE-*b*-P(MMA) and PE-*g*-P(MMA) materials as compatibilisers for PE and P(MMA) homopolymer blends;[17, 18, 19] although synthetic procedures to such materials currently available require multiple reaction steps, often involving interconversion of functional groups in order to generate the P(MMA) component. We therefore investigated whether PE-*i*-DIB could be copolymerised with MMA under the same simple free radical polymerisations as those successfully conducted for acrylates and vinyl esters.

Table 4.3 - Free radical polymerisations of MMA in presence of PE-*i*-DIB.

Run	Init.	Time (min)	Yield (g/%)	M_p [d] (g/mol)	M_n [d] (g/mol)	M_w [d] (g/mol)	$Đ$ [d]	PE-*i*-DIB Conversion (%)[e]
9[a]	BP	240	0.363/19	7000	4300	9000	2.1	100
10	BP	10	0.332/15	7900	3500	8900	2.5	78
	BP	20	0.343/16	10100	4300	10900	2.3	100
	BP	40	0.341/16	7400	4500	9800	2.1	100
	BP	60	0.328/15	8400	4400	9700	2.2	100
	BP	120	0.321/14	8200	4600	9600	2.1	100
	BP	180	0.345/16	7800	4100	9500	2.3	100
	BP	240	0.366/19	8100	4200	9400	2.3	100
11[b]	BP	10	0.728/28	7200	4300	9800	2.3	100
	BP	20	0.706/27	7500	4800	9600	2.0	100
	BP	40	0.726/28	7400	5300	9600	1.8	100
	BP	60	0.702/27	7600	5200	9900	1.9	100
	BP	120	0.696/27	8900	5200	11400	2.2	100
	BP	180	0.748/29	8300	5100	11300	2.2	100
	BP	240	0.751/29	10100	5500	10800	2.2	100
12[c]	BP	10	0.786/16	9300	6000	14400	2.4	100
	BP	20	0.853/18	11900	6600	16300	2.5	100
	BP	40	0.858/18	12200	6700	16600	2.5	100
	BP	60	0.846/17	11200	6600	16700	2.5	100
	BP	120	0.851/18	12100	6700	17200	2.6	100
	BP	180	0.866/18	12000	6700	15800	2.4	100
	BP	240	0.855/18	12200	6400	15500	2.4	100

[a] Polymerisation conditions: PE-*i*-DIB = 0.2 g, Mn = 2100 g/mol, Đ = 2.1; initial [PE-*i*-DIB] = 0.011 mol/L; comonomer = MMA; mass MMA added = 0.88 g (1 ml); MMA:PE = 100:1 initiator = BP; [initiator] solution = 0.11 mol/L; solvent = toluene; total volume = 8.2 ml; temperature = 125°C.
[b] MMA added = 1.9 g (2 ml); MMA:PE = 200:1.
[c] MMA added = 3.7 g (4 ml); MMA:PE = 400:1.
[d] GPC data obtained at 160°C in 1,2,4-trichlorobenzene using universal calibration. PS standards were used to calibrate the system (see Chapter 6, Section 6.1 for further details).
[e] Calculated from ^{1}H NMR.

A copolymerisation of PE-*i*-DIB (M_n = 2100 g/mol, $Đ$ = 2.1) with 100 equivalents of MMA (Run 9, Table 4.3) was conducted under the same high temperature conditions as described earlier. The copolymer isolated by precipitation in methanol was shown by ^{1}H NMR to contain signals assignable to both PE and PMMA and full DIB end group conversion was observed. Kinetic runs (Runs 10-12, Table 4.3) were then conducted as

before to investigate the copolymerisation further with varying monomer:PE molar ratios (100:1, 200:1, 400:1 respectively). As with P(*n*-BA)/methanol system discussed in Chapter 3, the well-documented insolubility of P(MMA) in methanol means that it seems an illogical choice of anti-solvent to isolate the copolymer. However, in runs with lower monomer concentrations (Runs 10 and 11), it appeared that the P(MMA) produced was sufficiently low in molecular weight that multiple reprecipitations from toluene into methanol yielded a copolymer product with no evidence of homopolymer contaminant *e.g.* evidence of termination by disproportionation, which is known to be the dominant mechanism in MMA polymerisation[20, 21] (*c.f.* Section 4.5.3). However, products from copolymerisations with higher monomer concentration (*e.g.* Run 12) were precipitated from the main reaction mixture using methanol and then purification was attempted by soxhlet extraction.

In Run 10, macromonomer conversion was achieved by t = 20 min after which the molecular weights and dispersities remained consistent. In Runs 11 and 12 we observe that the macromonomer was fully converted more quickly (t = 10 min) and higher molecular weight products were obtained. In Run 11 the yields and molecular weights are similar throughout; the same trend is also observed in Run 12. The material recovered from the soluble fraction was shown to be PMMA by ^{1}H NMR and GPC analysis on the recovered homopolymer from Runs 11 and 12 showed consistent molecular weights and dispersities throughout the reactions of M_n *ca* 1600 g/mol, $Đ$ = 1.6 and 2700 g/mol, $Đ$ = 1.8 respectively by GPC in $CHCl_3$. The ^{1}H NMR spectra in $CDCl_3$ of the homopolymer recovered from the soluble fractions (Figures C.15. – C.16.) did indeed show vinyl end group signals at 5.4 and 6.2 ppm which we would expect to also be present in the NMR spectra of the copolymer products (*c.f.* Section 4.2.3) if the samples were impure. This does not rule out the presence of P(MMA) chains that have

terminated by combination in the NMR spectra of the copolymers but since the proportion of chains terminating in this way is *ca* 20%,[21] we can say that the majority of the homopolymer contaminant has been removed based on the absence of these signals. Mass balance would also suggest that most of the homopolymer either stayed in the methanol or was removed by reprecipitation or soxhlet extraction.

4.3.2 Myristyl (C14) methacrylate

Myristyl methacrylate (C14MA) is a commercially available methacrylate monomer with a long alkyl chain that has found use in wax crystal modification in both oil and diesel.[22]

A copolymerisation of PE-*i*-DIB (M_n = 2100 g/mol, $Đ$ = 2.1) with 200 equivalents of C14MA (Run 13, Table 4.4) with BP as the initiator. Attempts to separate the polymeric mixture were conducted by precipitation in acetone with multiple reprecipitations from toluene into acetone. The ^{1}H NMR spectrum of the precipitated product showed signals assignable to PE and P(C14MA), with 100% macromonomer conversion also observed. The high dispersity and the multimodal trace obtained from GPC suggested that the product still contained significant amounts of homopolymer even after multiple reprecipitations. This was also supported by the presence of ^{1}H NMR signals at 5.4 and 6.2 ppm corresponding to vinylidene end groups resulting from termination of C14MA polymerisation by disproportionation.

Table 4.4 - Free radical polymerisations of C14MA in presence of PE-*i*-DIB.

Run	Init.	Time (min)	Yield (g/%)	M_p [e] (g/mol)	M_n [e] (g/mol)	M_w [e] (g/mol)	$Đ$ [e]	PE-*i*-DIB Conversion (%)[f]
13[a]	BP	240	3.21/56	155500	39300	315300	8.0	100
14[b]	BP	10	0.327/20	4700	3000	5300	1.8	86
	BP	20	0.338/21	6900	4700	9200	2.0	100
	BP	40	0.350/23	6700	4100	10500	2.6	100
	BP	60	0.358/24	7400	4100	9700	2.4	100
	BP	120	0.347/23	6900	4300	9800	2.3	100
	BP	180	0.323/19	7300	4000	9000	2.3	100
	BP	240	0.352/23	7200	4500	10300	2.3	100
15[c]	BP	10	0.687/37	12000	6700	20000	3.0	92
	BP	20	0.715/40	12700	6700	22800	3.4	100
	BP	40	0.768/43	11800	6500	23000	3.5	100
	BP	60	0.681/37	12100	6800	22700	3.3	100
	BP	120	0.723/40	11900	6200	19400	3.1	100
	BP	180	0.656/35	13600	6500	23400	3.6	100
	BP	240	0.721/40	13200	6700	21900	3.3	100
16[d]	BP	10	1.03/31	22000	12600	60100	4.8	100
	BP	20	1.57/51	21200	12000	65000	5.4	100
	BP	40	1.77/58	22300	11800	68000	5.8	100
	BP	60	1.42/45	22900	11600	61700	5.3	100
	BP	120	1.56/50	25600	11500	64200	5.6	100
	BP	180	1.60/52	23800	12100	66700	5.5	100
	BP	240	1.63/53	25500	11600	64000	5.5	100

[a] Polymerisation conditions: PE-*i*-DIB = 0.2 g, M_n = 2100 g/mol, Đ = 2.1; initial [PE-*i*-DIB] = 0.011 mol/L; comonomer = C14MA; mass C14MA added = 200 equivalents, 5.4 g (6.2 ml); initiator = BP; [initiator] solution = 0.11 mol/L; solvent = toluene; total volume = 8.2 ml; temperature = 125°C.
[b] C14MA added = 25 equivalents, 0.65 g (0.75 ml).
[c] C14MA added = 50 equivalents, 1.3 g (1.5 ml).
[d] C14MA added = 100 equivalents, 2.7 g (3.1 ml).
[e] GPC data obtained at 160°C in 1,2,4-trichlorobenzene using universal calibration. PS standards were used to calibrate the system (see Chapter 6, Section 6.1 for further details).
[f] Calculated from ^{1}H NMR.

The difficulty in isolating copolymer from homopolymer led us to use lower monomer concentrations for the kinetic runs. We observe in Runs 14-16 (Table 4.4) that the molecular weight, dispersity and rate of macromonomer conversion increase with monomer:PE ratio. We also observe that recorded yields and polymer characteristics

remained fairly constant after macromonomer conversion in all three runs. The material recovered from the soluble fraction of Runs 14-16 was shown by ^{1}H NMR to contain both P(C14MA) and C14MA monomer. Familiar vinylidene proton signals at 5.4 and 6.2 ppm were detected and their absence in the copolymer NMR spectra indicates successful separation of products. Ambient temperature GPC analysis on the recovered homopolymer from Runs 15 and 16 showed low molecular weights and dispersities throughout the reactions of M_n *ca* 1300 g/mol, $Đ$ = 1.5 and 1600 g/mol, $Đ$ = 1.6 respectively.

4.4 Styrene

Much of the interest in PE-PS copolymers of various architectures comes from reports of their potential application in mediating blending of PE and PS mixtures.[23, 24] Although styrene has a substantially lower propagation rate constant than *e.g.* *n*-BA,[25] investigations of styrene/AMS copolymerisations under CCTP conditions produced similar AMS-terminated macromonomers to those formed in the *n*-BA/AMS system.[26, 27]

A copolymerisation of PE-*i*-DIB (M_n = 3000 g/mol, $Đ$ = 2.1) and 500 equivalents of styrene (Run 17, Table 4.5) was conducted under the same high temperature conditions using TP as the source of radicals because of its availability at the time of the run. The copolymer was isolated by precipitation in acetone and the ^{1}H NMR spectrum of the precipitated product showed the presence of signals corresponding to both PE and PS. 100% of the DIB end groups were converted and the copolymer M_n of 24,400 g/mol ($Đ$ = 2.1) was determined by GPC; substantially higher than most of the materials described above.

Table 4.5 - Free radical polymerisations of styrene in presence of PE-*i*-DIB.

Run	Init.	Time (min)	Yield (g/%)	M_p [e] (g/mol)	M_n [e] (g/mol)	M_w [e] (g/mol)	$Đ$ [e]	PE-*i*-DIB Conversion (%)[f]
17[a]	TP	360	1.60/40	39700	24400	52000	2.1	100
18[b]	BP	10	0.256/6	4700	2500	11000	4.4	85
	BP	20	0.294/9	4900	2800	9500	3.3	90
	BP	40	0.326/13	6000	3400	12700	3.7	>95
	BP	60	0.328/13	6300	3400	11000	3.1	>95
	BP	120	0.330/13	6700	3500	11400	3.2	>95
	BP	180	0.367/17	6400	3600	11800	3.3	>95
	BP	240	0.373/17	5900	3500	11600	3.3	>95
19[c]	BP	10	0.340/7	10700	5000	19000	3.8	>95
	BP	20	0.366/8	15100	6200	22900	3.7	>95
	BP	40	0.438/12	15400	7000	23800	3.4	>95
	BP	60	0.411/11	14500	6800	23700	3.5	>95
	BP	120	0.470/14	16200	7600	26600	3.5	>95
	BP	180	0.550/18	16100	7500	27000	3.6	>95
	BP	240	0.585/19	16800	8000	27800	3.5	>95
20[d]	BP	10	0.622/11	18100	16200	44500	2.8	100
	BP	20	0.756/14	22900	21000	67500	3.2	100
	BP	40	1.11/23	34500	22400	79100	3.5	100
	BP	60	1.24/26	35000	21100	71000	3.4	100
	BP	120	1.25/26	40000	22500	81000	3.6	100
	BP	180	1.34/29	39400	22200	75500	3.4	100
	BP	240	1.33/28	42000	23400	79600	3.4	100

[a] Polymerisation conditions: PE-i-DIB = 0.2 g, M_n = 3000 g/mol, Đ = 2.1; initial [PE-*i*-DIB] = 0.0083 mol/L; comonomer = Styrene; mass Styrene added = 3.5 g (3.8 ml); STY:PE = 500:1; initiator = TP; [initiator] solution = 0.081 mol/L; solvent = toluene; total volume = 8.2 ml; temperature = 125°C.
[b] PE-*i*-DIB = 0.2 g, M_n = 2100 g/mol, Đ = 2.0; initial [PE-*i*-DIB] = 0.011 mol/L; mass Styrene added = 1 g (1.1 ml); STY:PE = 100:1; initiator = BP; [initiator] solution = 0.11 mol/L.
[c] Styrene added = 2 g (2.2 ml); STY:PE = 200:1.
[d] Styrene added = 4 g (4.4 ml); STY:PE = 400:1.
[e] GPC data obtained at 160°C in 1,2,4-trichlorobenzene using universal calibration. PS standards were used to calibrate the system (see Chapter 6, Section 6.1 for further details).
[f] Calculated from ^{1}H NMR.

To further investigate this reaction, kinetic runs on copolymerisations of PE-*i*-DIB (M_n = 2100 g/mol, $Đ$ = 2.1) with S:PE molar ratios of 100:1, 200:1 and 400:1 respectively were conducted but this time in the presence of BP, which was chosen to try to convert the macromonomer more quickly and lower the final molecular weight of the products

by production of more propagating chains early on. In Runs 18 and 19 (Table 4.5), an increase in yield and molecular weight is observed as the polymerisation progresses but, unusually for these reactions, the macromonomer was not fully converted. In Run 20, with the monomer concentration increased further, full macromonomer conversion was achieved early on but the molecular weight of the products increased substantially. Under similar conditions, Moad and co-workers reported that the use of AMS in CCTP of styrene afforded a simple method for molecular weight control;[26] an observation that was supported by our own free radical copolymerisations of styrene with AMS in which we observed significant molecular weight reduction (M_n = 13000, $Đ$ = 2.2 compared to M_n = 20000, $Đ$ = 2.6) with as little as 2 mol% AMS. In Runs 18-20, the AMS-like PE-*i*-DIB is present at a maximum concentration of 1 mol% relative to the monomer (Run 18), which it appears is insufficient to control the styrene polymerisation effectively at this high temperature. This is consistent with our conclusion from Chapter 3 that PE-*i*-DIB is limited in its ability to mediate the polymerisation, which in this case was probably compounded by thermal self-initiation of styrene at high temperatures.[28] At lower temperatures, where the propagation rate is lower and the contribution of thermal initiation is reduced,[28, 29] we might expect to achieve better control over the PS block length. However, the solubility of the macromonomer limits the extent to which this can be utilised.

^{1}H NMR spectra showed that the soluble fractions isolated from Runs 18-20 consisted of PS. GPC analysis conducted on the PS homopolymer samples obtained from run 19 showed consistent molecular weights and dispersities of M_n = 2300 g/mol, $Đ$ = 2.7 throughout, whereas in Run 20 molecular weights increased with time up to M_n = 5700 g/mol, $Đ$ = 2.8 at t = 60 min and then remained consistent for the remainder of the polymerisation.

4.5 NMR analysis

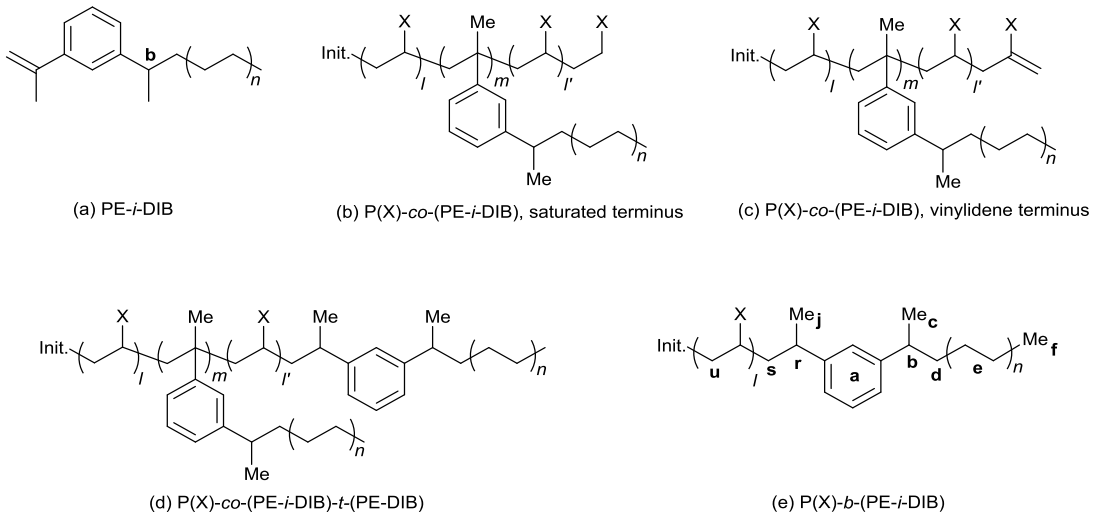

Figure 4.2 - PE-*i*-DIB and expected structures from copolymerisation with polar monomers.

4.5.1 PE-*b*-P(*n*-BA) NMR analysis

The structure of the precipitated products from the copolymerisations was investigated by NMR spectroscopy with the objective to ascertain whether the principal components were graft copolymers such as in Figure 4.2, (b) - (d), or a block copolymer (e). NMR analysis conducted previously on higher molecular weight copolymer samples yielded some evidence of block structure but many of the important correlations could not be detected due to significant overlap with large P(*n*-BA) signals that appeared in the same regions.[1] Analysis on copolymers with lower DP P(*n*-BA) segments could reasonably be expected to yield more substantial evidence of structure as a result of less signal overlap. Figure 4.3 shows the ^{1}H NMR spectrum of the final product recovered from run 9, Table 3.4 isolated by precipitation in methanol. A singlet peak is observed at $\delta = 1.30$ ppm corresponding to the PE backbone methylene protons. Peaks attributed to a P(*n*-BA) segment are also present.[30]

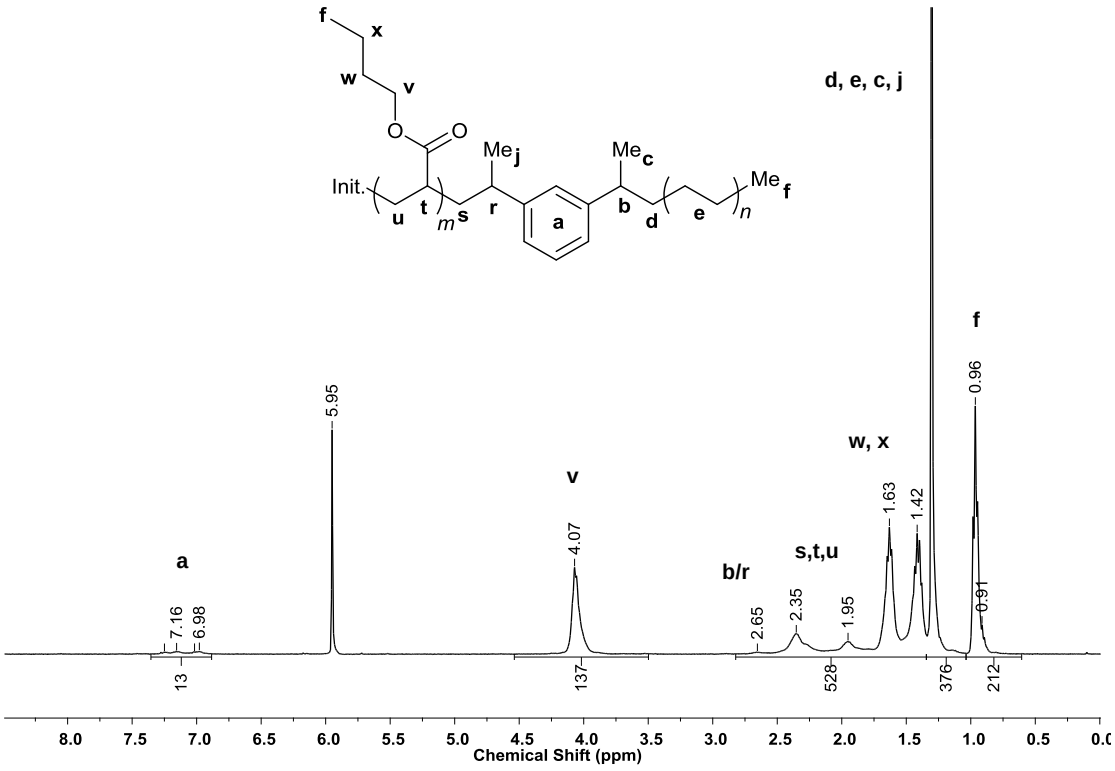

Figure 4.3 - ^{1}H NMR spectrum of PE-*b*-P(*n*-BA) in d^2-TCE at 100°C (400 MHz). Relaxation delay = 1 s. Integral of the *n*-BA signal at 4.07 ppm is set as follows: if we assume that an average of one PE-*i*-DIB macromonomer (M_n 2200 g/mol) is present in copolymer chains (M_n 11000 g/mol), the contribution of *n*-BA to the M_n of the copolymer is *ca* 11000-2200 = 8800 g/mol. Hence integral of *ca* 2 × (8800/128.2) = 137 H.

The absence of DIB end group vinylidene protons (δ = 5.07 and 5.34 ppm) in this and all similar samples is consistent with complete conversion of the PE-*i*-DIB starting material. Similarly the absence of P(*n*-BA) vinylidene end group signals (5.5, 6.2 ppm) indicates not only that the copolymer was successfully separated from P(*n*-BA) homopolymer species, but also that species (c) formed by polymerisation *through* PE-*i*-DIB macromonomer, followed by backbiting/*β*-scission, is absent. This does not however, allow us to exclude the presence of copolymer (d) formed by polymerisation through, and finally termination to PE-*i*-DIB units.

In the ^{1}H NMR spectra of these species, the signal for the PE chain at *ca* 1.3 ppm overlaps substantially with the signal for the P(*n*-BA) side chain methylene multiplet at

ca 1.4 ppm. Likewise the PE end group methyl signal overlaps with a broad P(*n*-BA) side chain CH_3 multiplet at *ca* 1 ppm. As a result the average number of PE segments per polymer unit (*i.e.* the degree of polymerisation of PE-*i*-DIB) cannot be reliably estimated by direct integration. Nevertheless, assuming for the moment that the copolymer (M_n = 11000 g/mol by universal calibration of GPC) includes a single macromonomer unit (2200 g/mol) we can readily calculate the expected integral of the P(*n*-BA) ester CH_2 signal at *ca* 4.1 ppm (Figure 4.3) to be *ca* 137 H. The relative integrals of the remaining groups correspond closely to expectations: (i) the somewhat overlapping peaks between *ca* 2.7 and 1.3 ppm have an integral of 903 H (expected 924 H) and the relative integrals within this group are appropriate, including the PE main chain of 375 (expected 396 H); (ii) the more isolated signal at *ca* 1.0 ppm containing P(*n*-BA) and PE methyl group resonances has an integral of 212 H (206 H expected); (iii) the isolated aromatic signal at *ca* 6.9-7.3 ppm has an integral of 13 H (9 H expected); noting that the sample contains a small amount of toluene. Hence, the assumption of the presence of *ca* one PE-*i*-DIB macromonomer per copolymer chain is consistent with integration of the high temperature ^{1}H NMR spectrum. If some polymer (d) is present, then the in-chain degree of polymerisation (*i.e. m*) is small.

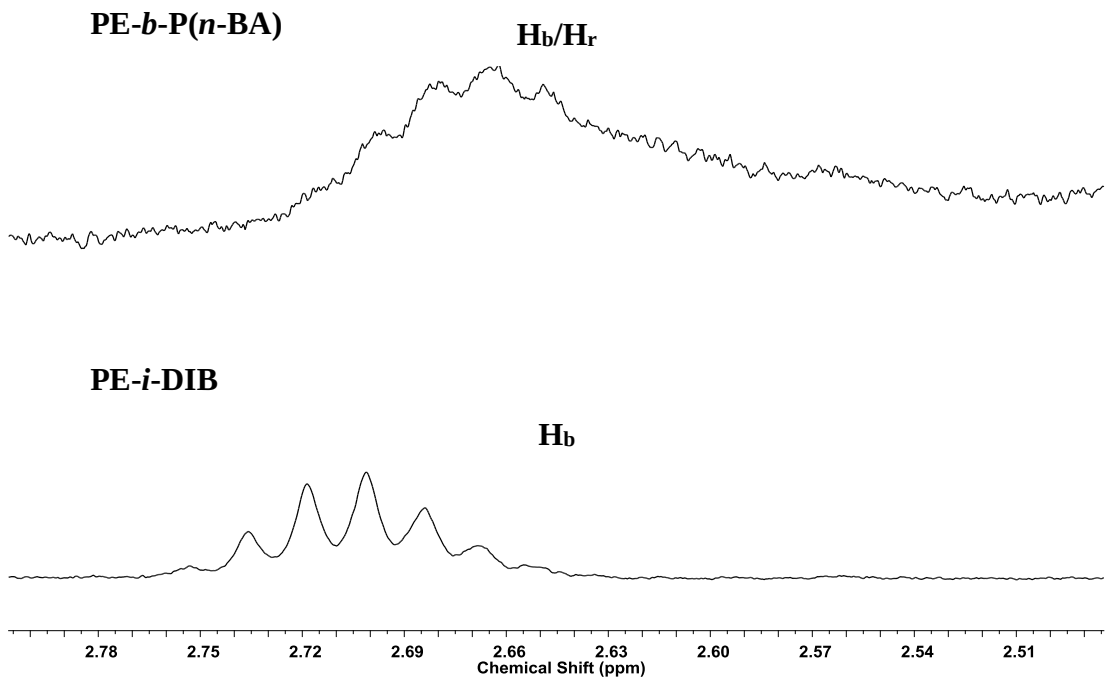

Figure 4.4 - ^{1}H NMR spectrum of PE-*i*-DIB and PE-*b*-P(*n*-BA) in d^{2}-TCE at 100°C, focussed on benzylic methine region (400 MHz).

The remaining architecture of Figure 4.2 – block copolymer (e) – is expected to have two inequivalent benzylic CH signals in the region 2.6-2.8 ppm, and while the above spectra are consistent with this, the significant overlap of the small signals in this region with those of the large P(*n*-BA) methine resonances at 2.35 ppm, renders integration unreliable. In Figure 4.4 we compare the benzylic regions of PE-*i*-DIB and the copolymer. In the former the centre of the sharp benzylic signal (**H$_b$**) is 2.70 ppm while in the latter a broader and higher relative intensity signal appears at 2.67 ppm (**H$_b$/H$_r$**). Figure 4.5, a segment of the ^{1}H-^{1}H COSY under the same conditons, shows that this methine signal gives a diagonally elongated cross-peak correlating to *ca* 1.2-1.25 ppm. Hence, although the individual correlations are unresolved, this is consistent with benzylic proton environments **H$_b$** and **H$_r$** coupling to methyl environments **Me$_c$** and **Me$_j$**

either side of the aromatic ring.[†] As shown in Figure 4.6, correlations between **H_r** and the neighbouring P(*n*-BA) methylene environments **H_s** at *ca* 1.75/1.78 ppm[‡] can be assigned readily, and while that between **H_b** and neighbouring PE methylene environments **H_d** at 1.54/1.59 ppm[‡] is broader, a further plot (Figure 4.7) shows this more clearly.

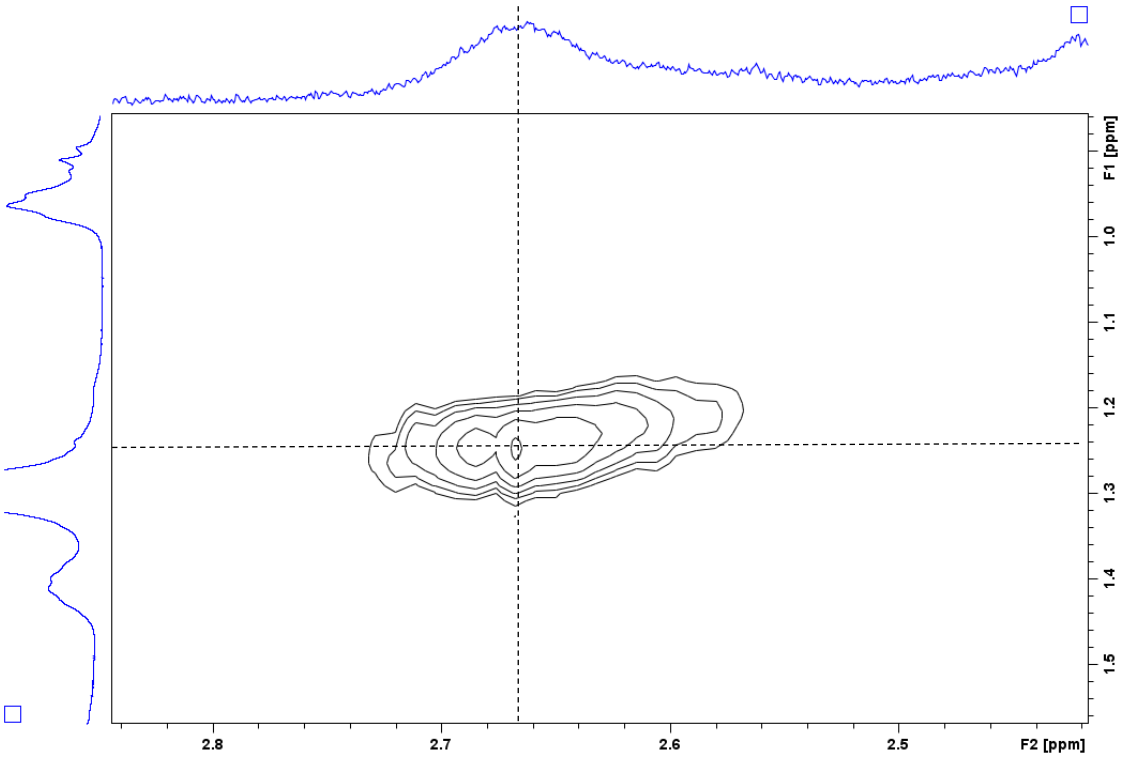

Figure 4.5 - Detail of a ^{1}H-^{1}H COSY NMR of PE-*i*-DIB-*b*-P(*n*-BA) in d^2-TCE at 100°C (500 MHz).

[†] Expected chemical shifts for Me_c and Me_j calculated by ACD/I-LAB to be 1.16 ± 0.23 and 1.29 ± 0.23 ppm respectively.
[‡] Expected chemical shifts for H_d and H_s calculated by ACD/I-LAB to be 1.52/1.76 ± 0.54 ppm and 1.82/2.08 ± 0.40 ppm respectively.

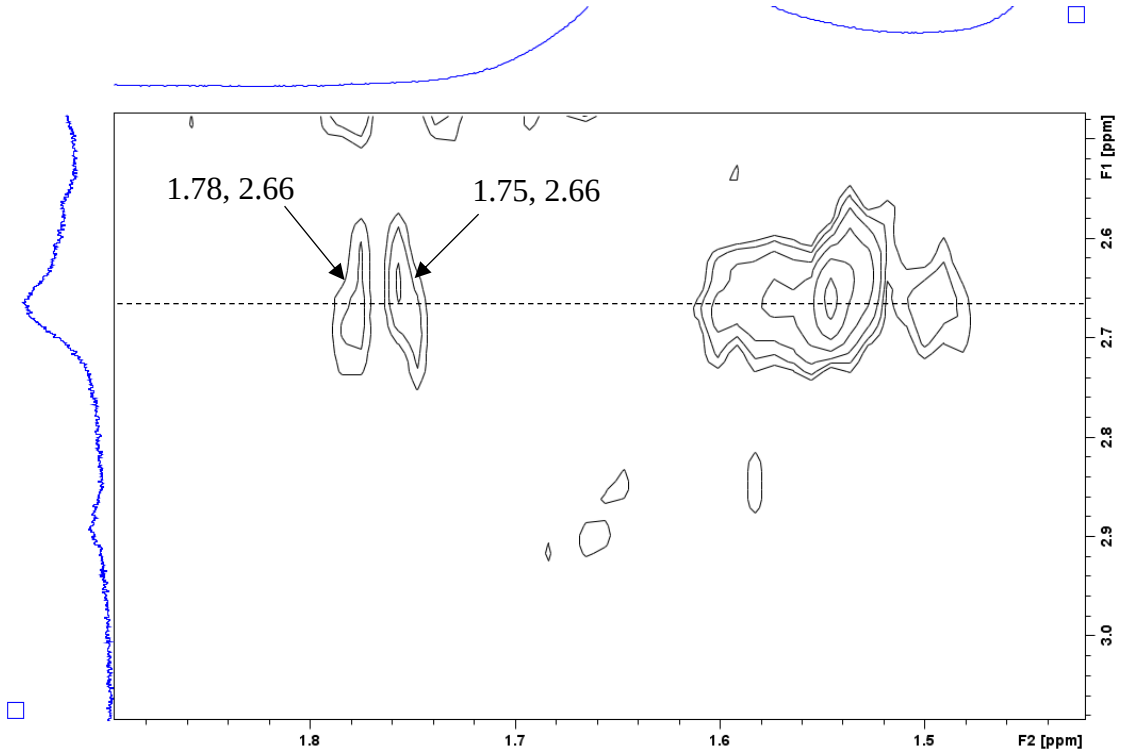

Figure 4.6 - Detail of a ^{1}H-^{1}H COSY NMR of PE-*i*-DIB-*b*-P(*n*-BA) in d^{2}-TCE at 100°C (500 MHz).

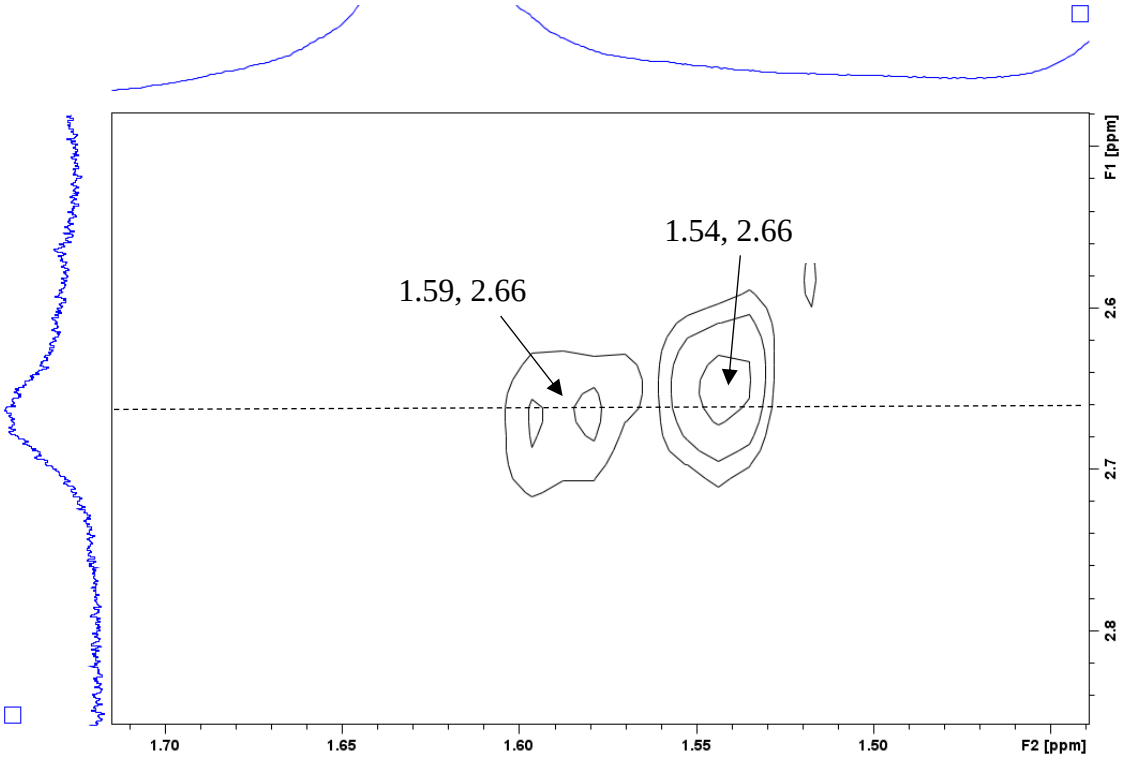

Figure 4.7 - Detail of a ^{1}H-^{1}H COSY NMR of PE-*i*-DIB-*b*-P(*n*-BA) in d^{2}-TCE at 100°C (500 MHz).

The ^{1}H-^{13}C HMQC (Figure 4.8) shows a cross-peak between the benzylic ^{1}H region and what are apparently overlapping ^{13}C signals at *ca* 40 ppm† in the expected chemical shift for **C$_b$** and **C$_r$**. A rather lower intensity ^{13}C signal appears nearby at 38.2 ppm but no ^{1}H correlation could be resolved.†

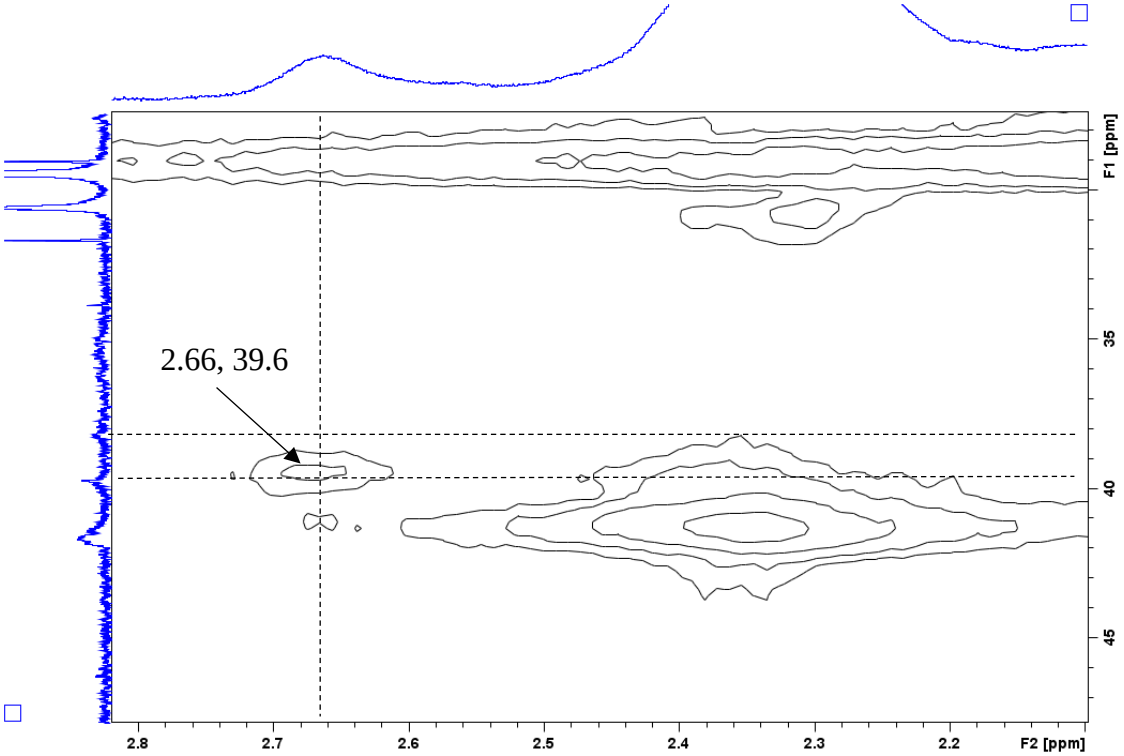

Figure 4.8 - Detail of ^{1}H-^{13}C HMQC NMR of PE-*i*-DIB-*b*-P(*n*-BA) in d^2-TCE at 100°C (500 MHz).

4.5.2 PE-*b*-P(VAc) NMR analysis

NMR spectroscopy was used again to investigate the structure of the PE-*b*-P(VAc) copolymers and to determine whether graft copolymers (b) - (d) or a block copolymer (e) was formed (Figure 4.2). Figure 4.9 shows the ^{1}H NMR spectrum at 100°C of the PE containing product isolated by precipitation from ethanol. A fully resolved triplet peak at δ = 0.91 ppm and a peak at δ = 1.30 ppm corresponding to PE methyl end group and

† Expected chemical shifts for C_b and C_r calculated by ACD/I-LAB to be 40.1 ± 2.4 and 37.9 ± 5.3 ppm respectively.

PE backbone methylene protons are observed, along with peaks attributed to a P(VAc) segment.[31]

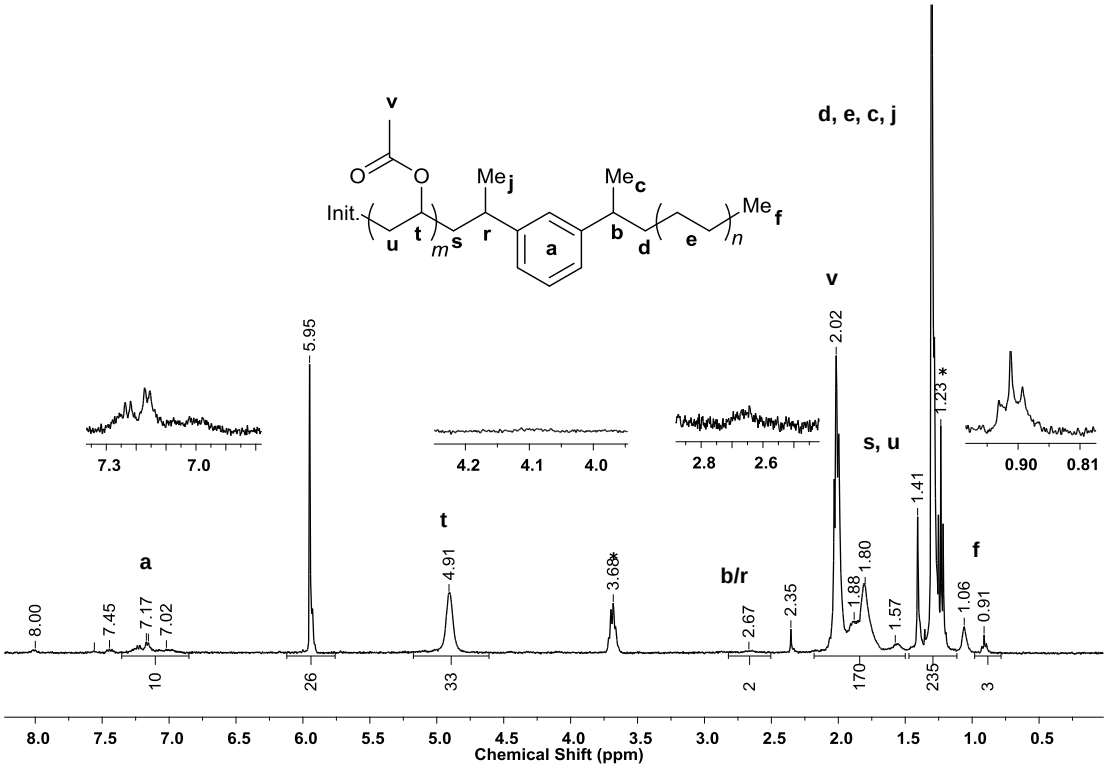

Figure 4.9 - ^{1}H NMR of PE-*b*-P(VAc) in d^2-TCE at 100°C (400 MHz). Relaxation delay = 1 s

As before, complete conversion of the macromonomer was confirmed by the absence of the DIB vinylidene protons at 5.07 and 5.34 ppm. Also detectable in some crude samples (though clearly absent in Figure 4.9) was a very small peak at 4.1 ppm which corresponds to the methylene end group of P(VAc), consistent with a small amount of homopolymer co-precipitating from the polymerisation mixture. This impurity was successfully removed by reprecipitation from toluene into ethanol for the sample shown above, but in some samples prepared using high monomer concentration this signal remained (*e.g.* Figure C.10.). The assignment of this peak as a methylene end group of P(VAc) was supported by the work of Lovell and Debuigne and confirmed by our own 2D NMR experiments on the homopolymer (Figures C.11. – C.12); the signal occurs as

a result of termination *via* chain transfer by H abstraction and also as a result of termination by disproportionation, which would also produce an equivalent number of vinylic end groups detectable in the ^{1}H and ^{13}C NMR spectra.[31, 32] The absence of such vinylic signals in the copolymer (Figure C.13.), even at high expansion, and their presence in the homopolymer (Figure C.14.) is consistent with separation of copolymer from homopolymer. We can thus also rule out polymerisation *through* PE-*i*-DIB followed by disproportionation to form architecture (c) on this basis. The presence of this CH_2 end group in the homopolymer and not the copolymer is consistent with the P(VAc) chain terminating to the macromonomer, which would suggest that polymerisation *through* followed by chain transfer to form architecture (b) is not prevalent.

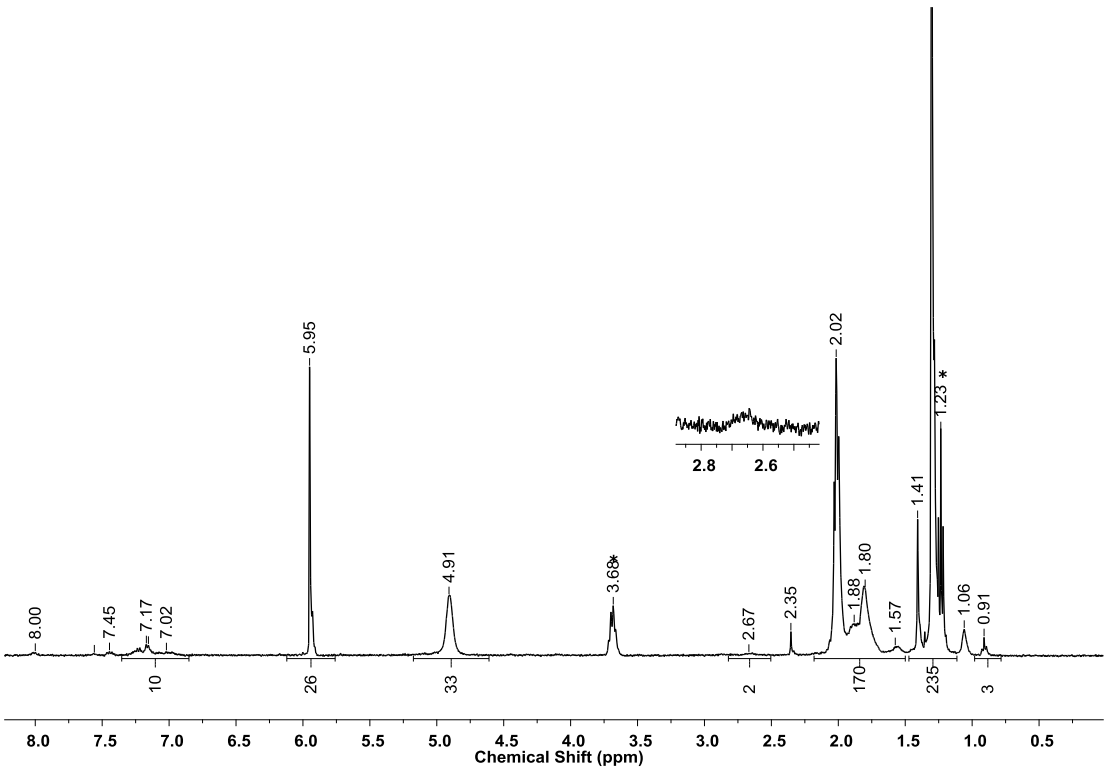

Figure 4.10 - ^{1}H NMR spectrum of PE-*b*-P(VAc) in d^{2}-TCE at 100°C (400 MHz). Relaxation delay = 1 s. Integral of the VAc signal at 4.91 ppm is set as follows: if we assume that an average of one PE-*i*-DIB macromonomer (M_n 2000 g/mol) is present in copolymer chains (M_n 4200 g/mol), the contribution of VAc to the M_n of the copolymer is ca 4200-2000 = 2200 g/mol. Hence integral of *ca* (2200/86.1) = 26 H.

In the case of PE-*b*-P(VAc) the PE methyl end group at δ = 0.91 ppm and P(VAc) backbone methine group at δ = 4.91 ppm are sufficiently well-separated for the copolymer molecular weight to be estimated more directly than for PE-*b*-P(*n*-BA) (*vide supra*). The degree of polymerisation of VAc was thus estimated by integration of the copolymer ^{1}H NMR spectrum as follows. With this integral set to 3, corresponding to the number of protons it represents in a block copolymer structure, the integral of the peak corresponding to the methine protons in the P(VAc) backbone was found to be 33 H, meaning a degree of polymerisation of VAc of 33. The M_n thus calculated for the copolymer is 4900 g/mol (M_n = 4200 g/mol by GPC). Further to this, we can perform a similar calculation to that discussed above for PE-*b*-P(*n*-BA) as follows: we assume for now the copolymer (M_n 4200 g/mol by universal calibration of GPC) includes a single macromonomer unit (2000 g/mol) we can readily calculate the expected integral of the P(*n*-BA) ester CH_2 signal at *ca* 4.91 ppm (Figure 4.10) to be *ca* 26 H. The relative integrals of the remaining groups again correspond closely with expectations: (i) the overlapping peaks between *ca* 1.7 and 2.2 ppm have an integral of 133 H (expected 130 H); (ii) the overlapping signal at *ca* 1.2-1.6 ppm has an integral of 183 H (expected 104 H) bearing in mind the presence of some ethanol; (iii) the isolated PE methyl end group signal at 0.9 ppm has an integral of 2 H (expected 3H) which is a little low but given the size of this peak relative to the rest this is not surprising. Indeed the fact that it is still so close is remarkable; (iv) the isolated benzylic signal at 2.65 ppm has an integral of 2 H (expected 2 H); (v) the isolated aromatic signal has an integral of 8 H (expected 9 H). The consistency of these methods of analysis would appear to support the assumption of the presence of *ca* one PE-*i*-DIB macromonomer per copolymer chain so if some polymer (d) is present, then the in-chain DP must be small.

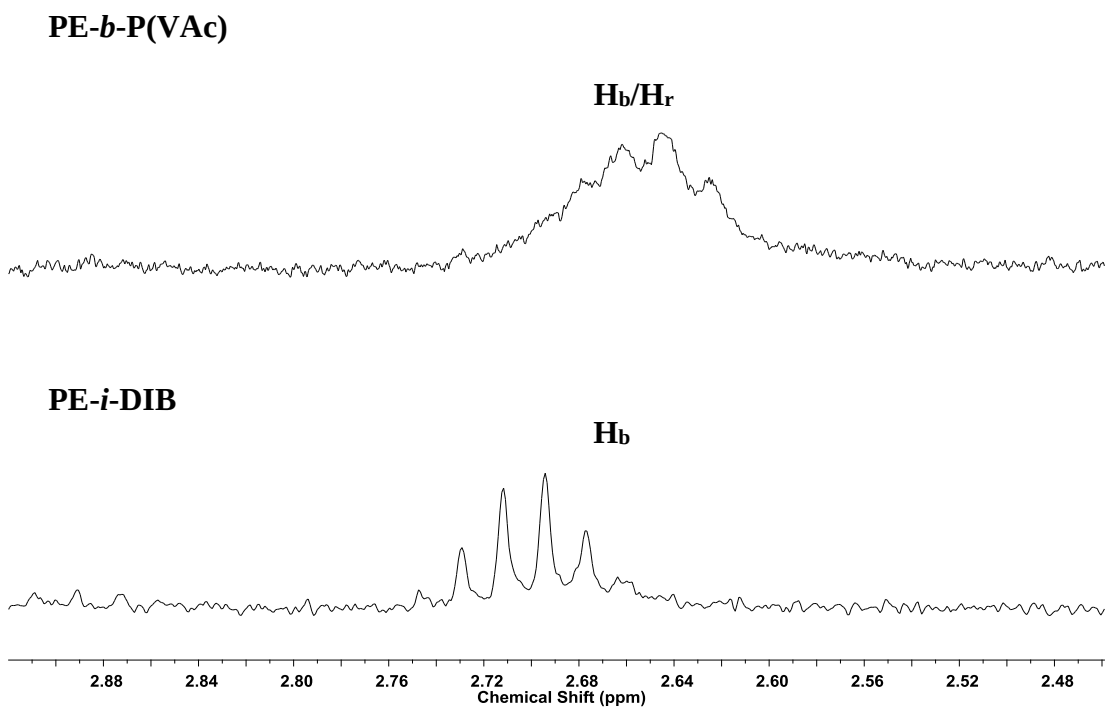

Figure 4.11 - ^{1}H NMR spectrum of PE-*i*-DIB and PE-*b*-P(VAc) in d^2-TCE at 100°C, focussed on benzylic methine region (400 MHz).

From the comparison of the two benzylic CH environments shown in Figure 4.11, we observe first that the benzylic signal in the block copolymer (e) is much better resolved than in PE-*b*-P(*n*-BA) (*vide supra*). As such, the integrals of these benzylic regions can be compared more reliably and we note a shift in the integral of this signal from 1 in the starting material to 2 in the copolymer relative to the PE methyl end group. We also note that the centre of the multiplet in the copolymer is shifted from 2.70 ppm (**H_b**) to 2.65 ppm (**H_b/H_r**).

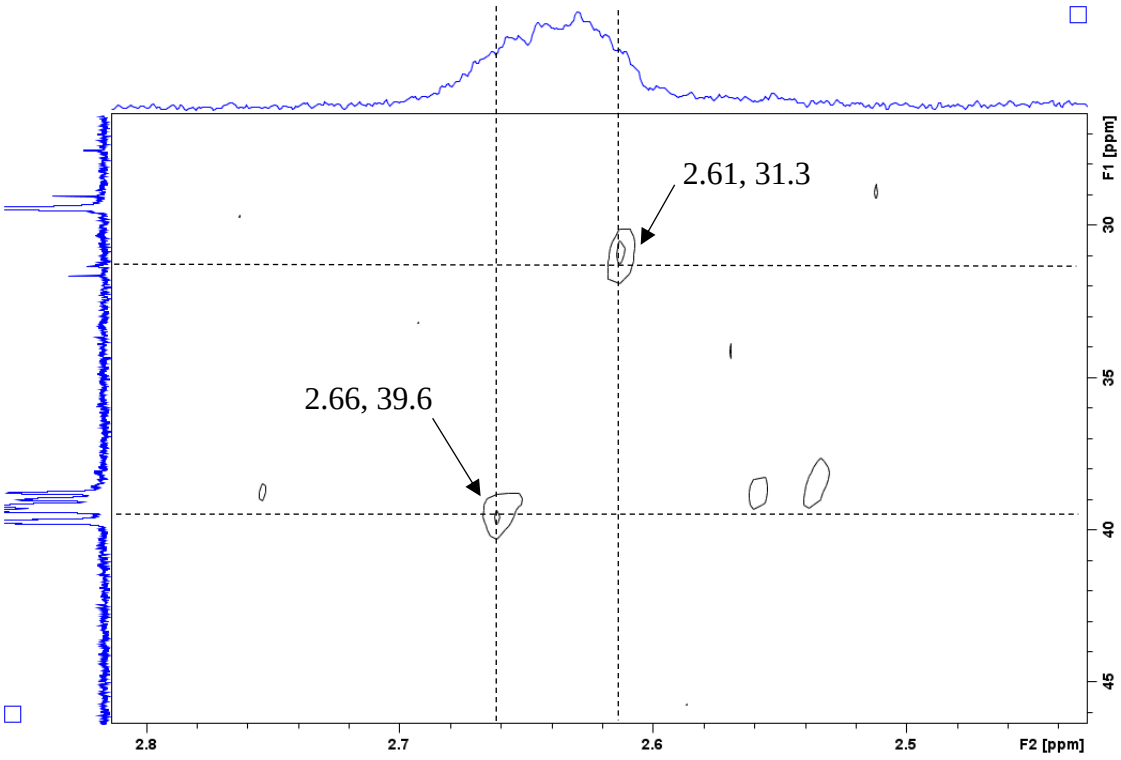

Figure 4.12 - Detail of ^{1}H-^{13}C HMQC NMR of PE-*i*-DIB-*b*-P(VAc) in d^2-TCE at 100°C (600 MHz).

The ^{1}H-^{13}C HMQC (Figure 4.12) indicates that this benzylic ^{1}H region correlates with a small signal at the expected chemical shift for **C$_b$** in the ^{13}C NMR (40 ppm)[†], which falls under the signals corresponding to the P(VAc) backbone CH_2 region. In the same ^{1}H benzylic methine region (2.61 ppm) a correlation with the appropriate chemical shift for **C$_r$** was detected at 31.3 ppm.[†]

[†] Expected chemical shifts for C_b and C_r were calculated by ACD/I-LAB to be 40.1 ± 2.4 and 36.7 ± 5.2 ppm respectively.

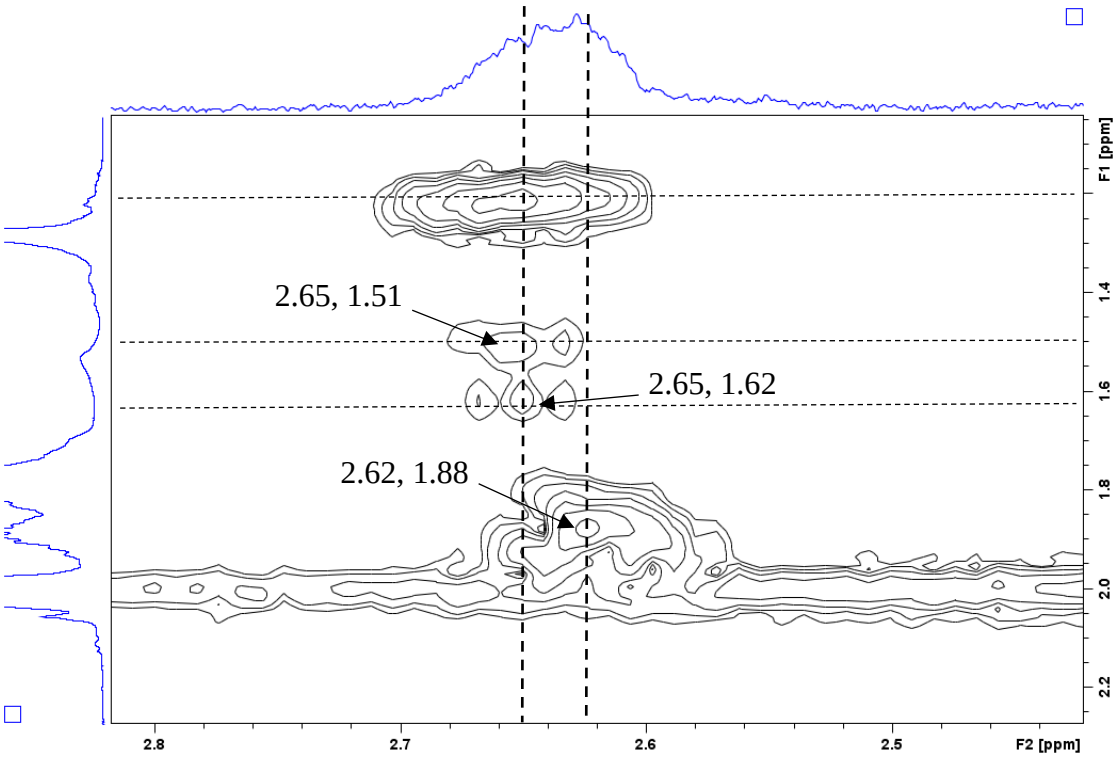

Figure 4.13 - Detail of a ^{1}H-^{1}H COSY NMR of PE-*i*-DIB-*b*-P(VAc) in d^{2}-TCE at 100°C (600 MHz).

The ^{1}H-^{1}H COSY (Figure 4.13) shows that, as before, the overlapping methine signal gives an elongated cross-peak correlating to *ca* 1.2 ppm, and in this instance two appropriate resonances are seen in the benzylic methyl region for **Me$_c$** and **Me$_j$**.[†] The same figure also shows separate correlations between: i) **H$_b$** and the neighbouring diastereotopic backbone methylene proton environments **H$_d$** at 1.51 and 1.62 ppm; and ii) **H$_r$** and methylene environment **H$_s$** at 1.88 ppm, shown more clearly in Figure 4.14.[‡] These observations are similar to those discussed above and are consistent with the block architecture, supporting the integration of 2 for the benzylic region seen in the ^{1}H spectrum.

[†] Expected chemical shifts for Me$_c$ and Me$_j$ calculated by ACD/I-LAB to be 1.16/1.25 ± 0.23 ppm.
[‡] Expected chemical shifts for H$_d$ and H$_s$ calculated by ACD/I-LAB to be 1.52/1.76 ± 0.54 and 1.75/1.94 ± 0.4 ppm respectively.

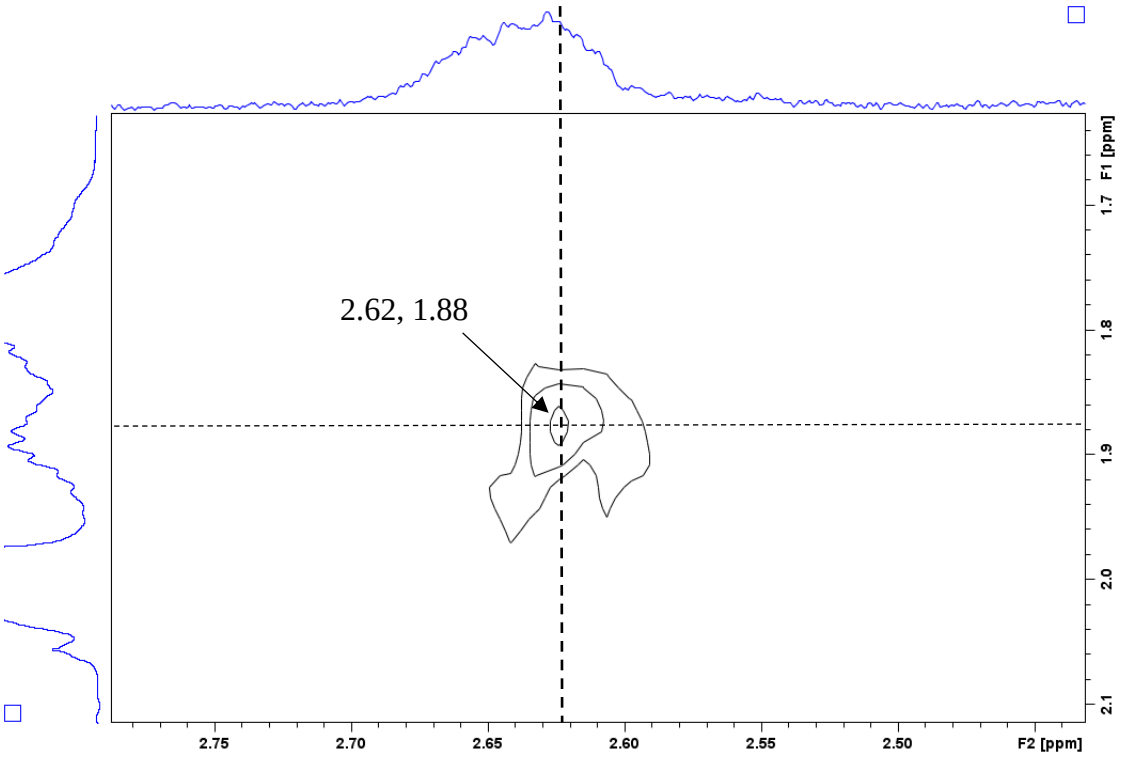

Figure 4.14 - Detail of a ^{1}H-^{1}H COSY NMR of PE-*i*-DIB-*b*-P(VAc) in d^{2}-TCE at 100°C (600 MHz).

4.5.3 PE-*b*-P(MMA) NMR Analysis

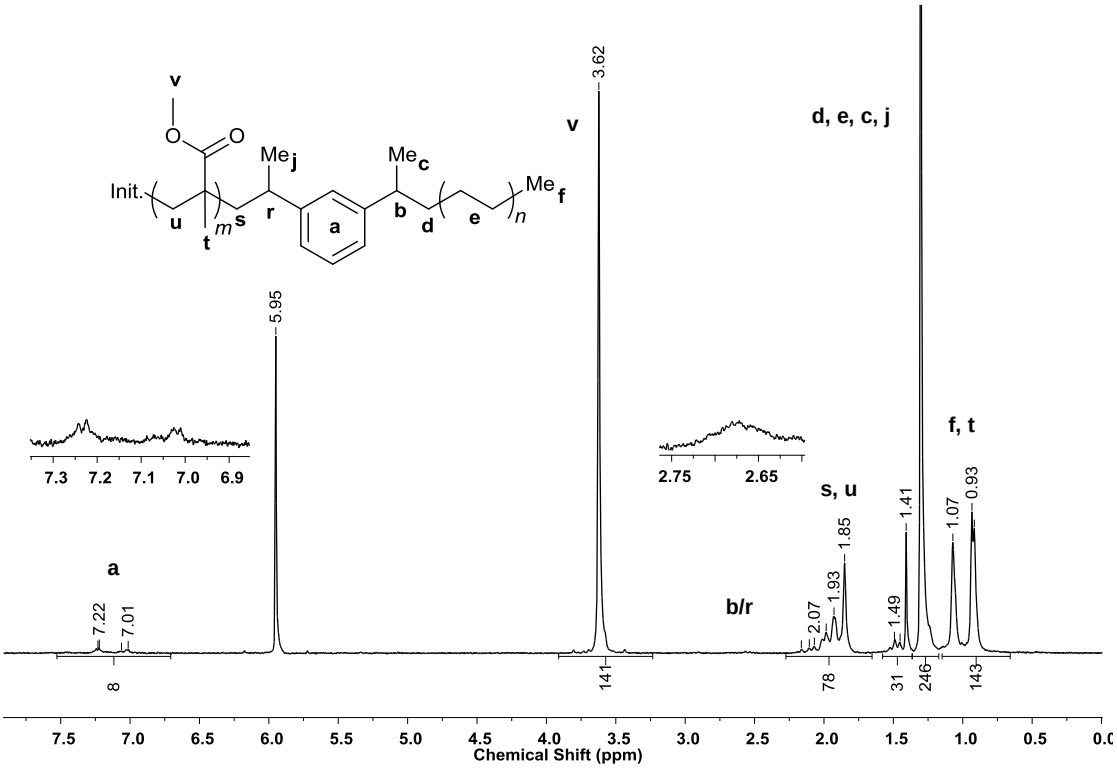

Figure 4.15 - ^{1}H NMR spectrum of PE-*b*-P(MMA) in d^2-TCE at 100°C (400 MHz). Relaxation delay = 1 s.

Figure 4.15 shows the ^{1}H NMR spectrum recorded at 100°C of the PE containing product isolated from the 240 min sample of Run 12 (Table 4.3). The PE methyl triplet peak at *ca* 0.91 ppm is obscured by P(MMA) methyl signals at *ca* 0.93 ppm but a peak at *ca* 1.30 ppm corresponding to PE backbone methylene protons is observed, along with signals that are attributable to a P(MMA) segment.[18, 33]

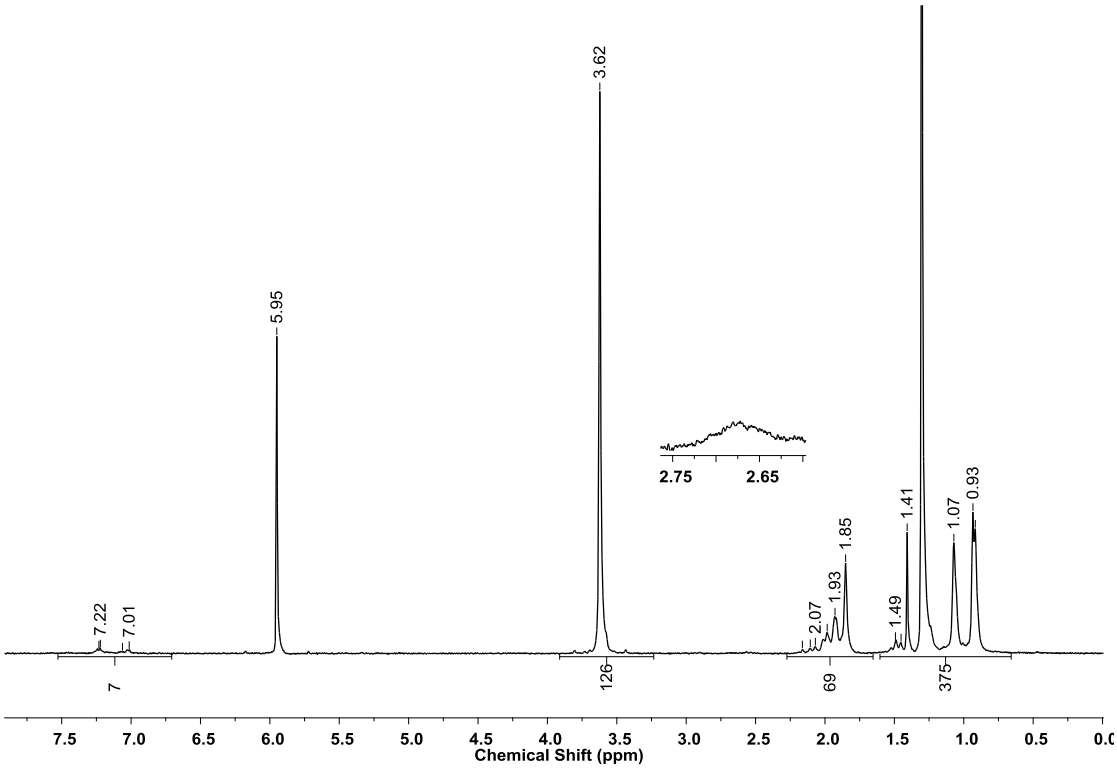

Figure 4.16 - ^{1}H NMR spectrum of PE-*b*-P(MMA) in d^{2}-TCE at 100°C (400 MHz). Relaxation delay = 1 s. Integral of the MMA signal at 3.6 ppm is set as follows: if we assume that an average of one PE-*i*-DIB macromonomer (M_n 2200 g/mol) is present in copolymer chains (M_n 6400 g/mol), the contribution of MMA to the M_n of the copolymer is *ca* 6400-2200 = 4200 g/mol. Hence integral of *ca* 3 × (4200/100.1) = 126 H.

The absence of the DIB vinylidene protons at 5.07 and 5.34 ppm confirms that the macromonomer was fully converted. In the P(MMA) homopolymer samples, signals at 5.47 and 6.20 ppm were detected, assignable as vinylidene end groups occurring as a result of termination by disproportionation.[20, 21, 33, 34] The absence of such signals in the copolymer NMR spectra suggests structure (c) is not prevalent. Given that the PE main chain CH_2 signal at 1.3 ppm and the P(MMA) ester methyl signal at 3.6 ppm are fairly well resolved, direct estimation of M_n by ^{1}H NMR was conducted as follows: from the ^{1}H NMR spectrum of PE-*i*-DIB we estimate a degree of polymerisation of 62 corresponding to an integral of the PE main chain CH_2 of 246 H. The integral of the P(MMA) ester methyl signal was thereby 141 H, which corresponds to a MMA DP of

47. The M_n thus calculated for the copolymer is 6800 g/mol (M_n = 6400 g/mol by GPC). Further to this, a similar comparison of the relative integrals and GPC measurements was conducted to determine the number of PE segments contained per chain. Using the copolymer M_n (6400 g/mol by universal calibration) and assuming a single PE macromonomer unit, we can readily calculate the expected integral of the P(MMA) ester CH_3 signal at *ca* 3.6 ppm. With the corresponding signal integral set to the appropriate number (here 126 H) the relative integrals of the remaining groups are close to expectations (Figure 4.16): (i) the somewhat overlapping peaks between *ca* 0.8 and 1.7 ppm have an integral of 375 H (expected 410 H) and the relative integrals within this group are appropriate, including the PE main chain of 219 H (expected 164 H), noting that we also expect one of the P(MMA) α-methyl signals to be under this region;[33] (ii) the signal at *ca* 0.8-1.2 ppm containing P(MMA) α-methyl and PE methyl group resonances has an integral of 126 H (123 H expected); (iii) the P(MMA) backbone CH_2 signals at 1.8-2.2 ppm has an integral of 69 H (expected 82 H); (iv) the isolated aromatic signal at *ca* 6.9-7.3 ppm has an integral of 7 H (9 H expected). Hence, the assumption of the presence of *ca* one PE-*i*-DIB macromonomer per copolymer chain is again consistent with integration of the high temperature ^{1}H NMR spectrum. If some of polymer (d) is present, the in-chain DP must be small.

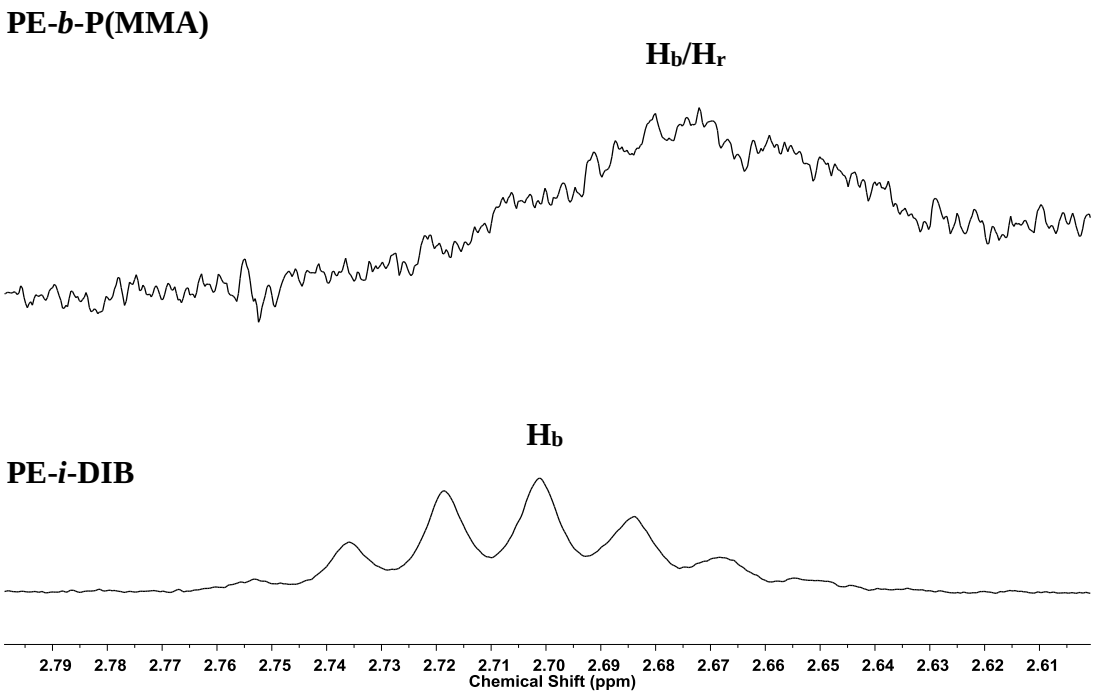

Figure 4.17 - ^{1}H NMR spectrum of PE-*i*-DIB and PE-*b*-P(MMA) in d^2-TCE at 100°C, focussed on benzylic methine region (400 MHz).

The spectra shown in Figure 4.17 are consistent with the expected two inequivalent benzylic CH signals at *ca* 2.6-2.8 ppm which, as with PE-*b*-P(VAc), appears to be relatively free from overlap with other signals in the copolymer. The benzylic signal (**H_b**) is shifted from 2.70 ppm in PE-*i*-DIB to 2.67 ppm in the copolymer (assigned as **H_b/H_r**) and a far broader benzylic signal in the product is noted, in this case to the extent that the signal is difficult to see in the ^{1}H NMR spectrum without high expansion.

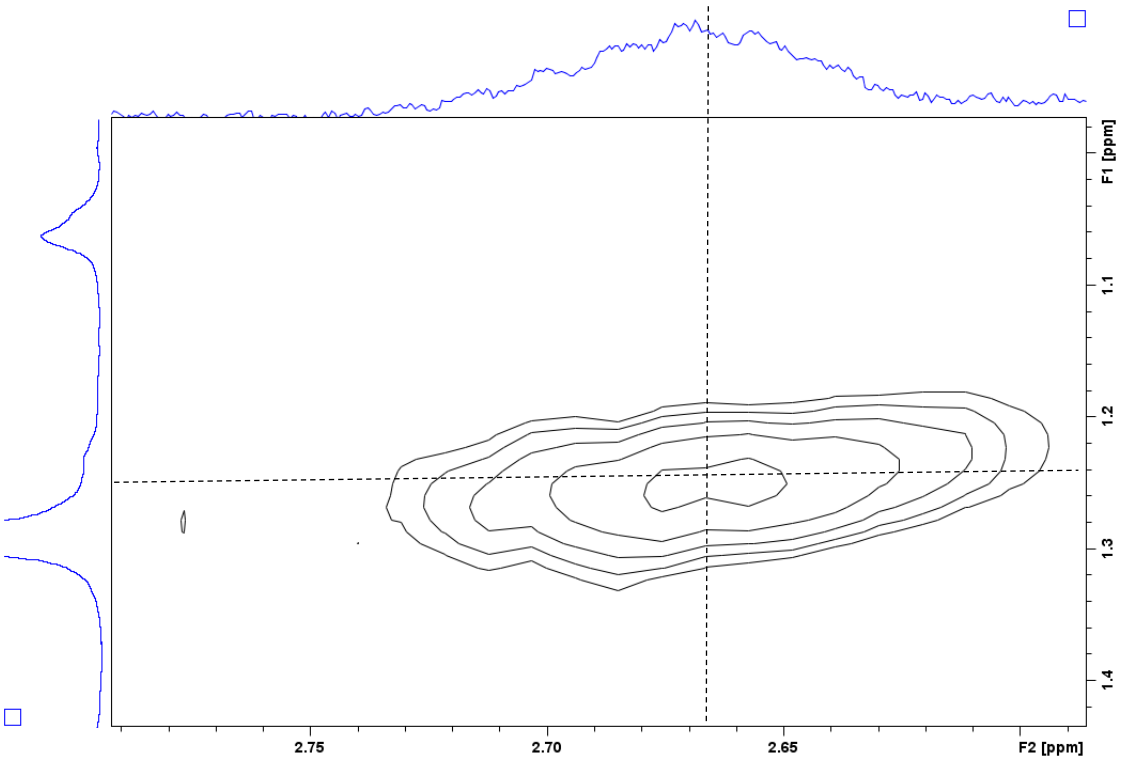

Figure 4.18 - Detail of a ^{1}H-^{1}H COSY NMR of PE-*i*-DIB-*b*-P(MMA) in d^{2}-TCE at 100°C (500 MHz).

The broadness of the benzylic signal in the ^{1}H NMR spectrum of these materials suggests that 2-D correlations analogous to those discussed for the materials above are likely to be hard to see. Nonetheless, 2-D NMR experiments were conducted as before and are discussed here. Figure 4.18 shows a familiar diagonally elongated cross-peak correlating to *ca* 1.2-1.3 ppm in the ^{1}H-^{1}H COSY. Again the individual correlations are unresolved but it is nonetheless consistent with $\mathbf{H_b}$ and $\mathbf{H_r}$ coupling to methyl environments $\mathbf{Me_c}$ and $\mathbf{Me_j}$.[‡] The expected correlation between $\mathbf{H_b}$ at 2.66 ppm and the adjacent PE methylene protons ($\mathbf{H_d}$) at 1.59 ppm was also detectable from the ^{1}H-^{1}H COSY (Figure 4.19).[†] In this case the expected analogous correlation between $\mathbf{H_r}$ and the P(MMA)

[‡] Expected chemical shifts for Me_c and Me_j calculated by ACD/I-LAB to be 1.16 ± 0.22 ppm.
[†] Expected chemical shifts for H_d and H_s calculated by ACD/I-LAB to be 1.54/1.76 ± 0.54 and 1.83/2.07 ± 0.62 ppm respectively.

backbone methylene proton environment **H_s** at *ca* 1.8 ppm was not detected,[†] though this is likely to be due to the broadness of the benzylic signal.

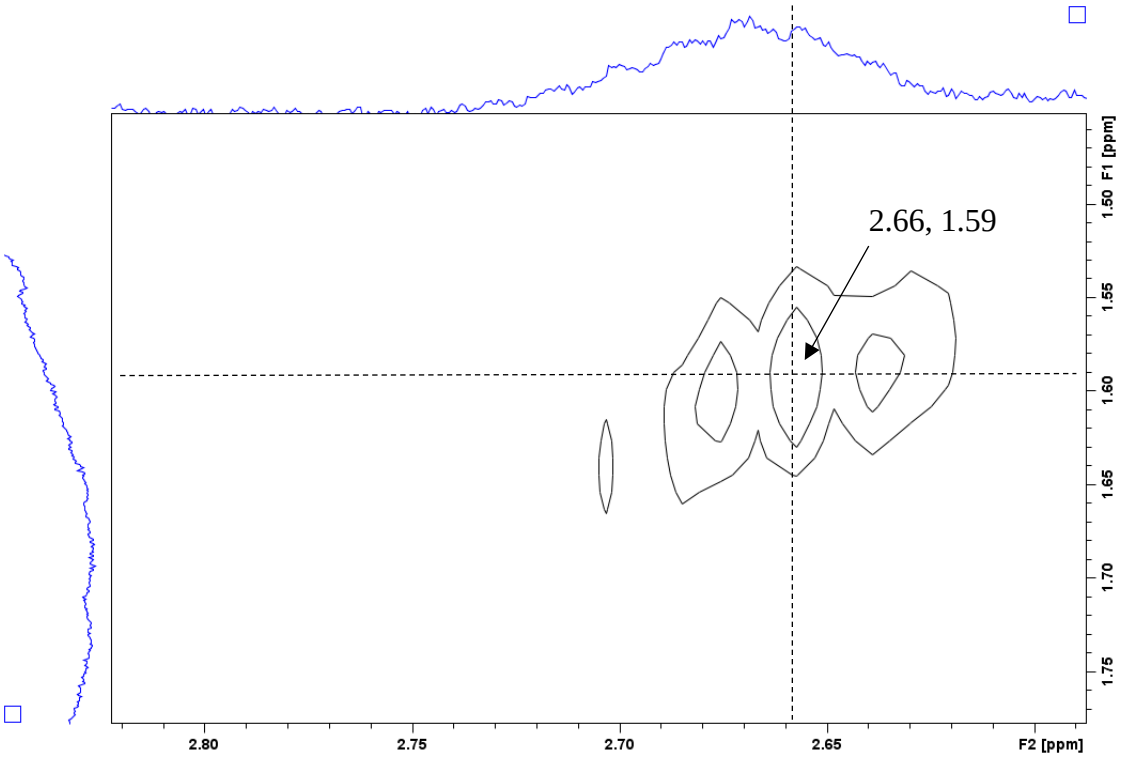

Figure 4.19 - Detail of a ^{1}H-^{1}H COSY NMR of PE-*i*-DIB-*b*-P(MMA) in d^2-TCE at 100°C (500 MHz).

Similar to PE-*b*-P(*n*-BA), the ^{1}H-^{13}C HMQC (Figure 4.20) shows a cross-peak between the benzylic ^{1}H region and what are apparently overlapping ^{13}C signals at *ca* 40 ppm[†] in the expected chemical shift for **C_b** and **C_r**.

[†] Expected chemical shifts for C_b and C_r calculated by ACD/I-LAB to be 40.1 ± 2.4 and 37.9 ± 5.3 ppm respectively.

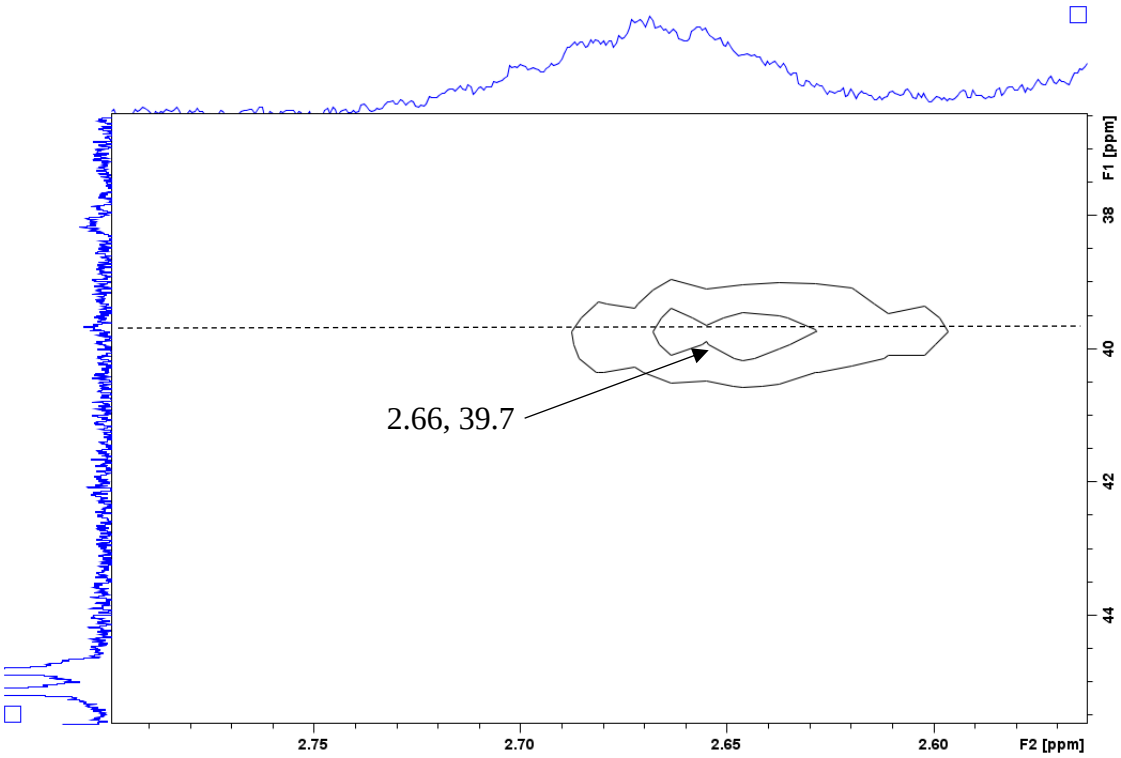

Figure 4.20 - Detail of ^{1}H-^{13}C HMQC NMR of PE-*i*-DIB-*b*-P(MMA) in d^{2}-TCE at 100°C (500 MHz).

4.5.4 PE-*b*-PS NMR Analysis

Shown in Figure 4.21 is the ^{1}H NMR spectrum recorded at 100°C of the PE containing product isolated from Run 17 (Table 4.5) after multiple reprecipitations from toluene into acetone. A broad peak at *ca* 1.30 ppm corresponding to PE backbone methylene protons is again observed; along with a small, isolated PE methyl triplet peak at *ca* 0.91 ppm. Also detectable are signals corresponding to a PS segment.[35] Again, the full conversion of the macromonomer was confirmed by the absence of DIB vinylidene proton signals at 5.07 and 5.34 ppm.

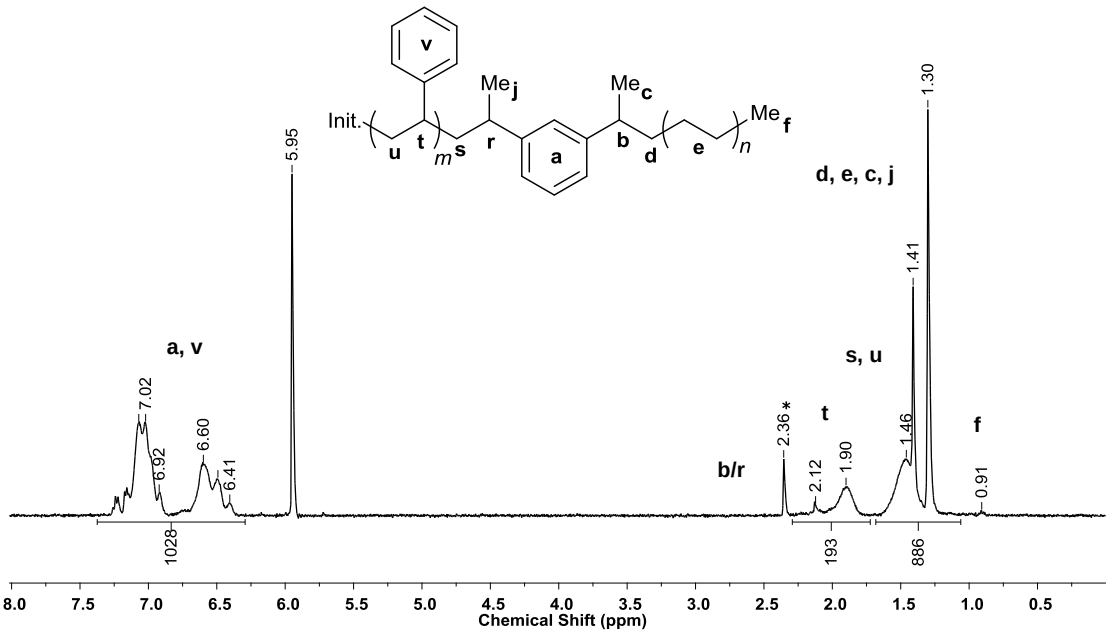

Figure 4.21 - ^{1}H NMR spectrum of PE-*b*-PS in d^{2}-TCE at 100°C (400 MHz). Relaxation delay = 1 s. Integral of the S signals at 6.3-7.3 ppm is set as follows: if we assume that an average of one PE-*i*-DIB macromonomer (M_n 3000 g/mol) is present in copolymer chains (M_n 24400 g/mol), the contribution of S to the M_n of the copolymer is ca 24400-3000 = 21400 g/mol. Hence integral of ca 5 × (21400/104.2) = 1028 H.

Backbiting and *β*-scission processes similar to those observed in acrylate polymerisations have been reported with styrene polymerisations but the temperature at which this is prevalent far exceeds that used here.[36] Polymerisation through PE-*i*-DIB followed by backbiting and *β*-scission to form species (c) is therefore unlikely and, correspondingly, we do not observe the vinylic signals in the ^{1}H NMR spectra of these materials. As with the PE-*b*-P(*n*-BA) materials discussed earlier, direct estimation of molecular weight by integration was not feasible here because of substantial overlap between the PE backbone methylene signal at 1.30 ppm and the broad signal at 1.4-1.7 ppm corresponding to the PS backbone methylene groups. Reliable integration of the PE methyl end group at 0.91 ppm was also not possible because of its size and broadness. We therefore conducted a similar comparison of the relative integrals and GPC

measurements to determine the number of PE segments contained per chain. Using the copolymer M_n (24400 g/mol by universal calibration) and assuming a single PE macromonomer unit, the expected integral of the PS aromatic signals at *ca* 6.3-7.3 ppm was readily determined. With the corresponding signal integral set to the appropriate number (here 1028 H) the relative integrals of the remaining groups are close to expectations (Figure 4.21): (i) the somewhat overlapping set of peaks between 1.2 and 1.7 ppm has an integral of 886 H (expected 822 H), including the PE main chain integral of 409 H (expected 428 H) and the PS backbone methylene signal integral of 477 H (expected 411 H), (ii) the peaks between *ca* 1.75 and 2.3 ppm have an integral of 193 H (expected 205 H). Again we thus find that the assumption of the presence of *ca* one PE-*i*-DIB macromonomer per copolymer chain is consistent with integration. If some of polymer (d) is present, the in-chain DP must be small, leaving the remaining architecture (e) as the major product.

In this PE-*b*-PS sample, the benzylic region at *ca* 2.7 ppm has been broadened to the extent that it was not visible in high temperature ^{1}H NMR. Given the molecular weight of the material and size of the other signals in the spectrum this is not surprising; but detection of correlations between this and surrounding environments were likely to be problematic as a result. This proved to be the case, with none of the correlations analogous to those discussed in the copolymers above detected in this material.

4.5.5 Diffusion-ordered NMR spectroscopy

Diffusion-ordered NMR spectroscopy (DOSY) is a powerful and non-invasive method that allows analysis of complex mixtures with little sample preparation and without the need for prior chemical separation.[37, 38] It relies on the principle that diffusion of molecules in solution depends on the size and shape of the molecule, as well as temperature and viscosity. Diffusion coefficients (*D*) of species can be described by the Stokes-Einstein equation (1) assuming a spherical shape. Smaller molecules tend to move more quickly and thus are associated with larger diffusion coefficients, while larger molecules are associated with smaller diffusion coefficients.

$$(1)\ D = \frac{kT}{6\pi\eta r_s}$$

Where *k* is the Boltzmann constant, *T* is temperature, η is viscosity of the liquid and r_s is the (hydrodynamic) radius of the molecule.

In the context of polymers, diffusion coefficients are related to hydrodynamic radius and molecular weight which has led to its use in the characterisation of homopolymers,[39, 40, 41, 42] block copolymers and mixtures of the two.[43, 44, 45] It has proved particularly useful in determining whether the sample contains one copolymer species, multiple homopolymer species or detecting the presence of contaminants *e.g.* homopolymer where ^{1}H NMR and GPC data are inconclusive. To the best of our knowledge however, the study below is the first example of polyethylene systems being characterised in this way.

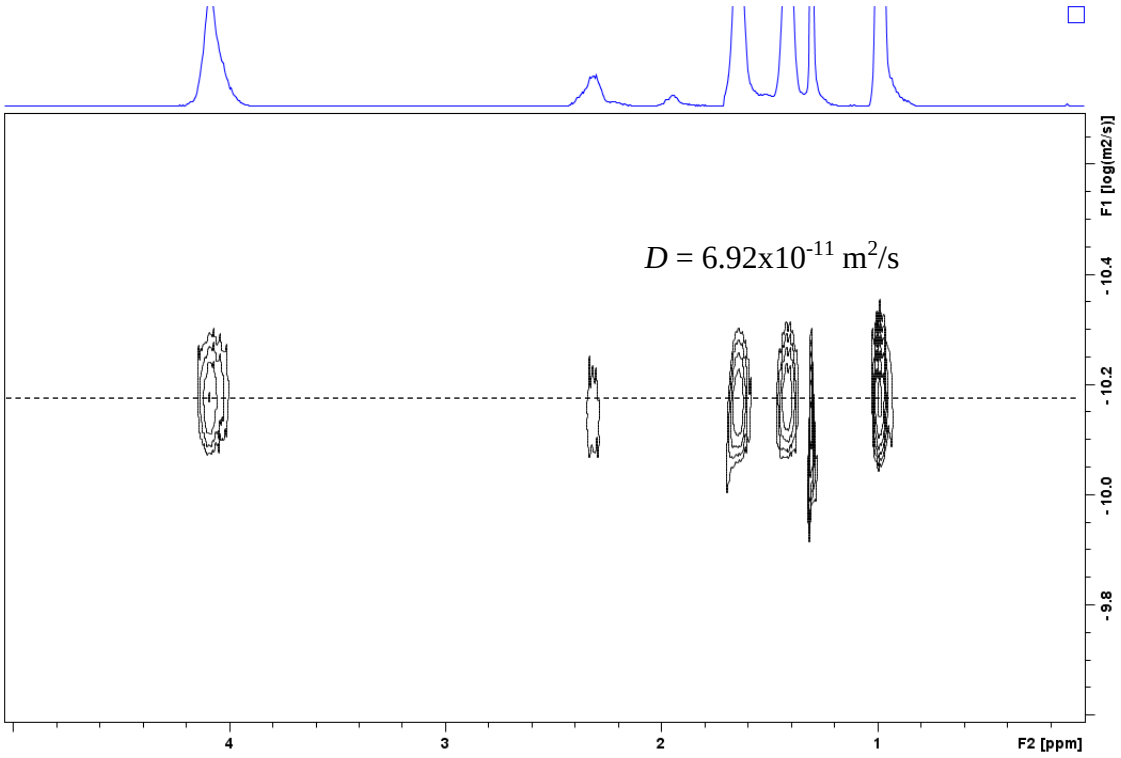

Figure 4.22 - DOSY ^{1}H NMR of PE-*b*-P(*n*-BA) in d^{2}-TCE at 25°C (500 MHz).

A DOSY experiment was conducted on a clear solution of the final PE-*b*-P(*n*-BA) sample from Run 9, Table 3.4 (M_n = 11000 g/mol, $Đ$ = 2.6) at 25°C. DOSY spectra were not available for the PE-*i*-DIB starting material due to the insolubility of the macromonomer at close to room temperature. The appearance (Figure 4.22) of all the ^{1}H resonances at a very similar diffusion coefficient is an indication either of the presence of one copolymer, or the presence of multiple species with the same diffusion coefficient. Given the differences in chemical nature and molecular weight of the two copolymer components, the likelihood of both having the same diffusion coefficient is small.

A separate DOSY experiment on a sample of the PE-*b*-P(*n*-BA) material that had been deliberately contaminated with P(*n*-BA) homopolymer (M_n = 2700 g/mol, $Đ$ = 2.0) was conducted as a control to see if the copolymer and homopolymer could be easily distinguished. The spectrum shown in Figure 4.23 still shows that the copolymer signals are aligned on the same horizontal line and the copolymer signal has a similar diffusion coefficient. However, there now appear to be two sets of P(*n*-BA) signals with one set now diffusing slightly faster. This is consistent with the presence of a second lower molecular weight species, though it was surprising that the presence of the low molecular weight homopolymer contaminant was not more clearly reflected in the diffusion rates.

Given the P(*n*-BA) was present as both homopolymer and as part of the copolymer, we considered the possibility that intermolecular interaction between the P(*n*-BA) homopolymer and the P(*n*-BA) outer component of a copolymer aggregate could be the reason for the two species being less distinct from each other than expected. This would support the VT NMR data (*vide infra*) which indicated the formation of aggregates in selective solvents, d^2-TCE in this case, which would be expected to be selective for the polar component of the copolymer.

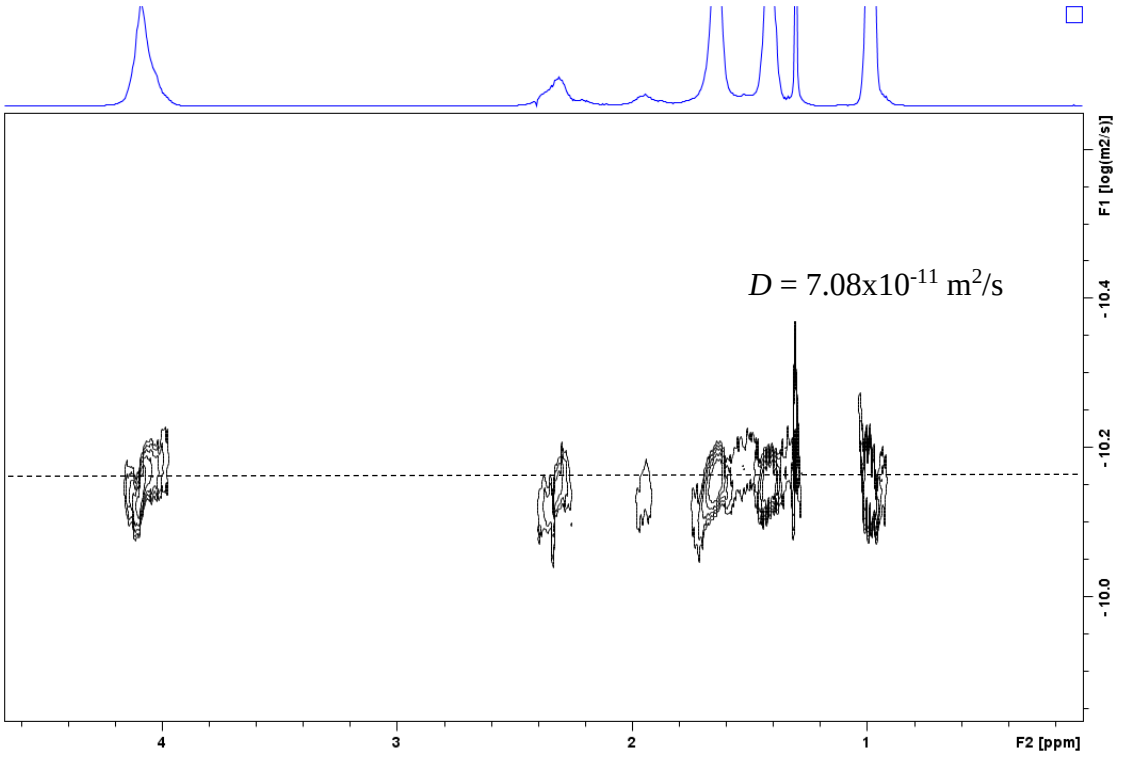

Figure 4.23 - DOSY ^{1}H NMR of PE-*b*-P(*n*-BA) contaminated with P(*n*-BA) homopolymer in d^2-TCE at 25°C (500 MHz).

To investigate this further, a similar DOSY experiment was conducted on a sample of the PE-*b*-P(*n*-BA) material that had been deliberately contaminated with a chemically different homopolymer, in this case P(VAc) (M_n = 7400 g/mol, $Đ$ = 3.4). The spectrum shown in Figure 4.24 shows more clearly that multiple species are present, which is consistent with our suggestion that the P(*n*-BA) homopolymer is interacting with the outer component of the copolymer aggregate in the previous spectrum. Interestingly the signal corresponding to PE seems now to diffuse faster than the P(*n*-BA) signals, the reasons for which are currently unclear, and the copolymer signals seem to be diffusing faster as a whole than the homopolymer.

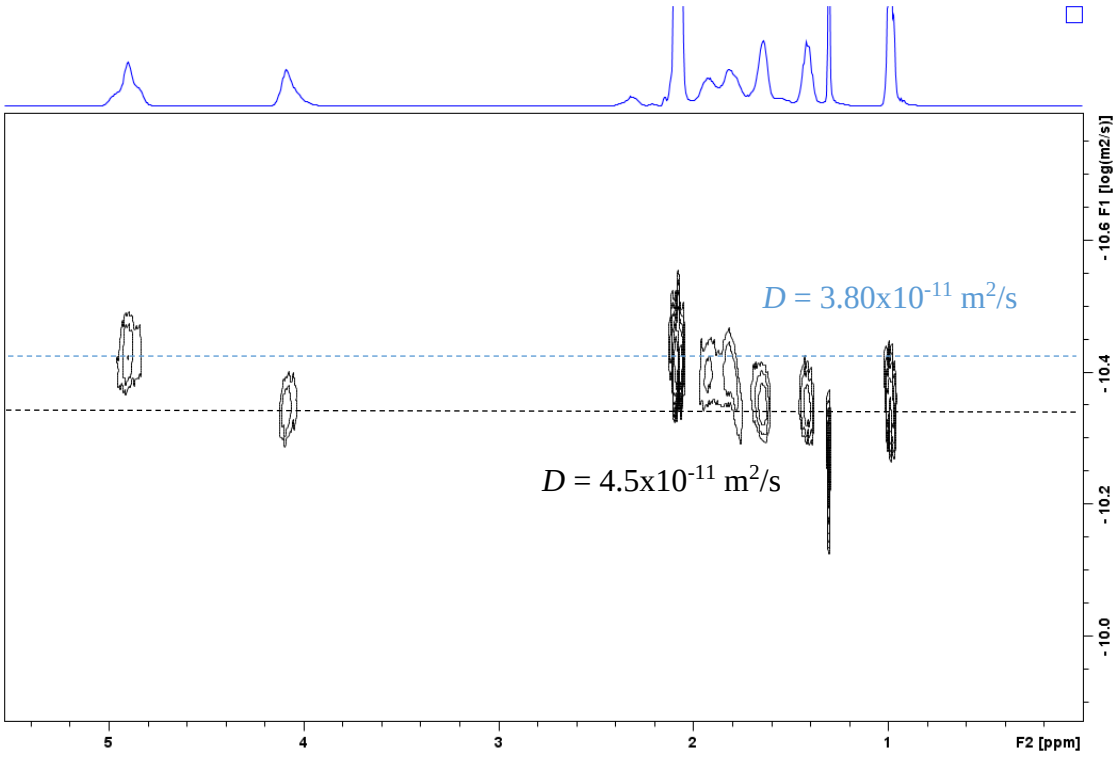

Figure 4.24 - DOSY ^{1}H NMR of PE-*b*-P(*n*-BA) contaminated with P(VAc) homopolymer in d^2-TCE at 25°C (500 MHz).

This observation led us to conduct further experiments on separate samples of the same material contaminated with lower and higher molecular weight P(VAc) respectively. Figure 4.25 is a stacked DOSY spectrum with the three samples depicted with different colours depending on which molecular weight homopolymer they contain (red = 3700, black = 7400, purple = 27600 g/mol). The signals corresponding to the PE copolymer in all three experiments overlay each other around the same diffusion coefficient of *ca* 4.5x10^{-11} m^2/s The signals for the P(VAc) homopolymers appear in the expected order of diffusion coefficient *i.e.* red > black > purple in Figure 4.25. These observations demonstrate the substantial effect that both the *nature* and molecular weight of a polymer can have on its diffusion rate.

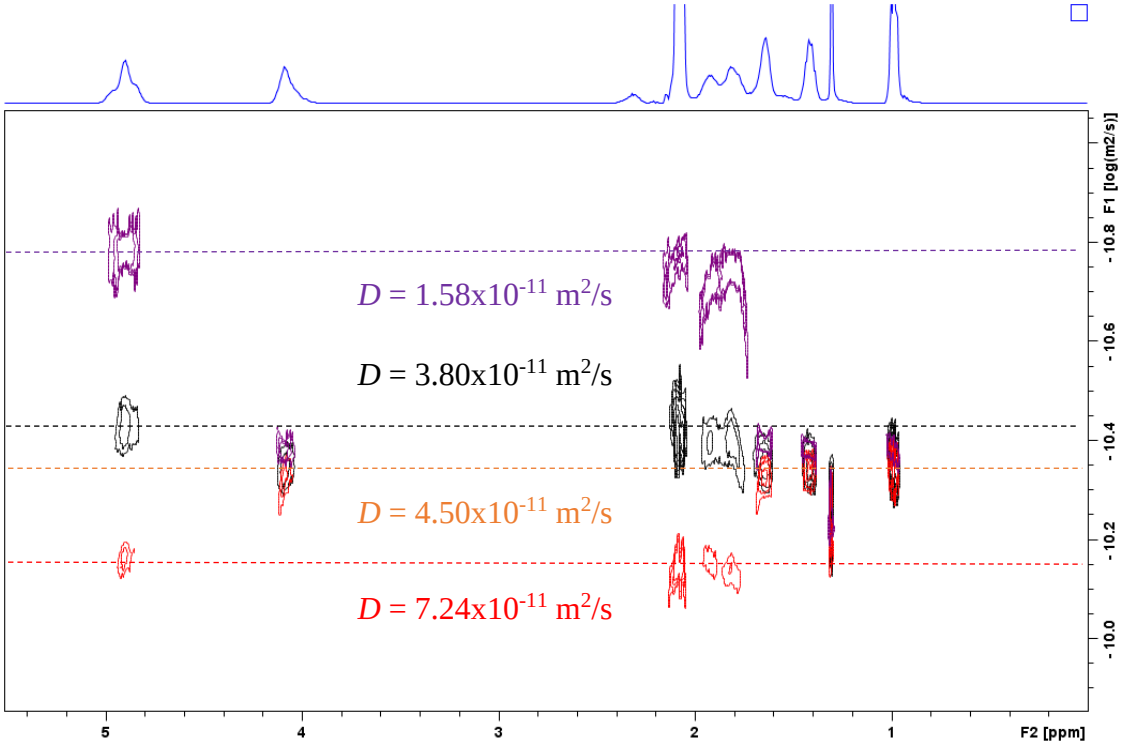

Figure 4.25 - Stack-plot of ^{1}H DOSY experiments on samples of PE-*b*-P(*n*-BA) (M_n = 11000 g/mol) contaminated with P(VAc) homopolymers of M_n: 3700 g/mol; 7400 g/mol; 27600 g/mol. Experiments recorded in d^2-TCE at 25°C (500 MHz).

Figure 4.26 shows a DOSY ^{1}H NMR spectrum of a clear solution of the PE-*b*-P(VAc) sample isolated from Run 1 (Table 4.1) at 25°C. The signals corresponding to PE and P(VAc) are aligned tightly around a single diffusion coefficient.

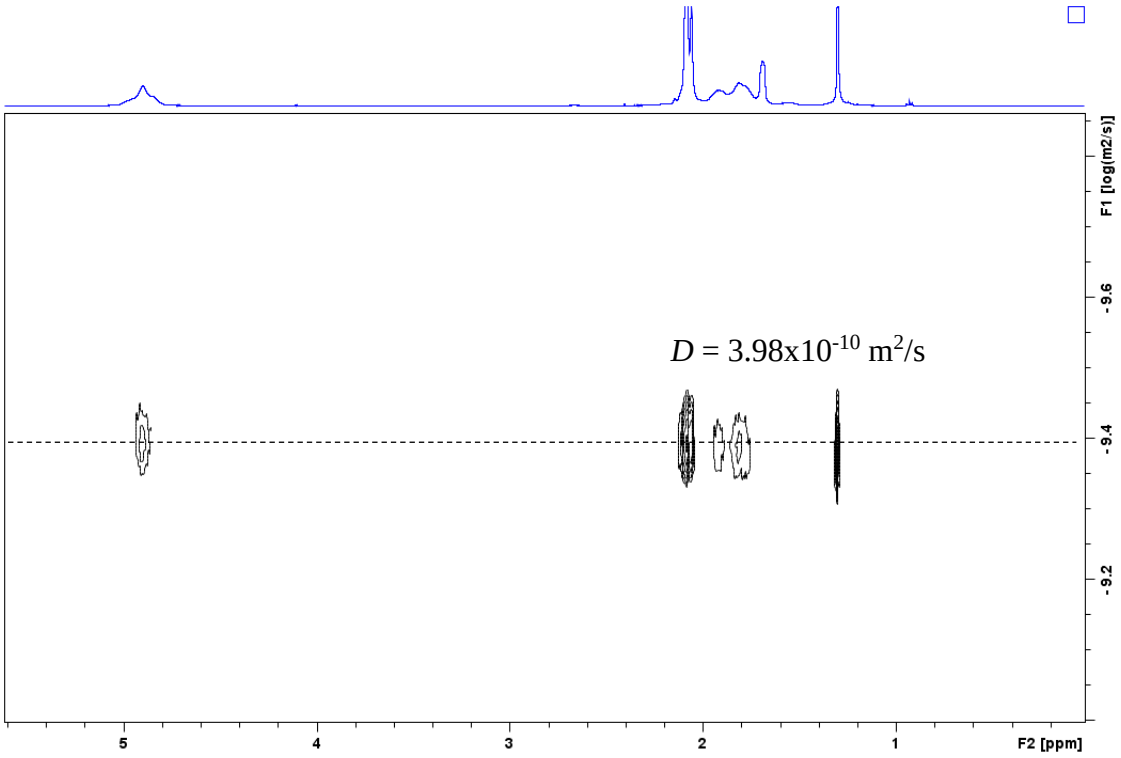

Figure 4.26 - DOSY ^{1}H NMR of PE-*b*-P(VAc) in d^{2}-TCE at 25°C (500 MHz).

Based on the above observations, separate DOSY experiments were run using PE-*b*-P(VAc) (M_n = 8000 g/mol, $Đ$ = 2.4) which had been deliberately contaminated with P(VAc) homopolymer M_n = 7400 g/mol, $Đ$ = 3.4 (Figure 4.27) and M_n = 3700 g/mol, $Đ$ = 2.2 (Figure 4.28). In the former, where the copolymer and homopolymers have similar molecular weights, resonances appear to be clustered around a single diffusion coefficient, while in the latter the lower part of the P(VAc) signals tail off towards higher diffusion rates (*cf.* Figure 4.28).

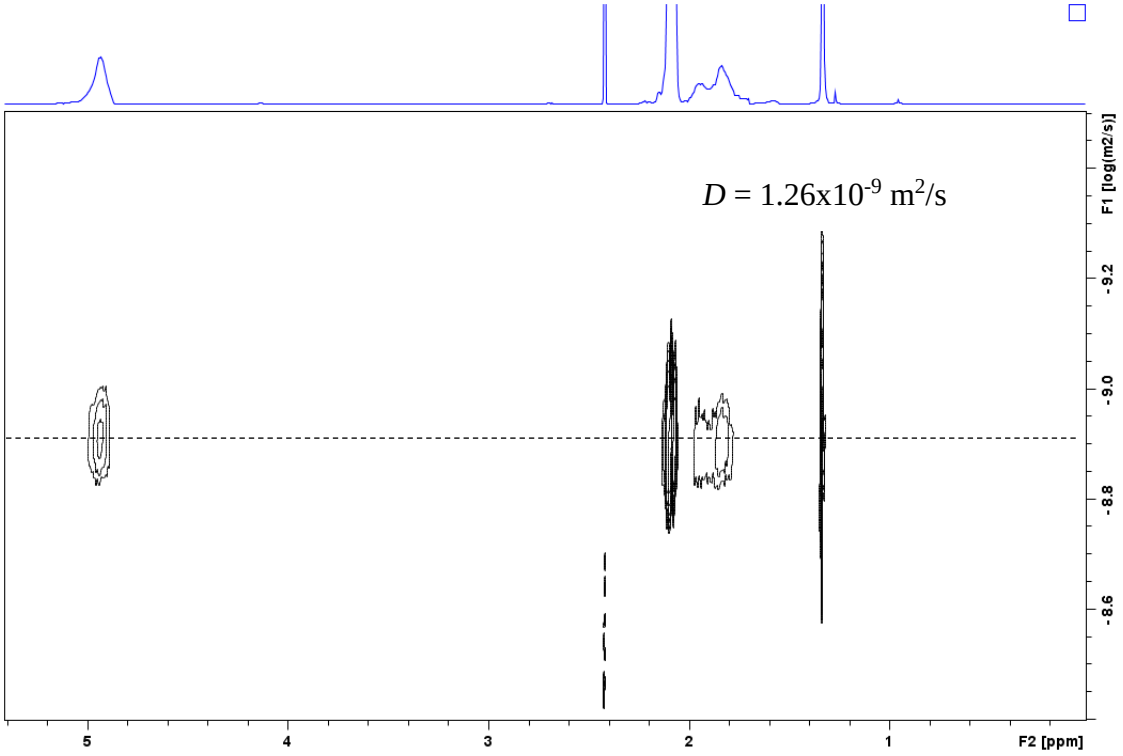

Figure 4.27 - DOSY ^{1}H NMR of PE-*b*-P(VAc) spiked with P(VAc) homopolymer in d^{2}-TCE at 25°C (500 MHz).

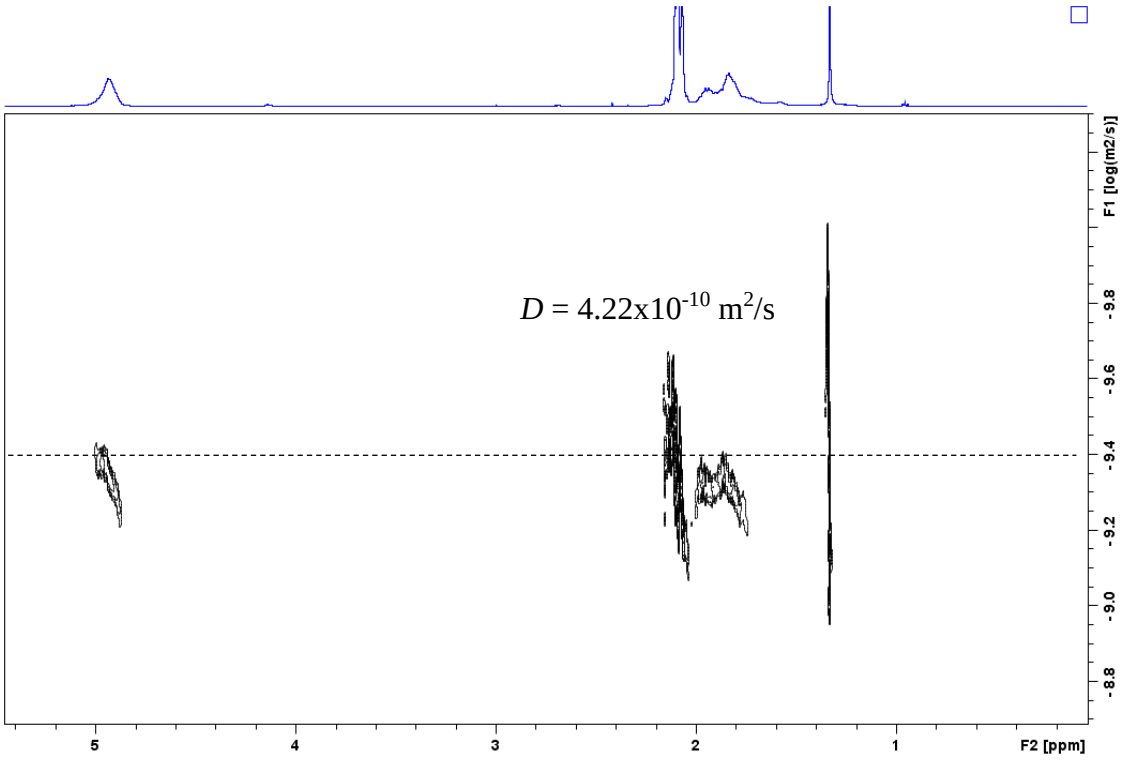

Figure 4.28 - DOSY ^{1}H NMR of PE-*b*-P(VAc) spiked with P(VAc) homopolymer in d^{2}-TCE at 25°C (500 MHz).

Given our observations from these experiments and in those discussed earlier for PE-*b*-P(*n*-BA), another DOSY experiment was conducted on a sample containing the same block copolymer spiked with a different homopolymer, in this case P(*n*-BA) (M_n = 2700 g/mol, Đ = 2.0). Figure 4.29 clearly shows the expected two distinct diffusion coefficients of the copolymer and the homopolymer. These observations are consistent with the experiments shown in Figures 4.24 and 4.25 and seem to support the proposal that aggregation of the copolymer and interaction between homopolymer and the polar outer component of the copolymer aggregate could be a contributing factor for the apparent single coefficient observed in Figure 4.27 and the small separation of the signals in Figure 4.28 where two species might have been expected to be clearly visible.

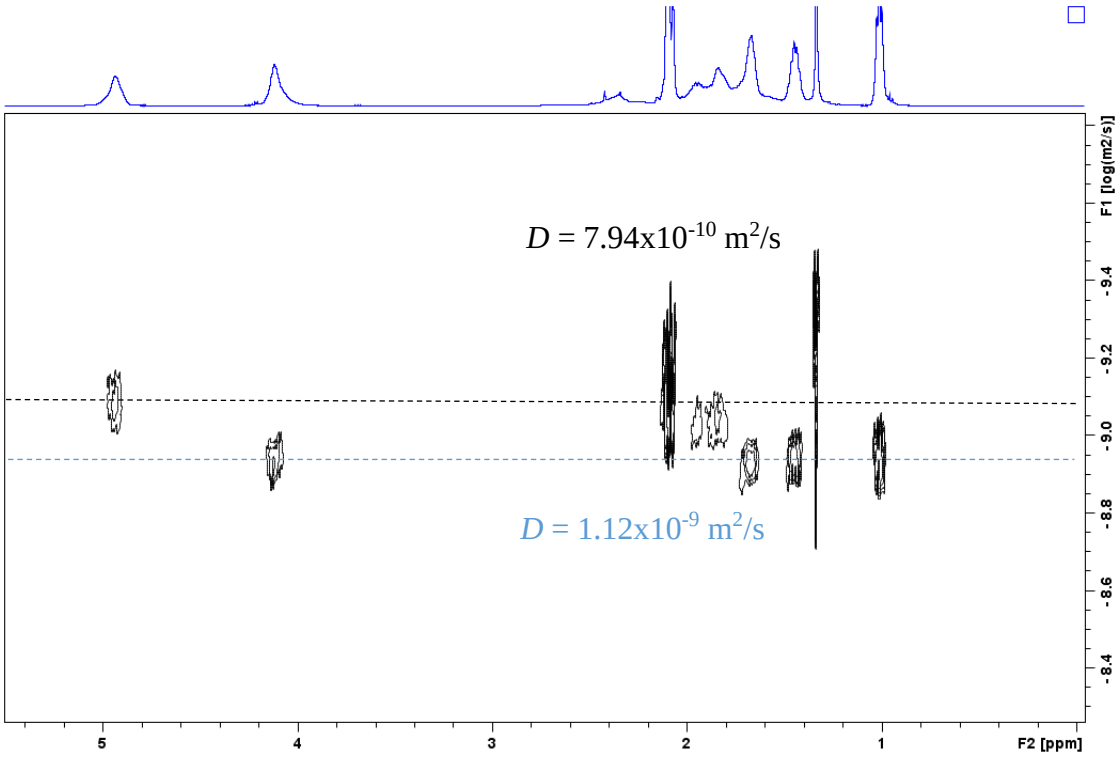

Figure 4.29 - DOSY ^{1}H NMR of PE-*b*-P(VAc) spiked with P(*n*-BA) homopolymer in d^2-TCE at 25°C (500 MHz).

The spectra obtained from these DOSY experiments clearly demonstrate that the chemical nature and molecular weight of species both have profound effects on the rates

of diffusion in a given solvent. They also suggest that aggregation behaviour and interaction between aggregate and contaminant could also have a significant impact on the results of such experiments conducted on amphiphilic materials.

4.5.6 Variable temperature ^{1}H NMR

Variable temperature ^{1}H NMR experiments were conducted using the same PE-*b*-P(*n*-BA) as used in the correlation and DOSY experiments (M_n = 11000 g/mol, $Đ$ = 2.6). Figures 4.30 and 4.31 are ^{1}H NMR spectra of a clear solution of this PE-*b*-P(*n*-BA) material recorded at 50°C and 25°C respectively. Though the polymer was apparently still soluble by eye, the relative integrals and chemical shifts recorded at the lower temperatures differ substantially to the spectrum recorded at 100°C for the PE signals. Using the integral corresponding to the NMR solvent d^2-TCE at δ = 5.95 ppm as a reference, the ratio of the peaks corresponding to the P(*n*-BA) ester CH_2 at 4.1 ppm and the PE backbone CH_2 at 1.3 ppm changed from 137:376 (1:1.4) at 100°C to 126:215 (1.2:1) at 50°C (Figure 4.30) and then to 110:132 (1.7:1) at 25°C (Figure 4.31).

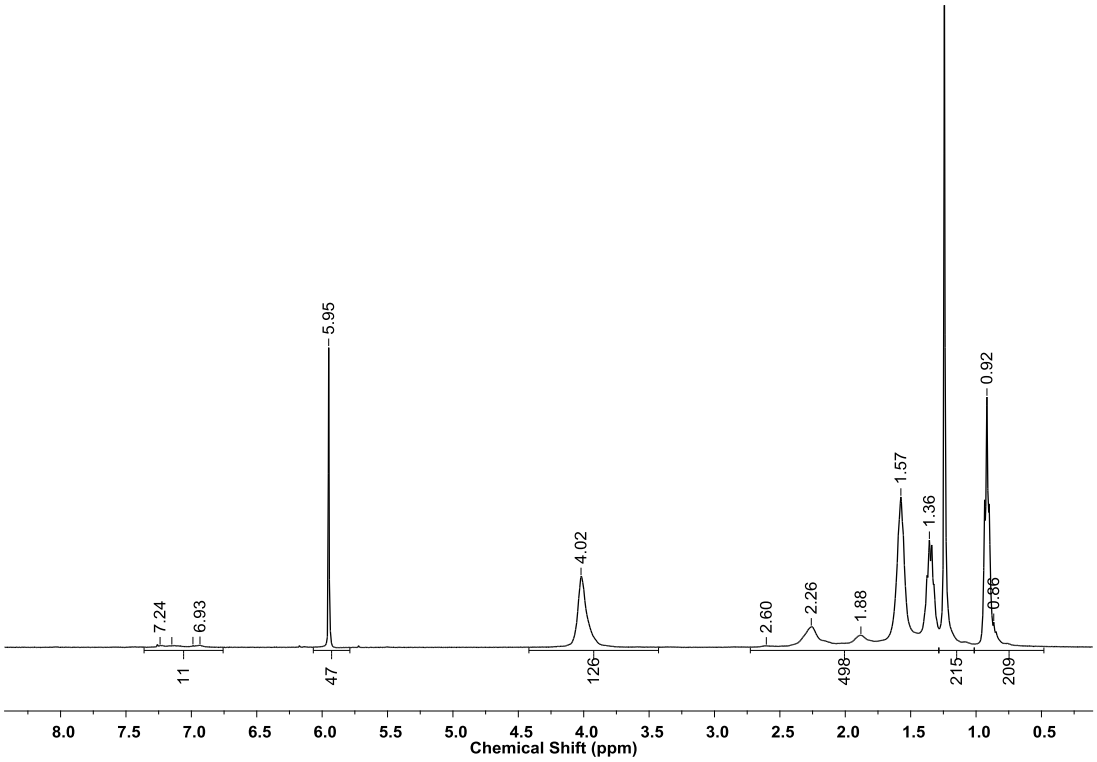

Figure 4.30 - ^{1}H NMR of PE-*b*-P(*n*-BA) in d^{2}-TCE at 50°C (400 MHz). Relaxation delay = 1 s.

It is expected that the intensity of polymer signals should fall with temperature,[46] but the PE signal intensity falls far more dramatically than the P(*n*-BA) signals. This data is consistent with a tendency of these copolymers to form aggregates, a commonly observed phenomenon with block copolymers in selective solvents,[47] where the molecular motion of the insoluble PE block is reduced to a greater extent than that of the soluble P(*n*-BA) block due to the protection provided by the more compatible polar outer component of the aggregate.

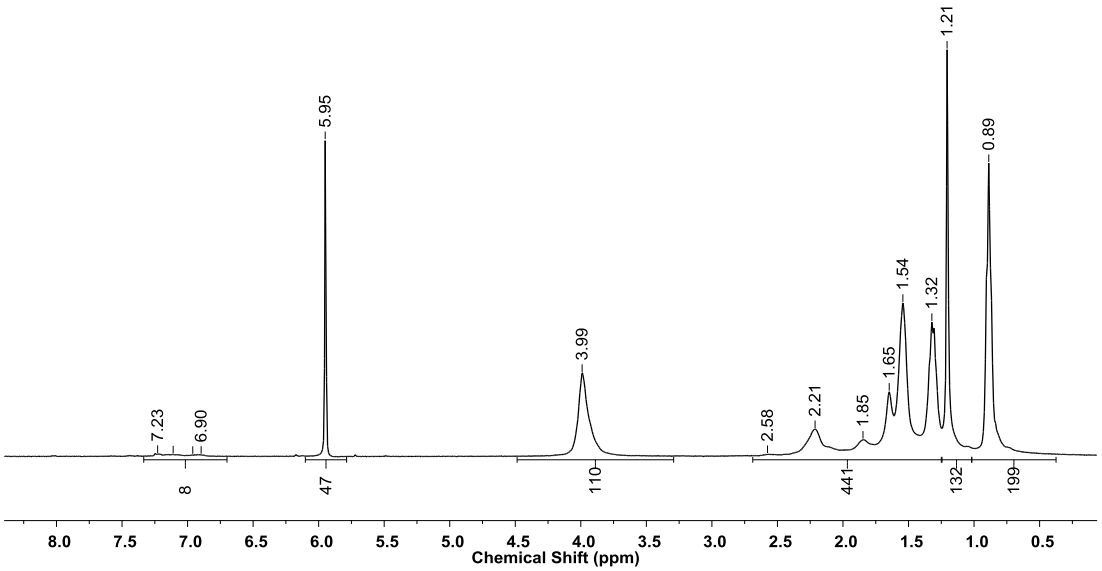

Figure 4.31 - ^{1}H NMR of PE-*b*-P(*n*-BA) in d^{2}-TCE at 25°C (400 MHz). Relaxation delay = 1 s.

4.6 DLS analysis

The solubility of the PE copolymers containing larger polar segments of *n*-BA, VAc, V2EH, MMA, C14MA and styrene permitted their analysis by dynamic light scattering (DLS) to investigate their aggregation properties further. Samples were prepared in a solvent selective for the polar block (THF) at a concentration of 1 mg/ml and a set of three measurements was recorded for each sample after sonication for 10 min in an ultrasound cleaning bath. This process was repeated twice to see whether variation of sonication periods affected the particle sizes.

4.6.1 PE-*b*-P(*n*-BA)

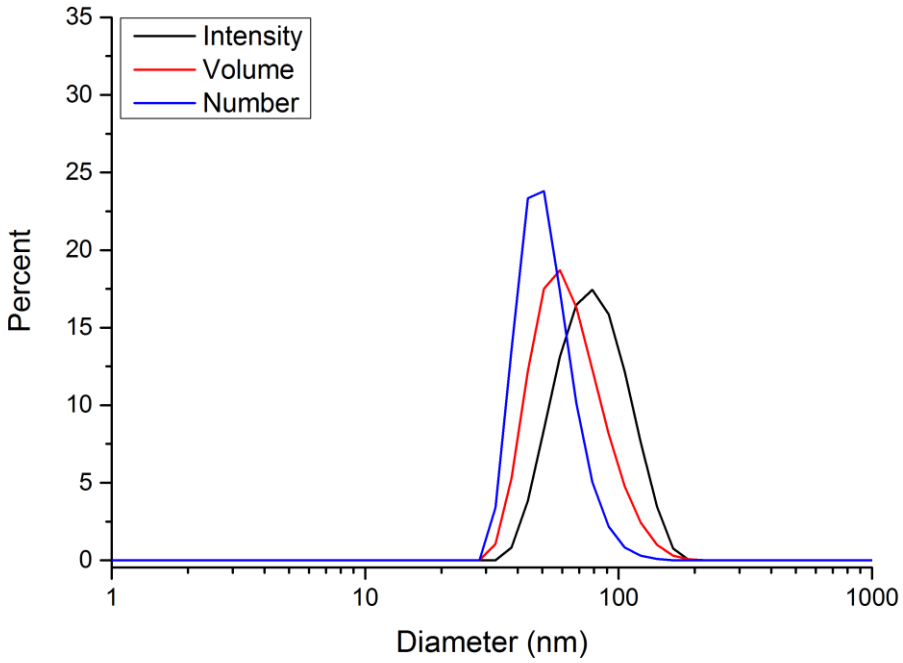

Figure 4.32 - DLS intensity/volume/number size distributions of sample 3-180, Table 3.1 in THF (1 mg/ml) after sonication (averages of three measurements).

Sample 3-180 (Chapter 3) gave an apparently clear solution when the material was dispersed in THF. Following a 10 min sonication period, a regular correlation plot (y-intercept *ca* 0.9), a count rate of 264 kcps and a single feature in the intensity distribution were obtained with a polydispersity index (PDI) of 0.082 (Figure 4.32). Whilst noting the assumptions regarding shape, refractive index, precision of the intensity data and the homogeneity of the sample that must be made,[48, 49, 50] the data indicates that the majority of the aggregates in this sample correspond to spherical particles of *ca* 60 nm in diameter. Further sonication of the dispersion did not significantly affect the results obtained, nor were they affected when the sample was re-analysed a week after the original run.

Tanford[51] proposed an equation (2) that allows an estimation of the expected diameter for an aggregate formed from a copolymer to be made. Using the distance between alternate carbons atoms of a fully extended chain (2.53 Å), the van der Waals radius of the terminal methyl group (2.1 Å) and one half of the bond length to the first atom not contained in the hydrophobic core (~0.6 Å), the maximum chain length (l_{max}) for n'_c embedded carbon atoms is obtained in angstroms.

$$(2)\ l_{max} = 1.5 + 1.265n'_c$$

Assuming that the M_n (19200 g/mol) by GPC is correct, a reasonable assumption as demonstrated by the consistency with the NMR studies (*vide supra*), we can obtain DP's of ethylene and *n*-BA in this sample of 75 and 134 respectively which then yields a value for the n'_c of 529 embedded carbon atoms. We would therefore expect a particle of diameter *ca* 670 Å or 67 nm, which is consistent with the value obtained for the majority of the particles detected in DLS for this sample (*ca* 60 nm).

4.6.2 PE-*b*-P(VAc)

Sample 3-240 (Table 4.1) at 1 mg/ml in THF gave a regular correlation plot (y-intercept *ca* 0.9 and count rate *ca* 234 kcps) along with a single feature in the intensity distribution with a PDI of 0.12 (Figure 4.33). The data indicates that the majority of the aggregates in this sample correspond to spherical particles of *ca* 50 nm in diameter. Using the same equation as above, we obtain an expected particle diameter for this sample of 32 nm, which is reasonably similar to the particle size indicated by DLS.

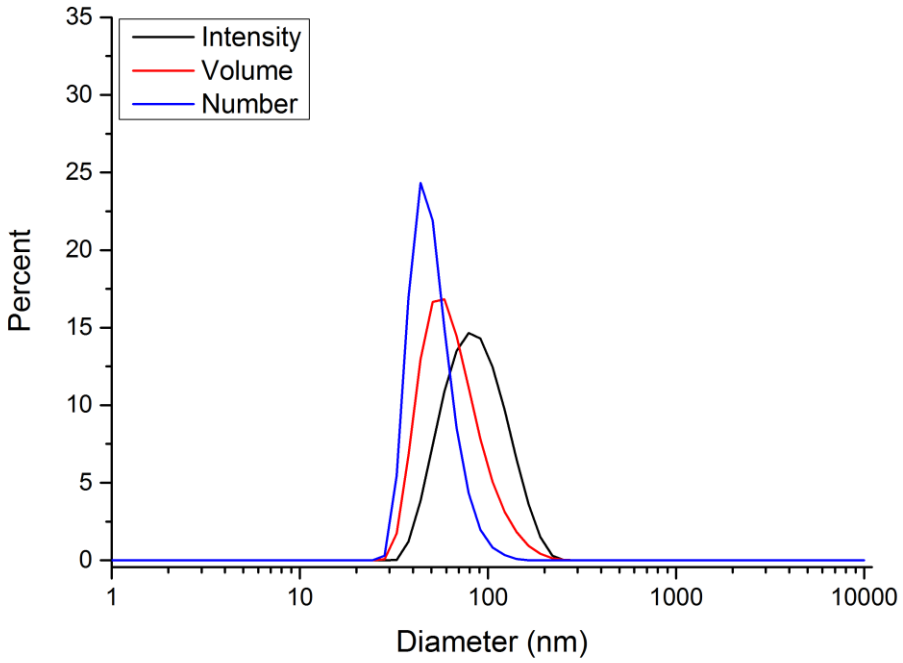

Figure 4.33 - DLS intensity/volume/number size distributions of sample 3-240 in THF (1 mg/ml) after sonication (averages of three measurements).

4.6.2 PE-*b*-P(V2EH)

Sample 7-240 again gave a regular correlation plot (y-intercept *ca* 0.95 and count rate *ca* 112 kcps) along with a single feature in the intensity distribution though with a significantly higher PDI of 0.24 (Figure 4.34). The data for this sample indicates the detection of slightly larger aggregates of *ca* 70 nm in diameter. Using the same equation as discussed above, we obtain an expected particle diameter for this sample of 43 nm.

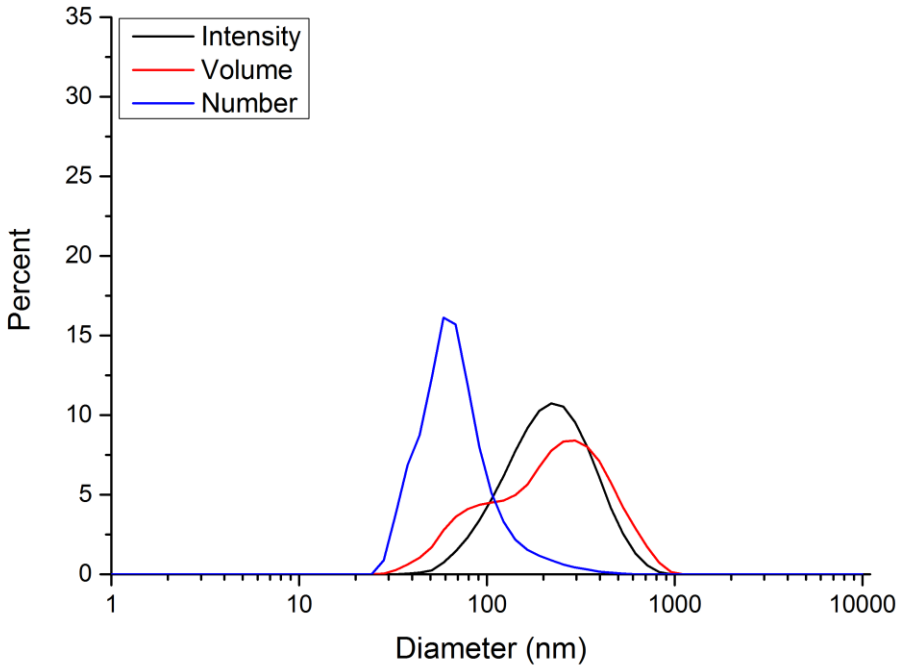

Figure 4.34 - DLS intensity/volume/number size distributions of sample 9-240 in THF (1 mg/ml) after sonication (averages of three measurements).

4.6.3 PE-*b*-P(MMA)

A regular correlation plot (y-intercept *ca* 0.84 and count rate *ca* 265 kcps) was obtained for the PE-*b*-P(MMA) sample isolated from Run 12-240 and a single feature observed in the intensity distribution with a PDI of 0.17. The data indicates that the majority of particles detected were *ca* 80 nm in diameter (Figure 4.35). Using equation (2), we obtain an expected particle diameter for this sample of 33 nm which, while it is not as close to the experimental result as the other materials, is not unrealistic compared to the experimental value indicated by DLS.

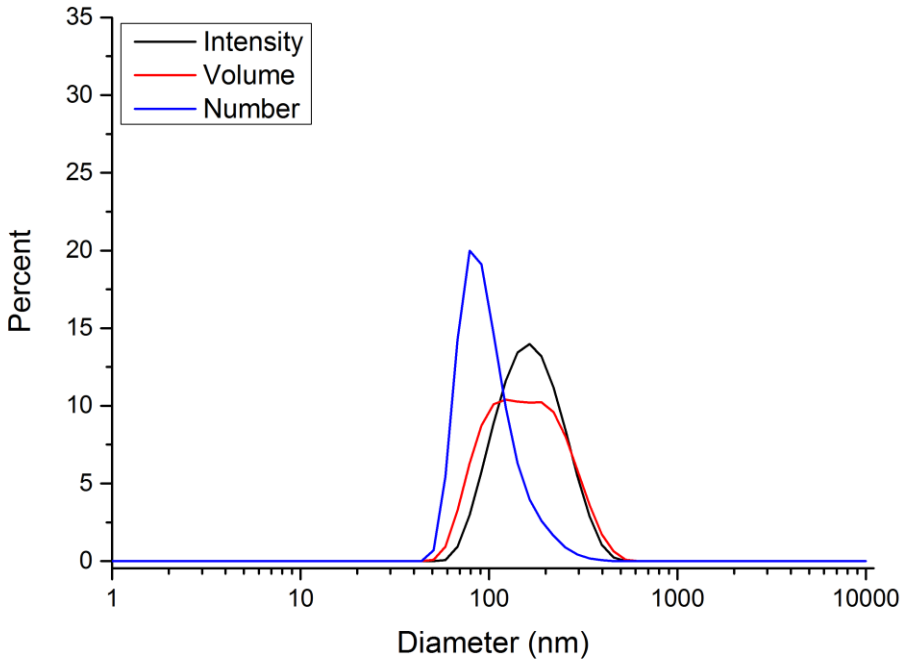

Figure 4.35 - DLS intensity/volume/number size distributions of sample 12-240 in THF (1 mg/ml) after sonication (averages of three measurements).

4.6.4 PE-*b*-P(C14MA)

In the case of the PE-*b*-P(C14MA) materials, sample 16-240 gave a single feature in the intensity distribution with a PDI of 0.18 (Figure 4.36) as well as a regular correlation plot (y-intercept *ca* 0.9 and count rate *ca* 284 kcps). Slightly larger particles of *ca* 100 nm in diameter were detected and an expected particle diameter for this sample of 35 nm was obtained. Again the two values are not as close as with some of the other samples but it is not unrealistic.

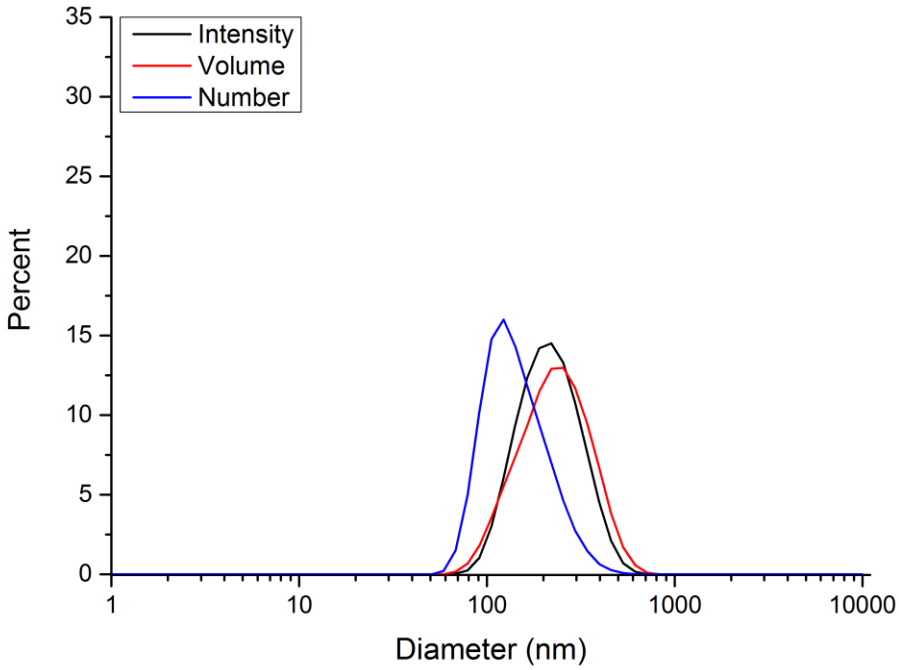

Figure 4.36 - DLS intensity/volume/number size distributions of sample 16-240 in THF (1 mg/ml) after sonication (averages of three measurements).

4.6.5 PE-*b*-PS

For the PE-*b*-P(S) materials, sample 20-240 gave a regular correlation plot (y-intercept *ca* 0.9 and count rate *ca* 138 kcps) and a single feature in the intensity distribution with a PDI of 0.09 (Figure 4.37). The data in the figure below indicates that the majority of the aggregates in this sample correspond to spherical particles *ca* 80 nm in diameter which is similar to those obtained in the PE-*b*-P(*n*-BA) sample with a comparable molecular weight. An expected particle diameter for this sample of *ca* 89 nm was obtained, which is consistent with the value obtained by DLS.

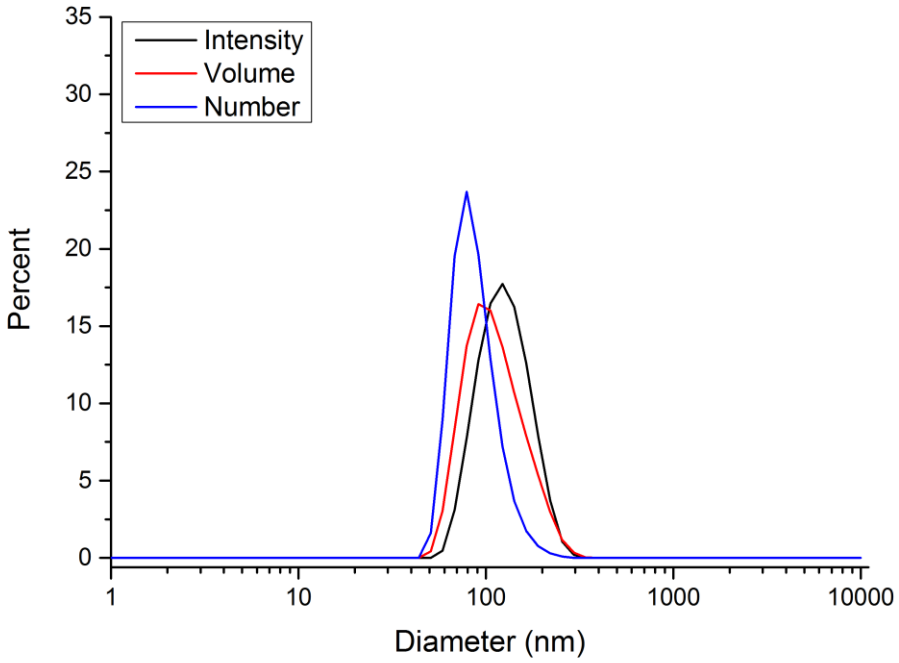

Figure 4.37 - DLS intensity/volume/number size distributions of sample 20-240 in THF (1 mg/ml) after sonication (averages of three measurements).

Given the general consistency of the experimental size distributions with the calculated particle sizes, as well as the surprisingly narrow polydispersities, we can reasonably say from the analysis that nanoscopic structures are formed in this medium under these conditions and that the size of these structures depend on the size of the polar block and also on the nature of the polar block. The data also supports the observations made from variable temperature and DOSY NMR experiments regarding the behaviour of these materials in selective solvents. However, in order to determine the morphology of the aggregates formed and the effect of the size and nature of the polar blocks on the morphology we would require DLS experiments on a larger range of samples and analysis by microscopy to corroborate the DLS data.

4.7 DSC analysis

The copolymers in the solid state are expected to consist of a semi-crystalline PE segment and an amorphous segment attributed to the polar component, with the thermal properties depending on both the nature and the molecular weight of the polar segments. DSC was used to investigate the phase separation and structure of the blocks.[30] Comparisons of the third heating and cooling curves of the PE-*i*-DIB macromonomer and low, medium and higher molecular weight examples of the copolymers are given in the following sections.

4.7.1 PE-*b*-P(*n*-BA)

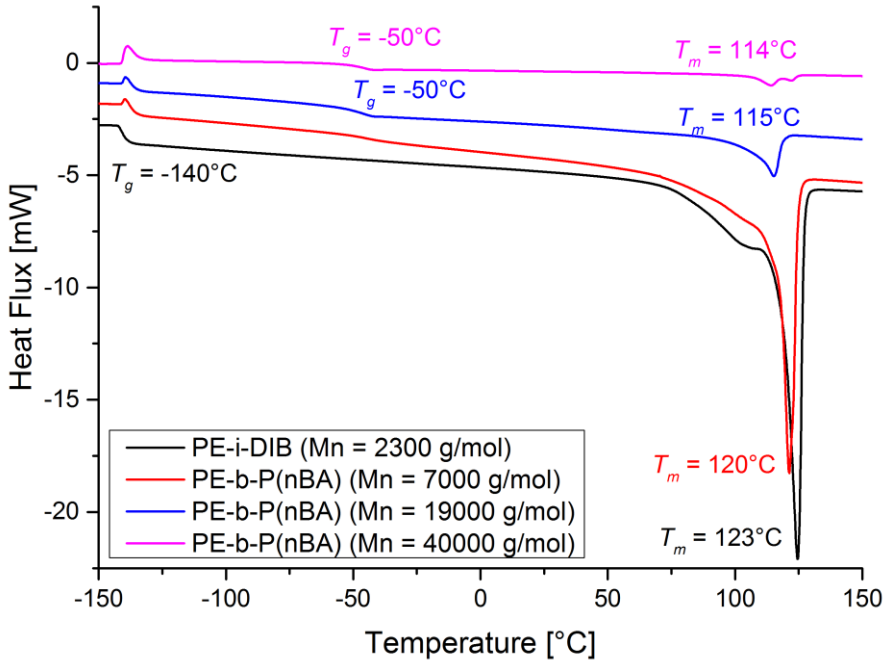

Figure 4.38 - Third heating curves (10°C/min) from DSC traces of PE-*i*-DIB, mass used = 5.23 mg; PE-*i*-DIB-*b*-P(*n*-BA) (Runs 2-4, Chapter 3), masses used: 8.62 mg, 9.51 mg, 5.59 mg.

The PE-*i*-DIB (M_n = 2300 g/mol) macromonomer from Runs 2-4 (Chapter 3) had a glass transition temperature (T_g) at -140°C and its melting temperature (T_m) appeared as a sharp peak at 123°C (Figure 4.38). The T_g corresponding to the PE segments in the copolymers were very similar to the starting material, indicating that amorphous regions of PE and P(*n*-BA) have phase separated. T_m values for the copolymers decreased modestly from 123°C in PE-*i*-DIB down to 114°C with increasing P(*n*-BA) block length. Determination of the %-crystallinity (X_c) of PE from DSC curves is normally accomplished by comparison of the enthalpy of melting of the sample with the enthalpy of 100% crystalline PE (294 J/g).[52, 53, 54] The enthalpies of fusion of the test sample and of totally crystalline PE (depicted in equation 3 as $\Delta H_f(T_m)$ and $\Delta H_f^0(T_m^0)$ respectively) are measured at the equilibrium melting point T_m^0 in J/g. Here, T_m is principally a property of the PE segment and it is important to consider that each sample contains a different proportion of PE by mass.[1] This was estimated as follows: The relative crystallinity of the sample is calculated by the instrument using equation 3. The differing proportions of PE in each sample were then accounted for by dividing this value by the mass fraction of PE in the material (PE-*i*-DIB, 100%; Run 2-180 54%; Run 3-180 14%; Run 4-180 6%). The crystallinities of the PE blocks in these materials were calculated on this basis to be PE-*i*-DIB, 75%; Run 2-180, *ca* 61%; Run 3-180, *ca* 42%; Run 4-180, *ca* 33%.

$$(3)\ X_c = \frac{\Delta H_f(T_m)}{\Delta H_f^0(T_m^0)} \times 100$$

The PE-*i*-DIB sample used for the synthesis of copolymers under starved feed conditions (Runs 8-11, Chapter 3) had a T_g at -140°C, which again remained similar in the copolymers. A similar reduction in T_m was also observed from 121°C in the macromonomer down to 115°C in the highest molecular weight copolymer.

The observation of a second T_g at -50°C which is attributed to the amorphous P(*n*-BA) segment (Figure 4.38 and 4.39) is further evidence of phase separation. This T_g does not change when the molecular weight distribution increases from 3.6 to 7.4 (Table 3.1). The P(*n*-BA) T_g is more difficult to resolve when the molecular weight of the P(*n*-BA) segment is low (Run 2-180).

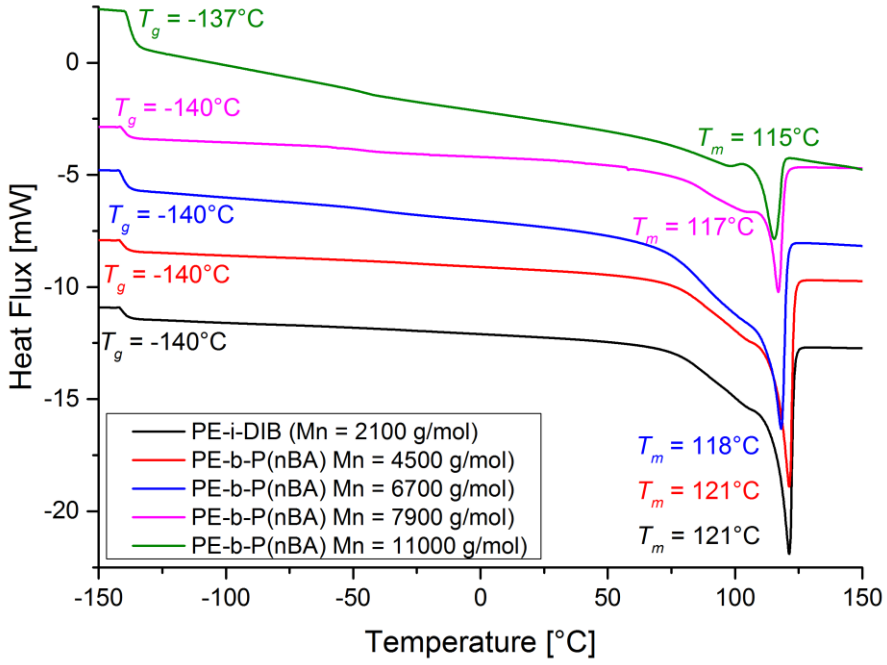

Figure 4.39 – Third heating curves (10°C/min) from DSC traces of PE-*i*-DIB, mass used = 5.23 mg; PE-*i*-DIB-*b*-P(*n*-BA) (Runs 8-11, Chapter 3), masses used: 6 mg, 12.06 mg, 8.36 mg, 4.67 mg.

From the above calculations we can conclude that the crystallinity of the PE component falls steadily from 71% in PE-*i*-DIB to *ca* 66%, 58%, 52% and eventually 38% as the added P(*n*-BA) block becomes larger (Runs 8-11). Increasing the P(*n*-BA) chain length further to M_n = 19000 g/mol and then to M_n = 40000 g/mol (Runs 3 and 4) does not lead to further reduction in crystallinity, as observed previously.[1, 18]

We also note the presence of a broad pre-melting curve in the DSC trace of the macromonomer starting at *ca* 50°C, thought to be caused either by the presence of defects or a broad size distribution of crystallites,[54] which is conspicuously absent in the copolymer traces. We suggest that the drop in crystallinity from 71% to *ca* 38%, which is in agreement with previous findings, is consistent with the loss of this region of low-melting PE, but the reason that no further loss of crystallinity is observed is because the PE and amorphous P(*n*-BA) are phase-separated. The second T_g at -50°C is not as obvious in these materials as with those above, presumably because the P(*n*-BA) segment is smaller in these materials so the transition is smaller. This T_g does not change over a range of copolymer molecular weights and dispersities (Tables 3.1, 3.3 and 3.4).

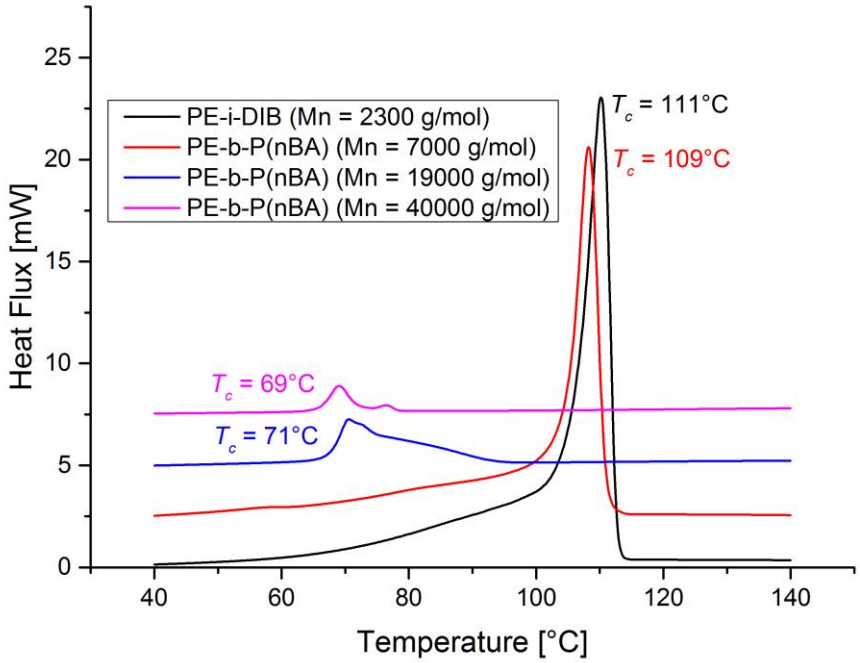

Figure 4.40 - Third cooling curves (10°C/min) from DSC traces of PE-*i*-DIB, mass used = 5.23 mg; PE-*i*-DIB-*b*-P(*n*-BA) (Runs 2-4, Chapter 3), masses used: 8.62 mg, 9.51 mg, 5.59 mg.

Figures 4.40 and 4.41 show the third cooling curves for the PE-*i*-DIB macromonomer and the PE-*b*-P(*n*-BA) copolymer samples prepared by batch and starved feed processes respectively. The P(*n*-BA) block length has a more pronounced effect on T_c than on T_m. There is a substantial discrepancy between T_m and T_c (supercooling)[55] and the size of this discrepancy increases with an increasing P(*n*-BA) block length for those materials prepared under batch conditions. The difference between T_m and T_c in the macromonomer is 12°C, which rises to 45°C in the largest molecular weight batch-prepared copolymer.

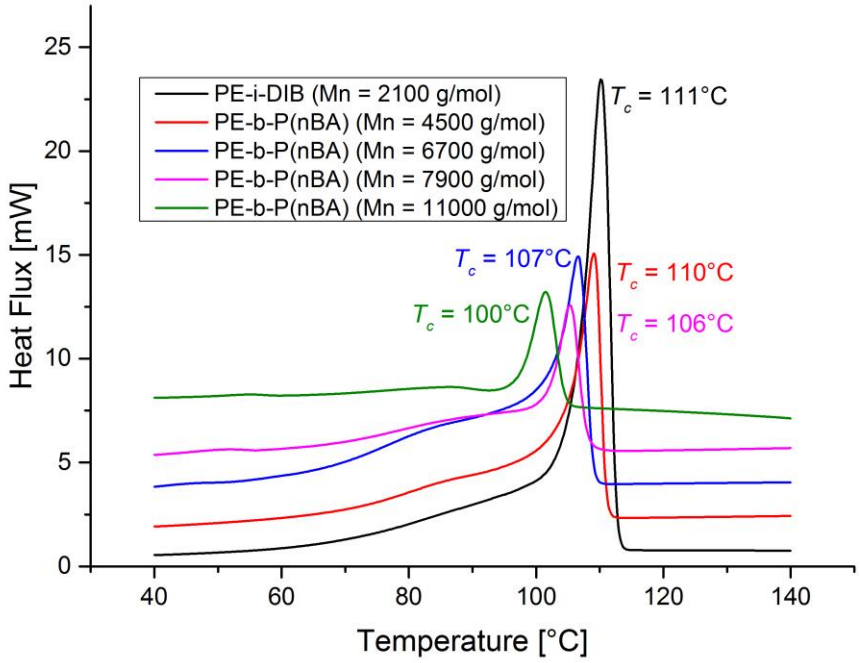

Figure 4.41 - Third cooling curves (10°C/min) from DSC traces of PE-*i*-DIB, mass used = 5.23 mg; PE-*i*-DIB-*b*-P(*n*-BA) (Runs 8-11, Chapter 3), masses used: 6 mg, 12.06 mg, 8.36 mg, 4.67 mg.

The degree of supercooling is, unsurprisingly given the lower range of molecular weights, far less pronounced for those materials prepared under starved feed conditions. Indeed the difference between T_m and T_c remains at 11°C until the copolymer molecular weight is increased to M_n = 11000 g/mol, where it rises to 15°C. The T_m falls by 9°C in

the batch samples and by 7°C in the starved feed samples. Our previous suggestion that this observation was a result of inhibition of PE block nucleation caused by the presence of the P(*n*-BA) chains appears consistent with present findings. Certainly the dramatic difference between T_m and T_c in the higher molecular weight batch-produced materials and the much less pronounced difference in the lower molecular weight starved-feed produced materials would suggest that the degree of inhibition is increased by larger P(*n*-BA) block length.[55, 56]

4.7.2 PE-*b*-P(VAc)

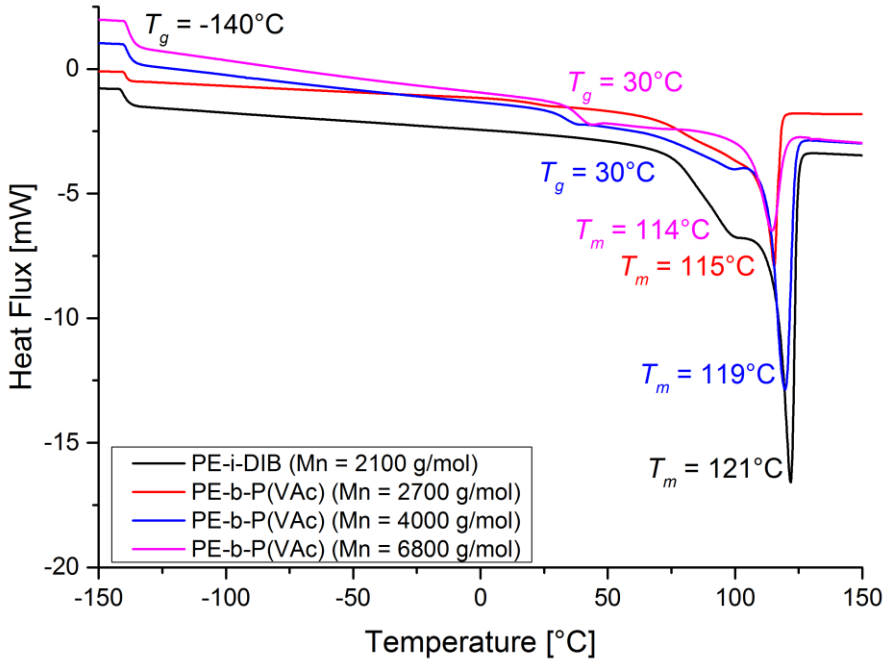

Figure 4.42 - Third heating curves (10°C/min) from DSC traces of PE-*i*-DIB, mass used = 5.23 mg; PE-*i*-DIB-*b*-P(VAc) (Runs 2-4, Table 4.1), masses used: 4.86 mg, 8.34 mg, 9.66 mg.

The PE-*i*-DIB (M_n = 2100 g/mol) macromonomer used in Runs 2-4 (Table 4.1) had a T_g at -140°C and a sharp T_m peak at 121°C. Again the T_g corresponding to the PE segments in the copolymers were very similar to the starting material, to indicate phase separation

between the two segments. Increasing P(VAc) block length caused T_m values for the copolymers to decrease modestly from 121°C in PE-*i*-DIB down to 114°C (Figure 4.42). Using the calculation discussed above and taking account of the differing proportions of PE the samples contain (PE-*i*-DIB, 100%; Run 2-240 70%; Run 3-240 47%; Run 4-240 16%); the crystallinities of the PE blocks in the macromonomer and copolymers were calculated to be: PE-*i*-DIB, 75%; Run 2-240, *ca* 59%; Run 3-240, *ca* 56%; Run 4-240, *ca* 50%. The reduction in relative crystallinity as the polar block length increases is again evident but the reduction is not as substantial as observed for the PE-*b*-P(*n*-BA) copolymers.

Further evidence of phase separation is observed in the form of a second T_g at 30°C which is attributed to the amorphous P(VAc) segment (Figure 4.42). As before, this T_g does not change when the molecular weight distribution increases (Table 4.1) and is more difficult to resolve when the polar segment is small.

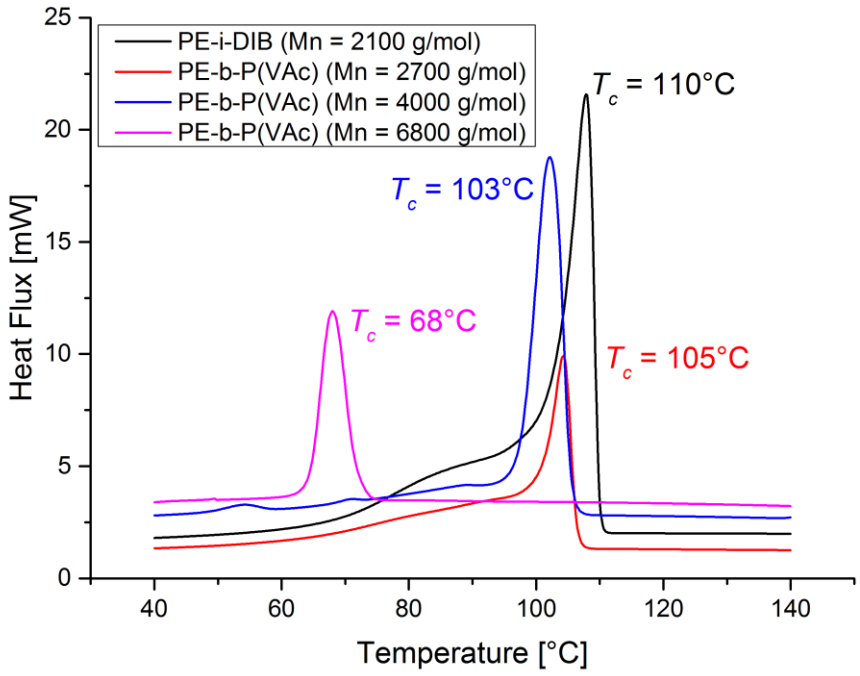

Figure 4.43 - Third heating curves (10°C/min) from DSC traces of PE-*i*-DIB, mass used = 5.23 mg; PE-*i*-DIB-*b*-P(VAc) (Runs 2-4, Table 4.1), masses used: 4.86 mg, 8.34 mg, 9.66 mg.

As with the PE-*b*-P(*n*-BA) copolymers discussed earlier, the influence of the P(VAc) segment is more pronounced in the decreasing T_c than the T_m (Figure 4.43). The degree of supercooling increases substantially with increasing block length from 11°C in the macromonomer to 46°C in the copolymer containing the largest P(VAc) block (sample 4-240). The degree of supercooling observed in the copolymer with the largest P(VAc) block is comparable with that of the PE-*b*-P(*n*-BA) material despite the substantially smaller polar block. We suggest that the P(VAc) block inhibits PE block nucleation to a greater extent than P(*n*-BA) and again that the inhibition increases with block length.

4.7.3 PE-*b*-P(V2EH)

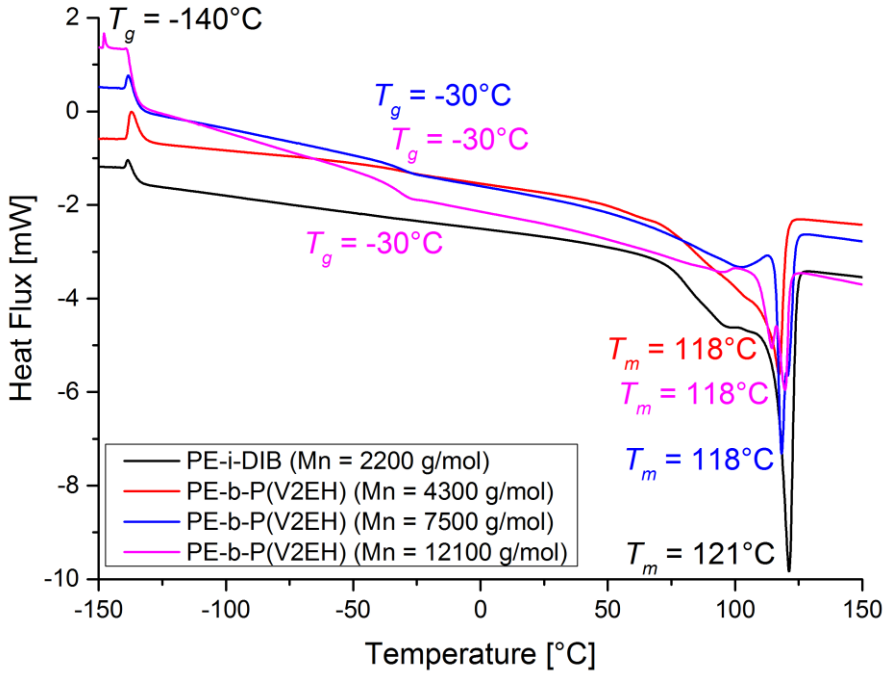

Figure 4.44 - Third heating curves (10°C/min) from DSC traces of PE-*i*-DIB, mass used = 5.23 mg; PE-*i*-DIB-*b*-P(V2EH) (Runs 6-8, Table 4.2), masses used: 5.10 mg, 6.34 mg, 8.13 mg.

As with PE-*b*-P(VAc), the PE-*i*-DIB (M_n = 2200 g/mol) macromonomer from runs 7-9 (Table 4.2) had a T_g at -140°C, which remained the same after copolymerisation with V2EH, and a sharp T_m peak at 121°C. The addition of a P(V2EH) block caused a small drop in the copolymer T_m from 121°C to 118°C but no further drop in T_m was observed when the P(V2EH) block length was increased (Figure 4.44). The relative crystallinities of the PE segments were calculated to be: PE-*i*-DIB, 75%; Run 6-240, *ca* 55%; Run 7-240, *ca* 47%; Run 8-240, *ca* 35%. The reduction in relative crystallinity of the PE segments in these materials is comparable to those of the PE-*b*-P(*n*-BA) samples prepared under the same conditions, though as with the PE-*b*-P(VAc) materials the lengths of the polar blocks were far lower indicating a larger effect on nucleation

inhibition of PE chains per monomer unit than P(*n*-BA). A second T_g was observed at -30°C which corresponds to the amorphous P(V2EH) block.

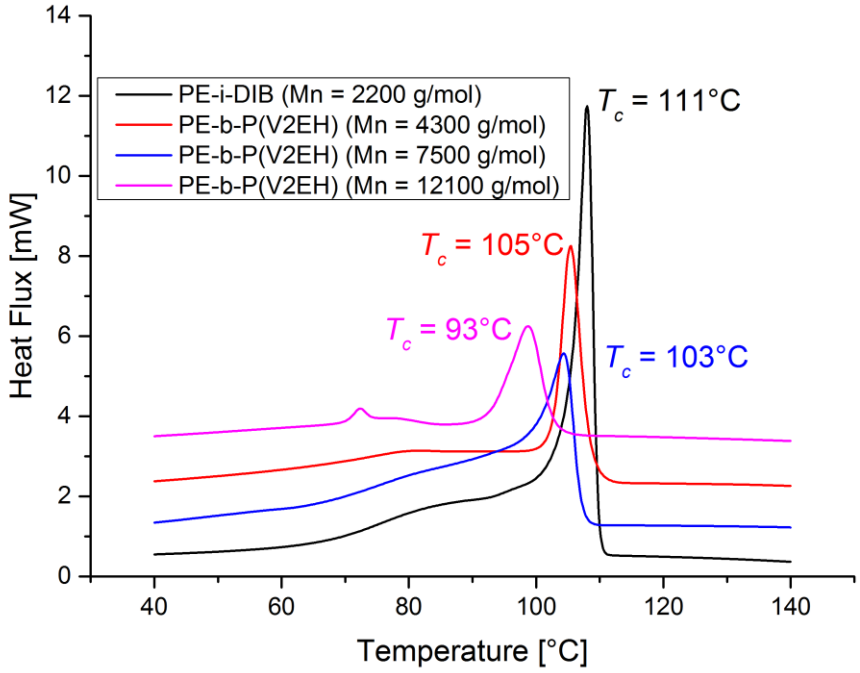

Figure 4.45 - Third cooling curves (10°C/min) from DSC traces of PE-*i*-DIB, mass used = 5.23 mg; PE-*i*-DIB-*b*-P(V2EH) (Runs 7-9, Table 4.2), masses used: 5.10 mg, 6.34 mg, 8.13 mg.

While the copolymer T_m did not decrease below 118°C as the P(V2EH) block length was increased (a difference of 3°C from the PE-*i*-DIB) the effect on the copolymer T_c was more significant (Figure 4.45), though not as large as with the PE-*b*-P(VAc) or the PE-*b*-P(*n*-BA) materials. In these samples the difference between T_m and T_c increased from 10°C in the macromonomer to 28°C in the copolymer containing the largest P(V2EH) segment (sample 8-240).

4.7.4 PE-*b*-P(MMA)

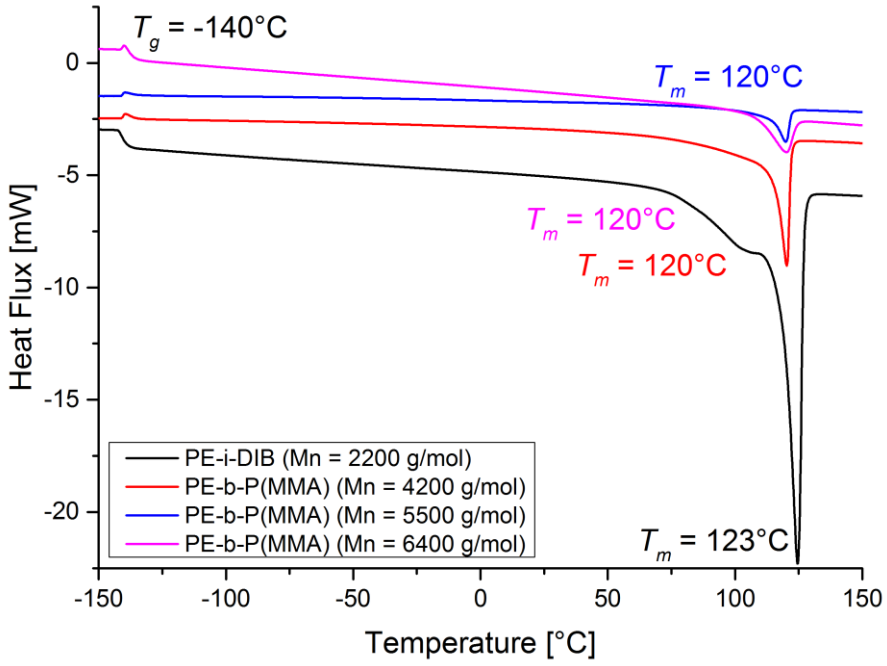

Figure 4.46 - Third heating curves (10°C/min) from DSC traces of PE-*i*-DIB, mass used = 5.23 mg; PE-*i*-DIB-*b*-P(MMA) (Runs 10-12, Table 4.3), masses used: 3.03 mg, 1.63 mg, 7.52 mg.

The PE-*i*-DIB (M_n = 2200 g/mol) macromonomer from Runs 10-12 (Table 4.3) had a familiar T_g at -140°C, which remained the same after copolymerisation with MMA, and a sharp T_m peak at 123°C. The addition of a P(MMA) block caused a small drop in the copolymer T_m from 123°C to 120°C, but no further drop in T_m was observed when the P(MMA) block length was increased (Figure 4.46). The relative crystallinities of: PE-*i*-DIB, 75%; Run 10-240, *ca* 67%; Run 11-240, *ca* 57%; Run 12-240, *ca* 32% were determined for the PE in each sample. Again, the reduction in relative crystallinity of the PE segments in these materials is comparable to those of the PE-*b*-P(*n*-BA) samples, but achieved with far smaller polar blocks. The T_g for the amorphous P(MMA) expected to occur at 105°C[57] is obscured by the large PE melting curve occurring from *ca* 50°C

and as such was not detected in the copolymer samples, even when the P(MMA) block is increased.

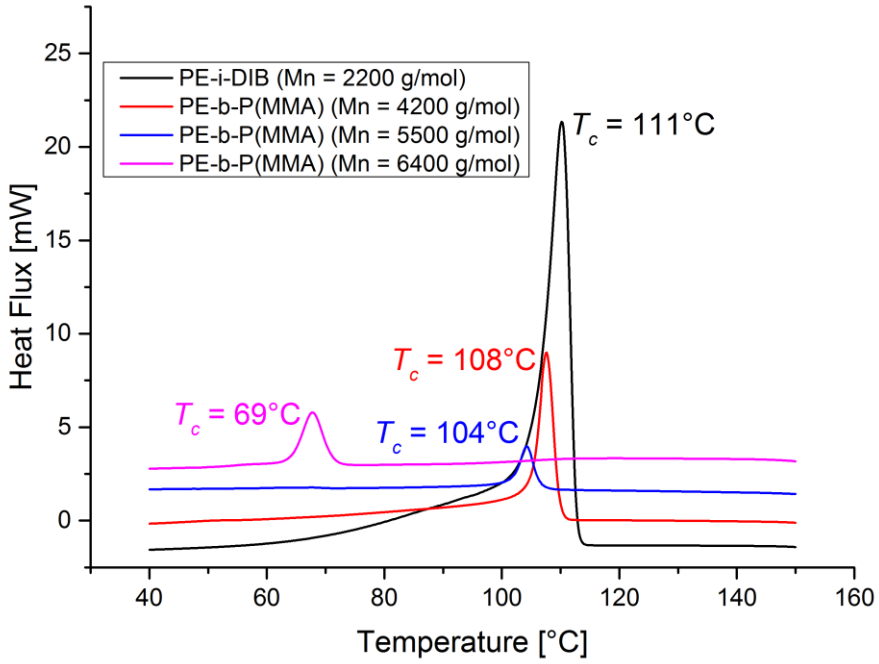

Figure 4.47 - Third cooling curves (10°C/min) from DSC traces of PE-*i*-DIB, mass used = 5.23 mg; PE-*i*-DIB-*b*-P(MMA) (Runs 10-12, Table 4.3), masses used: 3.03 mg, 1.63 mg, 7.52 mg.

Again the effect on the copolymer T_c was far more substantial than the T_m (Figure 4.47). The difference between T_m and T_c increased from 12°C in the macromonomer to 51°C in the copolymer containing the largest P(MMA) segment (sample 12-240). Again the degree of polymerisation of MMA required to achieve a comparable degree of supercooling is much smaller than that of *n*-BA, which again we suggest is a result of greater propensity of P(MMA) for disrupting the nucleation of PE chains than P(*n*-BA).

4.7.5 PE-*b*-P(C14MA)

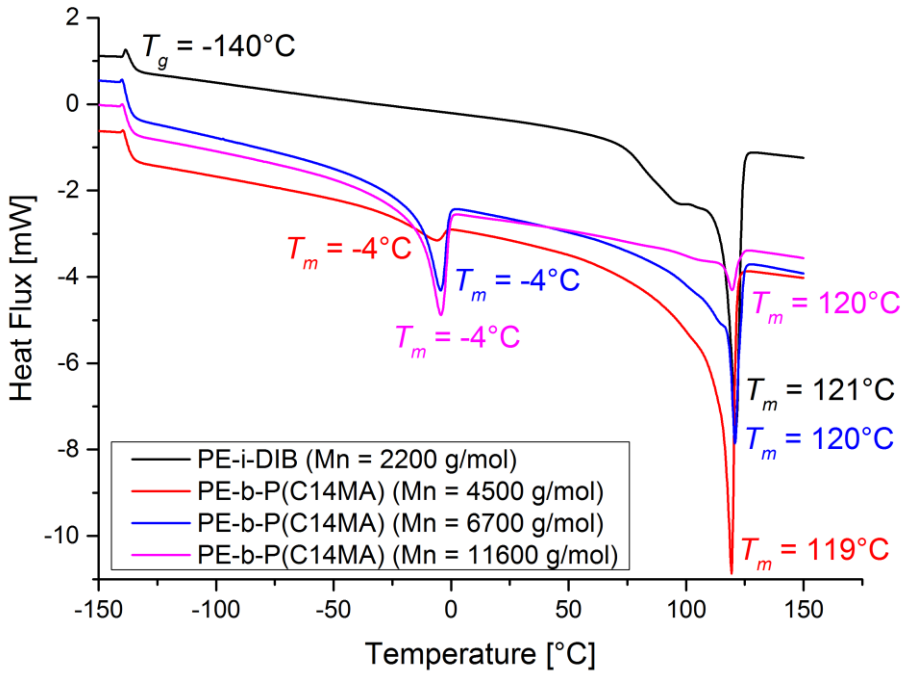

Figure 4.48 - Third heating curves (10°C/min) from DSC traces of PE-*i*-DIB, mass used = 5.23 mg; PE-*i*-DIB-*b*-P(C14MA) (Runs 14-16, Table 4.4), masses used: 5.15 mg, 7.18 mg, 6.57 mg.

The macromonomer (PE-*i*-DIB, M_n = 2200 g/mol) used in Runs 14-16 (Table 4.4) had the same T_g at -140°C, which was maintained after copolymerisation with C14MA, and a sharp T_m peak at 121°C. After copolymerisation with C14MA, a small drop in the copolymer T_m from 121°C to 120°C was observed and no further drop in T_m was observed when the P(C14MA) block length was increased (Figure 4.48). Relative crystallinities of the PE segments were calculated to be: PE-*i*-DIB, 75%; Run 14-240, *ca* 64%; Run 15-240, *ca* 51%; Run 16-240, *ca* 42%. A second T_m at -4°C which is attributable to the alkyl side chains of the P(C14MA) segment[58] (Figure 4.48) was also detected. This T_m value does not change with molecular weight or dispersity but as the polar block length is increased it becomes correspondingly more intense, consistent with our assignment as a property of the side chains. The expected T_g at -9°C corresponding

to the amorphous P(C14MA) segment[58] was not detected, presumably because it is obscured by the melting curve for the P(C14MA) side chains.

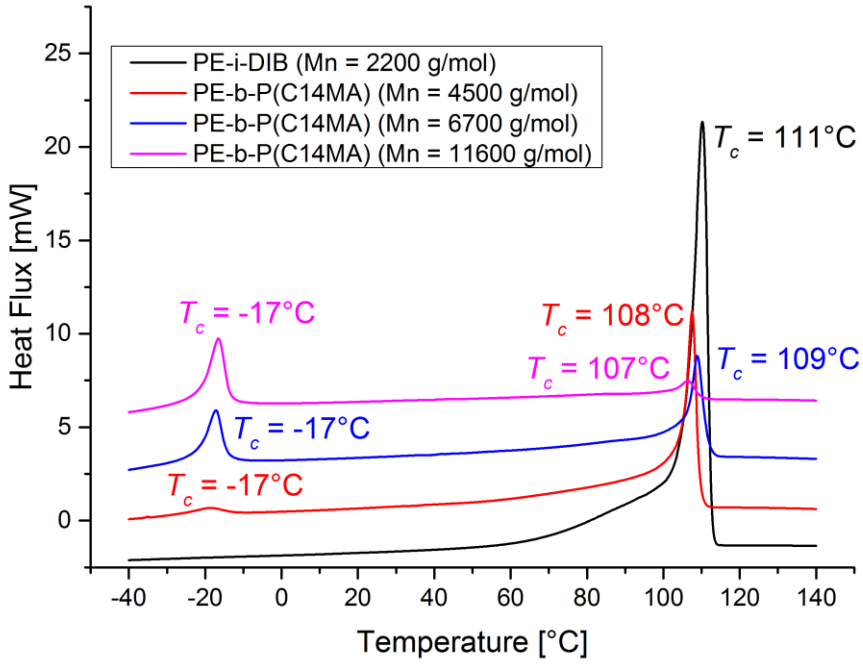

Figure 4.49 - Third cooling curves (10°C/min) from DSC traces of PE-*i*-DIB, mass used = 5.23 mg; PE-*i*-DIB-*b*-P(C14MA) (Runs 14-16), masses used: 5.15 mg, 7.18 mg, 6.57 mg.

In these materials, as with all the others discussed so far, we observe an increasing degree of supercooling as the polar block length is increased. In this case however, the increase is much more modest, from 10°C in the macromonomer to 13°C in the copolymer with the largest P(C14MA) block (Figure 4.49). Also detectable is the corresponding T_c for the P(C14MA) alkyl side chains at -17°C.

4.7.6 PE-*b*-PS

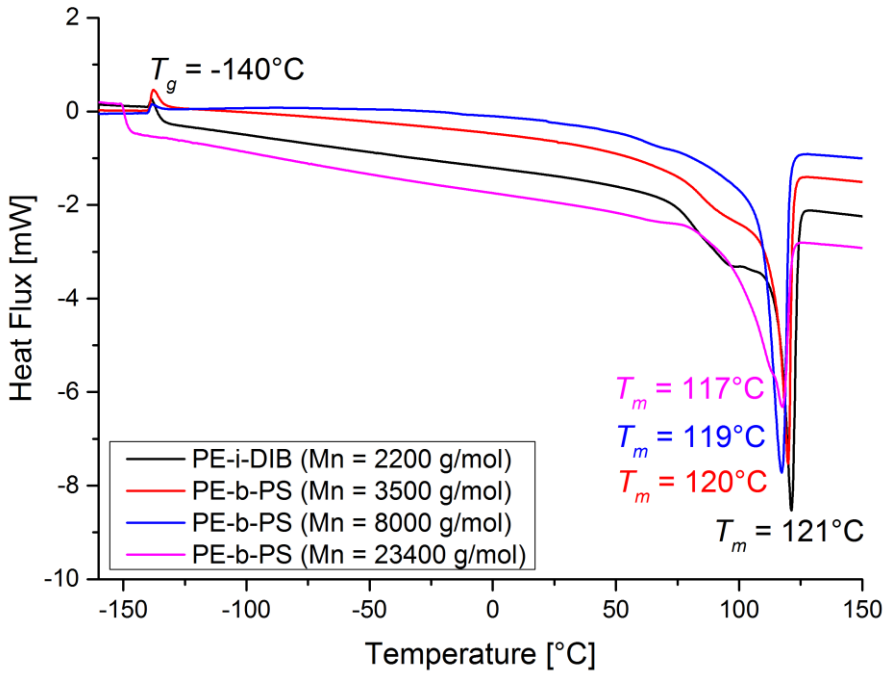

Figure 4.50 - Third heating curves (10°C/min) from DSC traces of PE-i-DIB, mass used = 5.23 mg; PE-*i*-DIB-*b*-PS (Runs 18-20, Table 4.5), masses used: 4.81 mg, 8.33 mg, 7.33 mg.

Figure 4.50 shows that the PE T_g at -140°C did not change after copolymerisation with styrene (Runs 18-20, Table 4.5), while the T_m peak was slightly reduced from 121°C in the macromonomer to 117°C in the PE-*b*-PS copolymer as the length of the PS block was increased. The relative crystallinities of the PE segments in the materials were calculated to be: PE-*i*-DIB, 75%; Run 18-240, *ca* 67%; Run 19-240, *ca* 65%; Run 20-240, *ca* 60%, suggesting that the PE segment in these materials retains crystallinity to a larger extent than in the other copolymers discussed here. As with PE-*b*-P(MMA), the T_g for the amorphous PS (95°C)[57] but was not detected as a result of overlap of the large PE melting curve occurring from *ca* 50°C.

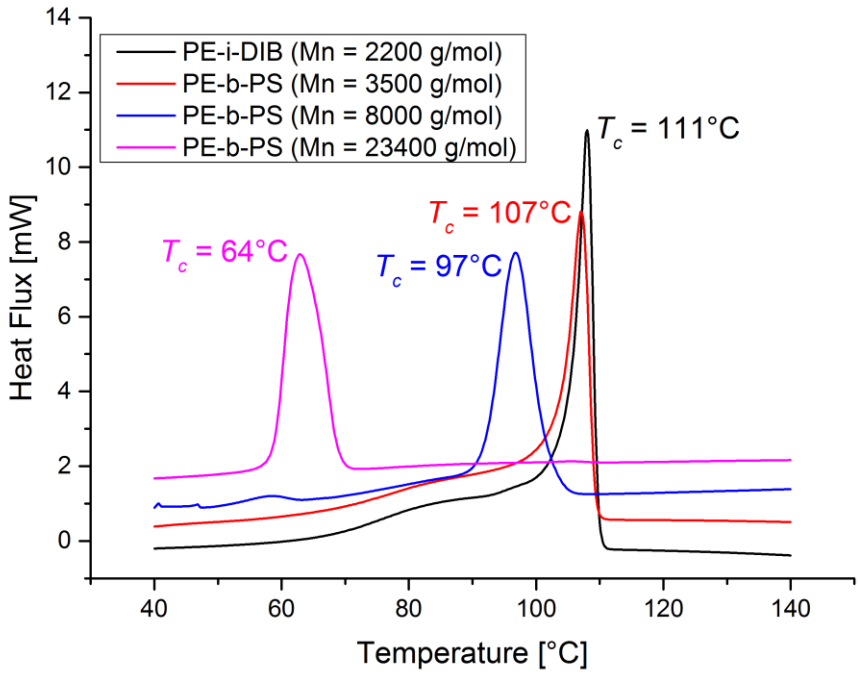

Figure 4.51 - Third cooling curves (10°C/min) from DSC traces of PE-i-DIB, mass used = 5.23 mg; PE-*i*-DIB-*b*-PS (Runs 18-20, Table 4.5), masses used: 4.81 mg, 8.33 mg, 7.33 mg.

Figure 4.51 shows the familiar reduction in T_c with increasing polar block length, as well as an increasing degree of supercooling from 10°C in the macromonomer to 53°C in the copolymer with the largest PS block. The change in the degree of supercooling is similar to that observed in the higher molecular weight PE-*b*-P(*n*-BA) samples but in this case the degree of polymerisation to achieve this was similar. This indicates a similar propensity for disrupting PE chain nucleation between PS and P(*n*-BA).

4.8 Conclusions

The versatility of the PE-*i*-DIB macromonomer was investigated through free-radical copolymerisations with a range of different polar monomers under similar conditions to those described in Chapter 3. PE copolymer products with vinyl esters, methacrylates and styrene were synthesised, isolated and purified. Kinetic runs allowed us to follow the progress of the polymerisations by GPC and NMR.

Detailed NMR studies were consistent with the presence of a block structure and the presence of a single diffusion coefficient in DOSY experiments suggested that there were no other materials present in the purified samples. Observations consistent with aggregate formation was also found in further DOSY NMR experiments as well as in VT NMR. As far as we know, this is the first example of polyethylene block copolymers being characterised by DOSY and the behaviour of these materials in the presence of other polymer species was discussed. Further evidence of aggregation in selective solvents was obtained from materials with larger polar blocks by their analysis using DLS and results from DSC studies were found to be consistent with phase separation of crystalline PE and amorphous polar blocks.

The simplicity of synthesis and purification, the range of compatible monomers, the ease with which molecular weights of both blocks can be tuned and the commercial availability of all reagents involved in both reaction steps make this a remarkably powerful and highly practical process that overcomes many of the technical and commercial drawbacks of the strategies discussed in Chapter 1.

4.9 References

1. Kay, C. J. Polyethylene Block Copolymers, PhD, University of Warwick, 2014.
2. Henderson, A. M., Ethylene-vinyl acetate (EVA) copolymers: a general review. *IEEE Electrical Insulation Magazine* **1993,** *9* (1), 30-38.
3. Wolf, B. A.; Will, B.; Obrecht, W.; Casper, R.; Baade, W.; Sylvester, G.; Meurer, K. P.; Zimmermann, H., Solution polymerization for the preparation of gel-free ethylene/vinyl acetate copolymers. Google Patents: 1990.
4. Orphanides, G. G., Vinyl acetate-ethylene copolymer binder emulsions for medical-surgical nonwoven fabrics. Google Patents: 1986.
5. Arsac, A.; Carrot, C.; Guillet, J., Rheological characterization of ethylene vinyl acetate copolymers. *J. Appl. Polym. Sci.* **1999,** *74* (11), 2625-2630.
6. Stenzel, M. H.; Cummins, L.; Roberts, G. E.; Davis, T. P.; Vana, P.; Barner-Kowollik, C., Xanthate Mediated Living Polymerization of Vinyl Acetate: A Systematic Variation in MADIX/RAFT Agent Structure. *Macromol. Chem. Phys.* **2003,** *204* (9), 1160-1168.
7. Iovu, M. C.; Matyjaszewski, K., Controlled/Living Radical Polymerization of Vinyl Acetate by Degenerative Transfer with Alkyl Iodides. *Macromolecules* **2003,** *36* (25), 9346-9354.
8. Debuigne, A.; Caille, J.-R.; Jérôme, R., Highly Efficient Cobalt-Mediated Radical Polymerization of Vinyl Acetate. *Angew. Chem.* **2005,** *117* (7), 1125-1128.
9. Kaneyoshi, H.; Matyjaszewski, K., Effect of Ligand and n-Butyl Acrylate on Cobalt-Mediated Radical Polymerization of Vinyl Acetate. *Macromolecules* **2005,** *38* (20), 8163-8169.
10. Dommanget, C.; D'Agosto, F.; Monteil, V., Polymerization of Ethylene through Reversible Addition–Fragmentation Chain Transfer (RAFT). *Angew. Chem. Int. Ed.* **2014,** *53* (26), 6683-6686.
11. Kermagoret, A.; Debuigne, A.; Jérôme, C.; Detrembleur, C., Precision design of ethylene- and polar-monomer-based copolymers by organometallic-mediated radical polymerization. *Nat. Chem.* **2014,** *6* (3), 179-187.
12. Prinos, J.; Bikiaris, D.; Theologidis, S.; Panayiotou, C., Preparation and characterization of LDPE/starch blends containing ethylene/vinyl acetate copolymer as compatibilizer. *Polymer Engineering & Science* **1998,** *38* (6), 954-964.
13. Mclennan, A. J.; Zeimentz, P. M.; Laborda, S., Vinyl acetate/vinyl 2-ethylhexanoate co-polymer binder resins. Google Patents: 2011.
14. Mclennan, A. J.; Zeimentz, P. M., Vinyl acetate/butenedioic acid cycloalkyl ester copolymers and uses thereof. Google Patents: 2010.
15. Lin, J.; Brown, G. I., Compositions comprising animal or vegetable derived oil and ethylene-vinyl ester copolymer. Google Patents: 2012.
16. Davies, B. W.; Brod, R. J.; Bock, J.; Ibrahim, T., Oil additive combinations, compositions and polymers for use therein. Google Patents: 1996.
17. Kawahara, N.; Kojoh, S.-i.; Matsuo, S.; Kaneko, H.; Matsugi, T.; Saito, J.; Kashiwa, N., Synthetic method of polyethylene-poly(methylmethacrylate) (PE-PMMA) polymer hybrid via reversible addition-fragmentation chain transfer (RAFT) polymerization with functionalized polyethylene. *Polym. Bull.* **2006,** *57* (6), 805-812.

18. Matsugi, T.; Kojoh, S.-I.; Kawahara, N.; Matsuo, S.; Kaneko, H.; Kashiwa, N., Synthesis and morphology of polyethylene-block-poly(methyl methacrylate) through the combination of metallocene catalysis with living radical polymerization. *J. Polym. Sci. A: Polym. Chem.* **2003,** *41* (24), 3965-3973.
19. Inoue, Y.; Matsugi, T.; Kashiwa, N.; Matyjaszewski, K., Graft Copolymers from Linear Polyethylene via Atom Transfer Radical Polymerization. *Macromolecules* **2004,** *37* (10), 3651-3658.
20. Hatada, K.; Kitayama, T.; Masuda, E., Studies on the Radical Polymerization of Methyl Methacrylate in Bulk and in Benzene Using Totally Deuterated Monomer Technique. *Polym. J.* **1986,** *18* (5), 395-402.
21. Zammit, M. D.; Davis, T. P.; Haddleton, D. M.; Suddaby, K. G., Evaluation of the Mode of Termination for a Thermally Initiated Free-Radical Polymerization via Matrix-Assisted Laser Desorption Ionization Time-of-Flight Mass Spectrometry. *Macromolecules* **1997,** *30* (7), 1915-1920.
22. Soldi, R. A.; Oliveira, A. R. S.; Barbosa, R. V.; César-Oliveira, M. A. F., Polymethacrylates: Pour point depressants in diesel oil. *Eur. Polym. J.* **2007,** *43* (8), 3671-3678.
23. Guo, H. F.; Packirisamy, S.; Mani, R. S.; Aronson, C. L.; Gvozdic, N. V.; Meier, D. J., Compatibilizing effects of block copolymers in low-density polyethylene/polystyrene blends. *Polymer* **1998,** *39* (12), 2495-2505.
24. Fayt, R.; Jerome, R.; Teyssié, P., Molecular design of multicomponent polymer systems, 13. Control of the morphology of polyethylene/polystyrene blends by block copolymers. *Makromol. Chem.* **1986,** *187* (4), 837-852.
25. Brandrup, J.; Immergut, E. H.; Grulke, E. A., *Polymer Handbook, 2 Volumes Set*. Wiley: 2003.
26. Chiefari, J.; Jeffery, J.; Krstina, J.; Moad, C. L.; Moad, G.; Postma, A.; Rizzardo, E.; Thang, S. H., Binary Copolymerization with Catalytic Chain Transfer. A Method for Synthesizing Macromonomers Based on Monosubstituted Monomers. *Macromolecules* **2005,** *38* (22), 9037-9054.
27. Kukulj, D.; Heuts, J. P. A.; Davis, T. P., Copolymerization of Styrene and α-Methylstyrene in the Presence of a Catalytic Chain Transfer Agent. *Macromolecules* **1998,** *31* (18), 6034-6041.
28. Moad, G.; Solomon, D. H., 3 - Initiation. In *The Chemistry of Radical Polymerization (Second Edition)*, Solomon, G. M. H., Ed. Elsevier Science Ltd: Amsterdam, 2005; pp 49-166.
29. Moad, G.; Solomon, D. H., 4 - Propagation. In *The Chemistry of Radical Polymerization (Second Edition)*, Solomon, G. M. H., Ed. Elsevier Science Ltd: Amsterdam, 2005; pp 167-232.
30. Kaneyoshi, H.; Inoue, Y.; Matyjaszewski, K., Synthesis of Block and Graft Copolymers with Linear Polyethylene Segments by Combination of Degenerative Transfer Coordination Polymerization and Atom Transfer Radical Polymerization. *Macromolecules* **2005,** *38* (13), 5425-5435.
31. Debuigne, A.; Caille, J.-R.; Jérôme, R., Synthesis of End-Functional Poly(vinyl acetate) by Cobalt-Mediated Radical Polymerization. *Macromolecules* **2005,** *38* (13), 5452-5458.
32. Britton, D.; Heatley, F.; Lovell, P. A., Chain Transfer to Polymer in Free-Radical Bulk and Emulsion Polymerization of Vinyl Acetate Studied by NMR Spectroscopy. *Macromolecules* **1998,** *31* (9), 2828-2837.
33. Hatada, K.; Kitayama, T.; Ute, K.; Terawaki, Y.; Yanagida, T., End-Group Analysis of Poly(methyl methacrylate) Prepared with Benzoyl Peroxide by 750

MHz High-Resolution 1H NMR Spectroscopy. *Macromolecules* **1997,** *30* (22), 6754-6759.
34. Kukulj, D.; Davis, T. P.; Gilbert, R. G., Chain Transfer to Monomer in the Free-Radical Polymerizations of Methyl Methacrylate, Styrene, and α-Methylstyrene. *Macromolecules* **1998,** *31* (4), 994-999.
35. Inoue, Y.; Matyjaszewski, K., Preparation of polyethylene block copolymers by a combination of postmetallocene catalysis of ethylene polymerization and atom transfer radical polymerization. *J. Polym. Sci. A: Polym. Chem.* **2004,** *42* (3), 496-504.
36. Chiefari, J.; Jeffery, J.; Mayadunne, R. T. A.; Moad, G.; Rizzardo, E.; Thang, S. H., Chain Transfer to Polymer: A Convenient Route to Macromonomers. *Macromolecules* **1999,** *32* (22), 7700-7702.
37. Morris, K. F.; Johnson, C. S., Diffusion-ordered two-dimensional nuclear magnetic resonance spectroscopy. *J. Am. Chem. Soc.* **1992,** *114* (8), 3139-3141.
38. Johnson Jr, C. S., Diffusion ordered nuclear magnetic resonance spectroscopy: principles and applications. *Prog. Nucl. Magn. Reson. Spectrosc.* **1999,** *34* (3–4), 203-256.
39. Chen, A.; Wu, D.; Johnson, C. S., Determination of Molecular Weight Distributions for Polymers by Diffusion-Ordered NMR. *J. Am. Chem. Soc.* **1995,** *117* (30), 7965-7970.
40. Jerschow, A.; Müller, N., Diffusion-Separated Nuclear Magnetic Resonance Spectroscopy of Polymer Mixtures. *Macromolecules* **1998,** *31* (19), 6573-6578.
41. Viel, S.; Capitani, D.; Mannina, L.; Segre, A., Diffusion-Ordered NMR Spectroscopy: A Versatile Tool for the Molecular Weight Determination of Uncharged Polysaccharides. *Biomacromolecules* **2003,** *4* (6), 1843-1847.
42. Li, W.; Chung, H.; Daeffler, C.; Johnson, J. A.; Grubbs, R. H., Application of 1H DOSY for Facile Measurement of Polymer Molecular Weights. *Macromolecules* **2012,** *45* (24), 9595-9603.
43. Thania S. Jiminez-Martinez, S. R.-M., Nuria Esturau-Escofet, Manuel Briseno-Teran, DOSY Experiments to Monitor Block Copolymer Polymerization. *J. Mex. Chem. Soc.* **2011,** *55* (2), 101-104.
44. Viel, S.; Mazarin, M.; Giordanengo, R.; Phan, T. N. T.; Charles, L.; Caldarelli, S.; Bertin, D., Improved compositional analysis of block copolymers using Diffusion Ordered NMR Spectroscopy. *Anal. Chim. Acta* **2009,** *654* (1), 45-48.
45. Monroy-Barreto, M.; Pérez-Vázquez, M. d. C.; Briseño-Terán, M.; Esturau-Escofet, N., Microstructural Characterization of Diblock Copolymers Formed by Styrene and Different Methacrylic Units. *Int. J. Polym. Anal. Char.* **2014,** *19* (1), 22-30.
46. Mirau, P. A., *A practical guide to understanding the NMR of polymers*. Wiley-Interscience: 2005.
47. Hamley, I., Neutral Block Copolymers in Dilute Solution. In *Block Copolymers in Solution: Fundamentals and Applications*, John Wiley & Sons, Ltd: 2005; pp 7-104.
48. van de Hulst, H., Light scattering by small particles. *New York: Dover, 1981* **1981**.
49. Dynamic Light Scattering Common Terms Defined. http://www.biophysics.bioc.cam.ac.uk/wp-content/uploads/2011/02/DLS_Terms_defined_Malvern.pdf (accessed 23/02/2017).

50. Berne, B. J.; Pecora, R., *Dynamic light scattering: with applications to chemistry, biology, and physics*. Courier Corporation: 2000.
51. Tanford, C., *The hydrophobic effect: formation of micelles and biological membranes*. Wiley: 1980.
52. Kong, Y.; Hay, J. N., The measurement of the crystallinity of polymers by DSC. *Polymer* **2002,** *43* (14), 3873-3878.
53. Kryuchkov, V. A.; Daigle, J.-C.; Skupov, K. M.; Claverie, J. P.; Winnik, F. M., Amphiphilic Polyethylenes Leading to Surfactant-Free Thermoresponsive Nanoparticles. *J. Am. Chem. Soc.* **2010,** *132* (44), 15573-15579.
54. Hatakeyama, T.; Quinn, F. X., *Thermal analysis: fundamentals and applications to polymer science*. Wiley: 1999.
55. Wunderlich, B., *Thermal analysis*. Academic Press: 1990.
56. Wunderlich, B., *Thermal Analysis of Polymeric Materials*. Springer Berlin Heidelberg: 2005.
57. Polymer Tg. http://polymerdatabase.com/polymer%20physics/Polymer%20Tg.html (accessed 10/05/2017).
58. Ellis, B.; Smith, R., *Polymers: A Property Database, Second Edition*. CRC Press: 2008.

Chapter 5: Application of Polyethylene diblock copolymers as wax crystal modifiers in diesel

5.1 Introduction

The crystallisation of paraffin waxes from middle distillate fuels is of great practical interest to the petroleum industry because of the problems associated with such events in the flow properties of the fuels at low temperatures.[1] In untreated fuels, rhomboid-shaped paraffin wax crystals grow very quickly with falling temperature and can interlock to form large "house of card" type structures.[2, 3] As a consequence, a small amount of precipitated wax is often sufficient to cause gelling of the fuel which can block pumps, transmission lines and filters, leading to engine failure.[4, 5] The addition of copolymer additives, variously called wax crystal modifiers or cold flow improvers, is by far the most practical and economically viable solution to this problem and as such is the most commonly used method.[6] There has been a great deal of work devoted to the synthesis of these additives and as a result, a wide variety of polymeric materials have been found to improve the low temperature operability of crude oils and middle-distillate fuels by altering the size and/or shape of the crystals formed. Included in this range of additives are random copolymers such as those of alkyl acrylates or methacrylates with α-olefins,[7, 8, 9] poly(vinyl ethers),[10] ethylene-vinyl ester, including ethylene-vinyl acetate (EVA),[5, 11] as well as more specific architectures like combs[3, 12, 13] and diblock copolymers.[14, 15, 16]

Just as the types of polymer additive are many and varied, so are the reported mechanisms by which they work. Much of the research into preparing new additives is governed by a desired or proposed method of interaction with the wax crystals. Among

many proposed mechanisms, the most widely accepted are: (a) nucleation, normally associated with additives that contain crystalline segments which provide multiple sites promoting crystal growth and amorphous segments that control the growth of said crystals leading to more numerous smaller crystals; (b) adsorption (growth inhibiting/arresting), where the additive physically binds to a face of a wax crystal and thus prevents further growth from that face, as well as preventing interlocking of crystals. This often results in needle-shaped crystals.[5, 17, 18, 19, 20, 21] Random copolymers like EVA or PE-*co*-PEB have previously been reported to act by the former mechanism, where the crystallisable ethylene segments form nucleation sites.[4, 22] Conversely, diblock copolymers like PE-*b*-PEP were thought to utilise the latter, physically adsorbing to the wax crystal to inhibit further growth and prevent aggregation of crystals.[23]

EVA copolymers in particular have been the mainstay of wax crystal modification in middle-distillate fuels for many years[24, 25] and, while they are generally reported be growth-arresting additives, there is a report that suggests that this can vary depending on the VAc content. Richter and co-workers describe EVA polymers that contain less VAc and more crystalline regions are perceived as acting like nucleating agents, while those with fewer crystalline segments and higher VAc content as behaving like growth arrestors.[5] These additives are normally sold as packages that consist either of mixtures of nucleator and growth arrestors or single shot grades which are thought to combine the nucleation and growth inhibition properties of the mixture.[5]

This chapter discusses the testing of some of the PE-polar monomer block copolymers synthesised in chapters 3 and 4 for their wax crystal modification properties in diesel as assessed by their performance in the cold filter plugging point test (CFPP) and further

investigated by DSC. Of those block copolymers that were soluble in diesel, a range of molecular weights were tested to study the effect of polar block length on performance. Based on the above literature reports, we would expect the amphiphilic diblock copolymers discussed in Chapters 3 and 4 to behave in a similar way to the PE-*b*-PEP diblocks; namely that the chemically similar non-polar PE block would adsorb to the face of a wax crystal and the chemically different polar block would inhibit further growth on that face of the crystal and prevent crystals aggregating to form larger structures.

5.2 Cold filter plugging point (CFPP)

The CFPP test is established around the world as the standard means for determining the limiting temperature of operability of cold, wax-bearing, middle-distillate fuels.[26] A small sample of the fuel is transferred to a test jar equipped with a thermometer and filter assembly, which is connected to a pipette and a vacuum source (Figure 5.1, Left). The test jar is then loaded into the cooling bath (Figure 5.1, Right) and the fuel is repeatedly drawn through the filter under vacuum at every 1°C as the sample is cooled.[26] The CFPP of a sample is defined as the highest temperature (in multiples of 1°C) at which either a given volume of fuel fails to pass under vacuum through a standardised filtration device within a specified time; or the fuel drawn up under vacuum fails to flow back into the sample vessel before the next vacuum cycle starts.[26]

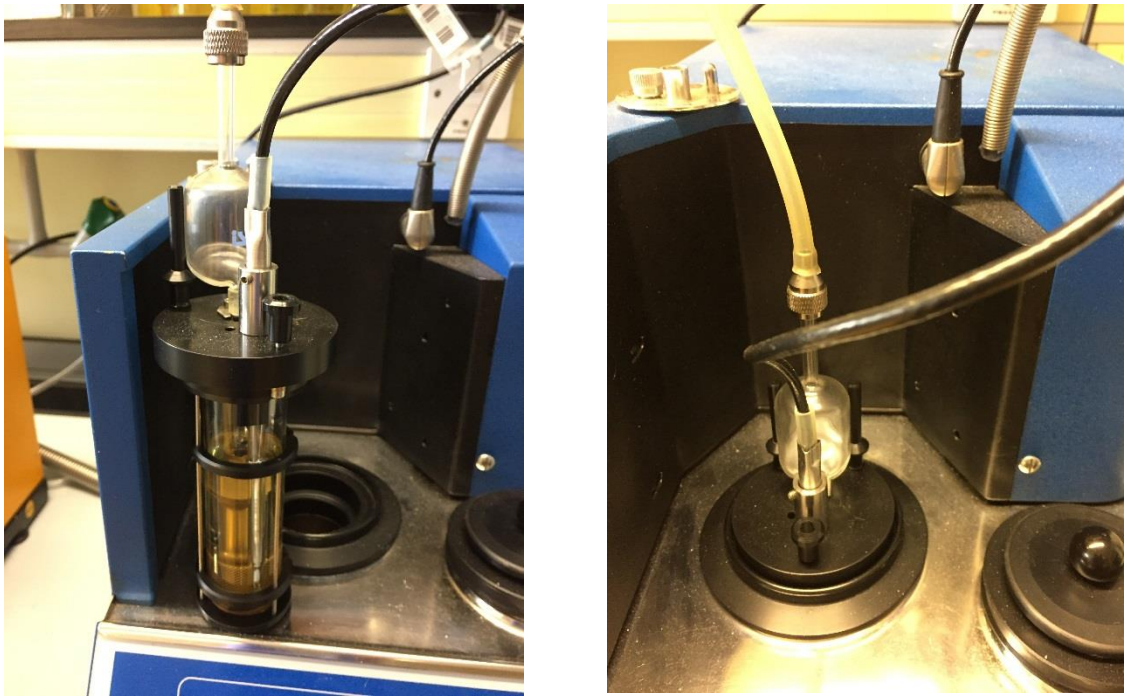

Figure 5.1 – (Left) Test jar containing fuel specimen, thermometer and filter assembly connected to a bulb pipette and a vacuum source. (Right) Test jar loaded into the cooling bath.

Solutions of the copolymers (10% w/v) were prepared in Solvesso 150®; a hydrocarbon solvent mixture with a high aromatic content and b.p. 175-205°C. Diesel test samples were treated with known concentrations of neat polymer, or with formulations consisting of known concentrations of polymer and commercial co-additives (growth arrestor, GA and nucleator, NU) in set ratios to try to establish the mode of action. Two tests were performed on each doped diesel sample over consecutive days under the same atmospheric conditions and the results did not differ from one test to the next within experimental error of the test equipment (±2°C). PE-*b*-P(MMA) and PE-*b*-P(S) copolymers were insoluble in diesel regardless of molecular weight or concentration and as such were not tested.

5.2.1 PE-*b*-P(*n*-BA) additives

CFPP testing was conducted on the PE-*b*-P(*n*-BA) copolymers prepared under batch conditions. Samples isolated after 180 min from runs 2-4 (Table 3.1, Chapter 3) were

dissolved in Solvesso 150 and doped into 50 g samples of diesel as a neat additive and in formulation with commercial additives. The CFPP results for the diesel samples doped with these materials are shown in Table 5.1. These additives did improve the CFPP of the diesel relative to untreated sample as a neat additive and in formulation with a commercial nucleator, but no difference was observed across the three polar block lengths in these formulations. We also note that the CFPP of diesel treated with neat nucleator was -17°C at the same treat rate, so the result with this formulation is likely to have been contributed to by the presence of a small amount of the nucleator. When combined with the growth arrestor, the two higher molecular weight PE-*b*-P(*n*-BA) additives did not significantly improve the CFPP performance of the diesel above the untreated sample. However, we do observe a modest improvement in performance when the lower molecular weight material was used. From these results we speculated that lowering the polar block length further may improve the performance of the additive in formulation with growth arrestor.

Table 5.1 – CFPP results for PE-*b*-P(*n*-BA) copolymers prepared under batch conditions.

Additive	PE M_n (g/mol)[a]	Copolymer M_n (g/mol) [a]	$Đ$ [a]	CFPP Polymer (°C)[b]	CFPP with GA (°C) [b]	CFPP with NU (°C) [b]
1	2100	7000	2.2	-13	-11	-15
2	2100	19000	3.6	-13	-8	-15
3	2100	40000	7.4	-13	-8	-15

[a] GPC data obtained at 160°C in 1,2,4-trichlorobenzene using universal calibration. PS standards were used to calibrate the system (see Chapter 6, Section 6.1 for further details).
[b] Total additive concentration = 250 ppm; polymer:GA treat ratio = 20:80; polymer:NU treat ratio = 80:20; untreated fuel CFPP = -7°C; CFPP of fuel treated with neat GA = -8°C; CFPP of fuel treated with neat NU = -17°C; CFPP of fuel treated with 80/20 formulation of GA:NU = -28°C.

As was demonstrated in Chapter 3, conducting the copolymerisation under starved feed conditions facilitated superior control over the reaction, thus allowing access to the lower molecular weight materials we were aiming for. Table 5.2 shows the results of

CFPP testing on the final samples obtained of these materials, where we observe considerable improvement in performance of the additive in formulation with the growth arrestor as the polar block length is reduced from additives 6 to 5 where the performance peaked at -21°C. By comparison the performance as neat additives and in formulation with the nucleator remained essentially the same. The additive with the shortest polar block (additive 4) precipitated when it was doped into the diesel, suggesting that the solubility limit for these materials has been reached. The best performance in this case was with additive 5 in a formulation with the commercial growth arrestor, which is consistent with activity as a nucleating agent *i.e.* providing sites for the promotion of wax crystal growth but also controlling the growth of the crystals (*vide supra*).

Table 5.2 – CFPP results from PE-*b*-P(*n*-BA) copolymers prepared under starved feed conditions.

Additive	PE M_n (g/mol)[a]	Copolymer M_n (g/mol) [a]	$Đ$ [a]	CFPP Polymer (°C)[b]	CFPP with GA (°C) [b]	CFPP with NU (°C) [b]
4	2100	4900	2.0	Insoluble	Insoluble	Insoluble
5	2100	6700	2.1	-13	-21	-16
6	2100	7900	2.1	-13	-12	-16

[a] GPC data obtained at 160°C in 1,2,4-trichlorobenzene using universal calibration. PS standards were used to calibrate the system (see Chapter 6, Section 6.1 for further details).
[b] Total additive concentration = 250 ppm; polymer:GA treat ratio = 20/80; polymer:NU treat ratio = 80:20; untreated fuel CFPP = -7°C; CFPP of fuel treated with neat GA = -8°C; CFPP of fuel treated with neat NU = -17°C; CFPP of fuel treated with 80/20 formulation of GA:NU = -28°C.

5.2.2 PE-*b*-P(VAc) additives

Although the use of EVA random copolymers in wax crystal modification applications is well documented, only the PE-*b*-P(VAc) copolymers with larger polar blocks discussed in Chapter 4 were found to be soluble in fuel and as such, only the higher molecular weight materials from the kinetic runs were tested in CFPP. The CFPP results for these additives are shown in Table 5.3.

Table 5.3 - CFPP results from PE-*b*-P(VAc) copolymers prepared under batch conditions.

Additive	PE M_n (g/mol)[a]	Copolymer M_n (g/mol) [a]	$Đ$ [a]	CFPP Polymer (°C)[b]	CFPP with GA (°C) [b]	CFPP with NU (°C) [b]
7	2100	4000	2.2	-8	-10	-15
8	2100	6800	3.0	-9	-21	-14

[a] GPC data obtained at 160°C in 1,2,4-trichlorobenzene using universal calibration. PS standards were used to calibrate the system (see Chapter 6, Section 6.1 for further details).
[b] Total additive concentration = 250 ppm; polymer:GA treat ratio = 20/80; polymer:NU treat ratio = 80:20; untreated fuel CFPP = -7°C; CFPP of fuel treated with neat GA = -8°C; CFPP of fuel treated with neat NU = -17°C; CFPP of fuel treated with 80/20 formulation of GA:NU = -28°C.

The fuel samples doped with neat polymer in both cases performed poorly, barely improving the performance beyond that of untreated fuel. Formulations with the nucleator produced similar CFPP performance to that of neat nucleator which, given the performance of the neat polymer samples, suggests that the presence of a small concentration of the commercial additive was the reason for the improvement. Little difference in performance was observed when the fuel was treated with a formulation of the lower molecular weight PE-*b*-P(VAc) copolymer and the growth arrestor, although there was a distinct improvement in performance with the higher molecular weight copolymer in the same formulation. The vastly improved performance of the higher molecular weight copolymer with growth arrestor would indicate that the block copolymer is acting as a nucleator. Unusually for these additives, the higher molecular weight material performed considerably better.

5.2.3 PE-*b*-P(V2EH) additives

The PE-*b*-P(V2EH) copolymers were far more soluble than the PE-*b*-P(VAc) materials on the whole as a result of the larger and bulkier side chain. As such all of these materials from the kinetic runs discussed in Chapter 4 were tested in CFPP.

Table 5.4 – CFPP results from PE-*b*-P(V2EH) copolymers prepared under batch conditions.

Additive	PE M_n (g/mol)[a]	Copolymer M_n (g/mol) [a]	$Đ$ [a]	CFPP Polymer (°C)[b]	CFPP with GA (°C) [b]	CFPP with NU (°C) [b]
9	2100	4300	1.8	-16	-23	-16
10	2100	7500	2.6	-17	-21	-18
11	2100	12100	3.5	-18	-21	-19

[a] GPC data obtained at 160°C in 1,2,4-trichlorobenzene using universal calibration. PS standards were used to calibrate the system (see Chapter 6, Section 6.1 for further details).
[b] Total additive concentration = 250 ppm; polymer:GA treat ratio = 20/80; polymer:NU treat ratio = 80:20; untreated fuel CFPP = -7°C; CFPP of fuel treated with neat GA= -8°C; CFPP of fuel treated with neat NU = -17°C; CFPP of fuel treated with 80/20 formulation of GA:NU = -28°C.

The results shown in Table 5.4 firstly suggest that the PE-*b*-P(V2EH) copolymers are far more active than the PE-*b*-P(*n*-BA) materials across all three formulations. The performance of the additives with the growth arrestor was the best of the three, which is consistent with the results from the PE-*b*-P(*n*-BA) materials and suggests that the materials are acting as nucleating agents. This is also supported by the consistency of the performance of each polymer as neat additives and in formulations with the nucleator. Again the additives with the lower polar block length gave the best results. The best performing formulation with these materials achieved a CFPP of -23°C (additive 9), which is fairly close to the CFPP achieved by the combination of the two commercial additives at the same treat rate (250 ppm). Interestingly, the performance of the neat additives and the formulations with the nucleator also improved with these materials and increasing the polar block length from M_n = 4300 g/mol to 12100 g/mol improved the performance in these formulations.

5.2.4 PE-*b*-P(C14MA) additives

As with the PE-*b*-P(V2EH) materials, the long alkyl side chain of C14MA meant that the PE-*b*-P(C14MA) copolymers were highly soluble in diesel (by comparison the PE-

b-P(MMA) materials were insoluble). The results shown in Table 5.5 show a sharp improvement in performance as a neat additive when the polar block length decreases from M_n = 39000 to 8300 g/mol (additives 15 to 13) but a drop in performance when the polar block length was decreased further. In fact the sample containing additive 13 as a neat additive gave the best CFPP performance to date with -25°C, very close to the CFPP achieved when growth arrestor and nucleator were combined. There was a significant improvement in CFPP in the formulations with the nucleator when the polar block was reduced between additives 14 and 13 but no more improvement when the polar block was decreased further (12). The performance in formulation with the growth arrestor was fairly consistent as the polar block length was varied, with a slight improvement between additives 14 and 13 but no further improvement with the smallest polar block in additives 12. Unusually for these block copolymer additives, which thus far have performed best in formulation with the growth arrestor, additive 13 performed well in formulation with both growth arrestor and the nucleator and even better as a neat additive. This indicates that additive 13 could have both nucleating and growth arresting properties and could be used as a single-shot additive, as with certain grades of EVA.

Table 5.5 – CFPP results from PE-*b*-P(C14MA) copolymers prepared under batch conditions.

Material	PE M_n (g/mol)[a]	Copolymer M_n (g/mol) [a]	$Đ$ [a]	CFPP Polymer (°C)[b]	CFPP with GA (°C) [b]	CFPP with NU (°C) [b]
12	2100	4500	2.3	-17	-23	-19
13	2100	6700	3.3	-25	-23	-20
14	2100	11600	6.1	-13	-22	-19
15	2100	39300	8	-11	-22	-13

[a] GPC data obtained at 160°C in 1,2,4-trichlorobenzene using universal calibration. PS standards were used to calibrate the system (see Chapter 6, Section 6.1 for further details).
[b] Total additive concentration = 250 ppm; polymer:GA treat ratio = 20/80; polymer:NU treat ratio = 80:20; untreated fuel CFPP = -7°C; CFPP of fuel treated with neat GA = -8°C; CFPP of fuel treated with neat NU = -17°C; CFPP of fuel treated with 80/20 formulation of GA:NU = -28°C.

5.3 Characterisation of additive effect on crystallisation events by DSC

The effect of the additives on the crystallisation of the wax was investigated by differential scanning calorimetry. Comparisons of the second cooling curve of untreated fuel and those of fuel treated with commercial growth arrestor and nucleator, with the neat PE-*b*-P(X) copolymer additives and formulations of the commercial and block copolymer additives are given in the following sections.

5.3.1 PE-*b*-P(*n*-BA) additives

The effect of the copolymer on wax crystallisation in the fuel sample is characterised in DSC by the changes in wax appearance temperature (WAT), identified by the onset temperature of crystallisation in the cooling curve (*e.g.* in Figure 5.1), and the size of the peak in the cooling curve indicating a change in the amount of wax crystallisation by the change in heat flux in mWg^{-1}. An increase in the WAT would be consistent with behaviour as a nucleating agent while a decrease in WAT would be consistent with growth arresting behaviour. The mass of the sample could be expected to have a significant effect on the size of the crystallisation peak so in order to gain meaningful information about the relative sizes of the peaks, the data has been corrected to take the mass differences into account.

As shown in Figure 5.2, the untreated fuel had a WAT of -12.4°C which in the presence of the commercial growth arrestor decreased to -13.0°C, consistent with the expected behaviour of a growth arrestor. In the presence of the commercial nucleator the WAT increased to -11.5°C, which is consistent with its expected behaviour. Both commercial additives caused a reduction in the size of the crystallisation peak but in the case of the nucleator the reduction was substantial. This could suggest a significant change in the

size of the wax crystals, as well as a likely change in the morphology (*vide supra*). When the two commercial additives were used in formulation, the WAT and the size of the peak remained the same as it had in the presence of neat nucleator which would initially indicate that the growth arrestor is not making a significant contribution. However the dramatic improvement in CFPP performance from neat nucleator (-17°C) to the formulation of both additives (-28°C) would suggest that the growth arrestor is making a significant difference to the morphology of the wax crystal as well as the size of such crystals.

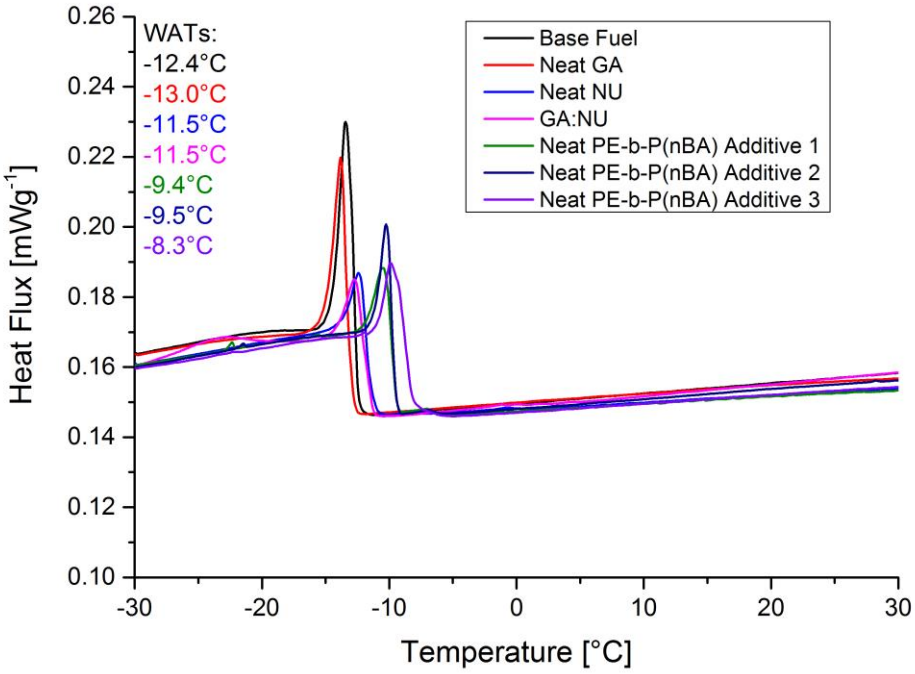

Figure 5.2 - Second cooling curve (5°C/min) from DSC traces of untreated fuel, mass used = 9.62 mg and treated fuel, masses used: GA 13.47 mg, NU 16.61 mg, GA:NU 9.70 mg, PE-*b*-P(*n*-BA) Additive 1 12.14 mg, PE-*b*-P(*n*-BA) Additive 2 15.35 mg, PE-*b*-P(*n*-BA) Additive 3 11.15 mg.

While the neat PE-*b*-P(*n*-BA) additives had a rather limited effect on the CFPP performance, all three copolymers showed promise in the DSC traces. A significant increase in the WAT of the fuel was observed (Figure 5.2), which is consistent with

activity as a nucleating agent. Indeed the increase in WAT was greater in the fuel samples doped with the block copolymers than with the commercial formulation package. This is interesting when we consider the rather inferior performance of the block copolymer additives in CFPP. We also observed a considerable reduction in the size of the crystallisation peak in the DSC traces. The increase in WAT and the reduction in peak size suggest that the block copolymers are affecting both the onset of crystallisation and the size and shape of the crystals wax but the performance in CFPP would indicate that the improvement is fairly modest. The similarity in WAT and peak sizes across the three block copolymer additives would suggest that increasing the molecular weight of the polar block had little impact on the effectiveness of the additive, which is also reflected in their CFPP performance.

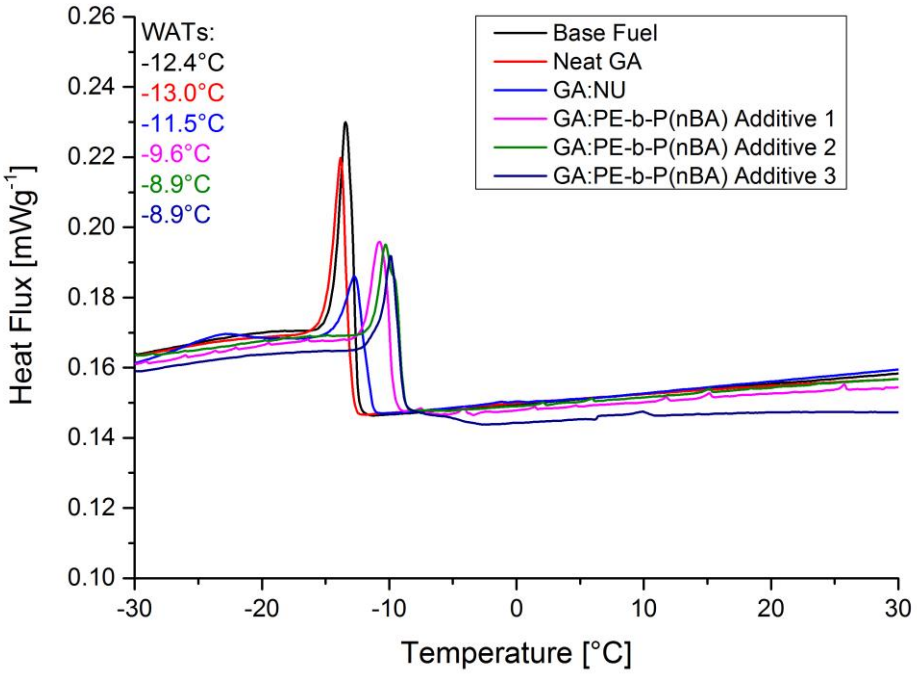

Figure 5.3 - Second cooling curve (5°C/min) from DSC traces of untreated fuel, mass used = 9.62 mg and treated fuel, masses used: GA 13.47 mg, GA:NU 9.70 mg, GA:PE-*b*-P(*n*-BA) Additive 1 11.77 mg, GA:PE-*b*-P(*n*-BA) Additive 2 11.31 mg, GA:PE-*b*-P(*n*-BA) Additive 3 9.3 mg.

Figure 5.3 shows the comparison of the DSC cooling traces for the untreated fuel sample with samples treated with the commercial additives and those treated with the three PE-*b*-P(*n*-BA) copolymers in formulation with the commercial growth arrestor (*i.e.* the block copolymer is being tested as a nucleator). Again we observe a similar increase in the WAT and a reduction in peak size in the samples treated with the block copolymer formulations and there seems to be very little difference in the effect of the additives as the size of the polar block is increased. While the effect of the additives in the DSC traces is evident, the CFPP performance of this formulation was poor. Noting the CFPP of the neat growth arrestor and given the difference in performance between the neat block copolymer and formulation with the growth arrestor and the similarity of the behaviour of the two sets of treated samples in DSC; we attribute this to the substantially reduced concentration of the block copolymer in this formulation (50 ppm) compared to the samples treated with neat copolymer.

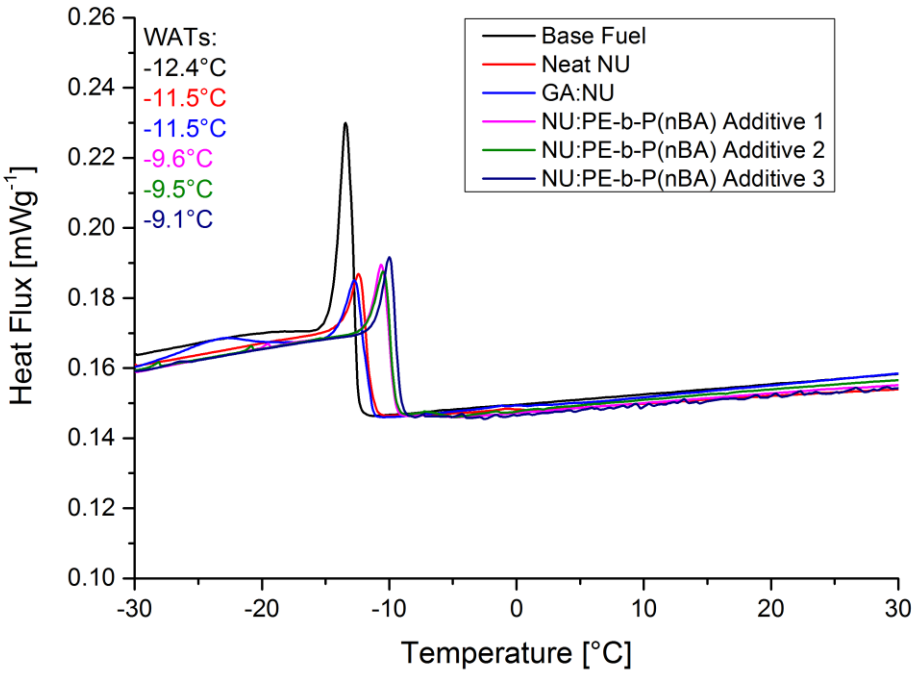

Figure 5.4 - Second cooling curve (5°C/min) from DSC traces of untreated fuel, mass used = 9.62 mg and treated fuel, masses used: NU 16.61 mg, GA:NU 9.70 mg, NU:PE-*b*-P(*n*-BA) Additive 1 15.46 mg, NU:PE-*b*-P(*n*-BA) Additive 2 17.04 mg, NU:PE-*b*-P(*n*-BA) Additive 3 17.09 mg.

When the fuel was treated with the block copolymer additives in formulation with the commercial nucleator (Figure 5.4), the traces were again rather similar to those for the fuel samples treated with neat block copolymer. In this formulation the block copolymer is being tested as a growth arresting agent and as such it is present in higher concentration (200 ppm) than the commercial nucleator (50 ppm), in fact a similar concentration to that in the neat sample (250 ppm). As a result, the fact that the WAT's and crystallisation peak sizes were rather similar to the fuel samples containing neat polymer is not a surprise and this is also reflected in the similarity of the CFPP performance of this formulation with that of the neat polymer samples. Again we see that increasing the size of the polar block had little effect on either the WAT or the peak size.

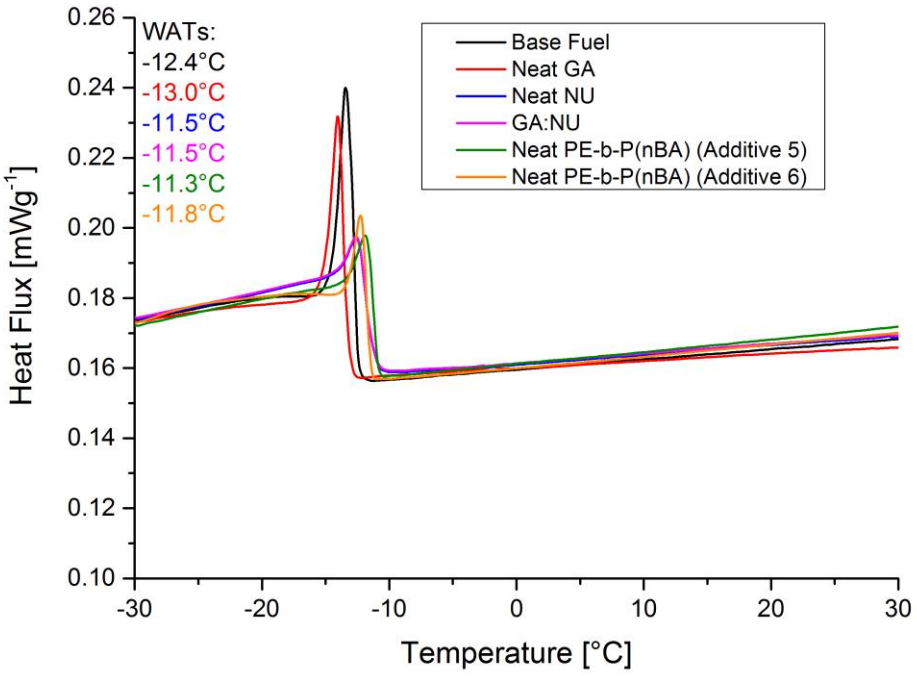

Figure 5.5 - Second cooling curve (5°C/min) from DSC traces of untreated fuel, mass used = 9.62 mg and treated fuel, masses used: GA 13.47 mg, NU 16.61 mg, GA:NU 9.70 mg, PE-*b*-P(*n*-BA) Additive 5 17.40 mg, PE-*b*-P(*n*-BA) Additive 6 10.13 mg.

Figure 5.5 compares the effect of the two PE-*b*-P(*n*-BA) additives prepared under starved feed conditions on the wax crystallisation in fuel with that of the commercial additives and untreated fuel. The increase in WAT for the fuel treated with the neat block copolymers (-11.8°C and -11.3°C) compared to untreated fuel is very similar to that achieved by the commercial nucleator and the commercial formulation (-11.5°C), but significantly lower than in the samples treated with the higher molecular weight batch-prepared block copolymers. The size of the crystallisation peak is also substantially reduced relative to the untreated fuel in both cases. Indeed both of the PE-*b*-P(*n*-BA) additives match the commercial formulation for the effect on the crystallisation peak despite the modest improvement in CFPP with the higher molecular weight additive (*vide supra*).

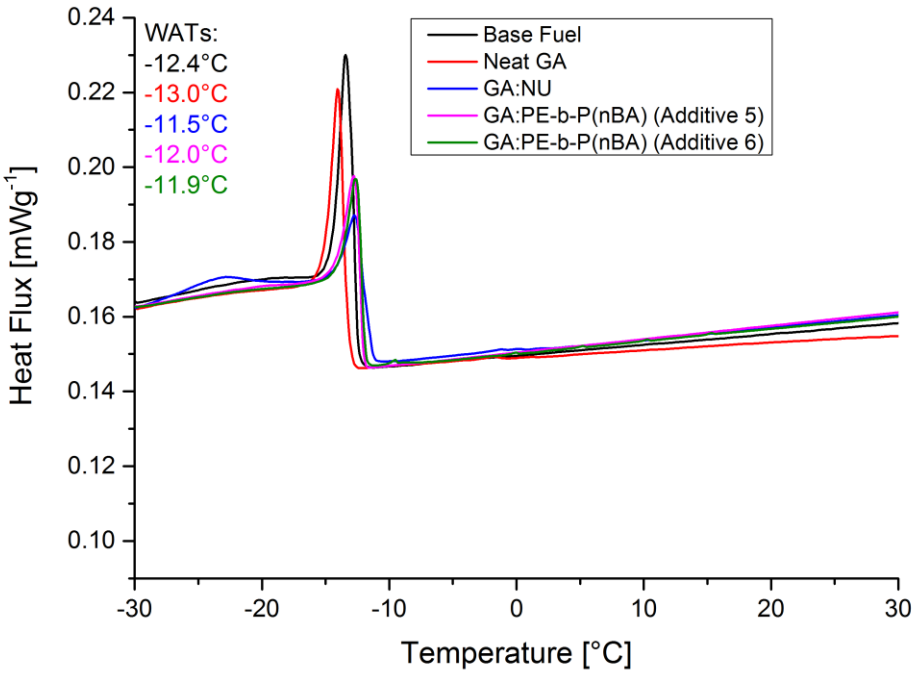

Figure 5.6 - Second cooling curve (5°C/min) from DSC traces of untreated fuel, mass used = 9.62 mg and treated fuel, masses used: GA 13.47 mg, GA:NU 9.70 mg, GA:PE-*b*-P(*n*-BA) Additive 5 13.23 mg, GA:PE-*b*-P(*n*-BA) Additive 6 14.52 mg.

When the DSC cooling traces are plotted for the fuel samples treated with formulations of copolymer and commercial growth arrestor (Figure 5.6), we observe a reduction in the size of the crystallisation peak compared to untreated fuel as expected, consistent with an effect on crystal size and shape. We also observe a slight reduction in the WAT compared to the samples treated with neat copolymer, which is not a surprise since the block copolymer additives are present in much smaller concentration (50 ppm *vs* 250 ppm) in this formulation.

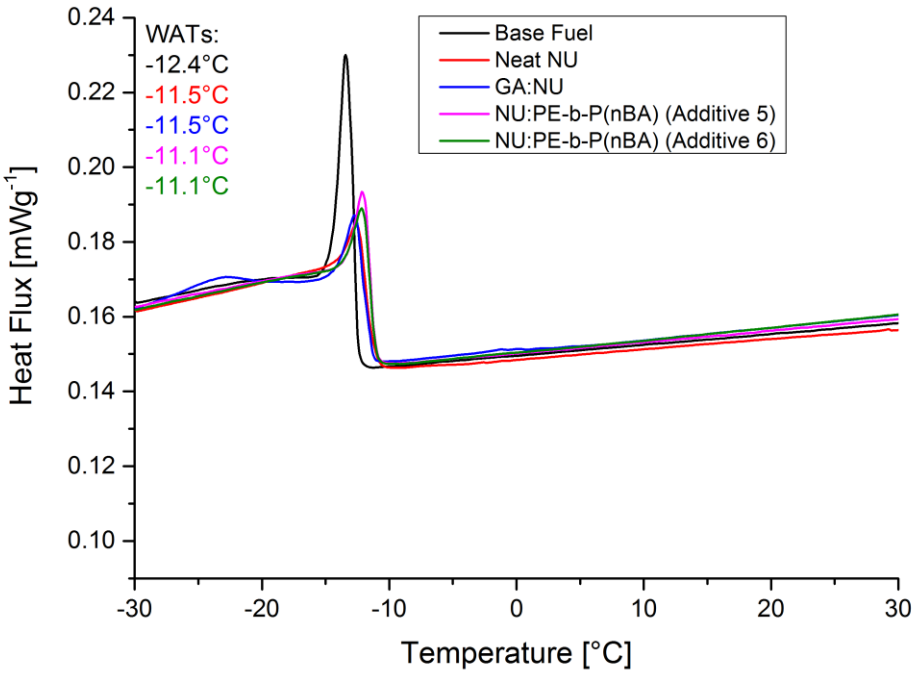

Figure 5.7 - Second cooling curve (5°C/min) from DSC traces of untreated fuel, mass used = 9.62 mg and treated fuel, masses used: NU 16.61 mg, GA:NU 9.70 mg, NU:PE-*b*-P(*n*-BA) Additive 5 14.91 mg, NU:PE-*b*-P(*n*-BA) Additive 6 8.09 mg.

The plots for the DSC cooling traces of the fuel treated using formulations of the copolymers with the commercial nucleator (Figure 5.7) show a substantial increase in the WAT and reduction in the size of the wax crystals in the treated samples relative to the untreated sample. We also observe very little difference in WAT and peak size between the treated samples. This suggests that the commercial nucleator and the copolymer additives are acting in a similar way which indicates that the PE-*b*-P(*n*-BA) additives are also acting as nucleators.

5.3.2 PE-*b*-P(VAc) additives

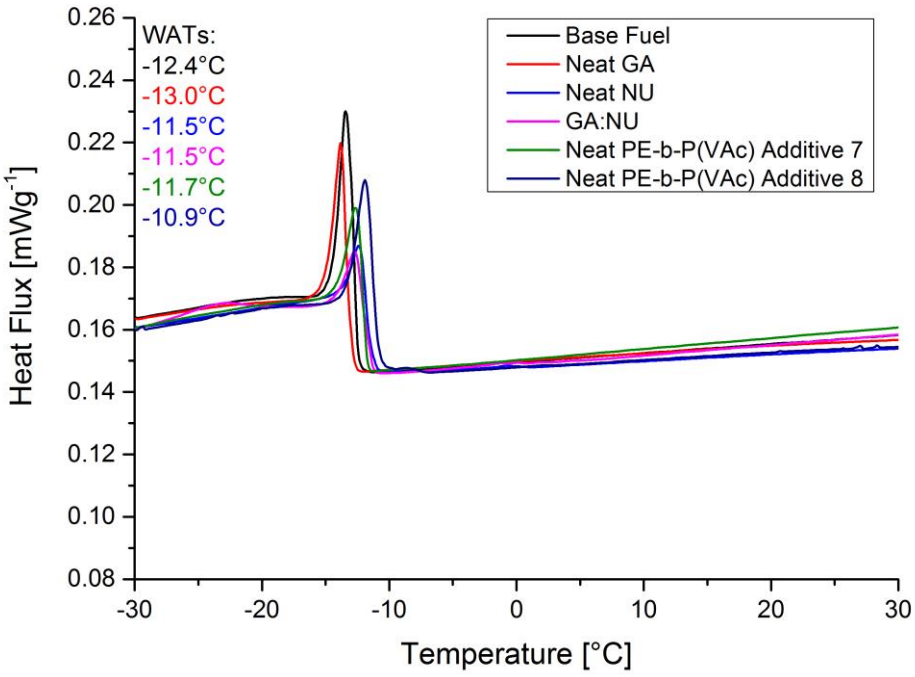

Figure 5.8 - Second cooling curve (5°C/min) from DSC traces of untreated fuel, mass used = 9.62 mg and treated fuel, masses used: GA 13.47 mg, NU 16.61 mg, GA:NU 9.70 mg, PE-*b*-P(VAc) Additive 7 10.13 mg, PE-*b*-P(VAc) Additive 8 17.40 mg.

Figure 5.8 shows the DSC cooling traces comparing the effect of the two neat PE-*b*-P(VAc) additives wax crystallisation in fuel with that of the commercial additives and untreated fuel. An increase in the WAT of the fuel is observed for both block copolymers, similar in fact to the WAT in the presence of the neat nucleator, which again is consistent with the additives acting as nucleating agents. Again we also observe a significant reduction in the size of the crystallisation peak, despite the poor CFPP performance.

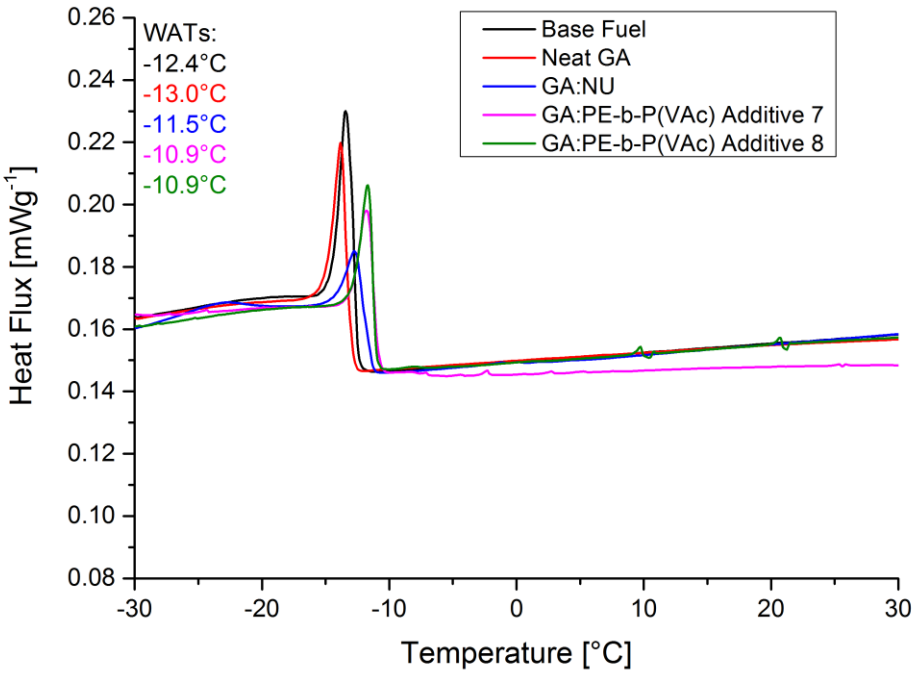

Figure 5.9 - Second cooling curve (5°C/min) from DSC traces of untreated fuel, mass used = 9.62 mg and treated fuel, masses used: GA 13.47 mg, GA:NU 9.70 mg, GA:PE-*b*-P(VAc) Additive 7 14.52 mg, GA:PE-*b*-P(VAc) Additive 8 13.23 mg.

When the additives are analysed by DSC in formulation with the growth arrestor, an increase in WAT similar to that in the presence of the commercial nucleator is again observed and the reduction in the size of the crystallisation peak is also similar. The somewhat similar appearance of the DSC cooling curves for the samples containing the two block copolymers is interesting given the far superior CFPP performance of the higher molecular weight additive (Additive 8) in this formulation. The vast improvement in CFPP performance of additive 8 in combination with the growth arrestor supports our proposal that these block copolymers may be less effective at controlling the size of the crystals that form.

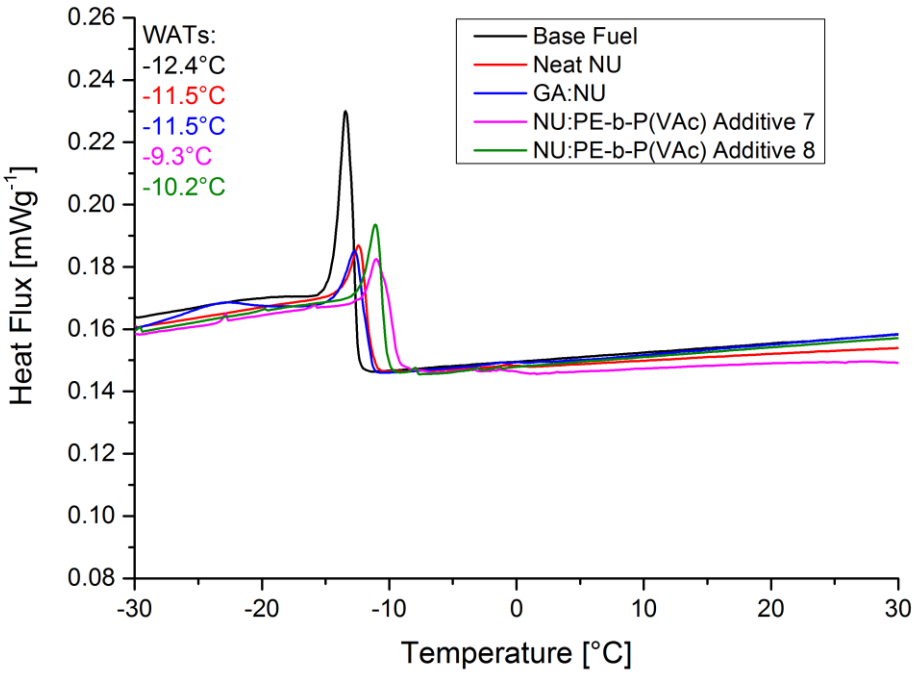

Figure 5.10 - Second cooling curve (5°C/min) from DSC traces of untreated fuel, mass used = 9.62 mg and treated fuel, masses used: NU 16.61 mg, GA:NU 9.70 mg, NU:PE-b-P(VAc) Additive 7 8.09 mg, NU:PE-b-P(VAc) Additive 8 14.91 mg.

Plotting the DSC cooling curves for the fuel samples treated with the block copolymer additives in formulation with the nucleator shows a substantial increase in WAT as well as a considerable reduction in the size of the crystallisation peak. We observed earlier with the PE-*b*-P(*n*-BA) additives that the DSC for the neat polymer samples and the polymer:nucleator formulation samples were somewhat similar, likely as a result of there being similar concentrations of block copolymer additive. This was also reflected in the similar CFPP performance of the two sets of samples. In the case of the PE-*b*-P(VAc) additives however, there was a stark contrast in the CFPP performance and the DSC curves for the neat polymer and polymer:nucleator formulations involving the PE-*b*-P(VAc). Given this difference, and noting that the DSC of the neat polymer samples also showed an increase in WAT, we attributed the improvement in CFPP performance and the observations in the DSC traces for the polymer:nucleator formulations was

mainly due to the presence of the commercial nucleator in this case despite the fact that it was present in far lower concentration than the block copolymer.

5.3.3 PE-*b*-P(V2EH) additives

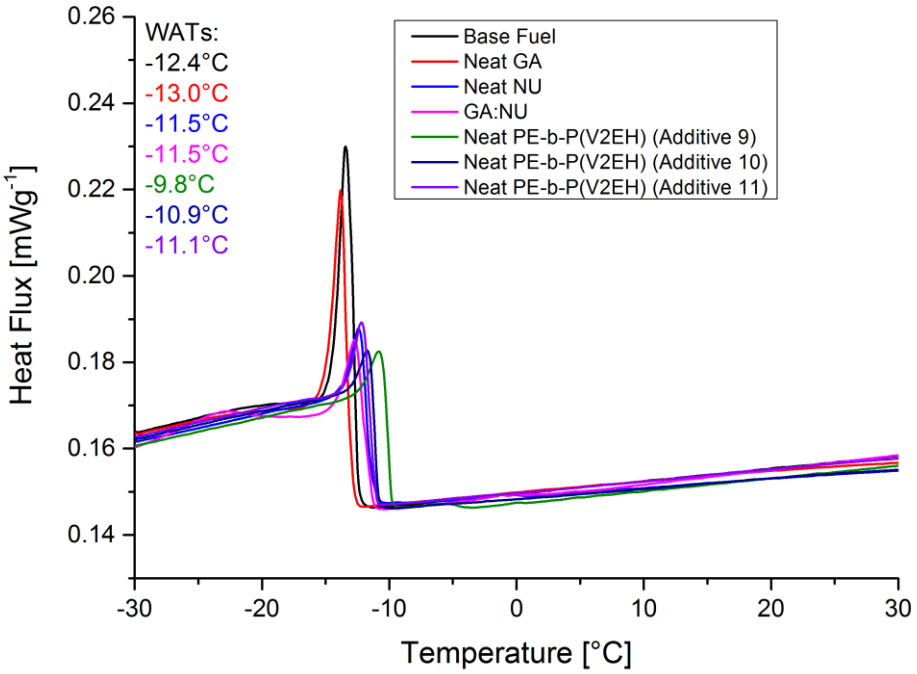

Figure 5.11 - Second cooling curve (5°C/min) from DSC traces of untreated fuel, mass used = 9.62 mg and treated fuel, masses used: GA 13.47 mg, NU 16.61 mg, GA:NU 9.70 mg, PE-*b*-P(V2EH) Additive 9 11.72 mg, PE-*b*-P(V2EH) Additive 10 14.87 mg, PE-*b*-P(V2EH) Additive 11 16.94 mg.

The cooling curves in Figure 5.11 show that the all three of the PE-*b*-P(V2EH) additives had a substantial effect on both the WAT and the size of the crystallisation peak. The WAT of the fuel sample containing the additive with the larger P(V2EH) blocks (additives 10 and 11) increased slightly to -11.1°C and -10.9°C respectively which is comparable with that of the commercial additive at -11.5°C. The additive with the smaller P(V2EH) block (additive 9) increased the WAT significantly beyond the commercial additives to -9.8°C. Again the advancing of the WAT is consistent with activity as nucleating agents and the nucleating effect of the additive was apparently

enhanced as the polar block length was reduced. The size of the crystallisation peak was also improved as the size of the P(V2EH) block was reduced and in this case the peaks for the samples containing additives 9 and 10 were smaller than that of the commercial formulation. This suggests that the additives are effective at controlling the size and morphology of the crystals formed through nucleation as evidenced by the CFPP performance of the neat additives.

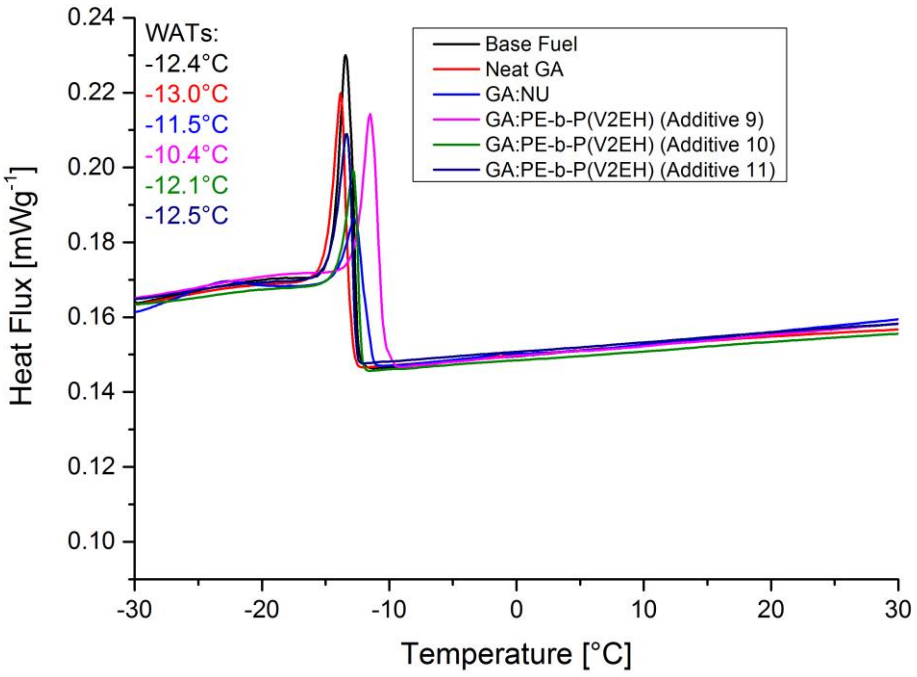

Figure 5.12 - Second cooling curve (5°C/min) from DSC traces of untreated fuel, mass used = 9.62 mg and treated fuel, masses used: GA 13.47 mg, GA:NU 9.70 mg, GA:PE-*b*-P(V2EH) Additive 9 12.26 mg, GA:PE-*b*-P(V2EH) Additive 10 13.33 mg, GA:PE-*b*-P(V2EH) Additive 11 13.99 mg.

Figure 5.12 shows the DSC cooling curves for the fuel samples treated with formulations of PE-*b*-P(V2EH) copolymers and the commercial growth arrestor. Again the WAT increases significantly in the presence of the block copolymer additives and the reduction in the size of the crystallisation peaks suggests the additives are having an effect on the size and shape of the crystals, though not as much as with the neat polymer

samples, which again we can attribute to the presence of a significant concentration of growth arrestor based on the data from the neat polymer samples. We note also that the WAT's are slightly lower than for the neat polymer samples, which can be attributed firstly to the presence of a lower concentration of block copolymer additive in this formulation and secondly to the presence of the growth arrestor which lowered the WAT when tested neat. The importance of the growth arrestor is again in evidence in this package given the difference between the CFPP's of the neat additives and this formultaion.

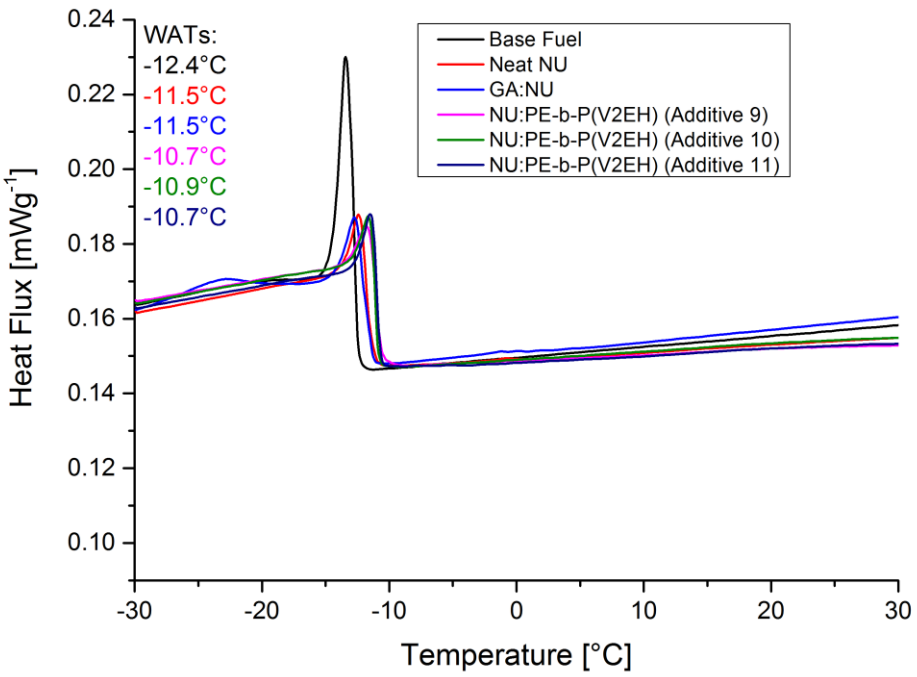

Figure 5.13 - Second cooling curve (5°C/min) from DSC traces of untreated fuel, mass used = 9.62 mg and treated fuel, masses used: NU 16.61 mg, GA:NU 9.70 mg, NU:PE-*b*-P(V2EH) Additive 9 9.35 mg, NU:PE-*b*-P(V2EH) Additive 10 11.29 mg, NU:PE-*b*-P(V2EH) Additive 11 10.80 mg.

When the DSC cooling curves for the fuel samples treated with the PE-*b*-P(V2EH) copolymers in formulation with the nucleator are plotted (Figure 5.13), the WAT's and the reduction in crystallisation peak sizes were found to be rather similar to the

commercial formulation, as well as the neat polymer samples, though a further reduction in the peak size was noted for the sample containing the smallest PE-*b*-P(V2EH) additive. This data combined with the CFPP results indicate again that the commercial nucleator additive and the block copolymer additives are both working in similar ways, thus further demonstrating the advantage of using a nucleator and growth arrestor in combination.

5.3.4 PE-*b*-P(C14MA) additives

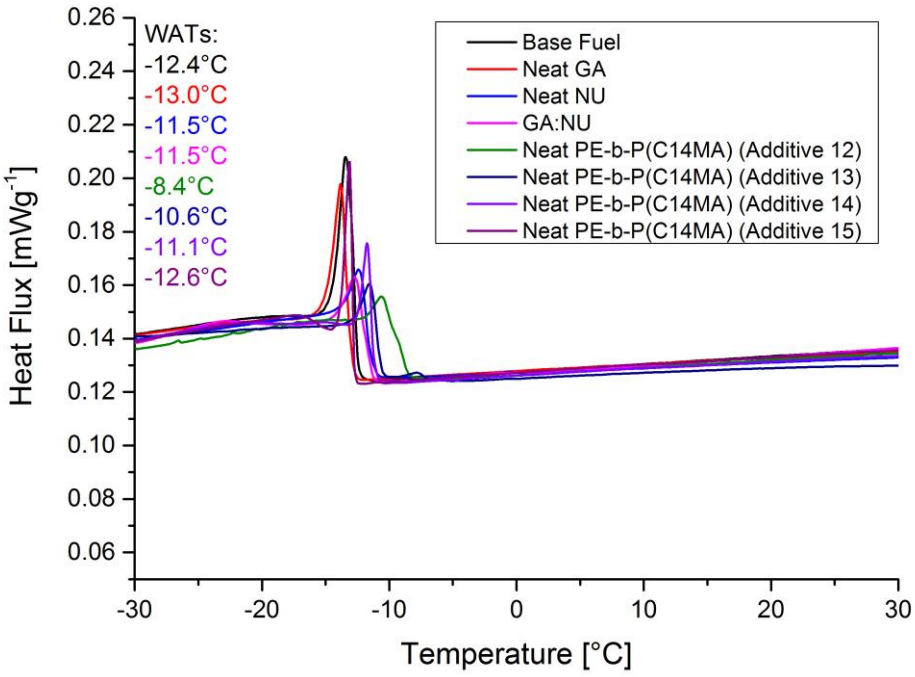

Figure 5.14 - Second cooling curve (5°C/min) from DSC traces of untreated fuel, mass used = 9.62 mg and treated fuel, masses used: GA 13.47 mg, NU 16.61 mg, GA:NU 9.70 mg, PE-*b*-P(C14MA) Additive 12 7.55 mg, PE-*b*-P(C14MA) Additive 13 12.97 mg, PE-*b*-P(C14MA) Additive 14 11.34 mg; PE-*b*-P(C14MA) Additive 15 10.02 mg.

Again the plots of the DSC cooling curves show that treating the fuel with the neat PE-*b*-P(C14MA) additives has a dramatic effect on both the WAT and the size of the crystallisation peak (Figure 5.14), peaking at -8.4°C with additive 12. We also observe

a similar trend towards the lower molecular weight copolymers which is consistent with the CFPP performance data. When compared to fuel treated with the commercial formulation, additives 12-14 significantly advanced the WAT, consistent with activity as nucleators, and reduced the size of the crystallisation peak. Indeed additives 12 and 13 advanced the WAT and reduced the size of the crystallisation peak further than the commercial formulation.

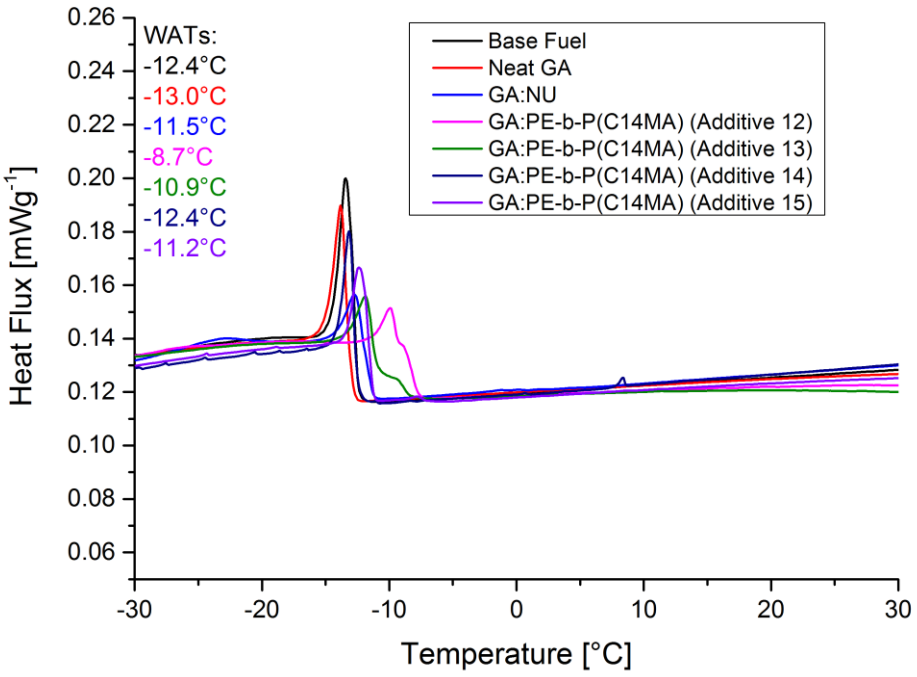

Figure 5.15 - Second cooling curve (5°C/min) from DSC traces of untreated fuel, mass used = 9.62 mg and treated fuel, masses used: GA 13.47 mg, NU 16.61 mg, GA:NU 9.70 mg, GA:PE-*b*-P(C14MA) Additive 12 8.15 mg, GA:PE-*b*-P(C14MA) Additive 13 13.40 mg, GA:PE-*b*-P(C14MA) Additive 14 9.89 mg; GA:PE-*b*-P(C14MA) Additive 15 14.15 mg.

When these copolymer additives were studied in formulation with the growth arrestor (Figure 5.15) a similar trend in WAT was observed; along with similar reductions in crystallisation peak sizes. In the case of the higher molecular weight additives, the formulation with the growth arrestor actually reduced the size of the crystallisation peak further despite the much smaller concentration of block copolymer. This effect is

reflected in the dramatic improvement in CFPP performance of these higher molecular weight additives with the growth arrestor compared to the neat additives (*vide supra*). Indeed, the CFPP performance of the higher molecular weight additives was similar to the lower molecular weight materials in the same formulation; whereas with the other materials discussed here there had been a distinct trend favouring the lower molecular weight additives.

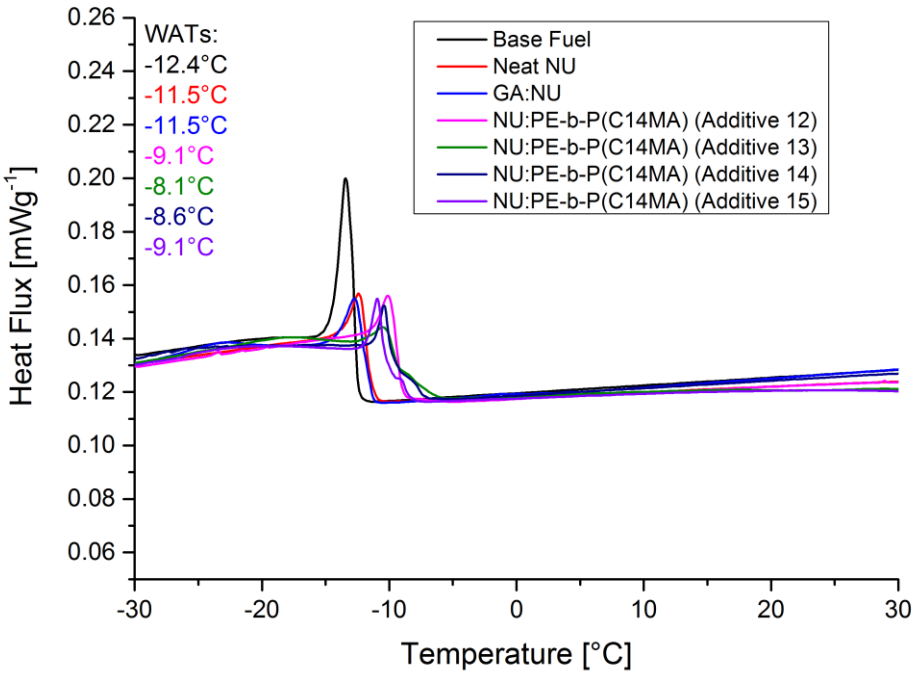

Figure 5.16 - Second cooling curve (5°C/min) from DSC traces of untreated fuel, mass used = 9.62 mg and treated fuel, masses used: GA 13.47 mg, NU 16.61 mg, GA:NU 9.70 mg, NU:PE-*b*-P(C14MA) Additive 12 11.85 mg, NU:PE-*b*-P(C14MA) Additive 13 11.23 mg, NU:PE-*b*-P(C14MA) Additive 14 7.26 mg; NU:PE-*b*-P(C14MA) Additive 15 16.05 mg.

The DSC cooling curves for the PE-*b*-P(C14MA) additives in formulation with the growth arrestor (Figure 5.16) are similar to those of the neat additives, again showing the significantly advancing WATs and the far smaller crystallisation peaks relative to the untreated fuel. As evidenced by the CFPP performance of these additives, they are unusual in that they seem to have a positive effect on the crystallisation of the wax

regardless of the formulation. As can be seen in Figure 5.15, even when the components of the formulation are expected to be behaving in the same way, there is still a significant observable effect of the block copolymer additives on the WAT when compared to both the neat nucleator and the formulation with the growth arrestor. The effect on the DSC cooling curves and the CFPP performance across the formulations suggest that these materials could also be useful as so-called single-shot additives *i.e.* they are able to behave both as nucleating agents and as growth arrestors to control the size and morphology of the wax crystals.

5.4 Conclusions

PE diblock copolymers synthesised using a range of polar monomers from the macromonomer PE-*i*-DIB as discussed in Chapters 3 and 4 were tested for their wax crystal modification properties in one type of diesel. The performance of the block copolymers was tested as a neat additive and in formulations with a commercial growth arrestor and a commercial nucleator in the CFPP test and the crystallisation events investigated by DSC. With the PE block molecular weight kept constant, varying the molecular weight of the polar block was found to have a dramatic effect on the CFPP performance, with materials containing smaller polar blocks generally performing considerably better than those containing larger blocks. The exception was the PE-*b*-P(VAc) materials where the material containing the larger polar block was more effective; we attribute this deviation from the rest of the data to a difference in solubility characteristics of the two additives in the formulation.

In general, the best performance in CFPP came when the copolymers were tested in formulation with the commercial growth arrestor, which is consistent with the PE block copolymers acting as nucleating agents. This is also supported by the DSC data

conducted on the neat polymer samples which show that the WAT in samples containing block copolymer were higher than for untreated fuel, which is what would be expected for a nucleating agent and is consistent with the activity of the commercial nucleating agent. Indeed some of the materials advanced the WAT to a greater extent even than the commercial nucleator and the commercial formulation and, in some more specific cases, *e.g.* PE-*b*-P(V2EH) and PE-*b*-P(C14MA), the reduction in the size of the crystallisation peak was greater than the commercial additives. The PE-*b*-P(V2EH) and PE-*b*-P(C14MA) materials were the best of the block copolymer additives that were tested; with the former yielding a best CFPP result of -23°C in formulation with the growth arrestor (Additive 9) and the latter a best result of -25°C as a neat additive (Additive 13). While additive 13 performed well across all formulations in this fuel, the fact that the best performance came as a neat polymer is particularly interesting because it indicates that the material is most productively used as a single shot additive *i.e.* it has both nucleating and growth arresting properties.

The results from this chapter show that even though none of the materials tested improved the performance of this particular batch of diesel further than the formulation of the two commercial additives; these block copolymers have significant potential as wax crystal modifiers in middle-distillate fuels. The potential for further work is also extremely broad, with further testing of the materials with different co-additives, in different types of fuel and at different treat rates being just some of the options available for the range discussed here alone. There is also potential for altering the size and nature of the olefin block as well as an almost endless range of polar monomers to utilise in the remarkably versatile copolymer synthesis.

5.5 References

1. Ribeiro, N. M.; Pinto, A. C.; Quintella, C. M.; da Rocha, G. O.; Teixeira, L. S. G.; Guarieiro, L. L. N.; do Carmo Rangel, M.; Veloso, M. C. C.; Rezende, M. J. C.; Serpa da Cruz, R.; de Oliveira, A. M.; Torres, E. A.; de Andrade, J. B., The Role of Additives for Diesel and Diesel Blended (Ethanol or Biodiesel) Fuels: A Review. *Energy & Fuels* **2007,** *21* (4), 2433-2445.
2. Wei, B., Recent advances on mitigating wax problem using polymeric wax crystal modifier. *Journal of Petroleum Exploration and Production Technology* **2015,** *5* (4), 391-401.
3. Soni, H. P.; Kiranbala; Agrawal, K. S.; Nagar, A.; Bharambe, D. P., Designing maleic anhydride-α-olifin copolymeric combs as wax crystal growth nucleators. *Fuel Process. Technol.* **2010,** *91* (9), 997-1004.
4. Ashbaugh, H. S.; Radulescu, A.; Prud'homme, R. K.; Schwahn, D.; Richter, D.; Fetters, L. J., Interaction of Paraffin Wax Gels with Random Crystalline/Amorphous Hydrocarbon Copolymers. *Macromolecules* **2002,** *35* (18), 7044-7053.
5. Ashbaugh, H. S.; Guo, X.; Schwahn, D.; Prud'homme, R. K.; Richter, D.; Fetters, L. J., Interaction of Paraffin Wax Gels with Ethylene/Vinyl Acetate Co-polymers. *Energy & Fuels* **2005,** *19* (1), 138-144.
6. Zhang, J.; Wu, C.; Li, W.; Wang, Y.; Han, Z., Study on performance mechanism of pour point depressants with differential scanning calorimeter and X-ray diffraction methods☆. *Fuel* **2003,** *82* (11), 1419-1426.
7. Nassar, A. M.; Ahmed, N. S., The Behavior of α-Olefins Butyl Acrylate Copolymers as Viscosity Index Improvers and Pour Point Depressants for Lube Oil. *Int. J. Polymer. Mat. Polymer. Biomat.* **2006,** *55* (11), 947-955.
8. Soldi, R. A.; Oliveira, A. R. S.; Barbosa, R. V.; César-Oliveira, M. A. F., Polymethacrylates: Pour point depressants in diesel oil. *Eur. Polym. J.* **2007,** *43* (8), 3671-3678.
9. Farag, R. K., Poly(Cinnamoyloxy Ethyl Methacrylate-Co-Octadecyl Acrylate) as Flow Improver for Egyptian Waxy Crude Oils. *Int. J. Polymer. Mat. Polymer. Biomat.* **2008,** *57* (3), 189-202.
10. A.K Chatterjee, P. K. C., P. S. N. Murthy, G. C. Joshi, A synthetic look at designing a flow improver additive in waxy indian diesel fuels. *Macromolec. Rep.* **1996,** *A33*, 23-31.
11. Castro, L. V.; Vazquez, F., Copolymers as Flow Improvers for Mexican Crude Oils. *Energy & Fuels* **2008,** *22* (6), 4006-4011.
12. Khidr, T. T., Synthesis and Evaluation of Copolymers as Pour-point Depressants. *Pet. Sci. Technol.* **2007,** *25* (5), 671-681.
13. R. A. Vora, D. P. B., Polymeric Flow Improvers. *Indian. J. Technol.* **1993,** *31*.
14. Richter, D.; Schneiders, D.; Monkenbusch, M.; Willner, L.; Fetters, L. J.; Huang, J. S.; Lin, M.; Mortensen, K.; Farago, B., Polymer Aggregates with Crystalline Cores: The System Polyethylene−Poly(ethylenepropylene). *Macromolecules* **1997,** *30* (4), 1053-1068.
15. Leube, W.; Monkenbusch, M.; Schneiders, D.; Richter, D.; Adamson, D.; Fetters, L.; Dounis, P.; Lovegrove, R., Wax-Crystal Modification for Fuel Oils by Self-Aggregating Partially Crystallizable Hydrocarbon Block Copolymers. *Energy & Fuels* **2000,** *14* (2), 419-430.
16. Radulescu, A.; Schwahn, D.; Stellbrink, J.; Kentzinger, E.; Heiderich, M.; Richter, D.; Fetters, L. J., Wax Crystallization from Solution in Hierarchical

Morphology Templated by Random Poly(ethylene-co-butene) Self-assemblies. *Macromolecules* **2006,** *39* (18), 6142-6151.
17. Holder, G. A.; Winkler, J., Crystal-Growth Poisoning of n-Paraffin Wax By Polymeric Additives and its Relevance to Polymer Crystallization Mechanisms. *Nature* **1965,** *207* (4998), 719-721.
18. Coutinho, J. A. P.; Dauphin, C.; Daridon, J. L., Measurements and modelling of wax formation in diesel fuels. *Fuel* **2000,** *79* (6), 607-616.
19. El-Gamal, I. M.; Khidr, T. T.; Ghuiba, F. M., Nitrogen-based copolymers as wax dispersants for paraffinic gas oils. *Fuel* **1998,** *77* (5), 375-385.
20. Qian, J. W.; Wang, X.; Qi, G. R.; Wu, C., Inter- and Intrachain Associations of an Ethylene−Vinyl Acetate Random Copolymer in Dilute 1,2-Dichloroethane Solutions. *Macromolecules* **1997,** *30* (11), 3283-3287.
21. El-Gamal, I. M.; Al-Sabbagh, A. M., Polymeric additives for improving the flow properties of waxy distillate fuels and crudes. *Fuel* **1996,** *75* (6), 743-750.
22. Schwahn, D.; Richter, D.; Wright, P. J.; Symon, C.; Fetters, L. J.; Lin, M., Self-Assembling Behavior in Decane Solution of Potential Wax Crystal Nucleators Based on Poly(co-olefins). *Macromolecules* **2002,** *35* (3), 861-870.
23. Ashbaugh, H. S.; Fetters, L. J.; Adamson, D. H.; Prud'homme, R. K., Flow improvement of waxy oils mediated by self-aggregating partially crystallizable diblock copolymers. *J. Rheol.* **2002,** *46* (4), 763-776.
24. Owen, K., *Gasoline and Diesel Fuel Additives*. Wiley: 1989.
25. K. Lewtas, R. D. T., D. H. M. Beiny, J. W. Mullin, In *Advances in Industrial Crystallization*, J. Gartside, R. J. D., A. G. Jones, Ed. Butterworth-Heinmann: London, 1991.
26. Standard Test Method for Cold Filter Plugging Point of Diesel and Heating Fuels. In *ASTM Standard D6371*, West Conshohocken, PA: ASTM International, 2005.

Chapter 6: Experimental

6.1 General Considerations

Where it was necessary the work detailed below was carried out under an inert atmosphere of argon, using standard Schlenk techniques. All glassware, cannulae and syringes were oven dried at 125°C for at least 24 h prior to use. Toluene was dried by reflux over sodium metal for three days prior to distillation, then degassed using three freeze-pump-thaw cycles before use. 1,3-diisopropenylbenzene (97%, Sigma Aldrich/97%, TCI Europe), (*R*)-limonene (97%, Sigma Aldrich), (*S*)-limonene (96%, Sigma Aldrich), 5-vinyl-2-norbornene (95% containing 80-150 ppm 2,6-di-*tert*-butyl-4-methylphenol (BHT) as inhibitor, Sigma Aldrich) and 5-ethylidene-2-norbornene (99% containing 100-200 ppm BHT as inhibitor, Sigma Aldrich) were passed through a column of alumina, transferred into glass ampoules and dried over 4Å molecular sieves. The ampoules were degassed by three freeze-pump-thaw cycles and stored under argon before use. Methylaluminoxane (AXION CA 310) was purchased from Chemtura as a 10 wt% solution in toluene, which was transferred to a graduated glass ampoule by cannula and used without further manipulation. Research grade ethylene (BOC) was passed through a drying train containing drying train consisting of BASF R3-11G deoxygenating agent and 3 Å molecular sieves as it was transferred *in situ* from the cylinder to the burette system as shown in Figure 6.1. High purity hydrogen (99.995%, BOC) was used as received. *n*-Butyl acrylate (≥99% contains 10-60 ppm monomethyl ether hydroquinone as inhibitor, Sigma Aldrich), vinyl acetate (99+% contains 3-20 ppm hydroquinone as inhibitor, Acros Organics), methyl methacrylate (99+% contains ≤30 ppm monoethyl hydroquinone as inhibitor, Acros Organics) and styrene (≥99% contains 4-*tert*-butyl catechol as inhibitor, Sigma Aldrich) were passed through an alumina

column to remove the inhibitor before use. Vinyl-2-ethyl hexanoate (97%, Infineum UK Ltd) and myristyl methacrylate (96%, Infineum UK Ltd) were used as received. Thermal initiators Dibenzoyl peroxide (75% remainder water, Sigma Aldrich) and di-*tert*-butyl peroxide (98%, Sigma Aldrich) were used as received. Solvents and anti-solvents used in the free-radical polymerisation procedures: Toluene (reagent grade, Sigma Aldrich), methanol (reagent grade, Fisher Scientific), ethanol (reagent grade, Fisher Scientific) and acetone (reagent grade, Fisher Scientific) were all used as received. 1,1,2,2-Tetrachloroethane-d^2 (99.6%, Cambridge Isotope Laboratories Inc.) toluene-d^8 (99.6%, Cambridge Isotope Laboratories Inc.) and chloroform-*d* (99.8%, Sigma Aldrich) were used as received. Zirconocene dichloride (≥98%, Sigma Aldrich) was stored in an MBraun glovebox at <5 ppm O_2. Dry toluene (25 ml) was transferred into a 25 ml graduated glass ampoule by cannula, which was then degassed by three freeze-pump-thaw cycles and sealed under vacuum. Zirconocene dichloride was weighed out, added to the toluene and the resulting solution stored in an MBraun glovebox at <5 ppm O_2.

^{1}H NMR spectra of the PE-containing samples were recorded on a Bruker AV-400 spectrometer at 100°C in 1,1,2,2-tetrachloroethane-d^2 (PE-*i*-DIB and PE-*i*-LIM-based samples) or toluene-d^8 (P(E-*co*-VNB) and P(E-*co*-ENB)-based samples). Residual protio-solvent was used as an internal reference.[1, 2] ^{13}C NMR spectra of PE-containing samples were recorded on a Bruker DRX-500 and DRX-600 spectrometers at 125 MHz and 150 MHz respectively (specified where necessary) in 1,1,2,2-tetrachloroethane-d^2 (PE-*i*-DIB and PE-*i*-LIM-based samples) or toluene-d^8 (P(E-*co*-VNB) and P(E-*co*-ENB)-based samples) at 100°C (>10,000 scans, 4 s relaxation time) ensuring that the sample was fully dissolved. ^{1}H NMR spectra of samples of polar homopolymers (P(*n*-BA), P(VAc), P(V2EH), P(MMA), P(C14MA) and PS) were recorded on a Bruker DPX-400 spectrometer at 25°C in chloroform-*d* and again, residual protio-solvent was

used as the internal reference. ^{13}C NMR spectra of polar homopolymer samples were recorded on a Bruker DPX-400 spectrometer at 100 MHz in chloroform-*d*. Routine NMR assignments (including polymer samples) were confirmed by ^{1}H-^{1}H (COSY), ^{13}C-^{1}H (HMQC) and ^{13}C-^{1}H (HMBC) correlation experiments where necessary.

High temperature GPC was performed on PE-containing polymer samples in 1,2,4-trichlorobenzene (≥99%, Sigma Aldrich) containing 250 ppm BHT (≥99%, Sigma Aldrich) antioxidant at 160°C at a flow rate of 1 ml/min on an Agilent PL220 equipped with differential refractive index (DRI), viscometry (VS) and dual angle light scatter (LS 90 + 15) detectors. The system was fitted with 2 x PLgel Mixed D columns (300 x 7.5 mm) and a PLgel 5 μm guard column. Polystyrene standards (Agilent EasyVials) were used to create a third order calibration. Analyte samples were filtered through a stainless steel frit with 10 μm pore size before injection. Respectively, experimental molar mass and dispersity ($Đ$) values of synthesized polymers were determined by universal calibration using Agilent GPC/SEC software. Universal calibration was used for the PE-based macromonomers and block copolymers in order to remove the chemical dependence of the calibration on the calibrants. The hydrodynamic volume of the copolymer samples will be different to the PS standards used to calibrate the system; consequently molecular weight data obtained for these samples with a conventional calibration will have substantial discrepancies from the true molecular weight. We therefore utilised a universal calibration which uses the concentration response from the RI detector and the intrinsic viscosity calculated from the response of the viscometer to generate a calibration curve of log (intrinsic viscosity × molecular weight) vs retention time (effectively log (size) vs retention time). As demonstrated by the work of Benoit *et al*,[3] the system separates by the size of samples in solution so the same calibration curve is generated regardless of the chemistry of the standards used to generate it. When

samples were analysed, the concentration and specific viscosity were determined from the response from the concentration detector and viscometer respectively. The specific viscosity was then converted to intrinsic viscosity which, along with the retention time, was compared to the calibration curve to generate the molecular weight of the sample. A PS standard was run alongside the copolymer samples and the peak molecular weight (M_p) of the standard was never more than 10% away from the stated molecular weight and, in the majority of cases, was no more than 5% away.

Room temperature GPC was carried out on soluble homopolymer samples in chloroform with 2 % TEA (triethylamine) additive at 30°C at a flow rate of 1 ml/min on an Agilent 390-LC MDS instrument equipped with differential refractive index (DRI), viscometry (VS), dual angle light scatter (LS) and two wavelength UV detectors. The system was equipped with 2 x PLgel Mixed C columns (300 x 7.5 mm) that uses 10 μm and 5 μm PLgel guard columns. Poly(methyl methacrylate) and poly(styrene) standards (Agilent EasyVials) were used for calibration depending on the analyte (specified where appropriate). Analyte samples were filtered through a GVHP membrane with 0.22 μm pore size before injection. Experimental molar mass and dispersity ($Đ$) values of synthesized polymers were determined by conventional calibration using Agilent GPC/SEC software.

Particle size distributions were measure by dynamic light scattering (DLS) using a Malvern Zetasizer Nano ZS. Samples for DLS measurements were prepared by weighing 10 mg of each polymer into a vial and making up to concentrations of 1 mg/ml with THF, which had been filtered using a GVHP membrane with 0.22 μm pore size to remove dust. To aid dissolution, the solutions were stirred using a vortex mixer for 5 min. Quartz cuvettes with two clear faces were filled to 1 cm depth with solutions for

ideal temperature control and two min temperature stabilisation time at 25°C was allowed. Each sample underwent three measurements of 15 scans each and the average of each set of measurements was reported.

Thermal analyses on copolymers were carried out on a Mettler Toledo DSC-400 system. Under an atmosphere of dinitrogen, the samples were heated to 160°C at 10°C/min, then cooled to -160°C at 10°C/min for recrystallization. This cycle was repeated three times in total and after the first melt to erase thermal history, all subsequent thermograms were identical. The thermal data (T_m, T_c, T_g) reported were taken from the third heating and cooling cycles. Thermal analyses on doped diesel samples were also carried out under dinitrogen. The samples were heated to 60°C at 5°C/min, held at 60°C for two min, then cooled to -30°C at 5°C/min and held at -30°C for two min. This cycle was repeated twice in total and after the first heat to erase thermal history, all subsequent thermograms were identical. The thermal data (wax appearance temperature, WAT) reported was taken from the second cooling cycle.

Cold filter plugging points (CFPP) of diesel samples were determined using an ISL CFPP 5GS instrument. Diesel was filtered through 30 μm filter paper and 50 g samples were prepared by doping with known concentrations of 10% w/v Solvesso® 150 cutbacks of copolymer additive. CFPP experiments were carried out according to the standard procedure outlined in ASTM D6371.[3, 4]

Software used in the project included CambridgeSoft ChemOffice, Endnote X7, MestReNova, Microsoft Office 2013, Origin Pro 9.1, STARe thermal evaluation software and Agilent GPC/SEC software.

6.1.1 Table values and equations

The values tabulated in Chapters 2-5 were calculated as follows:

$$M_n = \frac{\sum M_i N_i}{\sum N_i} \qquad M_w = \frac{\sum M_i^2 N_i}{\sum M_i\ N_i} \qquad Đ = \frac{M_w}{M_n}$$

Where possible, monomer conversion was determined gravimetrically, or otherwise by ^{1}H NMR spectroscopy (Chapters 3 and 4). Productivity measurements were calculated using equation (4).

$$(4)\ Productivity = \frac{kg\ polymer}{moles\ catalyst \times hours}$$

1,3-Diisopropenylbenzene (DIB) incorporation (mol%) was determined from quantitative ^{1}H NMR spectroscopy using equation (5).

$$(5)\ \frac{moles\ of\ comonomer}{moles\ of\ comonomer + moles\ of\ ethylene} \times 100$$

6.1.2 Gas burette system used to measure ethylene uptake during polymerisation

A gas pressure burette system was constructed by previous members of the research group to facilitate ethylene uptake measurements during polymerisation reactions, which would provide information on catalyst lifetime and allow determination of the productivity of the catalysis.[5] Gas is allowed to flow from a storage tank (burette) through a regulator into the reaction vessel. The gas uptake (in moles) by the polymerisation can be calculated by measuring the change in pressure of the storage tank.

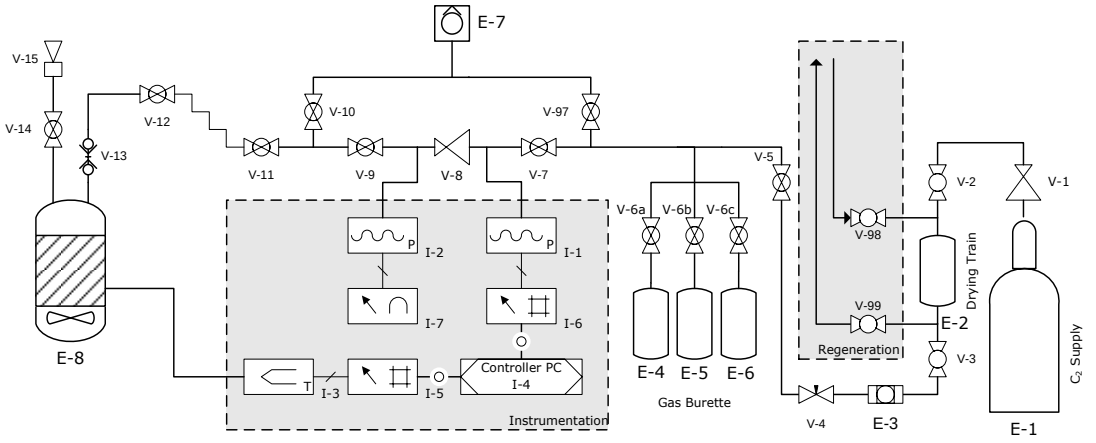

Figure 6.1 - Gas pressure burette schematic.

The equipment was constructed as shown schematically in Figure 6.1 (details are provided in Appendix B).[5] Prior to reaction, ethylene is passed through a drying train consisting of BASF R3-11G deoxygenating agent and 3 Å molecular sieves (E-2), and a filter (E-3), and then stored in an appropriately sized (300, 1000, 2250 cm^3) pressure burette (E-4, E-5, or E-6 respectively) at *ca* 16 bar. During the reaction, the supply valve (V-5) is closed, and gas passes from the burette through the regulator (V-8) into the reaction vessel (E-8) at between 1 and 7 bar as appropriate.

6.1.2.1 Data acquisition and processing

The pressure in the gas burette was measured by a pressure transducer (I-1), and the reactor temperature was measured by a thermocouple (I-3). Data from the sensors is digitised by process meters (I-5 and I-6), and recorded at the desired frequency (usually 1 s^{-1}) by an attached computer (I-4). Custom data acquisition software (Polymeister) was written by a previous group member for this setup in the Java programming language,[5] and this is used to display a chart of the ethylene uptake and temperature during the polymerisation. The software is controlled through a graphical user interface and outputs data in CSV format which can be tabulated in readily available spreadsheet software.

The control software also performs conversion calculations from pressure of ethylene remaining in the burette to moles of gas taken up during the reaction, by applying the second-order virial equation of state[6], shown in equation (6), to account for the non-ideal behaviour of ethylene.

$$(6)\ pV_m = RT\left(1 + \frac{B}{V_m}\right)$$

This may be rearranged to the quadratic form shown in equation (7), which in turn can be solved using the standard numerical quadratic solution, resulting in the form shown in equation (8), which the software solves for each recorded data point.

$$(7)\ \left(\frac{B}{V}\right) n^2 + n + \frac{-pV}{RT} = 0$$

$$(8)\ n = \frac{-1 \pm \sqrt{1 - 4\left(\frac{B}{V}\right)\left(\frac{-pV}{RT}\right)}}{2\left(\frac{B}{V}\right)}$$

Where:

B = 2nd virial coefficient, n = Number of moles, P = Pressure, R = Gas constant, T = Temperature, V = Total volume, V_m = Molar volume.

6.2 General procedure for polymerisations with monitored gas uptake

Polymerisations were conducted in a 250 ml stainless steel Parr reactor with an internal cooling coil, equipped with a thermocouple and linked to a burette system (*vide supra*) for monitoring of gas delivery. As a typical example, the reactor was dried under vacuum for 1 hour and in the meantime, a reaction solution was prepared by adding comonomer (*e.g.* 1,3-DIB (33 ml, 0.19 mol) and MAO (3 ml, 1800 equivalents relative to catalyst) to a graduated glass ampoule *via* cannula and then making up to 90 ml by adding dry toluene. The solution was then transferred to the reactor *via* cannula under an argon

atmosphere, with the reactor initially heated to 50°C. The reactor was purged for 10 min with hydrogen to switch the atmosphere in the reactor from argon to hydrogen before the addition of ethylene. After the ethylene uptake had stabilised a toluene solution of zirconocene dichloride catalyst ($2.5x10^{-6}$ mol) prepared in the glovebox was injected using an overpressure of argon. Following catalyst addition the reactor temperature and gas uptake were continuously monitored. The temperature was maintained at 60°C by use of a laboratory hot plate placed under the reactor and a supply of cold water running through the internal coil. At the appropriate time, the reaction was stopped by sealing the reactor to the ethylene supply then, following a cooling time of *ca* 10 min, careful addition of methanol (2 x 10 ml) to the vented reactor. The polymer product was isolated by precipitation in 5% HCl in methanol (500 ml) with stirring. The precipitated product was recovered by filtration, washed with THF (200 ml) to remove any unreacted comonomer and dried by heating overnight in a vacuum oven at 70°C.

6.3 General procedure for ampoule batch free-radical polymerisation in the absence of PE-*i*-DIB macromonomer

For a typical higher molecular weight example, a 10 ml glass ampoule equipped with a stirrer bar was charged in air with dibenzoyl peroxide (0.037 g, $9.5x10^{-5}$ mol, one equivalent), *n*-butyl acrylate (5.5 ml, 0.038 mol, 400 equivalents) and made up to 8.2 ml with toluene. The ampoule was then sealed and degassed by three freeze-pump-thaw cycles before it was sealed under vacuum. The ampoule was stirred and heated at 125°C using an aluminium heating block. At the appropriate time, the ampoule was cooled by plunging into liquid nitrogen, opened and the contents poured into stirring methanol. The precipitated product was recovered by filtration and dried *in vacuo* overnight. In the case of the lower molecular weight samples, the contents of the ampoules was

transferred to RBF's and the solvent and other volatiles were removed *in vacuo* to isolate the polymer, which was then dried in a vacuum oven overnight.

6.4 General procedure for ampoule batch free-radical polymerisations in the presence of PE-*i*-DIB macromonomer

For a typical example, seven 10 ml glass ampoules equipped with a stirrer bar were charged in air with PE-*i*-DIB macromonomer (0.2 g, 9.5×10^{-5} mol), *n*-butyl acrylate (2.7 ml, 0.019 mol, 200 equivalents), dibenzoyl peroxide (0.037 g, 9.5×10^{-5} mol, one equivalent), and made up to 8.2 ml with toluene. The ampoules were then sealed and degassed by three freeze-pump-thaw cycles before they were sealed under vacuum. The ampoules were stirred and heated simultaneously at 125°C using an aluminium heating block. At the appropriate time, the ampoules were removed from the heating block, cooled by plunging into liquid nitrogen, opened and the mixture poured into methanol (100 ml) with stirring to isolate the PE-containing products by precipitation. The precipitates were then allowed to settle before recovery by filtration. If required the crude products were purified by reprecipitation twice from toluene/methanol and dried overnight in a vacuum oven. Homopolymer by-products were isolated from the methanol-soluble mixture by transfer of the filtrate to an RBF and removal of the solvent and other volatiles *in vacuo*, then dried further in a vacuum oven.

6.5 General procedure for RBF batch free-radical polymerisations in the absence of PE-*i*-DIB macromonomer

For a typical example, a 250 ml 3-neck RBF equipped with a stirrer bar, a condenser (with bubbler) and two rubber seals was charged in air with *n*-butyl acrylate (8.2 ml, 0.057 mol, 50 equivalents) and toluene (60 ml). The system was purged by bubbling

argon through the reaction mixture using a needle connected to a Schlenk line with stirring for 15 min at room temperature. After purging, the inert atmosphere was maintained by turning on the dinitrogen supply as the argon supply was removed and the mixture was heated to 110°C with stirring. A separate RBF equipped with a stirrer bar was charged with dibenzoyl peroxide (0.37 g, 1.1×10^{-3} mol, one equivalent) and toluene (10 ml) and purged with argon for 15 min with stirring. A glass syringe was purged three times with argon then used to transfer the initiator solution into the reaction mixture. At appropriate intervals, sampling of the polymerisation was achieved by withdrawing a 2.5 ml aliquot from the reaction mixture with a syringe and the contents transferred to RBF's. At the appropriate time, the 3-neck RBF was opened and the remaining mixture was also transferred to an RBF. The polymer products in the aliquots and remaining reaction mixture were isolated by removal of the solvent and other volatiles *in vacuo* and the products were dried in a vacuum oven.

6.6 General procedure for RBF batch free-radical polymerisations in the presence of PE-*i*-DIB macromonomer

For a typical example, a 250 ml 3-neck RBF equipped with a stirrer bar, a condenser (with bubbler) and two rubber seals was charged in air with PE-*i*-DIB macromonomer (2.4 g, 1.1×10^{-3} mol), *n*-butyl acrylate (8.2 ml, 0.057 mol, 50 equivalents) and toluene (60 ml). The system was purged by bubbling argon through the reaction mixture with stirring for 15 min at room temperature. After purging, the inert atmosphere was maintained by turning on the dinitrogen supply as the argon supply was removed and the mixture was heated to 110°C with stirring to dissolve the macromonomer. A separate RBF equipped with a stirrer bar was charged with dibenzoyl peroxide (0.37 g, 1.1×10^{-3} mol, one equivalent) and toluene (10 ml) and purged with argon for 15 min with stirring.

A glass syringe was purged three times with argon then used to transfer the initiator solution into the reaction mixture. At appropriate intervals, sampling of the polymerisation was achieved by withdrawing a 2.5 ml aliquot from the reaction mixture with a syringe and the contents transferred into stirring methanol (30 ml) to isolate the PE-containing species. At the appropriate time, the 3-neck RBF was opened and the mixture poured into methanol (400 ml) with stirring to isolate the remaining PE-containing species. The precipitates of the aliquots and final product were then allowed to settle before their recovery by filtration. If required the crude products were purified by reprecipitation twice from toluene/methanol and dried overnight in a vacuum oven. Following filtration, the methanol-soluble filtrates were transferred to an RBF and the solvent and volatiles were removed *in vacuo* to isolate the homopolymer by-products.

6.7 General procedure for starved feed free-radical polymerisations in the absence of PE-*i*-DIB macromonomer

For a typical example, a 250 ml 3-neck RBF equipped with a stirrer bar, a condenser (with bubbler) and two rubber seals was charged in air with toluene (60 ml). The system was purged by bubbling argon through the reaction mixture with stirring for 15 min at room temperature. After purging, the inert atmosphere was maintained by turning on the dinitrogen supply as the argon supply was removed and the mixture was heated to 110°C with stirring. Separate RBF's were charged with a toluene solution of dibenzoyl peroxide (0.37 g, 1.1×10^{-3} mol, one equivalent) and *n*-butyl acrylate (8.2 ml, 0.057 mol, 50 equivalents) respectively and purged with argon for 15 min with stirring. Syringes were purged with argon three times and then used to draw up the required initiator and monomer feeds, which were then set into syringe pumps. The initiator solution and monomer were continuously fed into the reaction mixture at fixed rates and the total

amounts of monomer added and the feed rate were adjusted depending on the required rate to deliver the feeds over the desired reaction time. At appropriate intervals, sampling of the polymerisation was achieved by withdrawing a 2.5 ml aliquot from the reaction mixture with a syringe and the contents transferred to RBF's. At the appropriate time, the 3-neck RBF was opened and the remaining mixture was also transferred to an RBF. The polymer products in the aliquots and remaining reaction mixture were isolated by removal of the solvent and other volatiles *in vacuo* and the products were dried in a vacuum oven.

6.8 General procedure for starved feed free-radical polymerisations in the presence of PE-*i*-DIB macromonomer

For a typical example, a 250 ml 3-neck RBF equipped with a stirrer bar, a condenser (with bubbler) and two rubber seals was charged in air with PE-*i*-DIB macromonomer (2.4 g, 1.1×10^{-3} mol) and toluene (60 ml). The system was purged by bubbling argon through the reaction mixture with stirring for 15 min at room temperature. After purging, the inert atmosphere was maintained by turning on the dinitrogen supply as the argon supply was removed and the mixture was heated to 110°C with stirring to dissolve the macromonomer. Separate RBF's were charged with a toluene solution of dibenzoyl peroxide (0.37 g, 1.1×10^{-3} mol, one equivalent) and *n*-butyl acrylate (8.2 ml, 0.057 mol, 50 equivalents) respectively and purged with argon for 15 min with stirring. Syringes were purged with argon three times and then used to draw up the required initiator and monomer feeds, which were then set into syringe pumps. The initiator solution and monomer were continuously fed into the reaction mixture at fixed rates and the total amounts of monomer added and the feed rate were adjusted depending on the required rate to deliver the feeds over the desired reaction time. At appropriate intervals, sampling

of the polymerisation was achieved by withdrawing a 2.5 ml aliquot from the reaction mixture with a syringe and the contents transferred into stirring methanol (30 ml) to isolate the PE-containing species. At the appropriate time, the 3-neck RBF was opened and the remaining mixture poured into methanol (400 ml) with stirring to isolate the PE-containing product by precipitation. The precipitates were then allowed to settle before recovery by filtration. If required the crude product was purified by reprecipitation twice from toluene/methanol and dried overnight in a vacuum oven. Following filtration, the methanol-soluble filtrates were transferred to an RBF and the solvent and volatiles were removed *in vacuo* to isolate the homopolymer by-products.

6.9 General procedure for epoxidation of macromonomer vinyl groups[7]

A 250 ml 3-neck RBF equipped with a stirrer bar and a condenser was charged in air with P(E-*co*-VNB) macromonomer (0.3 g, 1.15×10^{-4} mol) and toluene (100 ml). On heating to 100°C with stirring the macromonomer dissolved and a solution of 3-chloroperbenzoic acid (1.3 g, 5.77×10^{-3} mol) in toluene (30 ml) was added rapidly. The mixture was then stirred at 100°C for 3 h. After the mixture was removed from the heat, the solvent was removed *in vacuo* and the product precipitated with methanol (80 ml). After recovery by filtration, the polymer was washed with 3 x 50 ml of methanol and dried overnight in a vacuum oven.

6.10 References

1. Gottlieb, H. E.; Kotlyar, V.; Nudelman, A., NMR Chemical Shifts of Common Laboratory Solvents as Trace Impurities. *J. Org. Chem.* **1997,** *62* (21), 7512-7515.
2. Fulmer, G. R.; Miller, A. J. M.; Sherden, N. H.; Gottlieb, H. E.; Nudelman, A.; Stoltz, B. M.; Bercaw, J. E.; Goldberg, K. I., NMR Chemical Shifts of Trace Impurities: Common Laboratory Solvents, Organics, and Gases in Deuterated Solvents Relevant to the Organometallic Chemist. *Organometallics* **2010,** *29* (9), 2176-2179.

3. Grubisic, Z.; Rempp, P.; Benoit, H., A universal calibration for gel permeation chromatography. *Journal of Polymer Science Part B: Polymer Letters* **1967,** *5* (9), 753-759.
4. Standard Test Method for Cold Filter Plugging Point of Diesel and Heating Fuels. In *ASTM Standard D6371*, West Conshohocken, PA: ASTM International, 2005.
5. Hammond, M. L. Imine Catalyst Stability. University of Warwick, 2006.
6. Atkins, P.; de Paula, J., *Atkins' Physical Chemistry*. OUP Oxford: 2010.
7. Sarazin, Y.; Fink, G.; Hauschild, K.; Bochmann, M., Copolymerization of Propene and 5-Vinyl-2-Norbornene: A Simple Route to Polar Poly(propylene)s. *Macromol. Rapid Commun.* **2005,** *26* (15), 1208-1213.

Appendix A: Dynamic light scattering (DLS) correlograms

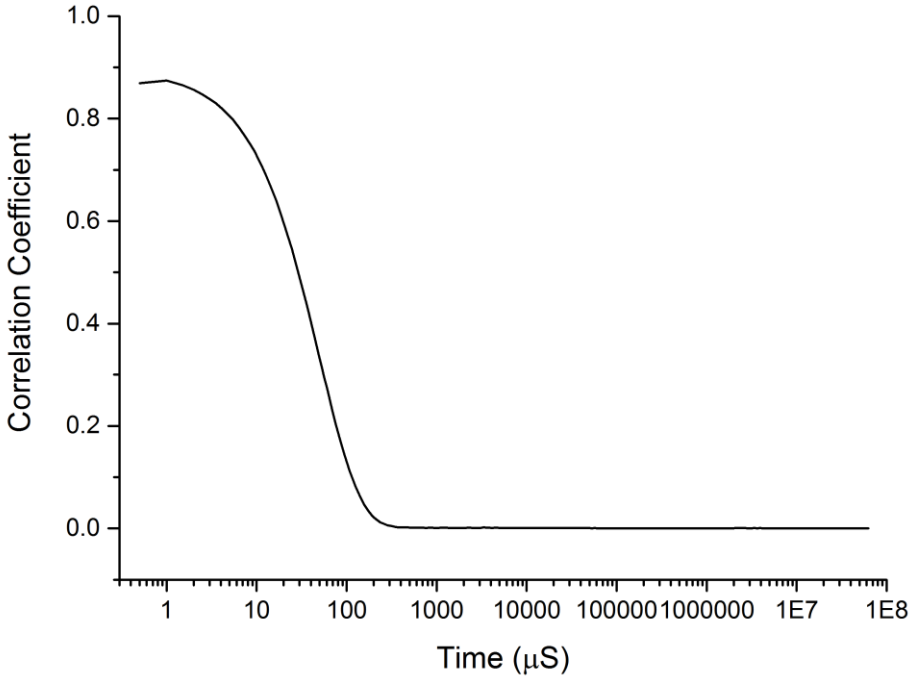

Figure A.1. - DLS correlogram of the product from Run 3-180, Chapter 3 in THF (1 mg/ml) after sonication (average of three measurements).

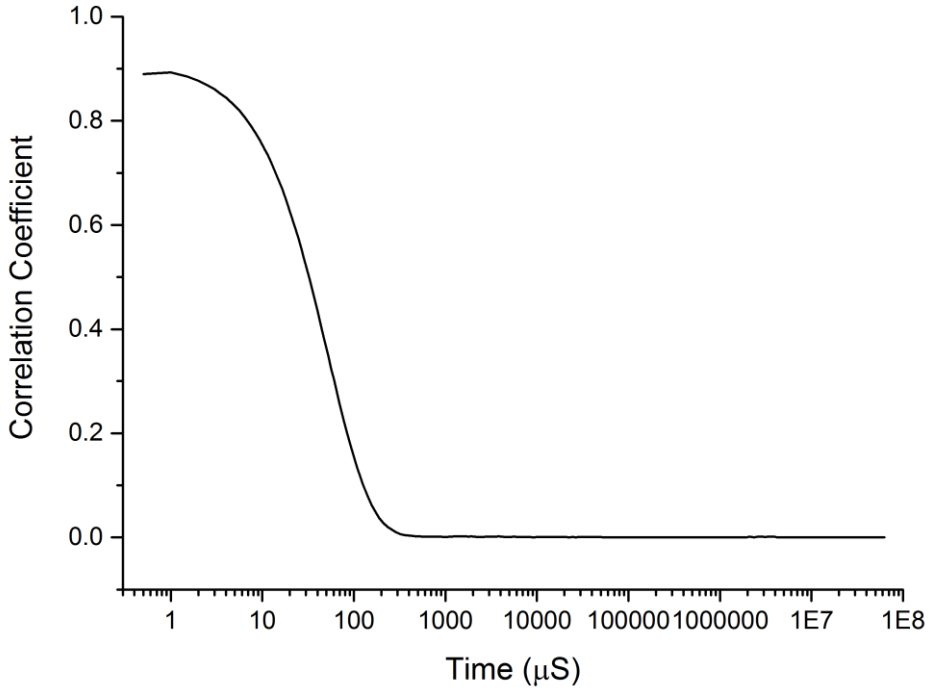

Figure A.2. - DLS correlogram of the product from Run 3-240, Chapter 4 in THF (1 mg/ml) after sonication (average of three measurements).

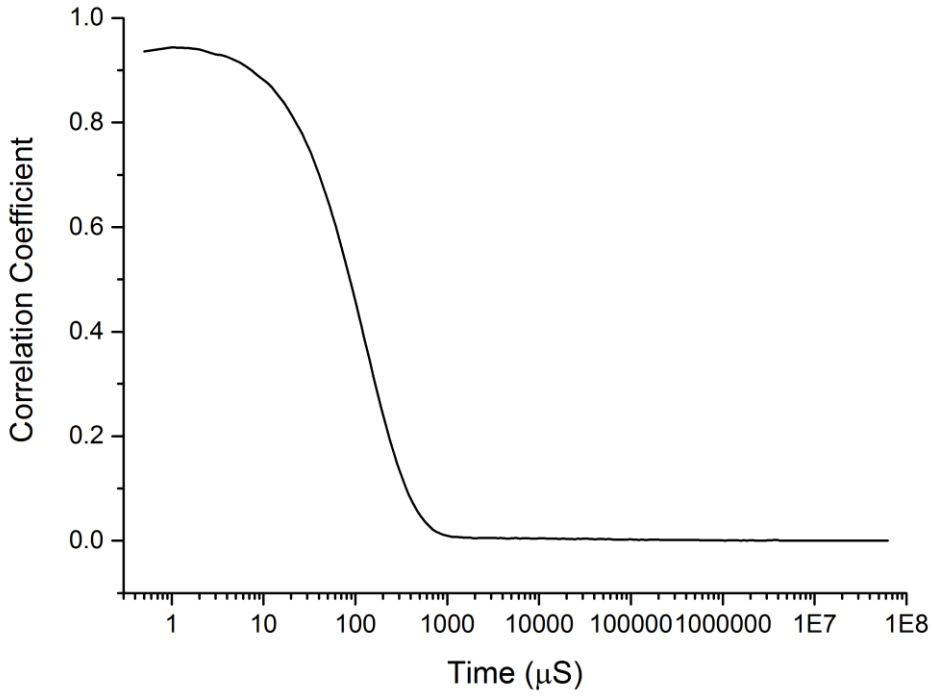

Figure A.3. - DLS correlogram of the product from Run 9-240, Chapter 4 in THF (1 mg/ml) after sonication (average of three measurements).

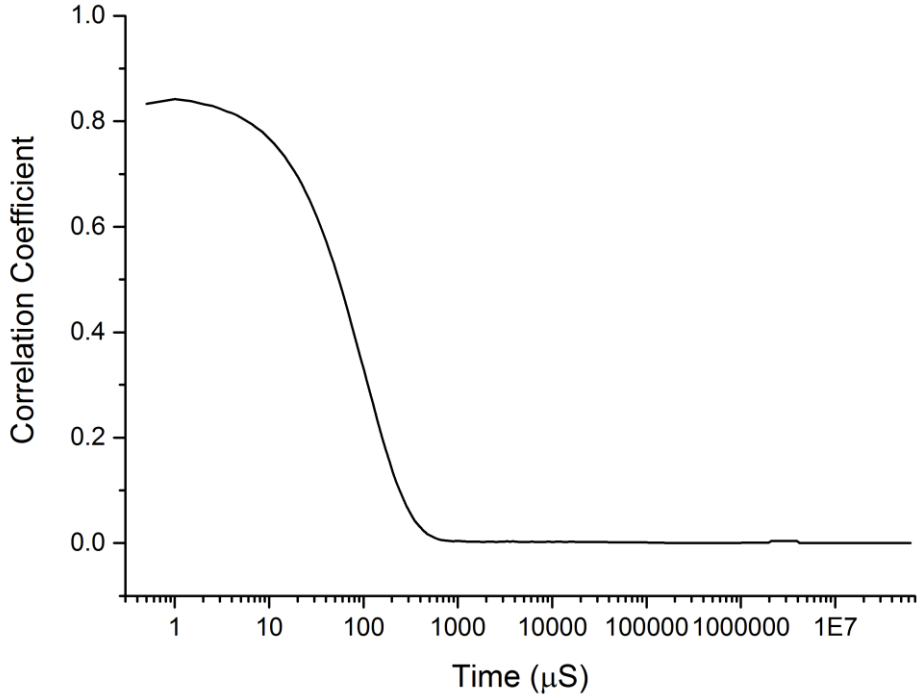

Figure A.4. - DLS correlogram of the product from Run 12-240, Chapter 4 in THF (1 mg/ml) after sonication (average of three measurements).

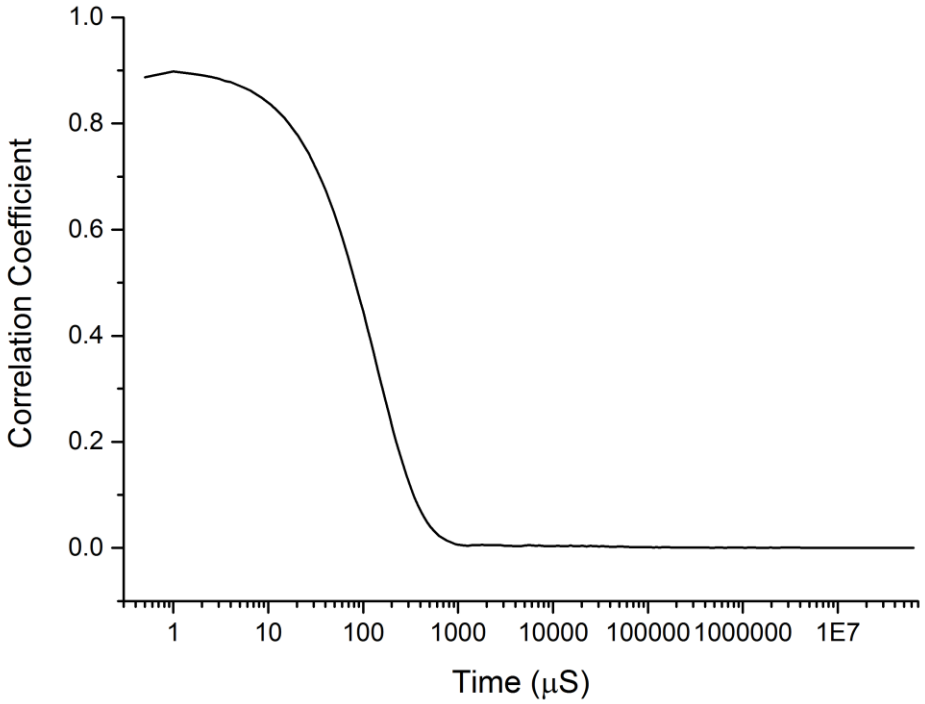

Figure A.5. - DLS correlogram of the product from Run 16-240, Chapter 4 in THF (1 mg/ml) after sonication (average of three measurements).

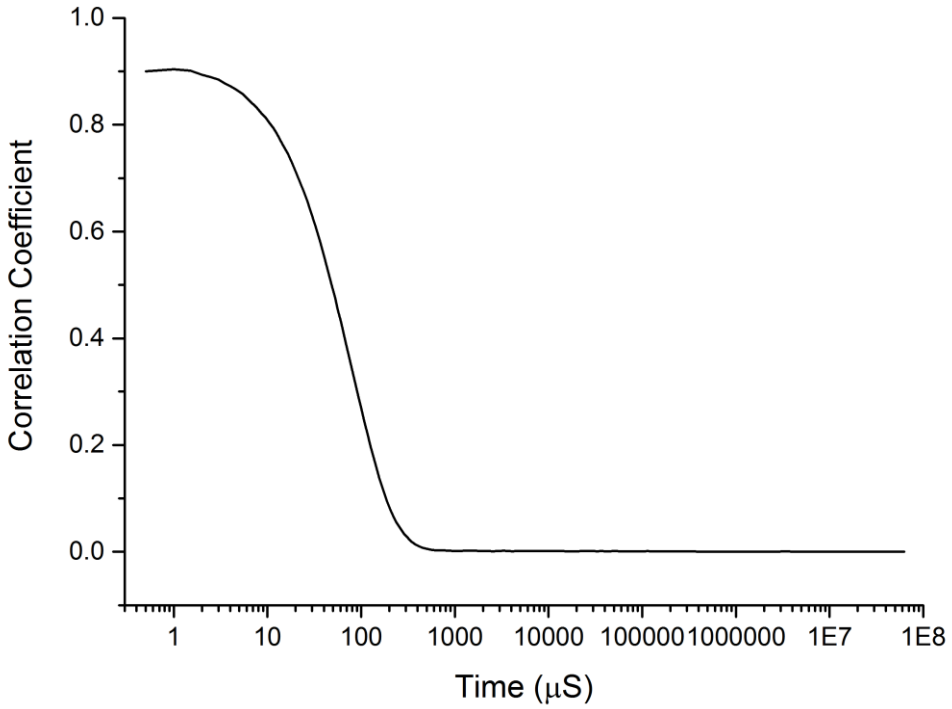

Figure A.6. - DLS correlogram of the product from Run 20-240, Chapter 4 in THF (1 mg/ml) after sonication (average of three measurements).

Appendix B: Design of the gas burette system used

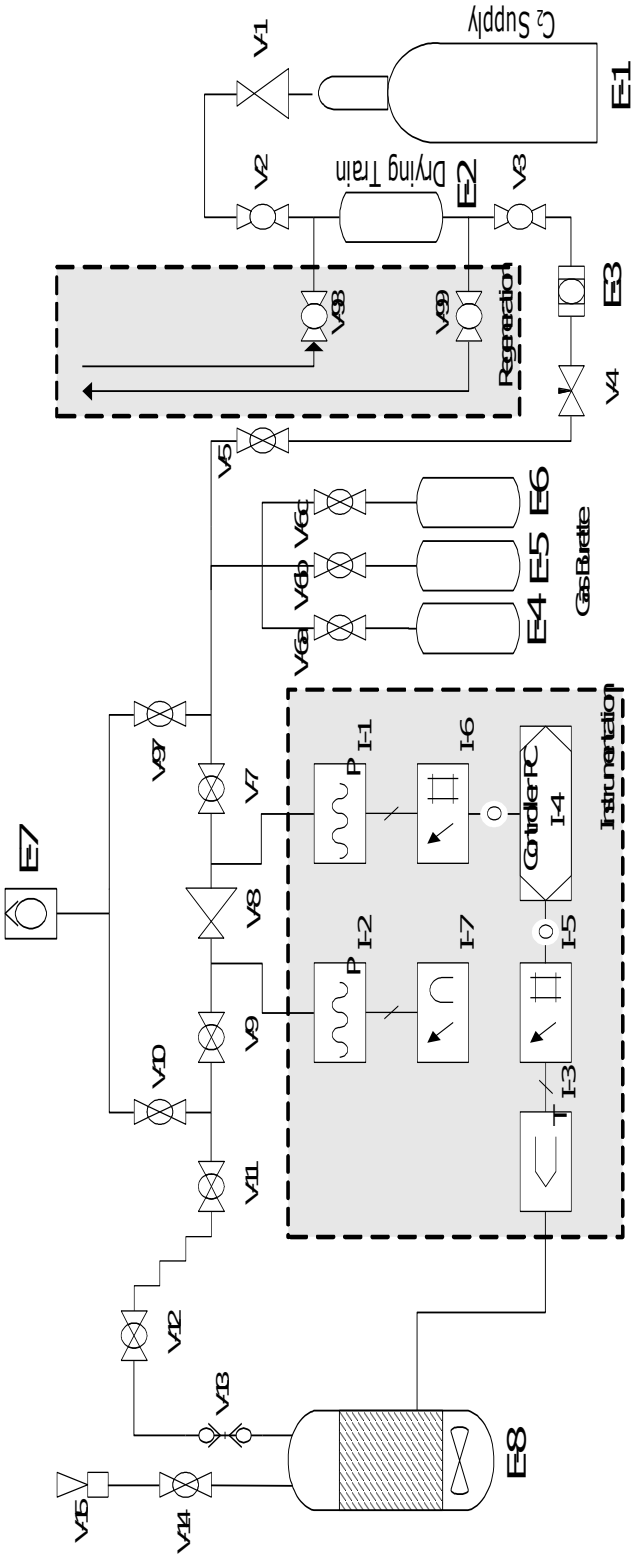

Figure B.1. – Gas burette schematic.[1]

Table B.1. - Gas burette components.[1]

Component	Description	Manufacturer	Model
E-1	Ethylene supply cylinder		
E-1	R-3-11G/3A molecular sieves drying train	Swagelok	304-HDF4-300
E-3	2 micron filter	Swagelok	SS-4FW-2
E-4	300CC sample cylinder	Swagelok	304L-HDF4-300
E-5	1000CC sample cylinder	Swagelok	304L-HDF4-1000
E-6	2250CC sample cylinder	Swagelok	304L-HDF4-2250
E-7	Connection to Schlenk line		
E-8	Reaction vessel		
I-1	Input gauge	Druck	PDCR-4010 (20 bar)
I-2	Output gauge	Tescom	4802-V200N
I-3	Thermocouple in reaction media		
I-4	Control		
I-5	Meter with RS232 interface	Druck	DPI282 with RS232 interface
I-6	ACD with RS232 interface	Druck	DPI282 with RS232 interface
I-7	Pressure dial	Tescom	4802-V200N
V-1	20 bar cylinder regulator	BOC	HP 1502B-GL-BS4
V-2	C2 isolation	Swagelok	SS-4P4T-BK
V-3	Rig isolation	Swagelok	SS-4P4T-BK
V-4	Meter valve	Swagelok	SS-4L2
V-5, V-6, V-7		Swagelok	SS-42S4
V-8	Reactor regulator	Tescom	44-2262-241
V-9, V-10, V-11, V-12		Swagelok	SS-42S4
V-13	Quick connect	Swagelok	SS-QC-D-400/SS-QC4-B-400
V-14	Catalyst injection valve	Swagelok	SS-43S4
V-15	Catalyst injection port	Swagelok	
V-97	Commissioning purge	Swagelok	SS-42S4
V-98	Regeneration gas connection	Swagelok	SS-4P4T-RD
V-99	Regeneration purge connection	Swagelok	SS-4P4T-RD
Catalyst injector	25CC Sample cylinder + Male quick connect	Swagelok	SS-4CS-TW-25/SS-QC6-D-600

References

1. Hammond, M. L. Imine Catalyst Stability, PhD, University of Warwick, 2006.

Appendix C: Selected polymer ^{1}H and ^{13}C NMR spectra

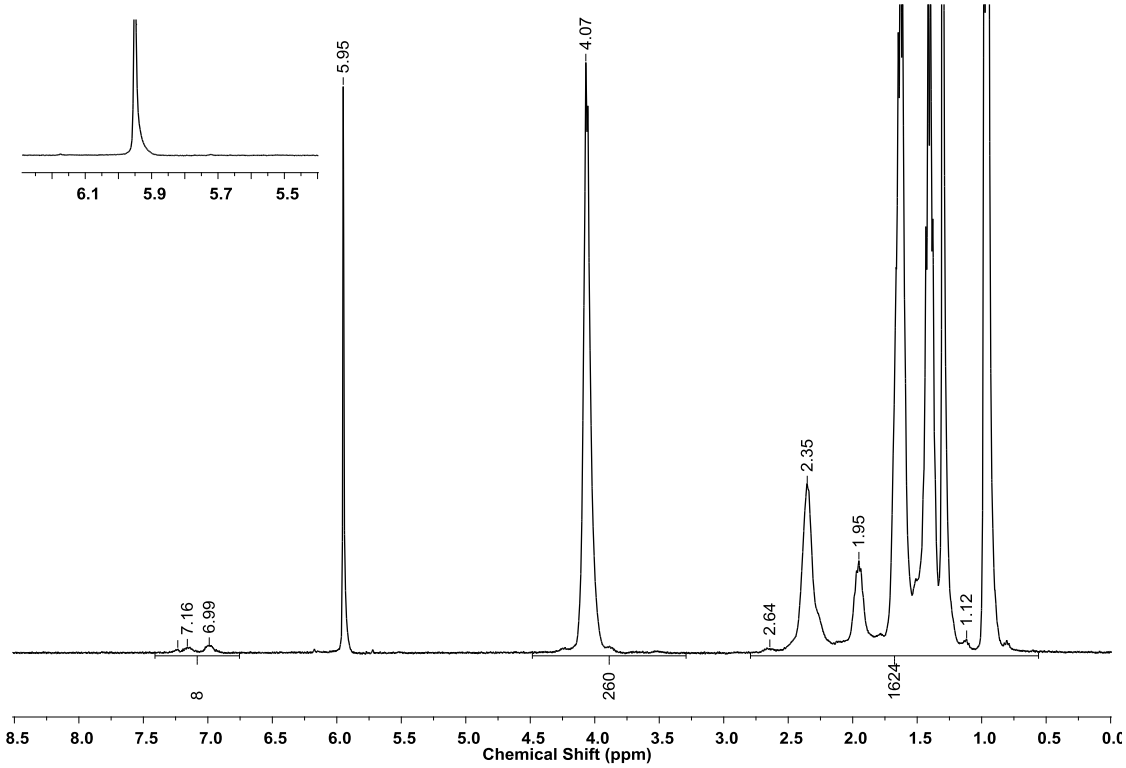

Figure C.1. - ^{1}H NMR spectrum of P(*n*-BA)-*b*-PE-*i*-DIB from Run 3, Chapter 3 in d^2-TCE at 100°C (400MHz) Relaxation delay = 1 s.

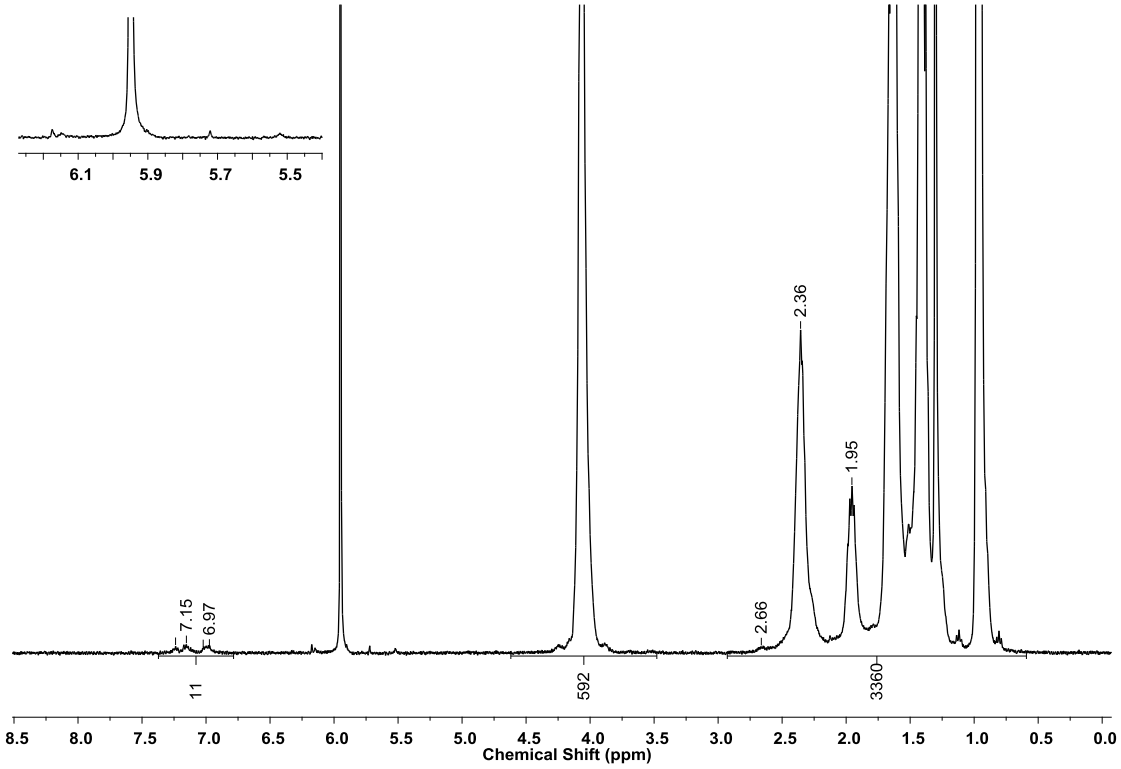

Figure C.2. - ^{1}H NMR spectrum of P(*n*-BA)-*b*-PE-*i*-DIB from Run 4, Chapter 3 in d^2-TCE at 100°C (400MHz) Relaxation delay = 1 s.

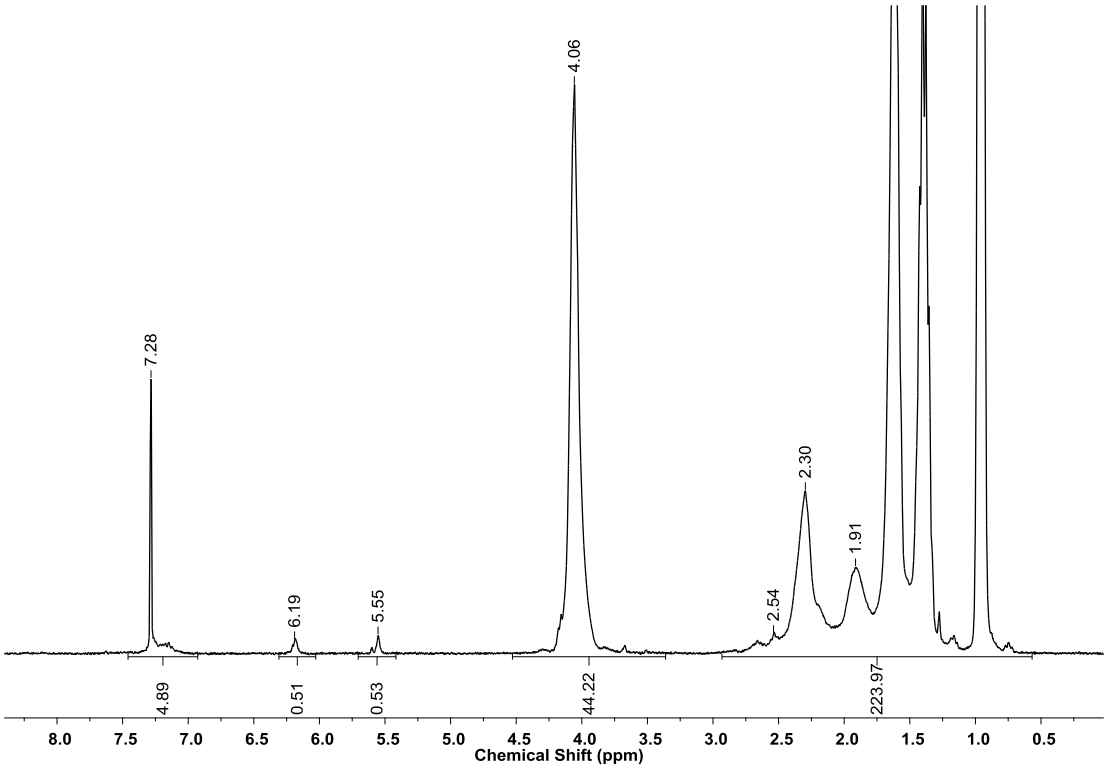

Figure C.3. - ^{1}H NMR spectrum of P(*n*-BA) by-product from Run 3 *t* = 180 min (M_n = 2800, $Đ$ = 2.5), Chapter 3 in $CDCl_3$ at 25°C (400MHz).

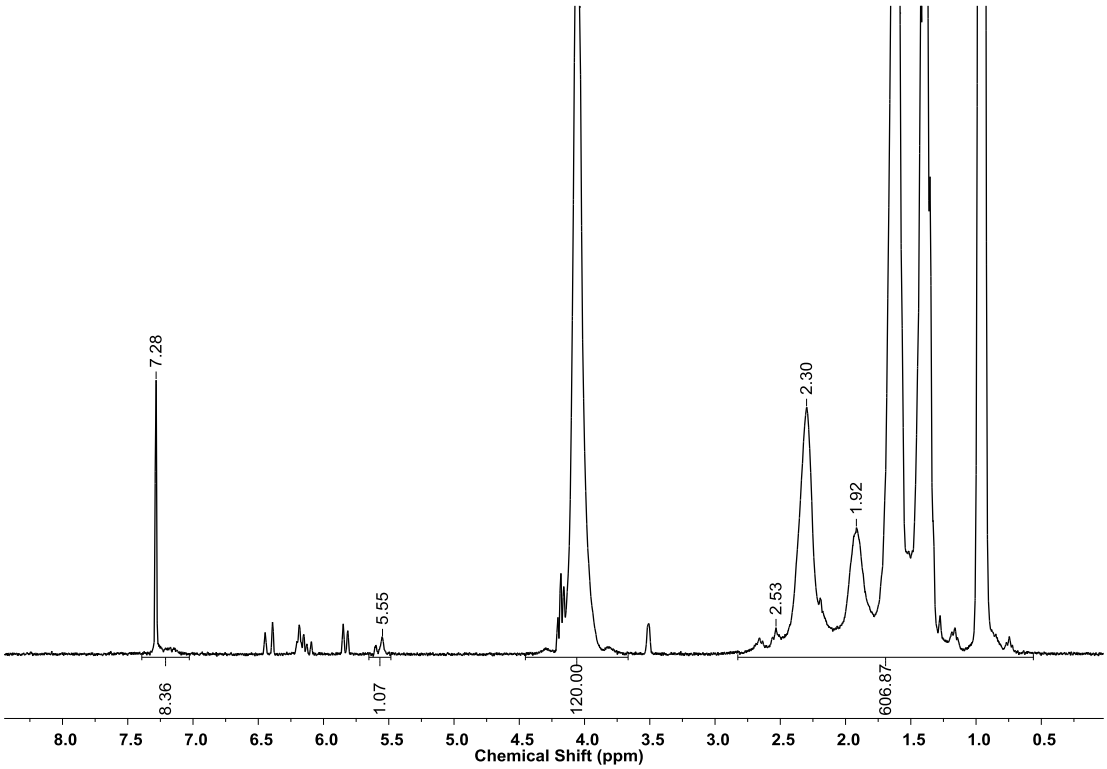

Figure C.4. - ^{1}H NMR spectrum of P(*n*-BA) by-product from Run 4 *t* = 180 min (M_n = 8000, $Đ$ = 2.4) Chapter 3 in $CDCl_3$ at 25°C (400MHz).

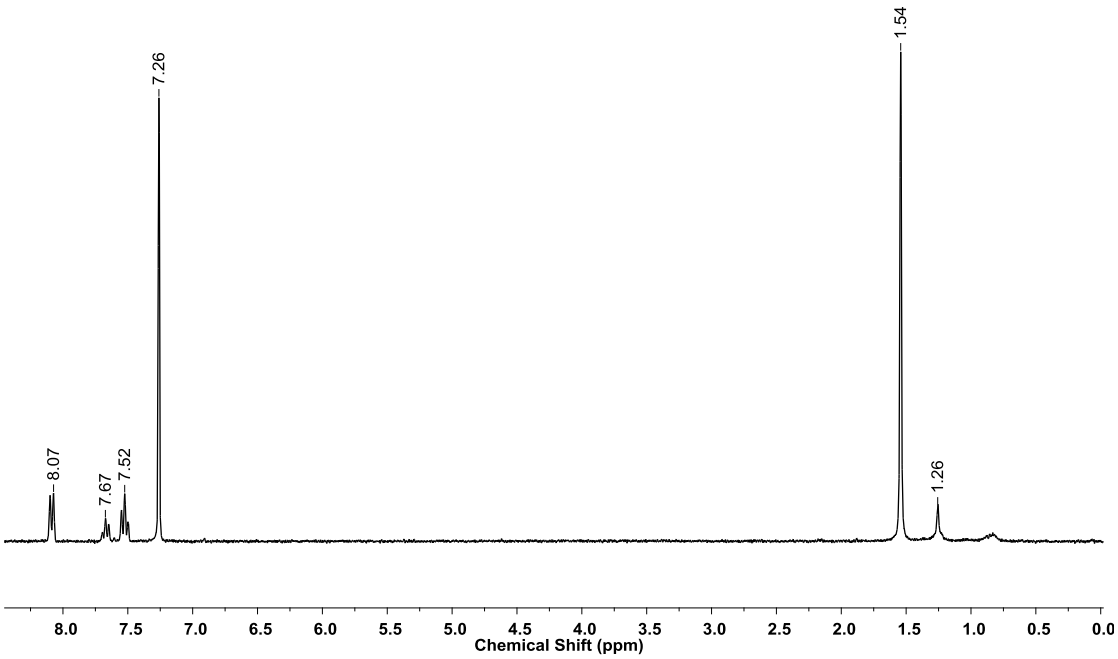

Figure C.5. - ^{1}H NMR spectrum of by-product from Run 8 *t* = 10 min, Chapter 3 in $CDCl_3$ at 25°C (400MHz).

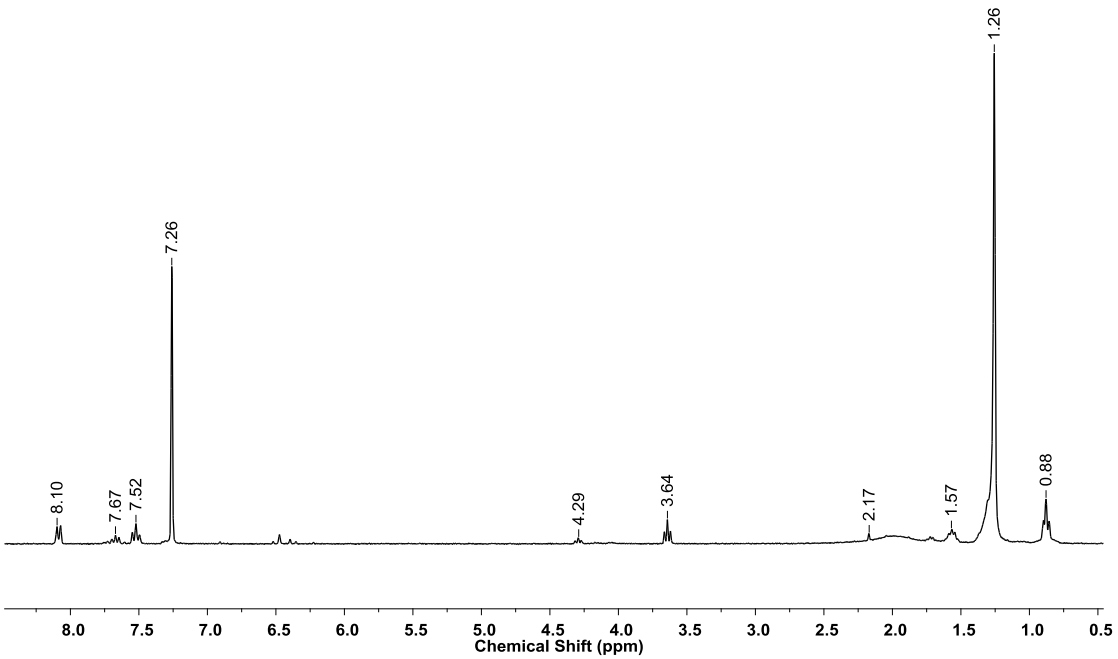

Figure C.6. - ^{1}H NMR spectrum of by-product from Run 8 *t* = 20 min, Chapter 3 in $CDCl_3$ at 25°C (400MHz).

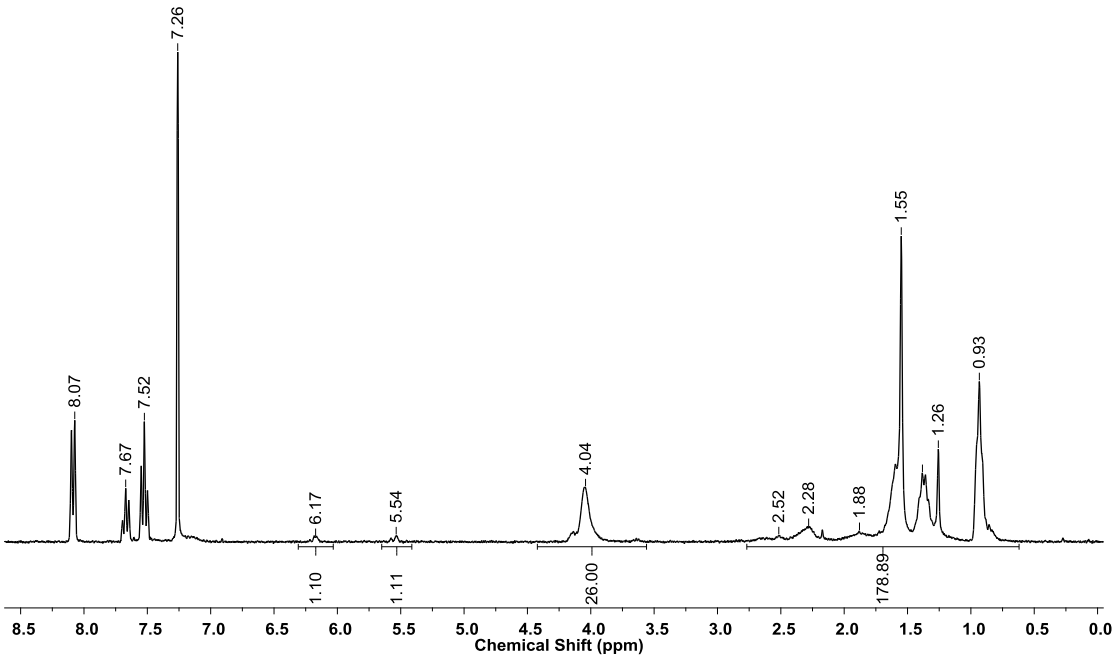

Figure C.7. - ^{1}H NMR spectrum of P(*n*-BA) by-product from Run 8 t = 40 min (M_n = 1600, $Đ$ = 1.6), Chapter 3 in $CDCl_3$ at 25°C (400MHz).

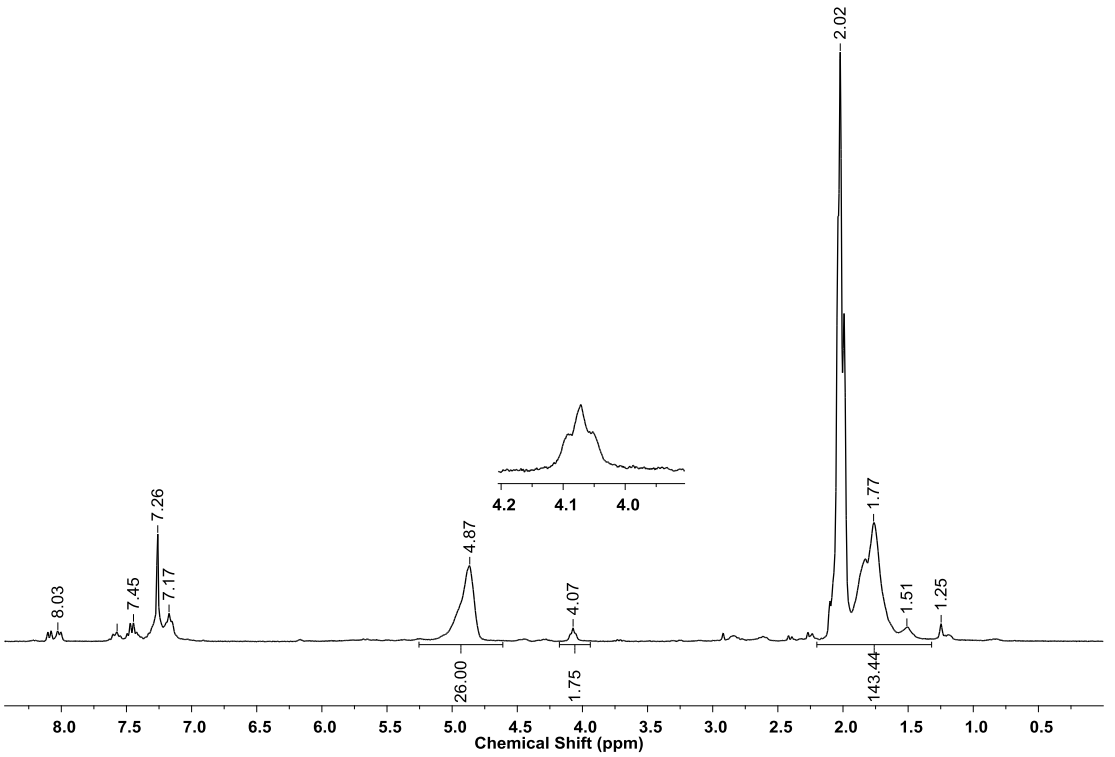

Figure C.8. - ^{1}H NMR spectrum of P(VAc) by-product from Run 3 t = 240 min, (M_n = 2200, $Đ$ = 1.6), Chapter 4 in $CDCl_3$ at 25°C (400MHz).

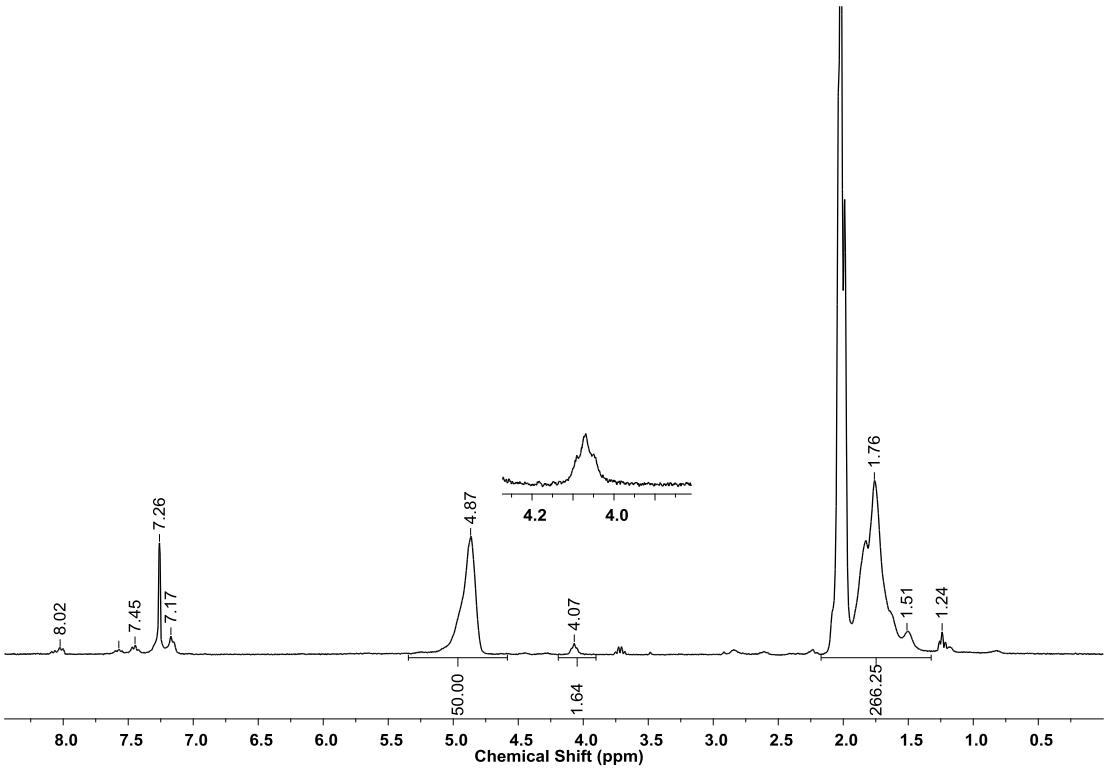

Figure C.9. - ^{1}H NMR spectrum of P(VAc) by-product from Run 4 t = 240 min, (M_n = 4300, Đ = 2.2), Chapter 4 in $CDCl_3$ at 25°C (400MHz).

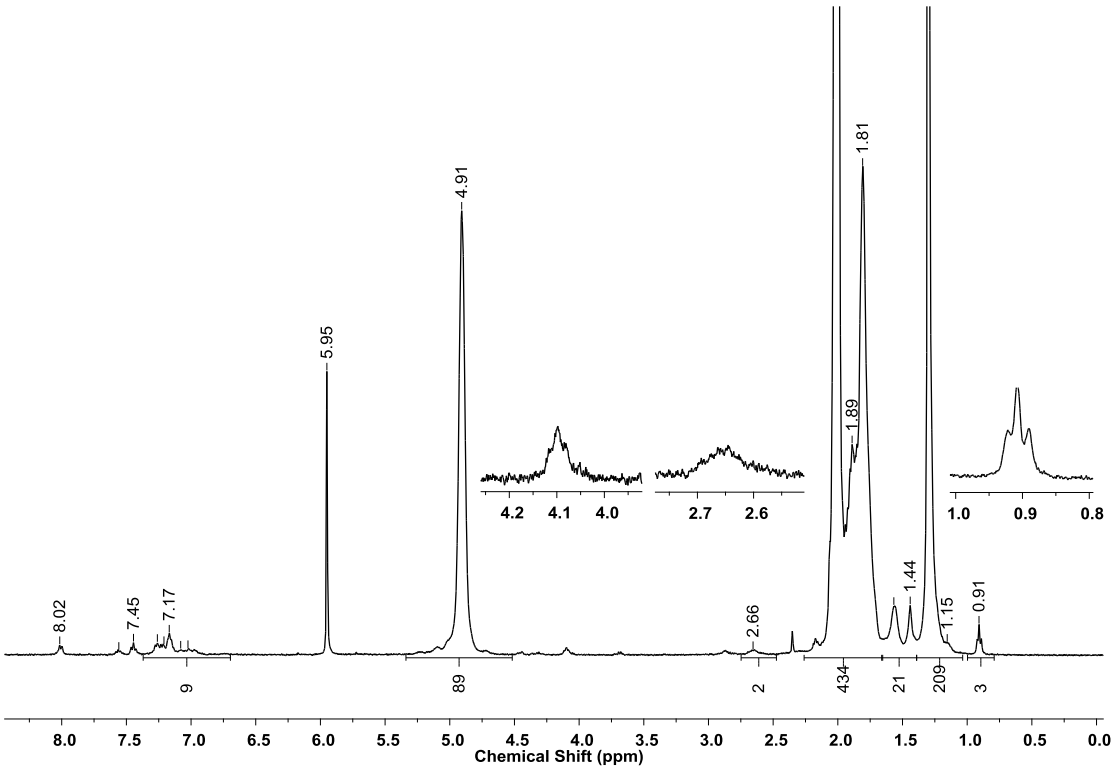

Figure C.10. - ^{1}H NMR spectrum of P(VAc)-*b*-PE-*i*-DIB from Run 4 t = 240 min (M_n = 6800 g/mol, Đ = 3.0), Chapter 4 in d^2-TCE at 100°C (400MHz).

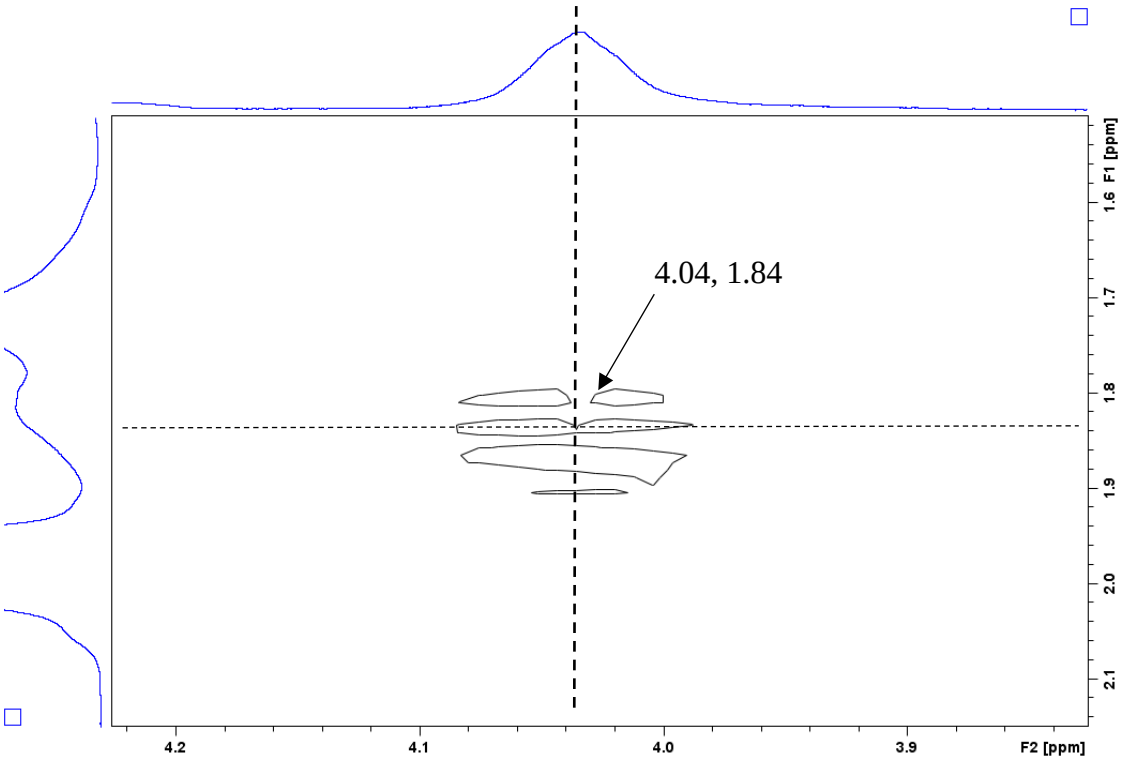

Figure C.11. - Detail of a ^{1}H-^{1}H COSY NMR of P(VAc) by-product from Run 4 *t* = 240 min, Chapter 4 in $CDCl_3$ at 25°C (400 MHz).

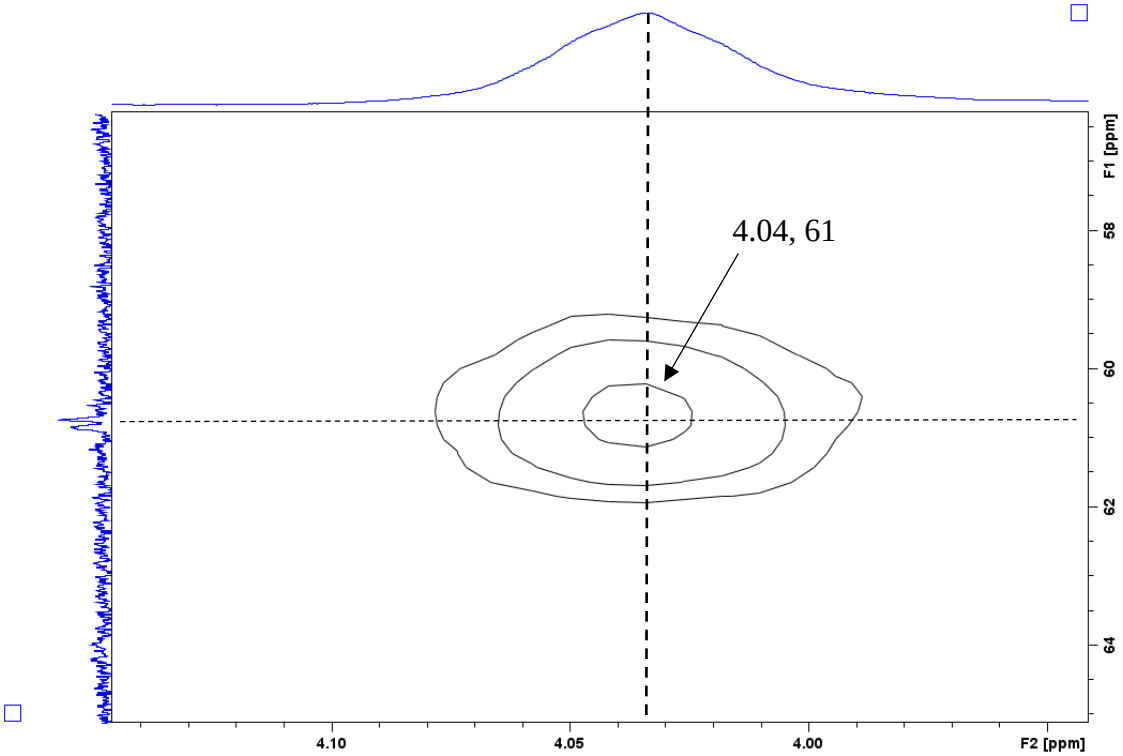

Figure C.12. - Detail of ^{1}H-^{13}C HMQC NMR of P(VAc) by-product from Run 4 *t* = 240 min, Chapter 4 in $CDCl_3$ at 25°C (400 MHz).

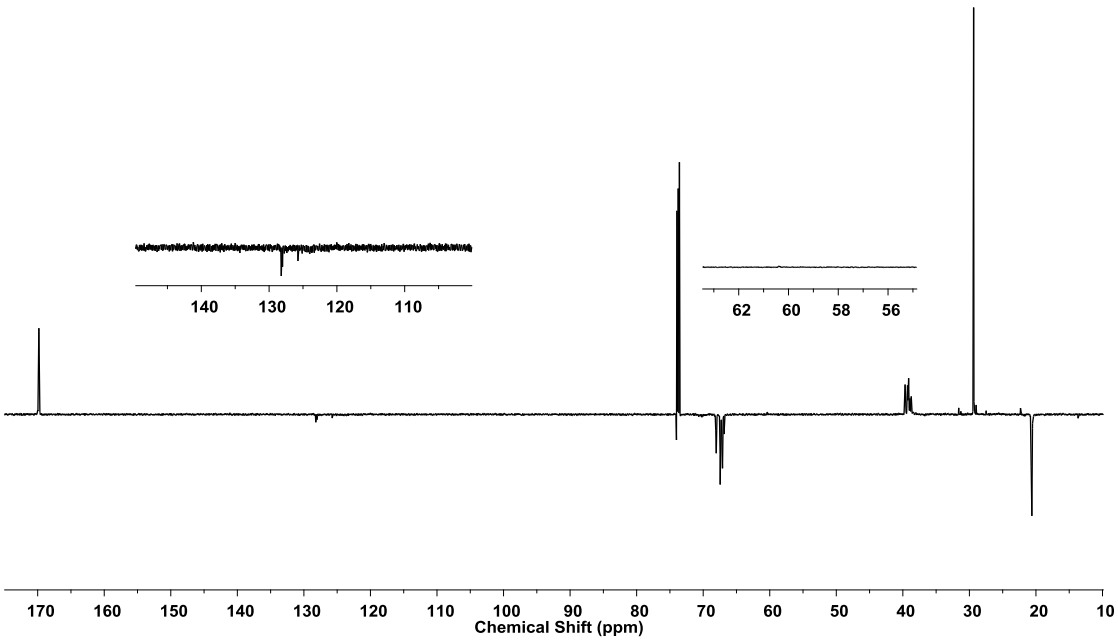

Figure C.13. – ^{13}C NMR spectrum of P(VAc)-*b*-PE-*i*-DIB from Run 4 t = 240 min (M_n = 6800 g/mol, $Đ$ = 3.0), Chapter 4 in d^2-TCE at 100°C (150 MHz) Relaxation delay = 4 s. The only signals present in the 100 – 150 ppm region are aromatic. No vinylic signals appear.

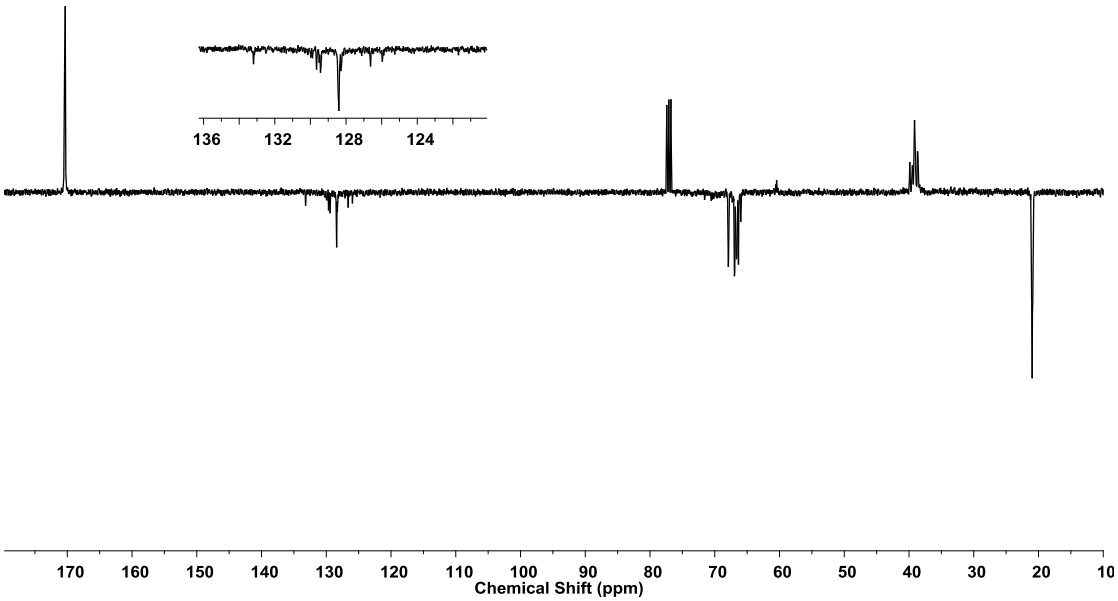

Figure C.14. - ^{13}C NMR spectrum of P(VAc) by-product from Run 4 t = 240 min (M_n = 4300 g/mol, $Đ$ = 2.4), Chapter 4 in $CDCl_3$ at 25°C (100 MHz) Relaxation delay = 4 s. Extra signals appear in the 100-150 ppm region at 126 ppm and 133 ppm, consistent with terminal vinylic groups.

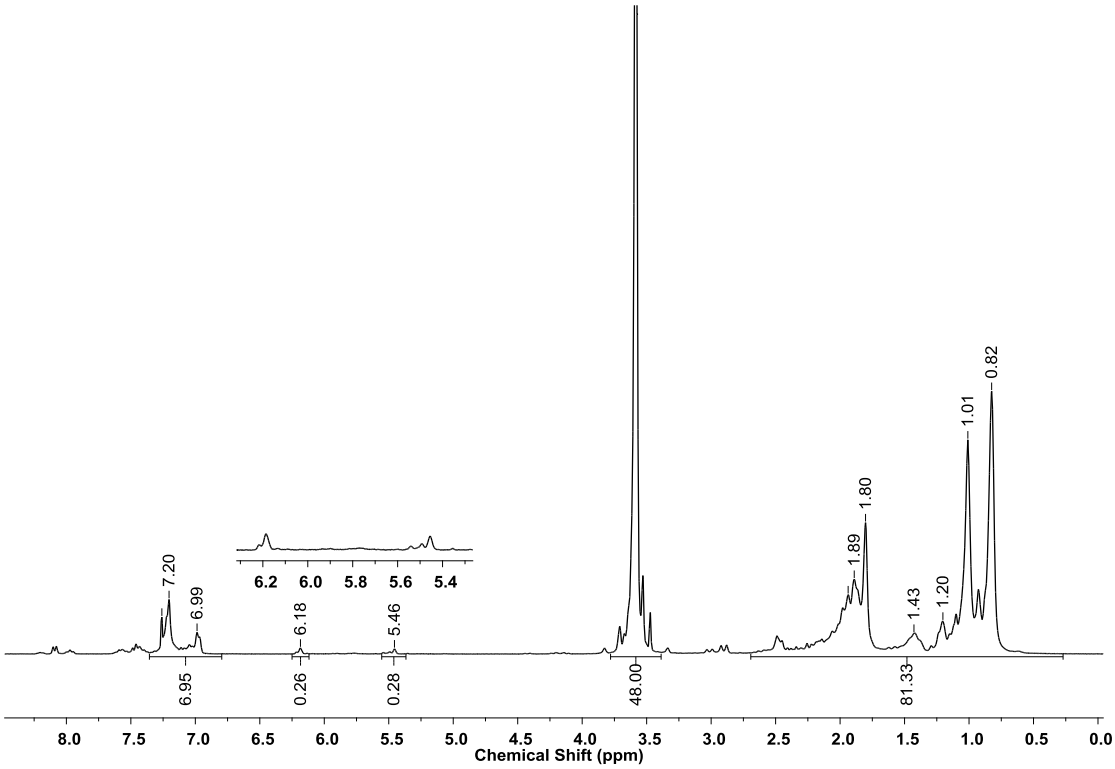

Figure C.15. - ^{1}H NMR spectrum of P(MMA) by-product from Run 11 t = 240 min, (M_n = 1600, $Đ$ = 1.6), Chapter 4 in $CDCl_3$ at 25°C (400MHz).

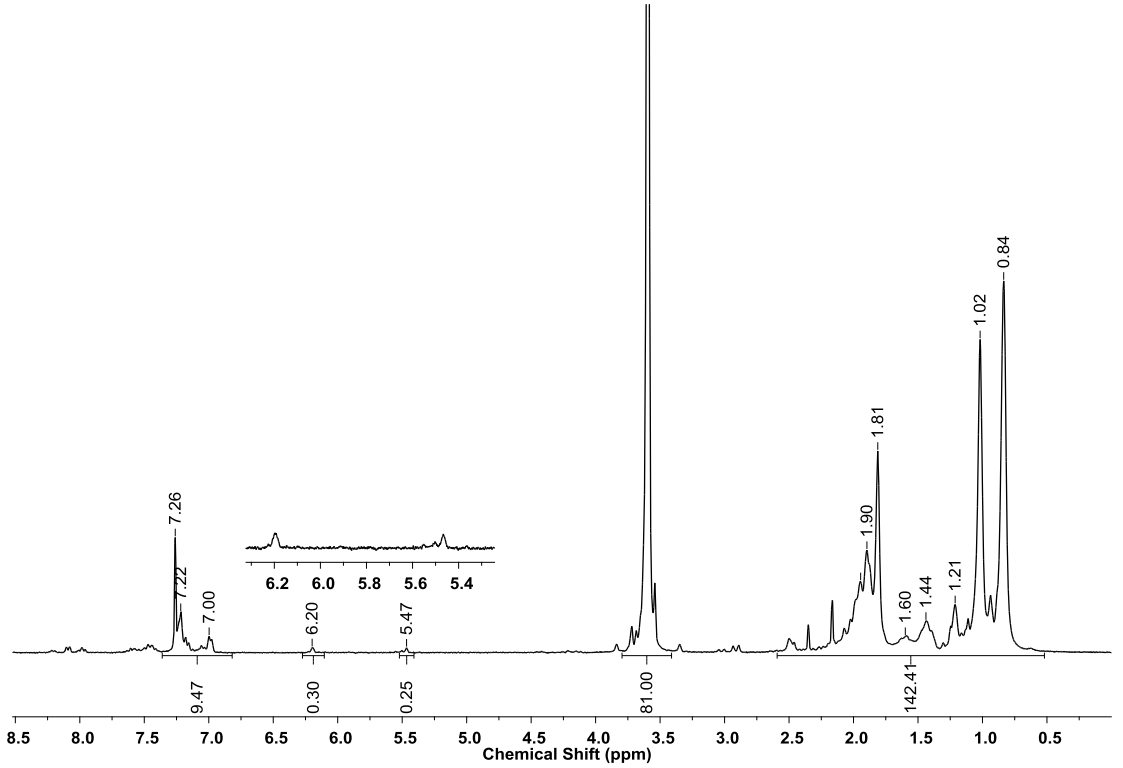

Figure C.16. - ^{1}H NMR spectrum of P(MMA) by-product from Run 12 t = 240 min, (M_n = 2700, $Đ$ = 1.8), Chapter 4 in $CDCl_3$ at 25°C (400MHz).

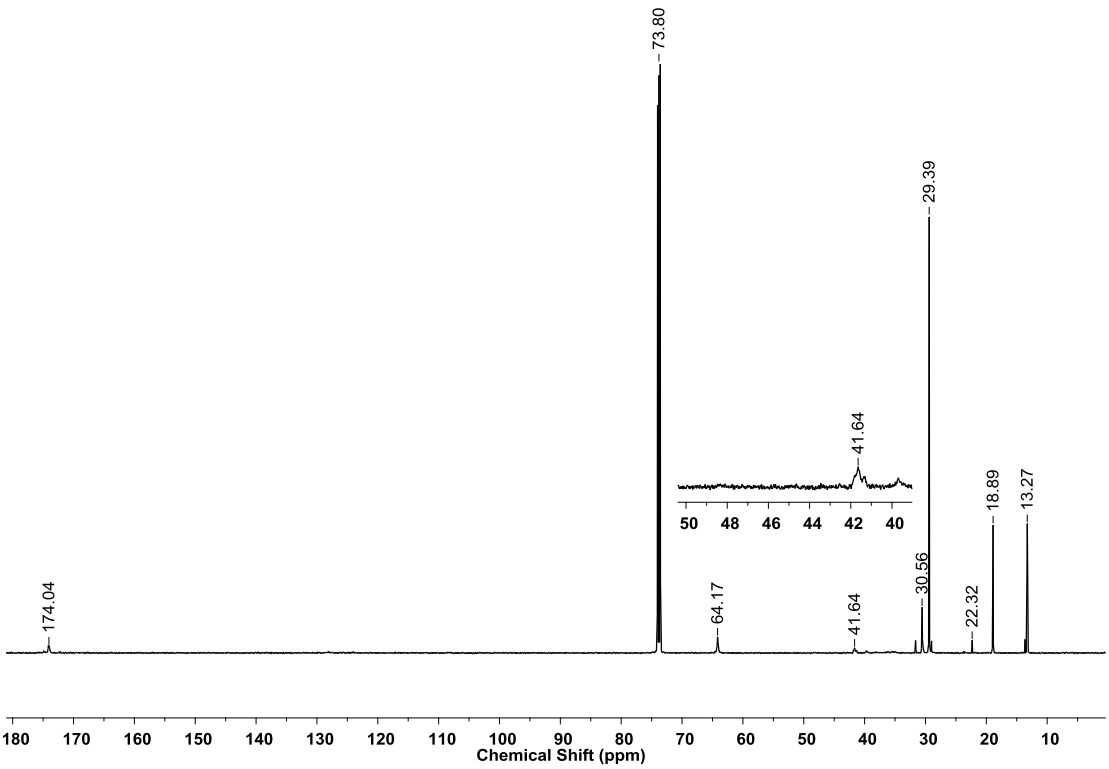

Figure C.17. - ^{13}C NMR spectrum of P(*n*-BA)-*b*-PE-*i*-DIB from Run 4 t = 60 min min (M_n = 11000 g/mol, Đ = 2.6), Chapter 3 in d^2-TCE at 100°C (125 MHz) Relaxation delay = 4 s. No P(*n*-BA) branching quarternary carbon environment signal at 47-49 ppm.